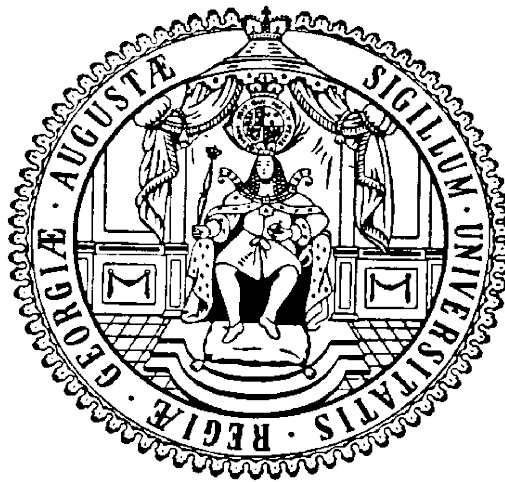# Characterization of the MIR23A Cluster in Diffuse Large B Cell Lymphoma

Regulation and Targetome Identification

Doctoral Thesis

In partial fulfillment of the requirements for the degree
"Doctor rerum naturalium (Dr. rer. nat.)"
in the Molecular Medicine Study Program
at the Georg-August University Göttingen

submitted by

Natalie Veronika Freytag

born in
Zabrze, Poland

Göttingen 2017

Members of the Thesis Committee:

Prof. Dr. Dieter Kube, Supervisor
        Department of Haematology and Oncology
        University Medical Center Göttingen

Prof. Dr. Peter Burfeind, Reviewer
        Department of Human Genetics
        University Medical Center Göttingen

Halyna Shcherbata, PhD, Reviewer
        Max Planck Research Group for Gene Expression and Signaling
        Max Planck Institute for Biophysical Chemistry Göttingen

Date of oral examination: 3.02.2017

Affidavit

Here I declare that my doctoral thesis entitled **"Characterization of the MIR23A Cluster in Diffuse Large B Cell Lymphoma - Regulation and Targetome Identification"** has been written independently with no other sources and aids than quoted.

Göttingen, October 2016

List of publications

Annica Vlad-Fiegen, **Natalie Veronika Freytag**, Susanne Dorn, Oliver Müller, Sonja Eberth
"The Wnt Pathway Target Gene CCND1 Changes Mitochondrial Localization and Decreases Mitochondrial Activity in Colorectal Cancer Cell Line SW480"
Journal of Biosciences and Medicines, 2016, 4, 132-143
DOI: 10.4236/jbm.2016.412017

Natalie V. Freytag, Claudia Pommerenke, Yvonne Merkhoffer, Hilmar Quentmeier, Hans G. Drexler, Sonja Eberth
"microRNAs encoded by the MIR23A-cluster on chr. 19 primarily target genes from the same chromosome"
Abstract and Poster
Transcription and Chromatin EMBL Conference, Heidelberg, 2016

Sonja Eberth, **Natalie Klytta**, Theres Lusansky, Andreas Rosenwald, Reiner Siebert, Hans G. Drexler, Hilmar Quentmeier
"Out of epigenetic control: Regulation of the miR-23a~27a~24-2 in B cell non-Hodgkin Lymphoma and classical Hodgkin Lymphoma"
Abstract Haematologica 2015: 760-760
20th European Hematology Association (EHA), Vienna, 2015

Natalie Klytta, Claudia Pommerenke, Dieter Kube, Lorenz Trümper, Michael Haid, Jessica Höll, Hilmar Quentmeier, Hans G. Drexler, Sonja Eberth
"The Role of microRNA Cluster MIR23A~27A~24-2 in the Development of Aggressive B-cell Lymphoma"
FEBS Journal 2015 (282): 160-160
Poster and oral presentation at the 40th Federation of European Biochemical Societies (FEBS) Congress, Berlin, 2015

Contents

List of Figures

List of Tables

Abbreviations

Abbreviation	Denotation
ABC	activated B cell like
Ago2	Argonaute 2
AKT	protein kinase B
ALL	Acute Lymphoblastic Leukemia
AML	Acute Myeloid Leukemia
anti-IgM/aIgM	anti-immunoglobulin M
BBC3	BCL-2 binding component 3
BCL6	B cell lymphoma 6
BCR	B cell receptor
BL	Burkitt lymphoma
bp	base pair
C2H2	Cystein(2)-Histidine(2)
CD40	soluble Cluster of Differerntiation 40
CD40L	Cluster of Differerntiation 40 ligand
cDNA	complementary DNA
CHX	cyclohexamide
CI	confidence interval
CSR	class switch recombination
C_T	threshold cycle
ctrl	control
DC	dendritic cell
DEG	differentially expressed genes
DLBCL	Diffuse Large B cell Lymphoma
DMSO	dimethylsulfoxide
DNA	desoxyribonucleic acid
dNTP	deoxyribose nucleoside triphosphate
DTT	dithiothreitol
E.coli	*Escherichia coli*
EBV	Epstein-Barr Virus
ECL	enhanced chemiluminescence
ELK1	E26-like kinase 1
ERK	extracellular signal regulated kinase
EZH2	enhancer of zeste homolog 2
FC	fold change
FCS	fetal calf serum
FDC	folicular dendritic cell
FDR	false discovery rate
FL	Follicular Lymphoma
GAPDH	glyceraldehyde 3-phosphate dehydrogenase

GC	germinal center
GCB	germinal center B cell
GFP	Green Fluorescent Protein
GO	gene ontology
h	hour
HRP	horseradish peroxidase
ICAM1	intercellular adhesion molecule 1
ICGC	International Cancer Genome Consortium
ID3	Inhibitor of DNA binding 3
Ig	immunoglobulin
IL	interleukin
JAK	Janus kinase
JNK	c-Jun N-terminal kinase
kDa	kilo Dalton
KRAB	Krueppel associated box
LIMK1	LIM domain kinase 1
lncRNA	long non coding RNA
LPS	lipopolysacharide
MAPK	mitogen-activated protein kinase
mBL	molecular Burkitt Lymphoma
MEK	Mitogen-activated protein kinase kinase
min	minute
MIR23A	miR-23a~27a~24-2 cluster gene
miRNA/miR	microRNA
MMML	Molecular Mechanisms in Malignant Lymphoma
mRNA	messenger RNA
NFAT	nuclear factor of activated T cells
NFκB	nuclear factor kappa-light-chain-enhancer of activated B cells
NHL	non-Hodgkin Lymphoma
ns	non-silencing
nt	nucleotide
P/S	Penicillin/Streptomycin
PAGE	Polyacrylamide-Gelelectrophoresis
PBS	PBS
PCR	polymerase chain reaction
PI	Propidium Iodide
Pol II	RNA polymerase II
pre-miR	precursor miRNA
pri-miR	primary miRNA
PUMA	P53 upregulated modulator of apoptosis
qRT-PCR	quantitative Reverse Transcriptase PCR
RIN	RNA Integrity Number
RIP	RNA immunoprecipitation

RISC	RNA induced silencing complex
RNA	ribonucleic acid
RT	room temperature or reverse transcriptase
s	second
sCD40L	soluble Cluster of Differerntiation 40 ligand
SDS	sodium dodecyl sulfate
Ser	serine
SHM	somatic hypermutation
siRNA	single interfering RNA
SLAMF7	signaling lymphocyte activation molecule family member 7
SNORD48	Small nucleolar RNA 48
SRF	serum response factor
STAT	signal transducer and activator of transcription
TCF3	transcription factor 3
Thr	threonine
TMC	tonsillar mononuclear cells
VDJ	Variable Diverse Joining
VRK3	vaccina related kinase 3
WHO	World Health Organization
x g	multiple of acceleration of gravity
ZNF	zinc finger

Abstract

During B cell maturation within the germinal centers of lymph nodes, genetical alterations, such as chromosomal translocations and mutations are introduced into the genome in order to increase the B cell receptor (BCR) specificity. Errors occurring during these processes, namely class switch recombination and somatic hypermutation, can affect the expression of tumor suppressors and proto-oncogenes, resulting in lymphomagenesis. Two major subtypes of germinal center derived aggressive Non-Hodgkin B cell lymphoma are Burkitt lymphoma (BL) and Diffuse Large B Cell Lymphoma (DLBCL). The MIR23A cluster, coding for miR-23a, miR-27a and miR-24-2 is induced during normal germinal center reaction. While the MIR23A cluster expression is low in germinal center B cells, it is upregulated in mature memory B cells. However, BL and DLBCL tumors have aberrantly high MIR23A expression levels compared to healthy controls, indicating that the cluster is de-regulated during lymphomagenesis. This study identified the BCR signaling, which plays a key role during germinal center reaction, as a general mechanism responsible for the induction of the MIR23A cluster in BL and DLBCL cell lines. MEK/ERK signaling was shown to be the major signaling cascade mediating this effect. Downstream transcription factors ELK1 and c-MYC are not involved in activation of the MIR23A cluster in DLBCL. Since the MIR23A cluster could not be induced by BCR signaling in normal germinal center B cells, this study hypothesizes that aberrant BCR signaling in BL and DLBCL is responsible for the increased MIR23A cluster levels. The MIR23A cluster is involved in many different solid cancers as well as leukemia and lymphoma. Its cellular function is discussed controversially among the different cancer entities, indicating that it is cell type and context specific. One study reported that DLBCL patients with high miR-23a levels show worse overall survival rates, suggesting an onco-miR function for the MIR23A cluster in DLBCL. However, the processes that are regulated by the MIR23A cluster in DLBCL remain unknown. In order to elucidate the biological function of the MIR23A cluster in the B cell lymphoma context, the targetomes of miR-23a and miR-27a were identified via Ago2-RNA immunoprecipitation in a DLBCL cell line stably overexpressing miR-23a, miR-27a or a non silencing control. By this approach 46 novel direct miR-23a and miR-27a targets in DLBCL were identified. LIMK1 and PUMA were validated as miR-27a targets on protein level. Furthermore, functional analyses demonstrated that miR-23a and miR-27a attenuate the ability of DLBCL cells to undergo apoptosis in response to DNA damage. This might be one plausible explanation why DLBCL patients with high miR-23a expression levels have a worse overall survival rate than patients with low levels, supporting the onco-miR hypothesis for the MIR23A cluster.

1. Introduction

A eukaryotic cell encounters many intra- and extracellular signals. These signals are integrated by sophisticated signaling cascades, resulting in activation or inhibition of genes directing the cell to grow, divide, rest or even to die. Normally, these processes are tightly controlled. If errors occur, the cell either undergoes apoptosis or it is eliminated by the immune system. However, in some cases mutations can lead to de-regulation of tumor suppressors or proto-oncogenes, leading to uncontrolled growth and proliferation (Hanahan and Weinberg, 2011). The resulting tumor mass is termed neoplasm. If the cells have the ability to invade the surrounding tissue or to spread into other tissues it is considered as malignant, otherwise it is said to be benign. A malignant neoplasm is also referred to as cancer. Cancer can affect any part of the body and is classified by its origin. Carcinomas arise from epithelial cells, sarcomas from connective tissue or muscle cells and leukemia and lymphoma from the hematopoietic system. While leukemias develop from the bone marrow and spread into the blood, lymphomas develop from the lymphatic system forming solid tumors in the lymph nodes, bone marrow, spleen and other non-lymphatic organs. According to the classification of the WHO to date 101 subtypes of leukemias and lymphomas exist (Swerdlow *et al.*, 2016). The classification is based on morphology, immunology, genetic aberrations and clinical aspects. The two main subgroups of lymphoma are Hodgkin lymphoma (HL) and Non-Hodgkin lymphoma (NHL). HL show big multi-nucleated Reed-Sternberg cells (Sternberg, 1897; Reed, 1902), which are lacking in NHL. NHL can further be divided in B cell or T cell derived and aggressive or indolent NHL (Armitage *et al.*, 2009). This study focuses on the aggressive B cell NHL (B-NHL) subtype, which constitutes the biggest group of NHL with about 90% of NHL cases (Armitage *et al.*, 2009). In developed countries aggressive NHL is one of the tenth most frequent cancer diagnosed (Torre *et al.*, 2015). Due to improved living circumstances and prolonged life expectancies, cancer is one of the leading cause of death worldwide (Ferlay *et al.*, 2013).

Although much progress has been made in the last decades of cancer research leading to a better understanding of the underlying mechanisms of malignant transformation, more effort must be put into the molecular characterization of each individual cancer entity in order to develop specific and effective treatments.

1.1. B cell development, maturation and malignant transformation

B lymphocytes (B cells) are part of the adaptive immune system and are essential for the humoral immune response against foreign antigens. They generate high affinity antibodies that are secreted to effectively inactivate the specific antigen. Antibodies are composed of four immunoglobulins (Ig): two identical heavy chain immunoglobulins (IgH) and two identical light chain immunoglobulins (IgL) linked by disulfide bonds. Each of these polypeptides consists of a carboxyterminal constant region (C) and an aminoterminal variable (V) region. Each mature B cell expresses a membrane bound antibody on its surface that is associated with cofactors (Igα and Igβ). Together they form the B cell receptor (BCR). This receptor gains its high specificity during B cell maturation where complex genomic modifications to the immunoglobulin genes are introduced.

Early development of B cells is initiated in the fetal liver and subsequently relocated into the bone marrow of the mammalian embryo (reviewed in (Melchers, 2015)). A multipotent hematopoietic stem cell in the bone marrow gives rise to a lymphoid progenitor, which develops into a precursor B cell that subsequently undergoes complex rearrangements of the immunoglobulin heavy and light chain variable region genes (reviewed in (Seifert *et al.*, 2013)). This process is called V(D)J recombination, because the variable region of the heavy and light chain immunoglobulin gene is encoded on different gene segments: variable (V), diversity (D) and joining (J) segments. From each of these segments one is randomly selected and step wise joined together with the other segments. This process leads to a high variability in newly formed immunoglobulins. Cells that express a functional, but non-autoreactive B-cell receptor survive the selection process and are released as naive B cells into the blood.

Upon encountering of a T cell dependent antigen these cells are activated, migrate into secondary lymphatic organs like the lymph nodes, tonsils, spleen, mucosa associated lymphoid tissue (MALT) or Peyer's patches, where they maturate their B-cell receptor, undergo clonal expansion and further differentiate into antibody secreting plasma cells or long lived memory cells (reviewed in (De Silva and Klein, 2015)).

One site of B cell maturation are the lymph nodes. They are characterized by follicles that are build up from naive B cells which are separated from each other by an interfollicular region that is surrounded by a T cell zone. Within the follicular centers a network of follicular dendritic cells (FDC) can be found. When a naive B cell encounters an antigen, it migrates to the border of T cell and B cell zone and forms long-lived interactions with antigen-specific T cells leading to full activation of the B cell. A subset of these B cells differentiate into short-lived plasmablasts, which secrete low affinity antibodies. Another subset of these cells enter the germinal center (GC) pathway, where the BCR is further refined. Activated T and B cells migrate to the follicular center and interact with the dendritic cells. The T cells become T follic-

ular helper cells (T_{FH}) thus they upregulate B cell lymphoma 6 (BCL6), the master regulator of T_{FH} and GC B cell development (Baumjohann *et al.*, 2011). The B cells start to divide rapidly and to populate the follicle displacing the naive B cells, which thereby form a so called "mantle zone" around the newly formed germinal center. Within the germinal center two different zones develop: a densely packed "dark zone" containing proliferating B cells (centroblasts) and reticular cells and a "light zone" containing non-proliferating B cells (centrocytes), T_{FH} cells, FDCs and macrophages. The centroblasts in the dark zone undergo somatic hypermutation (SHM), a process that further diversifies the rearranged IgV genes. SHM results in different B cell clones with a broad range of affinities against the antigen. The clones expressing a high-affinity antigen receptor are positively selected within the light zone. Effective antigen binding leads to enriched antigen capture followed by strong BCR signaling (see section 1.2.1) and longer interactions with FDCs and T_{FH} cells (fig. 1.1). The bystander cells (FDCs and T_{FH} cells) provide CD40L and secrete interleukine-4 and -21 (IL-4 and Il-21) (Liu *et al.*, 2015; Shulman *et al.*, 2014). In sum, these stimulations provide a survival signal, promoting positive selection. Cells expressing an auto-reactive or defective BCR undergo apoptosis. Induction of MYC expression during the selection process induces recircularization of the positive selected cells between dark and light zone resulting in further refinement of the antigen specificity (Dominguez-Sola *et al.*, 2012). CD40 stimulation leads to nuclear factor kappa-light-chain-enhancer of activated B cells (NF$\varkappa$B) mediated upregulation of Interferon Regulatory Factor 4 (IRF4) expression (Saito *et al.*, 2007), which represses BCL6 thereby terminating the dark zone program. Within the light zone the cells undergo class switch recombination (CSR) or finally differentiate into plasmablasts or memory cells and leave the germinal center (reviewed in (De Silva and Klein, 2015)). CSR is a process were the isotype of the immunoglobulin is switched (from IgM or IgD) by a new combination of the variable hypermutated VDJ gene elements with genes encoding for a different heavy chain (IgA, IgE or IgG), rendering their effector function.

Notably, most aggressive B cell lymphoma resemble germinal center B cells expressing markers that reflect their origin. The cells seem to be frozen at a particular differentiation step during germinal center reaction (reviewed in (Küppers, 2005)). Notably, some GC derived lymphoma still undergo SHM. Indeed, aberrant SHM and CSR can promote lymphomagensis (Lenz *et al.*, 2007; Pasqualucci *et al.*, 2008). If errors occur during CSR, free DNA ends are produced that can cause chromosomal translocations, a genetic hallmark of lymphoma. The translocations of proto-oncogene *MYC* and *BCL6* to immunoglobulin promoters are characteristic for aggressive B cell lymphoma. Moreover, constitutive expression of BCL6 maintains a pro-proliferative and DNA-damage tolerant phenotype leading to additional mutations which might further promote lymphomagensis (Cattoretti *et al.*, 2005). Enhanced expression of *MYC* results from the translocation into the immunoglobulin heavy chain or light chain loci and is characteristic for Burkitt lymphoma (BL) cells (section 1.3). Aberrant SHM acting in the 5′ regulatory or coding
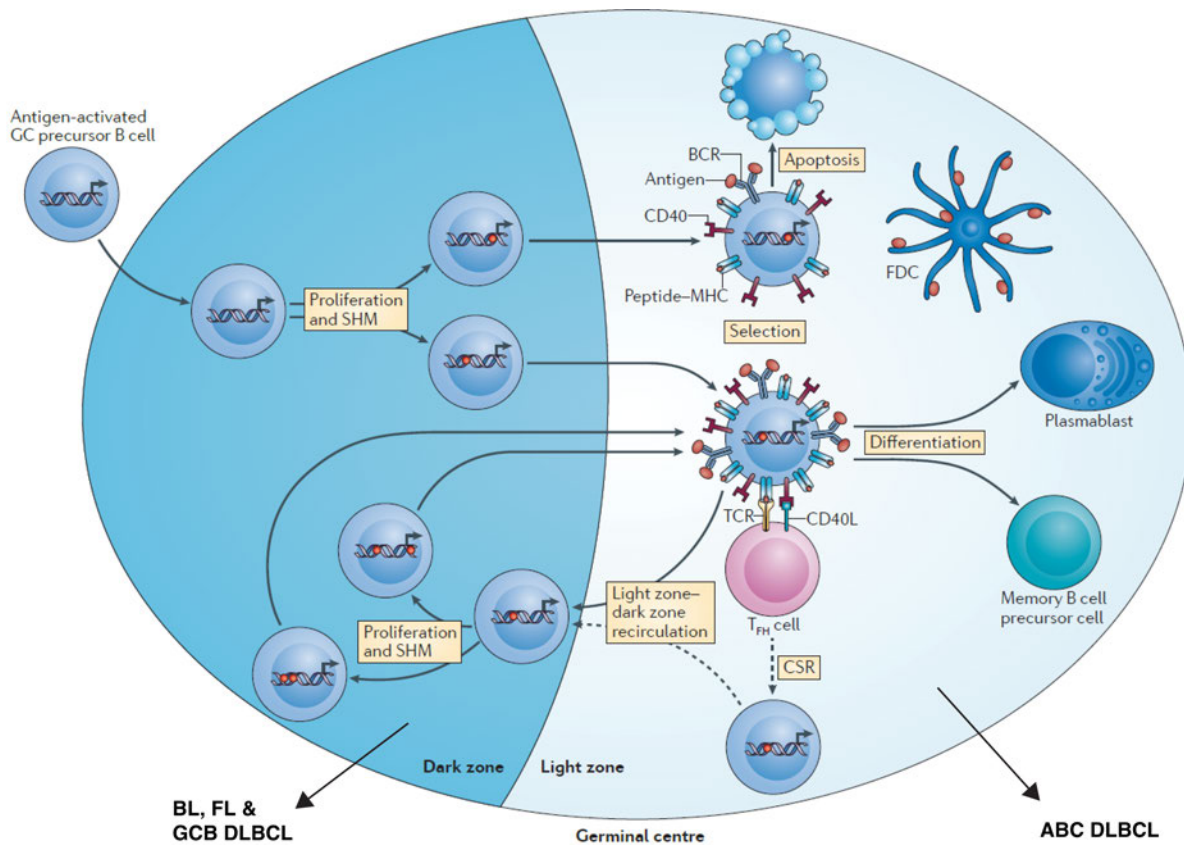
Figure 1.1.: Germinal center reaction

During germinal center reaction activated B cells generate due to genomic modification of the immunoglobulin genes high affinity antibodies and differentiate into antibody secreting plasmablasts or memory cells. Upon antigen binding, activated B cells differentiate into centroblasts that undergo clonal expansion and somatic hypermutation (SHM). SHM introduces point mutations into the V(D)J region of already rearranged immunoglobulin variable region (IgV) genes (red dots). These cells move into the light zone, were T follicular helper cells (T_{FH} cells) and follicular dendritic cells (FDCs) help to elect these cells, that generated an B cell receptor (BCR) with improved binding specificity. Higher affinity leads to increased antigen capture and promotes T_{FH} cell binding and CD40L signaling resulting in a survival signal. Cells with low binding capacity to the antigen undergo apoptosis. A subset of positive selected B cells recirculates into the dark zone to further refine the BCR, whereas another subgroup undergoes class switch recombination (CSR). CD40L = CD40 ligand, TCR = T cell receptor, MHC = major histocompatibility complex, BL = Burkitt Lymphoma, FL = Follicular Lymphoma, DLBCL = Diffuse Large B cell Lymphoma. (modified from de Silva and Klein, 2015)

regions of proto-oncogenes or tumor suppressors may cause deregulation of those genes. In fact, aberrant SHM mutates the negative regulatory region of *BCL6* in Diffuse large B cell lymphoma (DLBCL, see section 1.3) preventing BCL6 downregulation and termination of GC reaction (reviewed in (Klein and Dalla-Favera, 2008)).

In general, lymphomagensis is considered to be a multistep process. The gene arrangements performed during GC reaction are mutagenic processes that strongly increase the risk of malignant transformation, but tumor progression is also dependent on survival signals. These signals are provided by the microenvironment and dependent on the expression of a functional receptor (e.g. BCR and CD40 receptor (see sections 1.2.1 and 1.2.2)).

1.2. Signaling pathways involved in B cell activation

During B cell maturation autocrine signaling of the BCR is crucial for B cell survival, proliferation and differentiation. Only cells that express a functional BCR activate downstream signaling cascades including PI3K (phosphoinositol 3-kinase), MAPK (mitogen-activated protein kinase) and NFϰB (nuclear factor kappa-light-chain-enhancer of activated B cells) signaling, which in sum provide a survival signal (see section 1.2.1). This signal is enforced by co-stimulatory factors provided by the microenvironment within the GCs. FDCs and T_{FH} cells present important survival signals to the maturating B cell (reviewed in (De Silva and Klein, 2015)). In detail, the antigen activated B cell presents peptides of this antigen by the major histocompatibility complex II (MHCII) on its cell surface. This is recognized by the T_{FH} cells, which express membrane bound CD40L. This ligand activates the CD40 receptor of the B cell, resulting in CD40 mediated NFϰB signaling (Basso *et al.*, 2004). Besides, FDCs express soluble sonic hedgehog (Shh) providing an additional survival signal during GC reaction (Sacedon *et al.*, 2005). Moreover, it was shown that IL-21 and BAFF promote B cell survival by the activation of JAK/STAT and NFϰB signaling (Konforte *et al.*, 2009; Khan, 2009).

In summary, the B cell activation is dependent on complex mechanisms including cell-cell interactions, paracrine and autocrine signaling, which activates different signaling pathways that subsequently activate gene expression resulting in the induction of proliferation and differentiation of the GC B cell.

1.2.1. B cell receptor signaling

Each B cell expresses a unique membrane bound antibody, namely the B cell receptor (BCR). The BCR is a multimeric complex, consisting of two identical heavy chain immunoglobulins (IgH) and two identical light chain immunoglobulins (IgL) linked by disulfide bonds. Each of

these polypeptides consist of a carboxyterminal constant region (C) and an aminoterminal variable (V) region. The V region mediates the antigen binding whereas the C region anchors the antibody within the membrane (Janeway *et al.*, 2001). The antibody itself lacks signaling capacity, thus the transmembrane proteins CD79A (Igα) and CD79B (Igβ) are intracellular, but non-covalent associated to the C terminus of the immunoglobulin heavy chain (fig. 1.2). Both CD79 chains contain an immunoreceptor tyrosine based activation motif (ITAM) in their intra-cellular part, which are able to transduce signals intracellularly (reviewed in (Bojarczuk *et al.*, 2015)). Antigen binding induces BCR cross-linking followed by Sarcoma-family (SRC) kinase LYN (Lck/Yes novel tyrosine kinase) recruitment and phosphorylation of the ITAM. Phospho-rylated ITAM recruits spleen tyrosine kinase (SYK), which is subsequently phosphorylated by LYN. Phosphorylated SYK further propagates the signal via B cell linker protein (BLNK) to Burton's tyrosine kinase (BTK) and phospholipase Cγ2 (PLCγ2). PLCγ2 hydrolyses PIP2 (phosphatidyl inositol-4,5-bisphosphate) to IP3 (inositol-1,4,5-trisphosphate) and DAG (diacyl-glycerol). Increasing IP3 levels lead to the release of Ca^{2+} from the endoplasmatic reticulum and consequently to the activation of calcineurin and the transcription factor NFAT (nuclear factor of activated T cells). DAG activates protein kinase C (PKC), which in turn phosphory-lates the multiprotein complex CBM (consisting of CARD11, BCL-10 and MALT1), that acti-vates IϰBα kinase complex (IKK) thereby initiating NFϰB signaling. Another function of PLCγ2 is to activate mitogen-activated protein kinase (MAPK) pathway, including c-junNH2-terminal kinase (JNK), extracellular signal-regulated kinase 1/2 (ERK1/2) and p38 (Hashimoto *et al.*, 1998). Besides, LYN activated phosphorylation of co-receptor CD19 leads to activation of PI3K (phosphoinositol 3-kinase) which in turn activates AKT signaling.

The BCR signaling activates many different signaling pathways, which also show "cross-talk" with each other and also other signaling cascades (e.g. chemokine receptors) further increas-ing complexity (Seda and Mraz, 2015). These signaling cascades activate many different transcription factors, which regulate the expression of a set of GC-specific genes.

Beside the antigen induced activation of BCR signaling, a second form called "tonic" BCR sig-naling exists. The tonic signaling is found in mature B cells and ensures antigen-independent B cell survival.
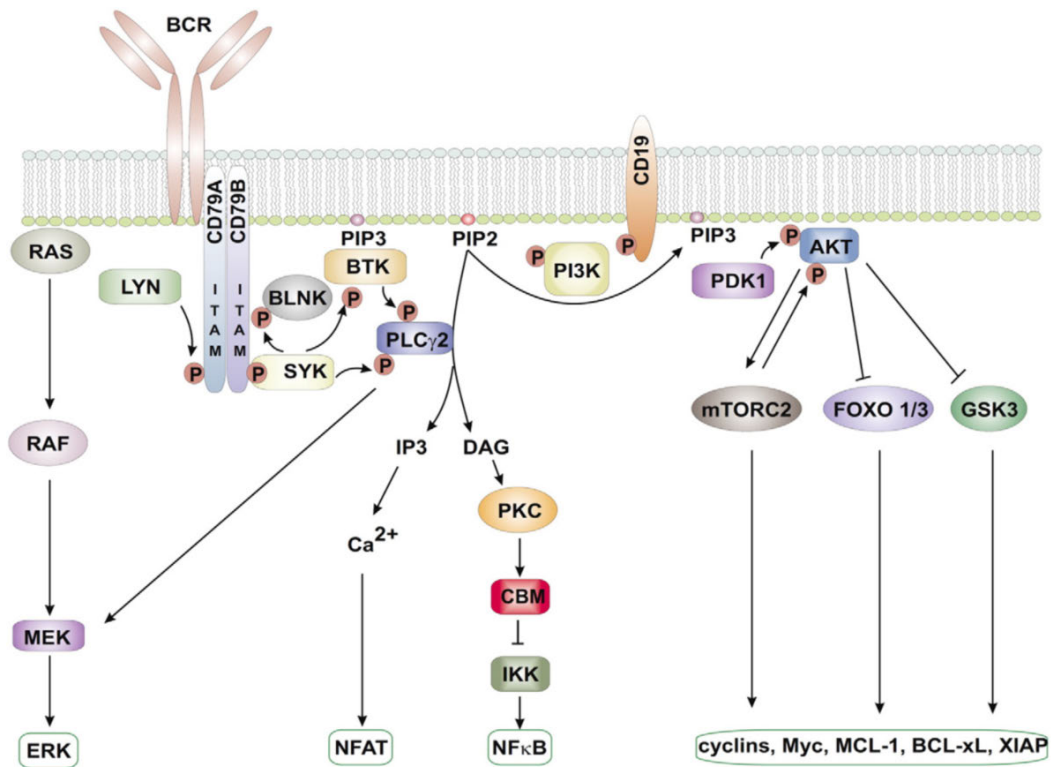
Figure 1.2.: Signaling cascades activated upon BCR activation
This figure depicts a simplified scheme of BCR downstream signaling cascades. The BCR consists of a pairs of immunoglobulin heavy (IgH) and light (IgL) chains, whose variable region allows the BCR to bind an antigen. It is intracellularly coupled to the heterodimer CD79A and CD79B, which mediates signal transduction. The immunoreceptor tyrosine based activation motif (ITAM) is phosphorylated upon antigen binding by the SRC-familiy kinase LYN, which initiates the recruitment and activation of several signaling proteins that spread the signal on different downstream signaling cascades as depicted in the scheme (for detailed description refer to the main text). Activation of these signaling cascades leads to activation of transcription factors (ERK, NFAT, NF$\varkappa$B, MYC etc.) that activate genes responsible for survival of the cell. Ras = rat sarcoma, RAF = rapidly accelerated fibrosarcoma, MEK = MAPK/ERK Kinase, ERK = extracellular signal regulated kinase, MYC = v-myc avian myelocytomatosis viral oncogene homolog, BTK = Burton's tyrosine kinase, PLCγ2 = phospholipase Cγ2, PI3K = phosphoinositol 3-kinase, PIP2 = phosphatidyl inositol-4,5-bisphosphate, IP3 = inositol-1,4,5-trisphosphate, DAG = diacylglycerol, PKC = protein kinase C, NFAT = nuclear factor of activated T-cells, PKC = protein kinase C, CBM = CARD11-BCL10-MALT1 signalosome, IKK = I$\varkappa$B kinase komplex, NF$\varkappa$B = nuclear factor kappa-light-chain-enhancer of activated B cells, AKT = protein kinase B, mTORC2 = mammalian target of Rapamycin complex 2, GSK3 = Glycogen synthase kinase 3, FOXO = forkhead box. (figure taken from Bojarczuk *et al*., 2015)

It is not surprising that lymphoma take advantage of the BCR signaling, thus it provides survival signals. In Burkitt lymphoma (section 1.3), which is characterized by *MYC* translocations, it was shown that tonic BCR signaling *via* PI3K allows the cell to tolerate the otherwise lethal ectopic *MYC* expression in absence of growth factors (Evan *et al.*, 1992). 70% of BL harbor *transcription factor 3 (TCF3)* mutations, that prevent the inhibition of TCF3 by ID3. Moreover frequent *ID3* mutations have been reported in BL (Richter *et al.*, 2012; Schmitz *et al.*, 2013). Hyperactive TCF3 leads to decreased SHP1 activity, a negative regulator of PI3K dependent BCR signaling, which results in enhanced BCR signaling.

Another lymphoma subtype, namely activated B cell like (ABC) DLBCL (see section 1.3) shows chronic active BCR signaling. Many ABC DLBCL patients carry Caspase recruitment domain-containing protein 11 (CARD11) mutations affecting the coiled-coil domain, causing it to form spontaneous aggregates that recruit all downstream signaling components of the NF$\varkappa$B pathway (Lenz *et al.*, 2008). Moreover, the ITAM of CD79 were reported to be mutated leading to an exchange of the tyrosine residue to another amino acid (Davis *et al.*, 2010). These mutations prevent endocytosis of the BCR and blunt the activity of LYN, a SRC-family tyrosine kinase that delivers negative feedback signals that attenuate BCR activity. Another mechanism for chronic active BCR signaling is the reactivity against self antigen (Young *et al.*, 2015). The presence of BCR clusters on the cell surface of ABC DLBCL, which resemble the clusters that are formed after antigen encountering, support this observation (Rui *et al.*, 2011).

The high complexity of BCR signaling, which is misused by lymphoma to survive and proliferate, provides many possibilities to interfere with, using targeted therapy. Indeed, many inhibitors were developed to target BCR downstream kinases, such as BTK, SYK, SRC family and PI3K, are already used in the clinics or in clinical trials (Young and Staudt, 2013; Gayko *et al.*, 2015).

1.2.2. CD40 signaling

Cluster of differentiation 40 (CD40) is a co-stimulatory receptor expressed on the surface of many cells, including B cells. It belongs to the tumor necrosis factor receptor (TNFR) superfamily and is activated by the soluble or membrane bound ligand CD40L. This ligand is regarded as the classical co-stimulatory signal presented by T helper cells during GC formation (section 1.1) and promotes GC formation, immunoglobulin isotype switching, somatic hypermutation and differentiation of GC B cells (reviewed in (Bojarczuk *et al.*, 2015)). Ligand binding to CD40 leads to the activation of downstream NF$\varkappa$B and MAPK signaling (reviewed in (Elgueta, 2009)). In detail, binding of CD40L to CD40 promotes CD40 clustering and recruits TNFR-associated factors (TRAFs) to the cytoplasmic domain of CD40. *In vivo* studies in mice showed that TRAF 1, 2, 3 and 5 are recruited to CD40 upon CD40L binding in B cells. TRAF1 activates canonical NF$\varkappa$B signaling, while TRAF 5 activates both canonical and non-canonical NF$\varkappa$B signaling (Xie *et al.*, 2006; Hauer *et al.*, 2005; Nakano *et al.*, 1999) (section 1.2.3). TRAF2 has multiple functions, hence it was shown to activate canonical NF$\varkappa$B signaling, while repressing non-canonical NF$\varkappa$B signaling and furthermore activating MAPK (including JNK and p38) signaling. In contrast, TRAF3 represents only a negative NF$\varkappa$B signaling regulator. In conclusion, CD40 signaling activates primarily TRAF mediated NF$\varkappa$B signaling with an autoregulatory loop, resulting in the expression of anti-apoptotic factors (BCL-XL, A20, survivin, Bfl-1, and c-FLIP). Studies with B-NHL cells showed that cells expressing low levels of CD40L are protected from

apoptosis (Pham *et al.*, 2002), while transient *in vitro* and *in vivo* activation of CD40L in BL, multiple myeloma and high-grade B cell lymphoma inhibited cell proliferation (Funakoshi *et al.*, 1994), indicating that quantitative levels might play a role in cell fate decision.

1.2.3. NFκB signaling

NFκB is a pleiotropic transcription factor involved in many biological processes such as inflammation, immunity, differentiation, proliferation, apoptosis and tumorigenesis (reviewed by (Vallabhapurapu and Karin, 2009)). Five different NFκB family members exist: NF-κB1 (p50 and its precursor p105), NF-κB2 (p52 and its precursor p100), p65 (RelA), c-Rel and RelB. These NFκB family members form homo- or heterodimers that bind to DNA to regulate specific target genes. In the inactive state their nuclear translocation sequence is shielded by the inhibitors IκBα, IκBβ and IκBε. The release from the IκBs is controlled by IκB kinases (IKKα/IKK1, IKKβ/IKK2 and IKKγ/NEMO). After activation by a given stimulus the IKKs phosphorylate IκB, leading to proteasomal degradation of IκB and the nuclear translocation of the NFκB dimer.

Many different stimuli can activate NFκB signaling (cytokines, chemokines and adhesion molecules) (Lawrence, 2009). Two NFκB signaling pathways are described: the canonical and the non-canonical pathway. They differ in the mode of activation and utilization of NFκB members. In the canonical pathway (e.g. activated by tumor necrosis factor (TNF) alpha) the NFκB dimers p65/p50 and c-Rel/p50 are activated by the proteasomal degradation of IκBs which is induced by phosphorylation from the trimeric IKK complex. The non-canonical pathway is activated by TNF family members, including CD40L (Berberich *et al.*, 1994). Subsequently NFκB inducing kinase (NIK) phosphorylates IKK which leads to partial proteasomal degradation of p100 precursor into p52 and subsequent activation of RelB/p52 dimers.

Deregulated NFκB signaling was shown to play an important role in B-NHL, thus hyperactivation of canonical NFκB signaling is characteristic for ABC DLBCL ((Davis *et al.*, 2001), see section 1.3).

1.2.4. MAPK/ERK signaling

The mitogen-activated protein kinase (MAPK) cascade is a central pathway that transmits signals from extracellular stimuli (growth factors, hormones, neurotransmitters and others) to regulate a broad variety of cellular processes, such as proliferation, differentiation, apoptosis and stress response (Plotnikov *et al.*, 2011). Each MAPK cascade consists of three main kinases: MAP3K, MAP2K and MAPK, which subsequently phosphorylate each other in response to a stimulus (reviewed in (Plotnikov *et al.*, 2011)). Four different MAPK cascades were identified:

extracellular signal-regulated kinase 1 and 2 (ERK1/2), c-Jun N-terminal kinase (JNK), p38 and ERK5. Each of this MAPKs is activated by different MAP2Ks (Raman *et al.*, 2007), leading to distinct responses to a specific stimulus. In the context of B cell activation ERK1/2 cascade plays a central role. Upon activation of the BCR (section 1.2.1), protein kinase C (PKC) activates rapidly accelerated fibrosarcoma 1 (RAF1) signaling dependent phosphorylation of ERK1/2 (Hashimoto *et al.*, 1998). Activated RAF1 (the MAPK3) phosphorylates MEK1/2 (the MAP2K), which in turn activates ERK1/2 (Ueda *et al.*, 1996). ERK1/2 are Ser/Thr kinases that phosphorylate a large number of downstream substrates of different cellular compartments (Plotnikov *et al.*, 2011). Among these substrates are many transcription factors, such as ELK1, c-MYC, c-Fos and Ets domain factors, but also dual-specificity MAPK phosphatases (MKPs or DUSPs) (Yoon and Seger, 2006). DUSPs are key negative regulators of MAPK signaling, which inactivate the MAPKs but can furthermore mediate crosstalk between different MAPK cascades (Kidger and Keyse, 2016). One of the first described ERK1/2 substrates was ETS domain-containing protein ELK1, a transcription factor responsible for the activation of immediate early genes (Gille *et al.*, 1995). In detail, it was shown in fibroblasts that ELK1 forms a ternary complex by p62^{TCF} with serum response factor (SRF) thereby binding to serum response element (SRE) of the *c-Fos* promoter, which facilitates *c-Fos* transcription. Induction of c-Fos is important for cell proliferation and differentiation (Hisanaga *et al.*, 1990; Shaulian and Karin, 2001). Interestingly, ERK1/2 phosphorylation of ELK1 induces binding of c-Fos to c-Jun, which together form the transcriptionally active AP-1 complex (Whitmarsh and Davis, 1996). AP-1 activity is required for cyclin D1 induction and cell cycle progression (Shaulian and Karin, 2001).

The MAPK/ERK pathway is a key signaling system for the decision of cell fate. It is frequently overactivated in human cancer due to genetic aberrations and is therefore considered to be a driver for cancer development (reviewed in (Fey *et al.*, 2016)). For aggressive lymphoma it was reported that the ERK substrate ELK1 binds to LMO2, which is overexpressed in GC derived B cell lymphoma (Cubedo *et al.*, 2012).

1.3. B cell non Hodgkin Lymphoma (B-NHL)

According to the WHO in 2012 the incidence for NHL was estimated with 93.4 cases per 100,000 people and a mortality of 37.9 cases per 100,000 people in male and female (Ferlay *et al.*, 2013). More than 85% of newly diagnosed NHL cases are from B-cell origin and affect men more frequently than women (Armitage *et al.*, 2009). Aggressive B-NHL includes diffuse large B-cell lymphoma (DLBCL), mantle-cell lymphoma (MCL), Burkitt lymphoma (BL) and follicular lymphoma (FL) (Maxwell and Mousavi-Fard, 2013). The most common subtype with approximately 40% of all NHL cases is DLBCL (Küppers, 2005).

DLBCL mostly affects patients with an average age of mid-60. Symptoms can be swollen lymph nodes, sweating at night, fever and dramatic weight loss (CancerresearchUK, 2016). DLBCL is clinically, morphologically and genetically a heterogeneous disease. Morphologically it is characterized by nuclei that have double or more than double times the size of a macrophage nucleus and a diffuse growth pattern (Paepe and Wolf-Peeters, 2007; Armitage *et al.*, 2009). According to their origin, DLBCL can be further be subdivided by gene expression profiling on molecular level in germinal center B-like (GCB) and activated B-like (ABC) DLBCL (Alizadeh *et al.*, 2000). Each subtype is characterized by specific chromosomal translocations and gene expression patterns.

A common feature of GCB DLBCL is the overexpression of *BCL6*, the master regulator and transcriptional repressor during germinal center formation. *BCL6* overexpression is caused by translocations of *BCL6* to heterologous promoters or point mutations in negative regulatory elements of *BCL6* promoter, which leads to the survival of DLBCL cells (Iqbal *et al.*, 2007; Ci *et al.*, 2008). These cells constantly undergo somatic hypermutations thereby accumulating further mutations (Shaffer III *et al.*, 2011). 20-30% of DLBCL harbor t(14;18) translocation leading to the juxtaposion of *BCL2* to immunoglobulin heavy chain gene (*IGH*) enhancer resulting in BCL2 protein overexpression and inhibition of apoptosis (Lu *et al.*, 2015). In 5-10% of the cases translocations that juxtapose *MYC* with the *IGH*, $\varkappa$, and λ genes (t(8;14), t(2;8) and t(8;22)) lead to an upregulation of *MYC* (Li *et al.*, 2012). *MYC* and *BCL2* or *BCL6* double hit lymphoma show highly aggressive behavior leading to extremely poor outcome (Caimi *et al.*, 2016). Furthermore, the amplification of *MIHG1* region, containing miR-17-92 cluster was observed in approximately 12% of the cases (De Jong and Balagué Ponz, 2011).

The second molecular subtype, ABC DLBCL, is characterized by a constitutive active NF$\varkappa$B signaling (Davis *et al.*, 2001). Several pathway components leading to NF$\varkappa$B activation have been shown to be mutated. Deletions and mutations in *A20*, a negative regulator, were found in 20% of ABC DLBCL cases (Compagno *et al.*, 2010). In 10% of ABC DLBCL cases missense mutations in the coiled-coiled domain of CARD11, which mediates oligomerization and is crucial for NF$\varkappa$B activation, occur (Lenz *et al.*, 2008). Moreover, somatic mutations in the ITAM tyrosine kinase motifs of BCR signaling proteins CD79A and CD79B were demonstrated to produce a sustained pseudo-BCR signal (Davis *et al.*, 2010), which leads to chronic BCR signaling that is important for ABC DLBCL cell survival (Davis *et al.*, 2001). The large number of NF$\varkappa$B targets contribute to poor prognosis of ABC DLBCL patients by the prevention of apoptosis, which reduces the sensitivity of the cells to chemotherapy (Baldwin, 2001). In general, the prognosis for GCB DLBCL is better than for ABC DLBCL patients (Paepe and Wolf-Peeters, 2007).

Usually, DLBCL arises *de novo,* but it can also develop from an indolent lymphoma, such as follicular lymphoma (Martinez-Climent *et al.*, 2003), chronic lymphocytic leukemia (Rossi

and Gaidano, 2009), marginal zone lymphoma or nodular lymphocytic predominant Hodgkin lymphoma (Fanale and Younes, 2008).

Nowadays the standard therapy for aggressive B-NHL, independent of the molecular subtype, is R-CHOP (cyclophosphamide, doxorubicin, vincristine and prednisone and the monoclonal antibody rituximab), a combination of cytostatic and immunosuppressive drugs with a chimeric human/murine immunoglobulin G1 monoclonal antibody that specifically binds to CD20, a surface antigen expressed on each B cell (Feugier, 2005). Crosslinking of CD20 induces complement-mediated cell lysis, antibody dependent cellular cytotoxicity and antibody dependent apoptosis (Shan *et al.*, 2000). Although the response rates, event free survival and overall survival significantly improved compared to CHOP therapy alone, there are still patients that do not respond to treatment or suffer from relapse (30-40%) or refractory disease (10%) (Coiffier *et al.*, 2002; Kahl, 2008; Cultrera and Dalia, 2012; Raut and Chakrabarti, 2014).

Another type of aggressive B-NHL is Burkitt lymphoma (BL). It was first described by Denis Burkitt in 1958 as the most prevalent African childhood lymphoma which localizes to the mandible and other extranodal sites (Burkitt, 1958). This type of BL is the endemic form of BL which can be found in Equatorial Africa and is in 98% of the cases associated with Epstein-Barr virus (EBV) infections (McNally and Parker, 2006). In contrast, the sporadic form of BL occurs worldwide and accounts for 2% of lymphoma in adults and up to 40% of lymphoma in children in Western countries (Ferry, 2006). A third subtype of BL is associated with immunodeficiency and affects HIV carriers (Franceschi *et al.*, 1999; Ferry, 2006) and patients that were treated with immunosuppressiva (Gong *et al.*, 2003). Characteristic for all three BL subtypes is the translocation of proto-oncogene *MYC* into one of the three immunoglobulin gene loci (Hummel *et al.*, 2006). These translocations are considered to be the central event in Burkitt lymphomagensis
(Dalla-Favera *et al.*, 1982). BL develops within the germinal centers of the lymph node, hence they display germinal center like features: expression of *CD10* and *BCL6*, but no expression of *BCL2* or *CD5* (Stein and Hummel, 2007). The prognosis of BL is favorable with cure rates > 90% in low stage BL and 70% in high stage BL, if treated intensively with multi-agent chemotherapy for at least 48-72h in order to target all tumor cells passing through mitosis (De Jong and Balagué Ponz, 2011).

According to their gene expression profile BL and GCB DLBCL are thought to derive from centroblasts of the dark zone of the germinal center, while ABC DLBCL are thought to derive from terminal determined centroblasts that differentiate into plasmablasts of the light zone (Tamaru *et al.*, 1995; Rosenwald *et al.*, 2002; Pasqualucci and Dalla-Favera, 2014; Sehn and Gascoyne, 2015).

One major challenge in the clinics is to discriminate BL from DLBCL. Two studies aimed to distinguish them on molecular level using gene expression profiles and cytogenetic analyses (Hummel *et al.*, 2006; Dave *et al.*, 2006). Hummel and colleagues developed a molecular classifier that reliably distinguishes BL from other mature aggressive B cell lymphoma. Cases with an index score (I) greater than 0.95 were classified as molecular BL (mBL) and cases with a score lower than 0.05 as non-molecular Burkitt lymphoma (non-mBL). Cases in between were designated as intermediate group, resembling mostly DLBCL cases. While this study used predominantly genes that are NFκB target genes for discrimination, Dave and colleagues applied a gene set composed of MYC target genes, several germinal center B cell and major-histocompatibility-complex (MHC) class I genes (Dave *et al.*, 2006). Although, the classification of aggressive B cell lymphomas can be achieved using different gene sets, not every subtype can be identified by this approach alone. Characterization is crucial to identify the best treatment strategy for the patients.

1.4. MicroRNAs

MicroRNAs (miRNAs or miRs) are small, single stranded and non-protein coding RNAs (ca. 21 nt) that mediate post-transcriptional gene silencing. The first miRNA lin-4 was identified in *Caenorhabditis elegans* in 1993 and reported to have antisense complementarity to lin-14 messenger RNA (mRNA) (Lee *et al.*, 1993). With the discovery of let-7 (Reinhart *et al.*, 2000) and its high conservation among many vertebrates, including humans (Pasquinelli *et al.*, 2000), the miRNA field rapidly expanded. Since then thousands of miRNAs have been identified in various species (Kozomara and Griffiths-Jones, 2011). The expression of miRNAs is tissue and cell type specific. About 60% of human protein coding genes are thought to be targeted by miRNAs, thus harboring conserved miRNA binding sites in their mRNA sequences (Friedman *et al.*, 2009). One miRNA can target multiple mRNAs thereby regulating different cellular processes. However, it was shown that one miRNA can inhibit multiple targets of gene networks thereby applying additional levels of regulation (Na and Kim, 2013). Furthermore, they can also act at different genes within a linear pathway resulting in a potentiation of the inhibitory effect. *Vice versa*, one mRNA can be targeted by several different miRNAs, suggesting that different miRNAs might act in concert to effectively downregulate their target. Furthermore, miRNAs are frequently found in feedforward or feedback loops that mediate the amplification or downregulation of the respective signal. Nowadays the mechanisms of miRNA biogenesis is mostly understood, while the exact mode of action is still being debated on (reviewed in (Filipowicz *et al.*, 2008; Ameres and Zamore, 2013)). However, it is clear that miRNAs are involved in the regulation of many important cellular processes. Therefore, deregulation may lead to severe defects and result in diseases and cancer.

1.4.1. MicroRNA biogenesis

In vertebrates, miRNAs are transcribed by RNA polymerase II (Lee *et al.*, 2004) from miRNA genes, introns of other host genes or intergenic regions (van Rooij, 2011; Cai *et al.*, 2004) (fig. 1.3). Approximately one third of miRNAs derive from transcripts that code for several miRNAs and are termed miRNA clusters (Farazi *et al.*, 2013). MiRNA biogenesis can be exerted in canonical or non-canonical manner (reviewed in (Rottiers and Näär, 2012)). In the canonical pathway miRNAs are first transcribed into the primary transcript (pri-miRNA), which has a 5' cap and a 3' poly-A tail and forms one or more stem loop structures (Lee *et al.*, 2004). These stem loop structures are recognized by the microprocessor complex, which consists of DGCR8 (DiGeorge syndrome chromosomal region 8) and Dicer. During transcription of the primary transcript, DGCR8 binds to the double stranded part of the stem loop in the nascent pri-miRNA (Morlando *et al.*, 2008). Finally, DGCR8 assists Drosha to cleave the bound stem loop approximately 11 nt distant from the ssRNA to dsRNA junction thereby producing a ~70 bp long transcript called precursor miRNA (pre-miRNA) (Han *et al.*, 2006). In non-canonical miRNA pathway, miRNAs are either directly transcribed as short hairpin RNAs (shRNAs) or derive from spliced introns, that re-fold into hairpins (mirtrons). In both pathways the newly generated pre-miRNAs are transported by Exportin 5 into the cytoplasm (Bohnsack *et al.*, 2004). There Dicer and transactivation response RNA binding protein (TRBP) RNase III complex recognize the pre-miRNA and cleave off the loop generating a ~21 bp long miRNA dublex composed of sense and anti-sense (guide and passenger strand or miRNA and miRNA*) mature miRNAs (Hutvágner *et al.*, 2001). TRBP furthermore facilitates the loading of mature miRNA duplex into the RISC complex, consisting mainly of argonaute (Ago), Dicer and TRBP (Chendrimada *et al.*, 2005). The strand with the weaker base pairing at the 5' terminus of the miRNA duplex binds to Ago, the effector protein of the RNA-induced silencing complex (RISC) (Khvorova *et al.*, 2003). In most cases, the anti-sense strand is degraded (Matranga *et al.*, 2005). Four different Ago proteins are expressed in humans: Ago1-4. Ago proteins harbor three domains: the PAZ domain recognizes the two nucleotides that overhang at the 3' end of the miRNA, the Mid domain recognizes the cap structure of mRNAs and the PIWI domain has RNase-H-like features (Hutvagner and Simard, 2008). Several studies report a high overlap of miRNAs loaded into the different Ago isoforms (Burroughs *et al.*, 2011; Siomi and Siomi, 2008; Hafner *et al.*, 2010). Indeed, it was reported that all Ago isoforms repress miRNA-mRNA duplexes (Janas *et al.*, 2012). However, only Ago2 protein has endonuclease/slicer activity, mediating mRNA cleavage (Liu, 2004).
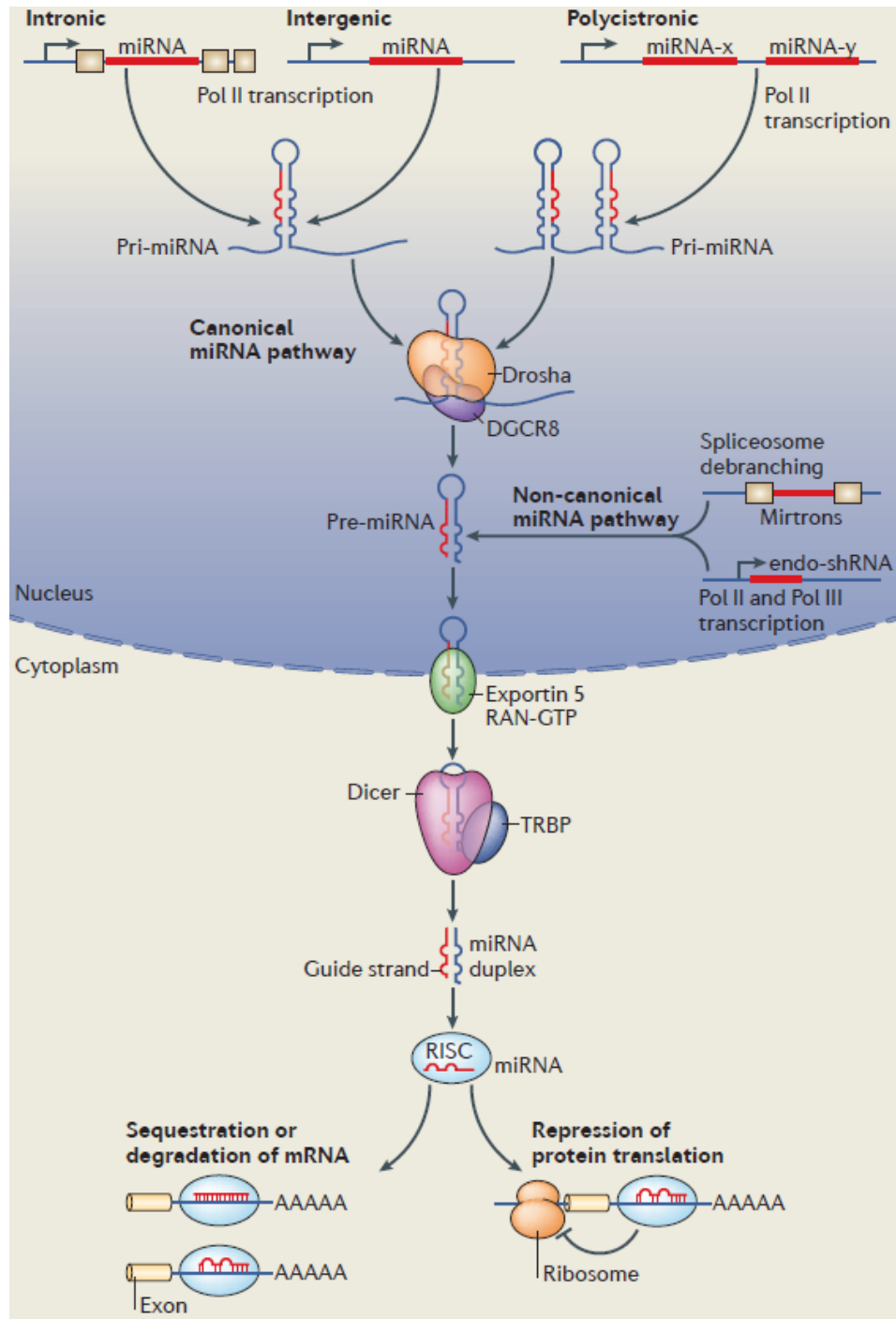
Figure 1.3.: MiRNA biogenesis pathway

In the canonical pathway RNA polymerase II (Pol II) transcribes miRNAs either from intergenic, intronic or poly-cistronic genomic loci. Drosha and DGCR8 recognize the stem loop sequence within the primary transcript (pri-miRNA) and trim it to produce the precursor transcript (pre-miRNA). In the non-canonical pathway pre-miRNAs are generated by splicing of introns (mirtrons) or are directly transcribed by short hairpins (shRNA). The pre-miRNA from both pathways is exported into the cytoplasm by exportin 5, where DICER and transactivation-response RNA-binding protein (TRBP8) cleave of the loop structure and produce a mature miRNA duplex. The guide strand of this duplex is incorporated into the AGO-containing RNA-induced silencing complex (RISC), which then mediates translational repression, mRNA degradation or sequestration. (figure taken from Rottiers *et al.* 2012)

Each of these biogenesis steps can be modulated. Drosha dependent cleavage of pri-miRNA to pre-miRNA can be modified by accessory proteins like hnRNP A1, KKSHP and SMAD (Michlewski and Cáceres, 2010; Davis *et al.*, 2008). Additionally, Drosha processing of pri-miRNAs can be prevented by RNA editing of adenine deaminases (ADARs), which change specific adenins into inosines (Siomi and Siomi, 2010; Iizasa *et al.*, 2010). Moreover, it was shown, that hyper-edited double stranded miRNAs are degraded within the RISC complex (Scadden, 2005). Besides RNA modification, the major factors of the miRNA biogenesis machinery can be regulated by post-transcriptional modifications, such as phosphorylation, hydroxylation or ubiquitination leading to alterations in their localization, activity and stability (reviewed in (Kim *et al.*, 2010)).

1.4.2. Mechanism of translational inhibition by microRNAs

Once the mature miRNA is incorporated into the RISC (miRISC), the miRNA guides the protein complex via its seed sequence to target mRNAs, leading to their translational inhibition or degradation (reviewed in (Filipowicz *et al.*, 2008)). In contrast to plants, where miRNAs are often fully complementary to their target mRNAs and induce mRNA cleavage and degradation, metazoan miRNAs bind only with partial complementarity and inhibit translation (Bartel, 2004). In mammalia, the miRNA recognizes its target by perfect base pairing of nucleotide 2-8 at the 5' end (Lewis *et al.*, 2003). This sequence is called "seed" sequence. Besides the seed pairing, supplementary pairing of the 3' part of the miRNA is supportive but plays a minor role in target recognition (Grimson *et al.*, 2007; Brennecke *et al.*, 2005). In principle miRNA binding sites can be recognized all over a mRNA (Lytle *et al.*, 2007), but effective translational repression was shown for mRNAs that harbor conserved miRNA binding sites within their 3'UTR (Kuersten and Goodwin, 2003).

While total complementarity of miRNAs to their target mRNAs (plant miRNAs or siRNAs) induces mRNA cleavage, the exact mechanism by which miRNA interfere with the translation machinery in mammalia is not well understood. However, it is known that Ago2 can compete with translation initiation factor eIF4E for the m^7G cap of the mRNA, disrupting translation initiation and mRNA circularization (Filipowicz *et al.*, 2008). Additionally, a drop-off model in which miRNAs render ribosomes prone to premature termination is discussed (Petersen *et al.*, 2006). Furthermore, translation inhibition can be mediated by mRNA deadenylation (Fabian *et al.*, 2009; Braun *et al.*, 2011) or sequestration in processing bodies (P-bodies) (Rottiers and Näär, 2012). P-bodies are cytoplasmatic foci, where enzymes that are involved in mRNA decay and translational repression (incl. GW182, Ago proteins and miRNAs) accumulate (Kulkarni *et al.*, 2010). The translational repression of mRNAs and their localization to P-bodies are shown to

be transient, thus they can be reactivated followed by ribosome recruitment and subsequent translation (Bhattacharyya *et al.*, 2006).

1.4.3. MiRNAs in tumorigenesis

MiRNAs regulate virtual all cellular processes, including genes that are associated with tumorigenesis: cell cycle regulation, differentiation, apoptosis, stress response, inflammation, migration and invasion. Therefore, dysfunctional expression of miRNA is considered as a hallmark of cancer (Lawrie, 2013). Alterations of miRNA expression is often observed due to genetical alterations, such as amplification, deletion or translocation of genes. Indeed, approximately 50% of annotated human miRNAs are located in fragile sites and associated with cancer (Esquela-Kerscher and Slack, 2006). MiRNAs function as tumor-suppressor miRNAs, when targeting an oncogene, or as onco-miRNAs, when targeting a tumor suppressor. Deletion of a tumor suppressive miRNA as well as amplification of an oncogenic-miRNA (onco-miR) can consequently lead to tumorigenesis.

Several miRNAs are deregulated in B cell lymphoma (e.g. miR-155, miR-17-92 cluster, miR-21, miR-34a, miR-125B etc., reviewed in (Lawrie, 2013)). These miRNAs were shown to play crucial roles during B cell development (reviewed in (de Yébenes *et al.*, 2013)). One well described example is miR-155, which is overexpressed in DLBCL (Kluiver *et al.*, 2005). MiR-155 is considered as a key regulator in immune function under normal physiological conditions, thus it can contribute to tumorigenesis in many different ways. MiR-155 negatively regulates somatic hypermutation by targeting AID (Teng *et al.*, 2008) and class switch recombination by targeting PU.1 (purine-rich DNA sequence (PU-box) binding protein) (Vigorito *et al.*, 2007). Furthermore, it was reported that miR-155 targets SMAD5, preventing the growth inhibitory effect of TGFβ1 and BMP2/4 (Rai *et al.*, 2010). Overexpression of miR-155 inhibits INPP5D which leads to TNFα dependent growth of DLBCL cells (Pedersen *et al.*, 2009). While miR-155 seems to have onco-miR function in DLBCL, it is downregulated in BL, indicating that it might have a tumor suppressor function in BL (Kluiver *et al.*, 2005, 2006). Therefore, the function of a miRNA seems to be dependent on the cellular context.

In summary, miRNA deregulation contributes to tumorigenesis by various means. However, the fact that miRNA levels are altered within lymphoma subtypes, can be used as markers for diagnosis (Lenze *et al.*, 2011; Roehle *et al.*, 2008). Furthermore, it was shown that miRNAs can have prognostic value (Goswami *et al.*, 2013) and can be used as therapeutic targets (reviewed in (Oom *et al.*, 2014)).

1.5. The MIR23A cluster

The miR-23a~27a~24-2 cluster (MIR23A) is a polycistronic cluster coding for miR-23a, miR-27a and miR-24 (fig. 1.4). It is encoded in an intergenic region on chromosome 19p13, which is conserved among vertebrates and harbors its own promoter region. In fact, the MIR23A cluster was one of the first miRNAs that were described to be transcribed by RNA polymerase II into a ~2.2 kb long pri-miR-23a~27a~24-2 transcript (pri-miR-23a) (Lee *et al.*, 2004). The MIR23a cluster promoter lacks common promoter elements, such as the TATA box, initiator element, downstream promoter element (DPE), TFIIB recognition element (BRE), downstream core element (DCE) and MED-1 (multiple start site element). Reporter gene assays showed that the region from -806 to -603 bp has negative regulatory function, while the region between -603 to +36 bp has the strongest positive function of all tested promoter sequences and strongly induces pri-miR-23a expression. The promoter region from -74 to -42 bp was absolutely necessary for transcription (Lee *et al.*, 2004).
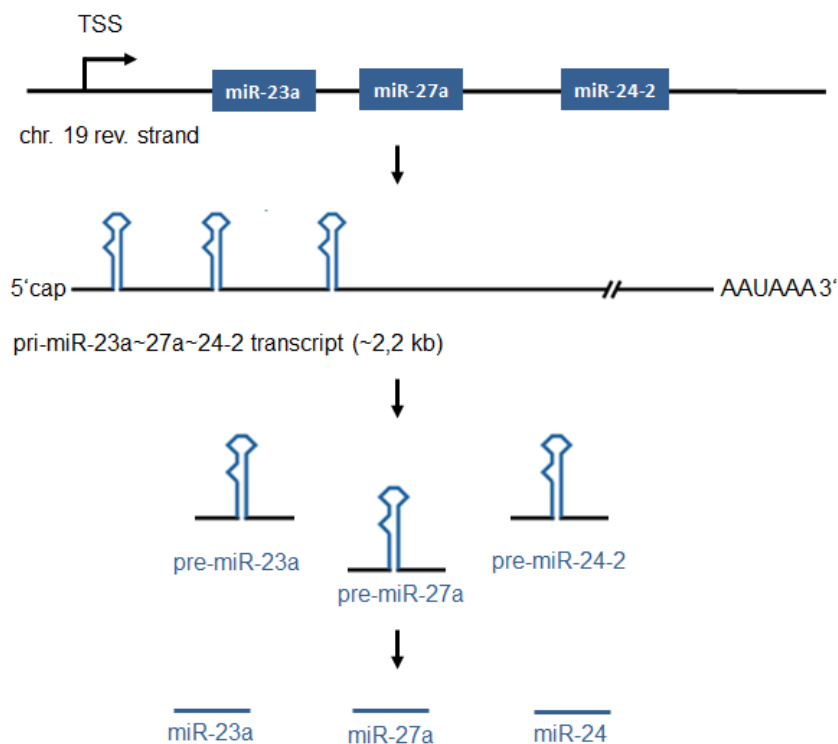
Figure 1.4.: MIR23A cluster
The polycistronic MIR23A cluster is localized on the reverse strand of chromosome 19 and codes for the 2.2 kb long primary transcript miR~23a~27a~24-2, which is processed into ~ 70 bp precursor transcripts pre-miR-23a, pre-miR-27a and pre-miR-24-2 and subsequently into mature miR-23a, miR-27a and miR-24.

Although all three miRNAs of this cluster are transcribed in one polycistronic transcript (pri-miRNA), it was observed that the mature miR-23a and miR-27a expression is inconsistent in leukemic cell lines, while miR-24 is not expressed (Yu *et al.*, 2006), indicating that regulation of the single miRNAs might be independent from each other, a well documented phenomenon for miRNAs (Buck *et al.*, 2010; Filipowicz *et al.*, 2008).

In mammals the paralogous cluster miR-23b~27b~24-1 (MIR23B), coding for miR-23b, miR-27b and miR-24, exists in an intronic region of a zinc-dependent metallopeptidase on chromosome 9q22. The sequences of miR-23a and miR-23b, miR-27a and miR-27b differ only in one base, while mature miR-24 sequence is identical and can only be distinguished from each other as precursor miRNAs. As the paralogous miRNAs harbor the same seed sequences, it has been suggested, that both clusters target the same set of mRNAs and might therefore have similar functions within the cell. However, the regulation of both clusters might be independent, as differential expression was reported in several cancer entities (reviewed in (Chhabra *et al.*, 2010)). Notably, the paralogous cluster is not expressed in leukemic cell lines (Yu *et al.*, 2006).

Interestingly, Karposi's sacroma-associated herpesvirus (KSHV) expresses a miR-23-Mimic (miR-K3) with high 5' sequence complementarity to miR-23a and miR-23b, harboring the identical seed-sequence as miR-23a and miR-23b thereby targeting the same mRNAs (Manzano *et al.*, 2013). Since KSHV infections are associated in tumorigenesis (Giffin and Damania, 2014), this might indicate a onco-miR function for miR-23a.

Various miRNA profiling studies have reported that all three members of the MIR23A cluster are deregulated in several diseases including muscle diseases, neurologic disorders and many different cancer entities (reviewed in (Chhabra *et al.*, 2010)). In particular, deregulation of MIR23A cluster was observed for acute promyelocytic leukemia (APL) caused by the fusion gene PML-RARA (Saumet *et al.*, 2009). Furthermore, the MIR23A cluster is differentially expressed between acute lymphoblastic leukemia (ALL; down) and acute myeloid leukemia (AML, up) (Mi *et al.*, 2007) as well as between BL (down) and DLBCL (up) (Lenze *et al.*, 2011; Iqbal *et al.*, 2015), indicating that aberrant factors or events during hematopoiesis might be responsible for MIR23A deregulation. Indeed, the MIR23A cluster was shown to play a crucial role during hematopoiesis, hence it is regulated by PU.1, a potent repressor of the lymphoid line, thereby promoting the myeloid line (Kong *et al.*, 2010). Very recently, it was reported that MIR23A germline knockout mice show an increased number of B lymphocytes in bone marrow and spleen and a decreased number of myeloid cells (Kurkewich *et al.*, 2016). For later steps of B cell development several groups showed by miRNA profiling (micro array, RNA sequencing or qRT-PCR) that the MIR23A cluster expression is induced during GC reaction in normal healthy B cells (Basso *et al.*, 2009; Tan *et al.*, 2009; Zhang *et al.*, 2009; Malumbres *et al.*, 2009)

(Iqbal *et al.*, 2015). Although none of these groups investigated the MIR23A cluster in detail, all show in principle the same expression pattern for the MIR23A cluster: naive B cells and GCB cells have low MIR23A cluster expression, while mature memory B cells have upregulated MIR23A cluster levels (Basso *et al.*, 2009; Tan *et al.*, 2009; Zhang *et al.*, 2009; Malumbres *et al.*, 2009; Iqbal *et al.*, 2015), indicating that a process within the GC might induce the MIR23A cluster. Notably, Iqbal *et al.* verified the MIR23A cluster data by qRT-PCR (Iqbal *et al.*, 2015). Only Thapa *et al.* show higher miR-23a levels in naive B cells, that are downregulated in GCBs and again upregulated in memory B cells (Thapa *et al.*, 2011). These differences might be explained by different cell surface markers used to sort distinct B cell subpopulations. However, the function of MIR23A cluster in B cells still remains unknown. Moreover, the mechanism by which it is induced under physiological conditions is still unclear. Considering the fact, that MIR23A cluster is differentially expressed between BL and DLBCL, which both develop from GCB cells (Tamaru *et al.*, 1995; Rosenwald *et al.*, 2002; Pasqualucci and Dalla-Favera, 2014; Sehn and Gascoyne, 2015), it can be suggested that pathways activated during GC reaction might be responsible for the regulation of MIR23A cluster expression. First indications supporting this hypothesis came from an arbitrary cell system, which mimics BL (P493-6) and demonstrated that MYC can repress MIR23A cluster expression (Gao *et al.*, 2009). Additionally, for non-small cell lung cancer cells the transcription factor ELK1, which acts downstream from MEK/ERK cascade, was reported to activate the MIR23A cluster (Acunzo *et al.*, 2013). Furthermore, the NFκB member p65 induced the MIR23A cluster in human leukemic T cells (Rathore *et al.*, 2012). However, experimental data supporting this hypothesis for DLBCL are still missing.

Recently, Wang and colleagues reported that tumor samples of DLBCL patients show aberrant high miR-23a levels compared to reactive lymph nodes of healthy control patients. Furthermore, they showed that patients with higher miR-23a levels have a worse overall survival rate than patients with lower levels, indicating an onco-miR function of MIR23A cluster in DLBCL (Wang *et al.*, 2014). In order to understand why miR-23a worsens prognosis, knowledge about the targets of the MIR23A cluster would be needed to explain which cellular processes are affected by the MIR23A cluster. Indeed, several targets were already described for all three members of the MIR23A cluster for different malignancies, except for lymphoma, indicating that this cluster acts in many different cellular processes and can have diverse functions.

In pancreatic cancer miR-27a is overexpressed and acts as an onco-miR by targeting Sprouty2, a negative regulator of Ras/MEK signaling, thereby inducing growth, colony formation and migration of pancreatic cells (Ma *et al.*, 2010). Similar results were gained in colon cancer, where miR-23a was shown to promote migration and invasion by targeting metastasis suppressor 1 (MTSS1) (Jahid *et al.*, 2012). Moreover, the same group showed that miR-27a promotes proliferation. In breast cancer miR-27a overexpression leads to downregulation of transcription fac-

tor FOXO1 and induced cell proliferation as well as survival (Guttilla and White, 2009). FOXO1 is a putative tumor suppressor, which is also activated upon BCR signaling (see section 1.2.1). In contrast, miR-23a acts as a tumor suppressor miRNA in osteosarcoma, where ectopic over-expression of miR-23a inhibited proliferation, migration and invasion by targeting RUNX2 and CXCL12 (He *et al.*, 2014). A tumor suppressor function was also reported for miR-27a in col-orectal cells (Bao *et al.*, 2014). This group demonstrated, that miR-27a inhibited proliferation, promoted apoptosis and attenuated migration. Furthermore, miR-27a inhibited tumor growth *in vivo* (Bao *et al.*, 2014). Gao *et al.* showed that miR-23a levels are downregulated in BL upon MYC expression (Gao *et al.*, 2009). Low miR-23a levels lead to increased mitochondrial glutaminase (GLS) levels promoting glutamine metabolism resulting in higher energy produc-tion. In this example, the oncogene *MYC* abolishes the tumor suppressor function of miR-23a in order to facilitate cancer metabolism.

Taken together, these current findings indicate that the MIR23A cluster is aberrantly regulated in DLBCL and that the biological function of the MIR23A cluster is cell type and context specific. A previous study suggests that the MIR23A cluster might act as an onco-miR in DLBCL patients (Wang *et al.*, 2014). However, neither the reason for MIR23A cluster deregulation, nor the biological function of the MIR23A cluster in DLBCL are understood.

1.6. Aims

The MIR23A cluster was shown to be deregulated in many different diseases, including leukemia and lymphoma. BL and DLBCL, two aggressive B-NHL subtypes, are derived from GCB cells. Gene expression profiles show, that naive B cells and normal GCBs have low MIR23A cluster levels compared to increased levels in memory B cells. Due to complex interactions with the microenvironment of the GC, many different signaling cascades are activated during GC reaction modulating survival, proliferation and differentiation of GCB cells. However, DLBCL patients show aberrant high MIR23A cluster levels compared to healthy controls, indicating that signaling cascades deregulated during GC reaction might be responsible for MIR23A cluster activation. However, experimental data for the factors responsible for aberrant MIR23A cluster regulation in DLBCL are missing.

The function of MIR23A cluster is controversially discussed, since onco-miR as well as tumor suppressive functions were reported for the MIR23A cluster in different cancer entities. Because miRNA function is dependent on the mRNAs targeted by the miRNA, its function is context and cell type specific. A previous study reported that DLBCL patients with increased miR-23a levels have a worse overall survival rate than patients with lower miR-23a levels. These observations indicate the MIR23A cluster to function as an onco-miR in DLBCL. However, the processes in which the MIR23A cluster is involved in DLBCL are unknown.

Consequently, this study aims to answer the following two questions:

1. Which signaling pathways are responsible for the aberrant regulation of the MIR23A cluster in DLBCL?

2. What is the DLBCL specific targetome of the MIR23A cluster? In detail, which mRNAs are targeted by miR-23a and miR-27a?

By the identification of the miR-23a and miR-27a targetomes the cellular function of MIR23A cluster in DLBCL can be predicted. Furthermore, the onco-miR hypothesis can be tested.

In order to investigate the MIR23A cluster regulation, MIR23A cluster levels were analyzed upon stimulation of B cell relevant signaling pathways with different factors from the GC microenvironment, followed by the inhibition of downstream factors within the respective signaling cascades. The cellular function of the MIR23A cluster was investigated by the identification of miR-23a and miR-27a targetomes in a DLBCL model cell line. Therefore, DLBCL cell lines overexpressing the respective miRNA or control were generated. These cell lines were used to establish an Ago2-RNA immunoprecipitation assay. By this *in vitro* approach several novel mRNA targets of the MIR23A cluster were identified for a DLBCL model cell line and were subjected to functional validation.

2. Materials and Methods

2.1. Biological Material

2.1.1. Primary Material and Data

Primary material of human pediatric tonsils was obtained with informed consent from the legal guardians of the children and ethical approval (34/7/06 Ethic-Commission University Göttingen). Tonsillectomies were performed in the University Medical Center Göttingen.

Patient RNA sequencing data were obtained from the data base of the International Cancer Genome Consortium (ICGC) Project "Determining Molecular Mechanisms in Malignant Lymphoma by Sequencing" (ICGC-MMML-Seq, https://ddc.icgc.org/releases/current/Projects/MALY-DE, release v22 24.08.2016, published in (Hezaveh *et al.*, 2016)).

2.1.2. Cell Lines

Cell lines used in this study are listed in table 2.1.

Table 2.1.: Cell lines

Cell line	Description	Distributor	Reference
BL-2	Burkitt Lymphoma	Bornkamm, Munich	(Bertrand *et al.*, 1981)
HEK293T	Embryonal kidney	DSMZ, Brunswick	(Rio *et al.*, 2015)
OCI-LY3	Diffuse large B cell lymphoma (ABC)	DSMZ, Brunswick	(Tweeddale *et al.*, 1987)
OCI-LY7	Diffuse large B cell lymphoma (GCB)	DSMZ, Brunswick	(Tweeddale *et al.*, 1987)
P493-6	MYC transformed lymphoblastoid cell line	Bornkamm, Munich	(Polack *et al.*, 1996)
U2932 R1	Diffuse large B cell lymphoma	DSMZ, Brunswick	(Quentmeier *et al.*, 2013)
U2932 R2	Diffuse large B cell lymphoma	DSMZ, Brunswick	(Quentmeier *et al.*, 2013)

2.1.3. Bacteria

E.coli Subcloning Efficiency DH5α Competent Cells were used for subcloning and plasmid DNA amplification (Thermo Fisher Scientific, Waltham, USA). Genotype: F- φ80*lac*ZΔM15 Δ(*lac*ZYA-*arg*F)U169 *rec*A1 *end*A1 *hsd*R17(r_k $^-$, m_k $^+$) *pho*A *sup*E44 *thi*-1 *gyr*A96 *rel*A1 λ$^-$

2.2. Chemicals, Buffers & Consumables

2.2.1. Chemicals

Chemicals used in thesis study are listed in table 2.2:

Table 2.2.: Chemicals and Solutions

Chemical or solution	Manufacturer
30% Acrylamid/Bis Solution (37,5:1)	Bio-Rad, California, USA
Adenosine 5'triphosphate, ATP	Roth, Karlsruhe, Germany
Agarose	Sigma-Aldrich, Steinheim, Germany
anti FITC microbeads	Miltenyi Biotec, Bergisch Gladbach, Germany
auto MACS rinsing buffer	Miltenyi Biotec, Bergisch Gladbach, Germany
β-Mercaptoethanol	Sigma-Aldrich, Steinheim, Germany
Bacillol	Bode, Hamburg, Germany
Biocoll Lymphoprep Solution	Biochrom, Berlin, Germany
Bovine Serum Albumin BSA	Serva, Heidelber, Germany
Brilliant Blue G	Sigma-Aldrich, Steinheim, Germany
Chloroform	J. T. Baker, Deventer, Netherlands
Complete protease inhibitor, EDTA-free	Roche, Mannheim, Germany
Coomassie Plus	Thermo Scientific, Massachusetts, USA
Disodiumhydrogenphosphate	Roth, Karlsruhe, Germany
Dithiothreitol (DTT)	Sigma-Aldrich, Steinheim, Germany
DMSO	Sigma-Aldrich, Steinheim, Germany
dNTPs	Peqlab, Erlangen, Germany
Dynabeads Protein G	Life Technologies AS, Oslo, Norway
EDTA	Sigma-Aldrich, Steinheim, Germany
EGTA	Sigma-Aldrich, Steinheim, Germany
Ethanol	J. T. Baker, Deventer, Netherlands
Ethidiumbromide	Sigma-Aldrich, Munich, Germany
FACS flow	Becton Dickinson, Heidelberg, Germany
FCS	Sigma-Aldrich, Steinheim, Germany
Formaldehyde	Sigma-Aldrich, Munich, Germany
Formic acid	Sigma-Aldrich, Steinheim, Germany
Glycerol	Roth, Karlsruhe, Germany
Glycine	Roth, Karlsruhe, Germany
IGEPAL CA-630	Sigma-Aldrich, St. Louis, USA
Methanol	J. T. Baker, Deventer, Netherlands
Methanol	J. T. Baker, Deventer, Netherlands
MTT (Thiazolyl Blue Tetrazolium Bromide)	Sigma-Aldrich, Steinheim, Germany
Nonidet P-40	Fluka, Missouri, USA
NXA931	GE Healthcare (Little Chalfont, UK)
PBS	Sigma-Aldrich, Steinheim, Germany
Penicillin/Strepomycin	Gibco, Massachusetts, USA
PhosSTOP	Roche, Mannheim, Germany
Ponceau S solution	Sigma-Aldrich, Steinheim, Germany
Potassiumchloride	Roth, Karlsruhe, Germany
Potassiumhydrogenphosphate	Roth, Karlsruhe, Germany
2-Propanol	J. T. Baker, Deventer, Netherlands
Propidiumiodid	Sigma-Aldrich, Steinheim, Germany
Puromycin	Invivogen, Toulouse, France

Continued on next page

Chemical or solution	Manufacturer
Random Primers	Invitrogen, Karlsruhe, Germany
Re-Blot Plus Mild Solution (10x)	Millipore, Massachusetts, USA
RNase away	Molecular BioProducts, San Diego, USA
RNase free H2O	Sigma-Aldrich, Steinheim, Germany
RNAse Out	Invitrogen, Karlsruhe, Germany
RPMI1640	Gibco, Massachusetts, USA
Sigma-AldrichAST Protease Inhibitor	Sigma-Aldrich, Steinheim, Germany
Sodiumchloride	Roth, Karlsruhe, Germany
Sodiumdeoxycholat	Roth, Karlsruhe, Germany
Sodiumfluoride	Sigma-Aldrich, Steinheim, Germany
Sodiumhydroxid	Roth, Karlsruhe, Germany
TEMED	Bio-Rad, California, USA
Triton X-100	Serva, Heidelberg, Germany
Tris Base	Sigma-Aldrich, Steinheim, Germany
Tris HCl	Sigma-Aldrich, Steinheim, Germany
Trypanblaue 0.4% in PBS	Sigma-Aldrich, Steinheim, Germany
Tween 20	Sigma-Aldrich, Steinheim, Germany
Western lightning Plus ECL	Perkin Elmer, Waltham, USA

2.2.2. Buffers and Solutions

Buffers and solutions used in this study are listed in table 2.3:

Table 2.3.: Buffers

Buffer	Recipe
Ago2-RIP lysis buffer	25 mM Tris HCl pH 7.5
	150 mM KCl
	2 mM EDTA
	0.5% (v/v) IGEPAL CA-630
	0.5 mM DTT
	4U/mL Rnase Out
	1x Protease Inhibitor Cocktail, EDTA free
Ago2-RIP wash buffer	50 mM TrisHCl pH 7.5
	300 mM NaCl
	5 mM MgCl2
	1 mM NaF
	0.1% (v/v) IGEPAL CA-630
	4U/mL Rnase Out
	1x Protease Inhibitor Cocktail, EDTA free
6x Laemmli buffer	375 mM Tris HCl pH 6,8
	9% SDS
	50% (v/v) Glycerol
	0.03% Bromphenoleblue
	9% (v/v) beta-Mercaptoethanol
MTT Solution I	5 mg/mL MTT in PBS
MTT Solution II	33 % DMSO (v/v),
	5 % (v/v) Formic acid
	62 % (v/v) Isopropanol
Nucl. extraction buffer A	10 mM HEPES pH 7.9
	10 mM KCl

Continued on next page

Buffer	Recipe
	10 mM EDTA
	10 mM EGTA
	1 mM DTT
Nucl. extraction buffer B	20 mM HEPES
	400 mM KCl
	1 mM EDTA
	1 mM EGTA
	1 mM DTT
RIPA lysis buffer	100 mM NaCl
	50 mM TrisHCl pH 7.4
	0.1% SDS
	1% (v/v) NP-40
	1x Protease Inhibitor Cocktail
	1x Phosphatase Inhibitor Cocktail
	0.25% Sodium-deoxycholat
Running buffer (1x)	25 mM Tris-base
	192 mM Glycin
	34.67 mM SDS
Separation gel mix	250 mM Tris-base, pH 8.8
	25% (v/v) Acrylamid/Bis solution (40 %)
	0.0004% (w/v) APS
	0.00125% (v/v) TEMED
Stacking gel mix	250 mM Tris Base pH 6.8
	12.5% (v/v) Acrylamid/bis solution (40 %)
	0.0004% (w/v) APS
	0.00125% (v/v) TEMED
TBS (1x)	20 mM Tris-base
	137 mM Sodium chloride
	Adjusted to pH 7.6
TBS-T	0.1% (v/v) Tween-20
Transfer buffer (1x)	25 mM Tris-base
	192 mM Glycin
	20% (v/v) MeOH

2.2.3. Inhibitors

Inhibitors used in this study are listed in table 2.4:

Table 2.4.: Inhibitors

Inhibitor	Final Concentration	Manufacturer
BEZ235	200 nM	Selleckchem, Munich, Germany
Cyclohexamide	100 µg/mL	Sigma-Aldrich, Steinheim, Germany
Etoposide	100 µM	Sigma-Aldrich, Steinheim, Germany
Ibrutinib	1 µM	Selleckchem, Munich, Germany
MK2206	3 µM	Selleckchem, Munich, Germany
Trametinib	125 nM	Selleckchem, Munich, Germany

2.2.4. Consumables

Consumables used in this study are listed in table 2.5:

Table 2.5.: Consumables

Consumable	Manufacturer
96 well PCR plates	Applied Biosystems, Foster City, California, USA
Agilent RNA 6000 Pico Kit	Agilent Technologies, Waldbronn, Germany
Agilent Small RNA kit	Agilent Technologies, Waldbronn, Germany
Cell culture flasks	Nunclon, Rosklide, Denmark
Cryotubes	Nunc, Wiesbaden, Germany
DNA loBind tubes 1,5 mL, safe lock PCR clean	Eppendorf, Hamburg, Germany
FACs tubes	Becton Dickinson, Franklin Lakes, USA
Falcon tubes 15 ml	Falcon, Reynosa, Mexico
Falcon tubes 50 ml	Greiner Bio-One, Kremsmuenster, Austria
MACS LS columns	Miltenyi Biotec, Bergisch Gladbach, Germany
MACS pre separation filters	Miltenyi Biotec, Bergisch Gladbach, Germany
Multiwell cell culture plates	Nunclon, Rosklide, Denmark
Nucleofection cuvettes	Amaxa-biosystems, Cologne, Germany
PVDF membrane	Biorad, Hercules, USA
Reaction tubes (0.5, 1.5, 2.0 mL)	Eppendorf, Hamburg, Germany
Siliconized Tubes, 1,7ml (25 Tubes)	Active Motif, La Hulpe, Belgium

2.3. Equipment

Equipment used in this study is listed in table 2.6:

Table 2.6.: Equipment

Instrument	Manufacturer
7500 Fast Real-Time PCR System	Applied Biosytems, Foster City, California, USA
Advanced Fluorescence Imager	Intas, Goettingen, Germany
Amaxa Nucleofector 4D	Lonza, Basel, Switzerland
Bioanalyzer2100	Agilent Waldbronn, Germany
FACS Calibur, FACS Aria III	Becton Dickinson, Franklin Lakes, USA
Heraeus Multifuge 3L	Thermo, Waltham, USA
Microcentrifuge 5424	Eppendorf, Hamburg, Germany
Multiscan Ex Platereader	Thermo, Waltham, USA
NanoDrop1000	Thermo, Waltham, USA
Neubauer Counting Chamber Improved	Lo Labor Optik, Friedrichsdorf, Germany
Thermocycler T3000	Biometra, Goettingen, Germany

2.4. Stimulants

Stimulants used in this study are listed in table 2.7:

Table 2.7.: Stimulants

Description	Final conc.	Manufacturer
F(ab')2 Fragment Goat α-human IgG	13 µg/mL	Jackson ImmunoResearch, Suffolk, UK
F(ab')2 Fragment Goat α-human IgM	13 µg/mL	Jackson ImmunoResearch, Suffolk, UK
sCD40L	200 ng/mL	Autogen bioclear, Wiltshire, UK
LPS	1 µg/mL	Sigma-Aldrich, Steinheim, Germany

2.5. Antibodies

Antibodies used for immunoblotting, FACS and Ago2-RIP are listed in table 2.8.

Table 2.8.: Antibodies

Antibody	Species	Order no.	Working solution	Manufacturer
Ago2 clone 11A9	rat	SAB4200085	1:1,000 5% BSA TBS-T 3.6 µg per 4.5 µg beads	SIGMA, St. Louis, USA
P-AKT (Ser473)	rabbit	4060P	1:1,000 5% BSA TBS-T	Cell Signalling Technology, Danvers, USA
AKT (67E7)	rabbit	4691P	1:1,000 5% BSA TBS-T	Cell Signalling Technology, Danvers, USA
BCL-6	rabbit	5650	1:1,000 5% BSA TBS-T	Cell Signalling Technology, Danvers, USA
BTK (D3H5)	rabbit	8547	1:1,000 5% BSA TBS-T	Cell Signalling Technology, Danvers, USA
P-BTK (Tyr223)	rabbit	5082	1:1,000 5% BSA TBS-T	Cell Signalling Technology, Danvers, USA
CD77	mouse	551353	50 µL per $1x10^8$ cells	Beckton Dickinson, New Jersey, USA
c-MYC	rabbit	ab32072	1:5,000 5% BSA TBS-T	Abcam, Cambridge, UK
ELK-1	rabbit	9182	1:1,000 5% BSA TBS-T	Cell Signalling Technology, Danvers, USA
P-ELK1 (Ser383)	rabbit	9180	1:1,000 5% BSA TBS-T	Cell Signalling Technology, Danvers, USA
ERK	rabbit	sc-94	1:1,000 5% BSA TBS-T	Santa Cruz, Dallas, US
P-ERK (Tyr204)	mouse	sc-7383	1:1,000 5% BSA TBS-T	Santa Cruz, Dallas, US
GAPDH	mouse	ab8245	1:10,000 5% BSA TBS-T	Abcam, Cambridge, UK
LIMK1	rabbit	3842	1:1,000 5% BSA TBS-T	Cell Signalling Technology, Danvers, USA
p53	rabbit	9282	1:1,000 5% BSA TBS-T	Cell Signalling Technology, Danvers, USA
PCNA	rabbit	ab19167	1:1,000 5% BSA TBS-T	Abcam, Cambridge, UK
PUMA	rabbit	12450	1:1,000 5% BSA TBS-T	Cell Signalling Technology, Danvers, USA
VRK3	rabbit	3260	1:1,000 5% BSA TBS-T	Cell Signalling Technology, Danvers, USA
IgG2a (aRTK2758) (iso type ctrl)	rat	ab18450	3.6 µg per 4.5 µg beads	Abcam, Cambridge, UK
mouse IgG HRP	sheep	NXA931	1:10,000 5% BSA TBS-T	GE Healthcare Chicago, USA
rabbit IgG HRP	donkey	NA934V	1:10,000 5% BSA TBS-T	GE Healthcare Chicago, USA
rat IgG HRP	goat	sc-2032	1:10,000 5% BSA TBS-T	Santa Cruz, Dallas, USA

2.6. Oligonucleotides

2.6.1. Primer

MiRNAs were detected using miScript Precursor Assays. Used primers are listed in table 2.9:

Table 2.9.: miScript primer

Order No	primer	description
MP00001645	Hs_mir-23a_PR_1	pre-miR-23a primer
MP00001701	Hs_mir-27a_PR_1	pre-miR-27a primer
MP00001666	Hs_miR-24-2_PR_1	pre-miR-24-2 primer
MS00031633	Hs_miR-23a_2	miR-23a-3p primer
MS00003241	Hs_miR-27a_1	miR-27a-3p primer
MS00006552	HS_miR-24_1	miR-24-3p primer
MS00007511	SNORD48_11	SNORD48 primer

Conventional primers used for qRT-PCR or conventional PCR are listed in table 2.10:

Table 2.10.: Primer

Primer	Sequence (5'-3')
c-MYC fw	CTACCCTCTCAACGACAGC
c-MYC rev	CTTGTTCCTCCTCAGAGTCG
CD58 fwd	ATGAAGATGAGTATGAAATGGAATCGCCA
CD58 rev	AGTGTGGGAGATGGAAGAGACTCAAGC
ICAM1 fw	TTCACAATGACACTCAGCGGTC
ICAM1 rev	AGTGCAAGCTCCCAGTGAAATG
ELK1 fw	CTGTCTGGAGGCTGAAGAGG
ELK1 rev	GCCTTGGTGGTTTCTGGCAC
GAPDH fw	TGGGTGTGAACCATGAGAAG
GAPDH rev	TCCACGATACCAAAGTTGTCA
miR-23a XhoI fw	CTCGAGTGCTCTCTCTCTCTTTCTCC
miR-23a MluI rev	ACGCGTACAGGCTTCGGGGCCTCT
miR-27a XhoI fw	CTCGAGTTCCAACCGACCCTGAGC
miR-27a MluI rev	ACGCGTTAGGCACGGGAGGCAGAGC
pri-miR-23a fw	CCAGGGATTTCCAACCGACC
pri-miR-23a rev	AGC TAA GCC CTG CTC CTC AG
pri-miR-23b fw	AGCTGAGGAAGATGCTCAC
pri-miR-23b rev	ACCAATCACTGTTCACCAATC
SLAMF7 fw	CAGAGAGCAATATGGCTGGTTCC
SLAMF7 rev	GCTGCTGACCCTGTGAGCTG

2.6.2. siRNAs

SiRNAs used in this study are listed in table 2.11:

Table 2.11.: siRNAs

siRNA	Cat. No.	Manufacturer
MYC_5	SI00300902	Qiagen, Hilden, Germany
ELK1_7	SI02662506	Qiagen, Hilden, Germany
all stars negative	SI03650318	Qiagen, Hilden, Germany

2.7. Ready to use reaction systems

Annexin V Apoptosis Detection kit PE (ebioscience, San Diego, USA), miRNeasy kit (Qiagen, Hilden, Germany), SsoFast EvaGreen Supermix with Low Rox (Biorad, California, USA), miScript SYBR Green PCR Kit (Qiagen, Hilden, Germany), miScript II RT Kit (Qiagen, Hilden, Germany), RNA 6000 Pico Kit (Agilent Technologies, Waldbronn, Germany), Small RNA kit (Agilent Technologies, Waldbronn, Germany), QiaEx DNA fragment isolation kit, Machery-Nagel Plasmid isolation kit. innuPREP Plasmid Mini Kit (Analytic Jena, Germany), NucleoBond® Xtra Midi EF (Machery-Nagel, Düren, Germany).

2.8. Software

The following software products were used: the present thesis was written with LyX and BibTeX. Literature-management and bibliography were generated using Mendeley Desktop Version 1.16.1. Graphs were created using Microsoft Excel 2010. Figures were assembled using GIMP and Microsoft Office PowerPoint 2010. Densidometry analyses were performed with ImageJ 1.49v. qRT-PCR analysis was performed using SDS 2.4 and RQ Manager 1.2.1 (Applied Biosystems). Bioanalyzer measurements were performed with Agilent Bioanalyzer expert B.02.08.SI648 software. Western Blot chemoluminescence was detected by Intas Chemostar Imager V 0.3.12.

2.9. Eukaryotic expression vectors
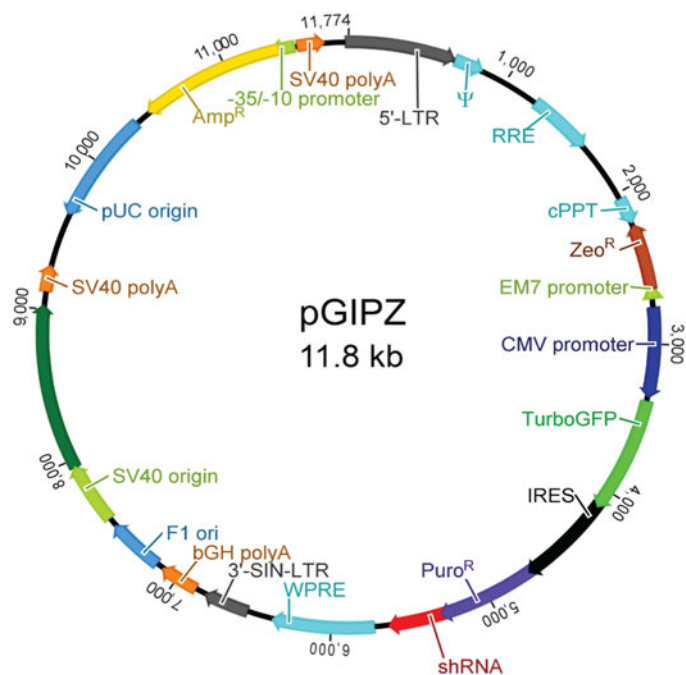
Figure 2.1.: Lentiviral vector pGIPZ

ns ctrl hairpin sequence: 5´TGCTGTTGACAGTGAGCGATCTCGCTTGGGCGAGAGTAAG-
TAGTGAAGCCACAGATGTACTTACTCTCGCCCAAGCGAGAGTGCCTACTGCCTCGGA 3´
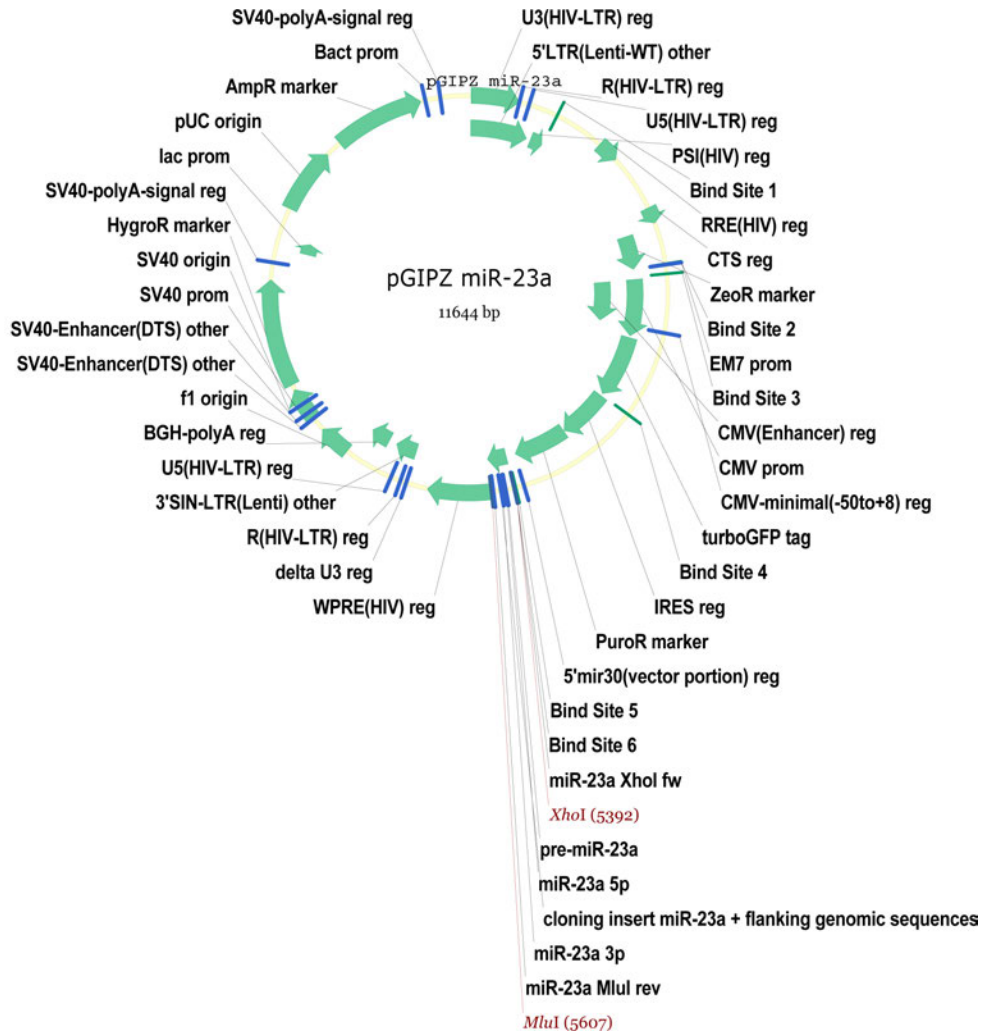
Figure 2.2.: MiR-23a pGIPZ
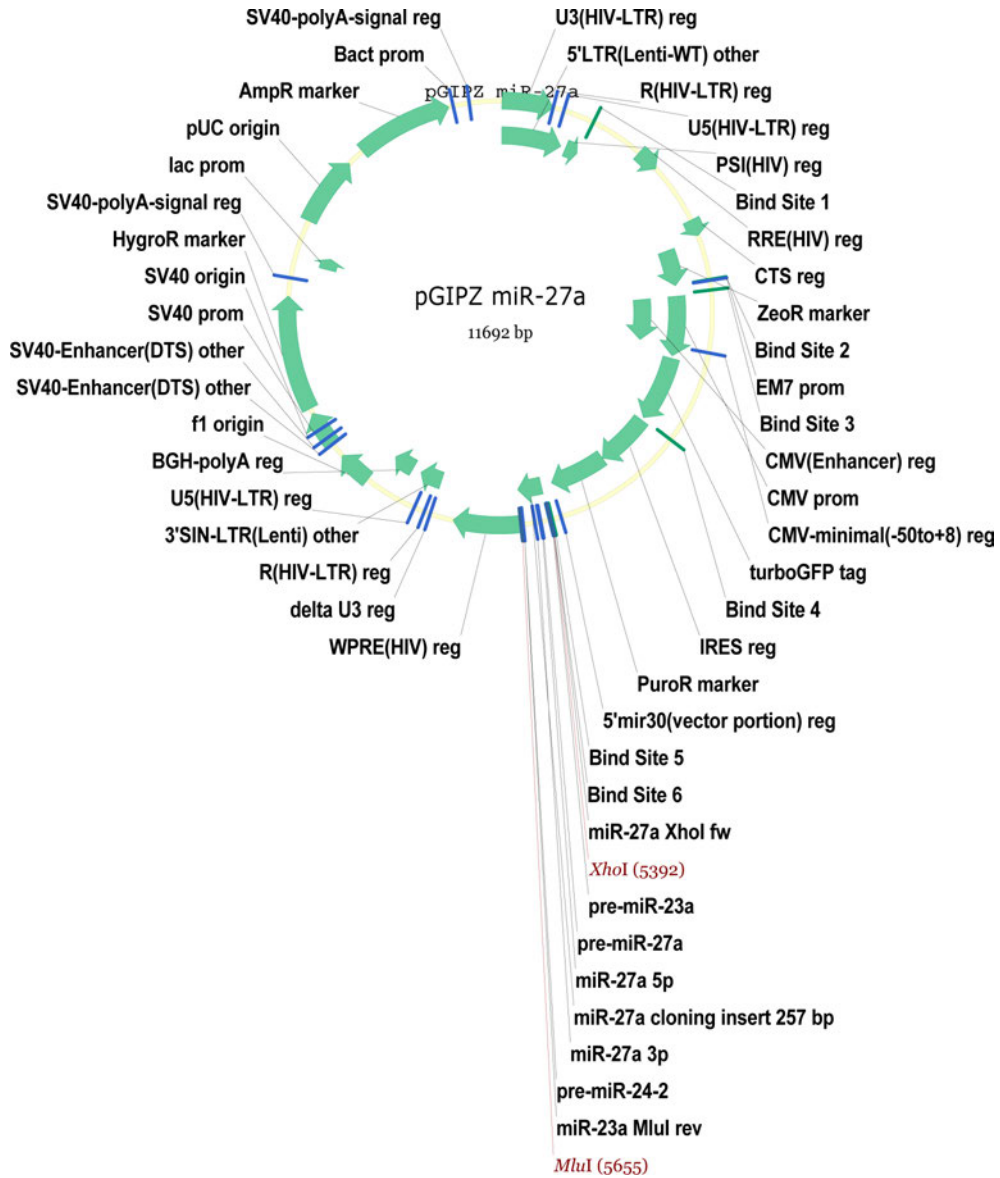
Figure 2.3.: MiR-27a pGIPZ
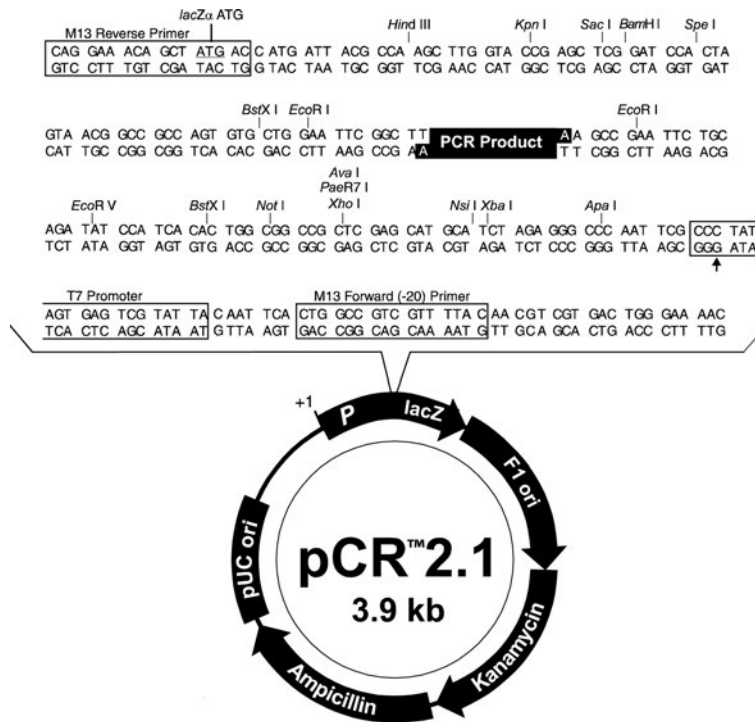
Figure 2.4.: Topo TA cloning vector pCR2.1
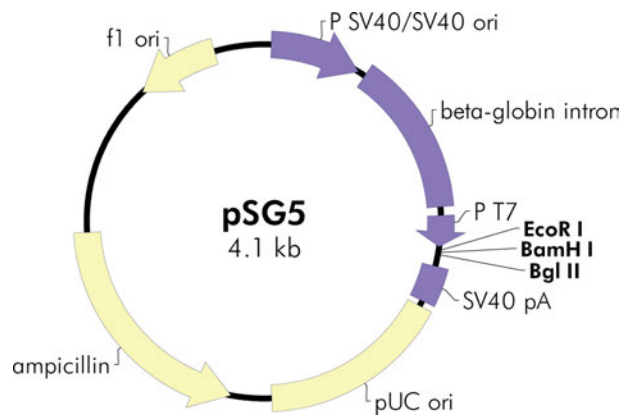
Figure 2.5.: Transient expression vector pSG5
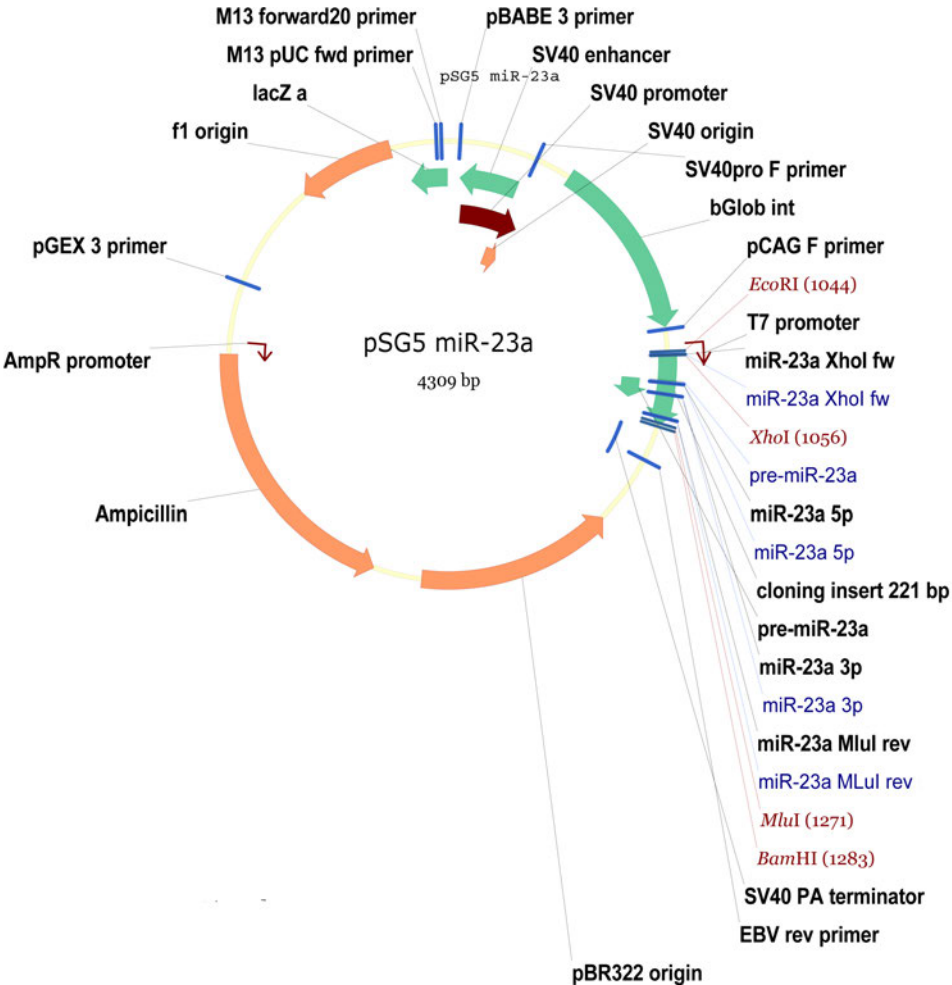
Figure 2.6.: MiR-23a in transient expression vector pSG5
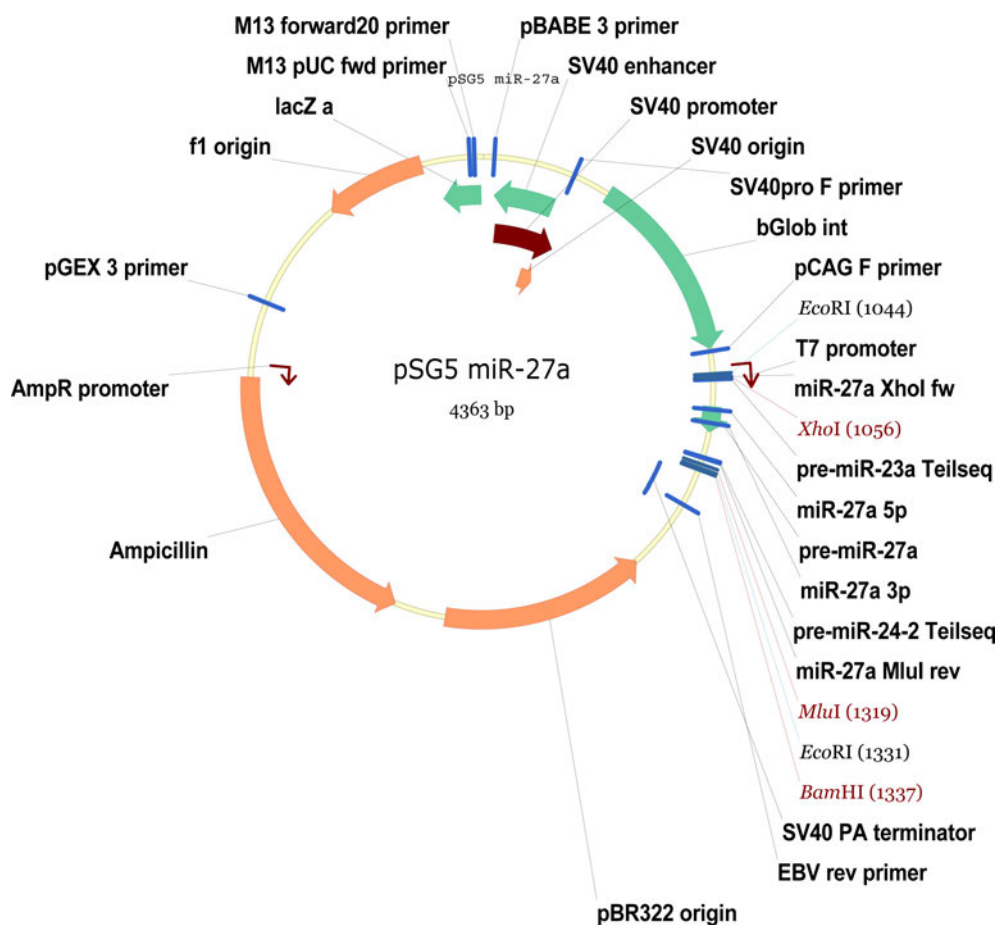
Figure 2.7.: MiR-27a in transient expression vector pSG5

2.10. Cell Biology

2.10.1. Cell culture

All cells were maintained at 37°C in 5 % CO_2 and subcultivated every second day. The BL cell line BL-2 was cultured in RPMI-1640 with 10% fetal calf serum (FCS), 200 U/mL Penicilin and 200 μg/mL Streptomycin. The DLBCL cell lines U2932 R1, U2932 R2 and OCI-LY3 were cultured in cell culture medium RPMI-1640 with 20% FCS, 200 U/mL Penicilin and 200 μg/mL Streptomycin and the DLBCL cell line OCI-LY7 was cultured in IMDM with 20% FCS, 200 U/mL Penicilin and 200 μg/mL Streptomycin. The BL cells were seeded at a density of 3 x 10^5 cells/mL the day before the experiment while DLBCL cell lines were seeded at a density of 5 x 10^5 cells/mL. HEK293T cells have been cultured in DMEM with 10% FCS. Approximately 2-3 x 10^6 cells/80 cm^2 have been seeded and subcultivated (ratio: 1:4 to 1:5) every three days. For cell number measurement cells were mixed in an equal ratio with 0.4 % Trypan blue and counted using the Neubauer counting chamber.

All cell lines have been tested regularly for mycoplasma contamination. Cells were no longer than four weeks continuously cultivated. For cell freezing 4-5 x 10^6 cells were centrifuged for 5 min at 120xg at RT and resuspended in 1 mL freezing medium (normal culture medium supplemented with 10% DMSO). For the freezing process cryo boxes which contain isopropanol were used to ensure a constant cooling of approximately 1°C/min. Cryo boxes were stored immediately at -80°C for 16-24 hours before they were transferred to liquid nitrogen for long-term storage. For thawing, cells were washed with their corresponding culture medium, counted and seeded in new culture medium (DLBCLs: 5 x 10^5 cells/mL; BLs: 3 x 10^5 cells/mL).

2.10.2. Isolation of CD77$^+$ GCB cells from primary pediatric tonsills

Isolation of tonsillar mononuclear cells

Primary tonsillar tissue was kept on ice after tonsillectomy. The tonsillar cells were extracted by mincing the tonsil in a petri dish with cold RPMI1640 plus P/S. To obtain tonsillar mononuclear cells (TMCs), the cell solution was overlaid with Lymphoprep™ solution and separated by density gradient centrifugation (400 x g, 30 min at RT without break). The interphase containing the TMCs was collected, washed once with cold RPMI1640 plus P/S and a second time with cold autoMACS™ buffer plus.

Enrichment of CD77$^+$ GC B cells

Cell enrichment was performed by an indirect labeling of the GC B cell marker CD77 on the cell surface with an antibody coupled to magnetic beads (MACS™ MicroBeads). The magnetic sorting was performed using MACS™ columns placed in a precooled MACS™ Separator, a strong permanent magnet. Thereby the MACS™ Column provides a magnetic field which retains labeled cells. Elution was achieved by removing the column from the magnet and rinsing the column with buffer. TMCs were counted and resuspended in autoMACS™ buffer plus (1x10^8 cells/250 μL). Cells were stained with anti CD77-FITC antibody (50 μL per 1x10^8 cells) for 10 min at 4°C in the dark. Cells were washed once with 50 mL autoMACS™ buffer plus P/S (centrifugation 300xg, 10 min, 4°C) and afterwards adjusted to a concentration of 40 μL/1x10^7 cells in autoMACS™ buffer plus P/S. 10 μL anti-FITC microbeads per 1x10^7 TMCs were added and incubated for 20 min at 4°C. Cells were washed with 50x volume of autoMACS™ buffer plus P/S and resuspended in autoMACS™ buffer plus P/S. CD77$^+$ cells were enriched using LS MACS™ separation columns topped with pre-separation filters (500 μL with 1x10^8 CD77 cells per column). After the equilibration of the columns and filters with 500 μL autoMACS™ buffer plus P/S in the magnetic field, 1x10^8 cells in 500 μL autoMACS™ buffer plus P/S were given onto each column. The columns were washed three times with 3 mL autoMACS™ buffer

plus P/S. The first washing step was executed through a pre-separation filter. Elution was per-
formed with 5 mL autoMACS™ buffer plus P/S. An aliquot of CD77$^+$ enriched cells was stored
at 4°C for cell characterisation by flow cytometry.

2.10.3. Nucleofection of cells

Small-interfering RNA (siRNA) against the indicated target genes or scrambled control were
transfected into the cells using Lonza Amaxa Nucleofection Kit (SF Cell Line 4D-Nucleofector®
X Kit L) and the Lonza Amaxa Nucleofector 4D device (100 pmol siRNA or 5 µg plasmid per
five million cells) according to the manufacturer's instructions (program: Primary cell P3, CD
137 for U2932 R1). After the nucleofection process, cells were incubated in pre-warmed RPMI
1640 supplemented with 20 % FCS for 24/48 hours at 37°C in 5 % CO_2. Knockdown quality
was verified with qRT-PCR and immunoblotting.

2.10.4. Inhibitor treatment

Cells were seeded in fresh cell culture medium at a density of 1 x 10^6 cells/mL and treated for
the indicated time span with the respective inhibitor (table 2.4). When performing combined
inhibitor and stimulation experiment, cells were pretreated 1-2 h before stimulation. Depending
on the experimental question, the cells were harvested for RNA isolation and/or for Western
blot analysis.

2.10.5. MTT Assay

For cell viability tests, the cell lines were treated with the inhibitor or solvent only as a control in
a cell density of 5 x 10^5 cells/mL for 24 h and 48 h at 37°C in 5 % CO_2 . After X-4 h incubation
100 µL cell suspension was seeded into a 96 well plate and 10 µL MTT I solution was added
following an incubation for four hours at 37°C in 5 % CO_2. Afterwards the cells were pelleted
for 10 min at 1200 rpm. The supernatant was discarded and the cell pellet was resuspended
in acidic MTT II solution. Optical density was afterwards determined at 560 nm and 750 nm
as reference wavelength using Thermo Multiscan Ex Platereader.

2.10.6. Stimulation of cells

One day prior to the experiment, cells were seeded at a cell density of 5 x 10^5 cells/mL in
the corresponding medium. At the day of the experiment cells were seeded at a density of
1 x 10^6 cells/mL in fresh medium without Penicillin and Streptomycin. The stimulant and the

corresponding solvent as control (table 2.7) were added to the cells and resuspended before incubation for the indicated time span at 37°C and 5% CO_2. For harvesting, cells were centrifuged 5 min at 210 x g and washed once with PBS. When analyzing phosphoproteins, cells were harvested in a pre-cooled centrifuge, washed once with cold PBS and handled on ice prior to cell lysis.

2.10.7. Generation of stable transduced U2932 R1 cells

Lentivirus production

For lentivirus production 5 x 10^6 HEK293T cells have been seeded per 10 cm^2 cell culture dish and grown to 80 % confluence in DMEM +10% FCS. Two hours prior to the experiment HEK293T medium has been renewed without disturbing cell confluence.

Expression vector (pGIPZ LEF1 shRNA or pGIPZ non-silencing control), packaging plasmid (pCMV delta R8.2) and envelope plasmid (pMD.2G) have been mixed in a ratio of 3:2:1. Calcium chloride solution has been added to a final concentration of 0.5 M. While the calcium chloride-plasmid mixture has been mixed thoroughly the same volume of 2x Hepes-buffered NaCl solution has been added drop by drop. The final mixtures have been incubated for 3 min at room temperature, mixed again and then carefully been added drop by drop to the HEK293T cells. The next day cell supernatant has been removed and 5 ml fresh culture medium was added carefully to each dish. HEK293T cells have been incubated for 24 hours at 37°C in 5 % CO_2 before the first virus harvest was performed. For that purpose HEK293T cell supernatant was removed, stored at 4°C and HEK293T cells were covered for a second time with 5 ml of cell culture medium per dish. After another day of incubation the second supernatants was removed and mixed with the respective first supernatant. The resulting virus solutions were centrifuged at 2,000 x g for 10 min at 4°C. To remove residual cell debris supernatants have been transferred to new tubes and sterile filtered (0.45 µm pores). Virus solution has either been used immediately for transduction or stored in liquid nitrogen.

Lentiviral transduction and selection of U2932 R1 pGIPZ

U2932 R1 cell concentration was adjusted to 1 x 10^6 cells/mL in RPMI1640 medium supplemented with 20 % FCS, 200 U/ml penicillin, 200 µg/ml streptomycin and 10 µg/mL protamin-sulfate. Equal volume of virus solution (concentrated, 1:2 or 1:3) was added to the cell suspension, mixed and centrifuged at 300 x g for 90 min at 37°C. 7 hours after transduction fresh Medium without protaminsulfate was added to the cells. If green fluorescing cells could be observed, 48h hours after transduction the selection process was started by addition of puromycin

to a final concentration of 1.5 µg/mL to the cells. To control the selection process untransduced cells were also treated with puromycin. Lentiviral transduced U2932 R1 cells have been expanded, checked for GFP expression and frozen for long-term storage as described in section 2.10.1. MiRNA overexpression was regularly confirmed using qRT-PCR.
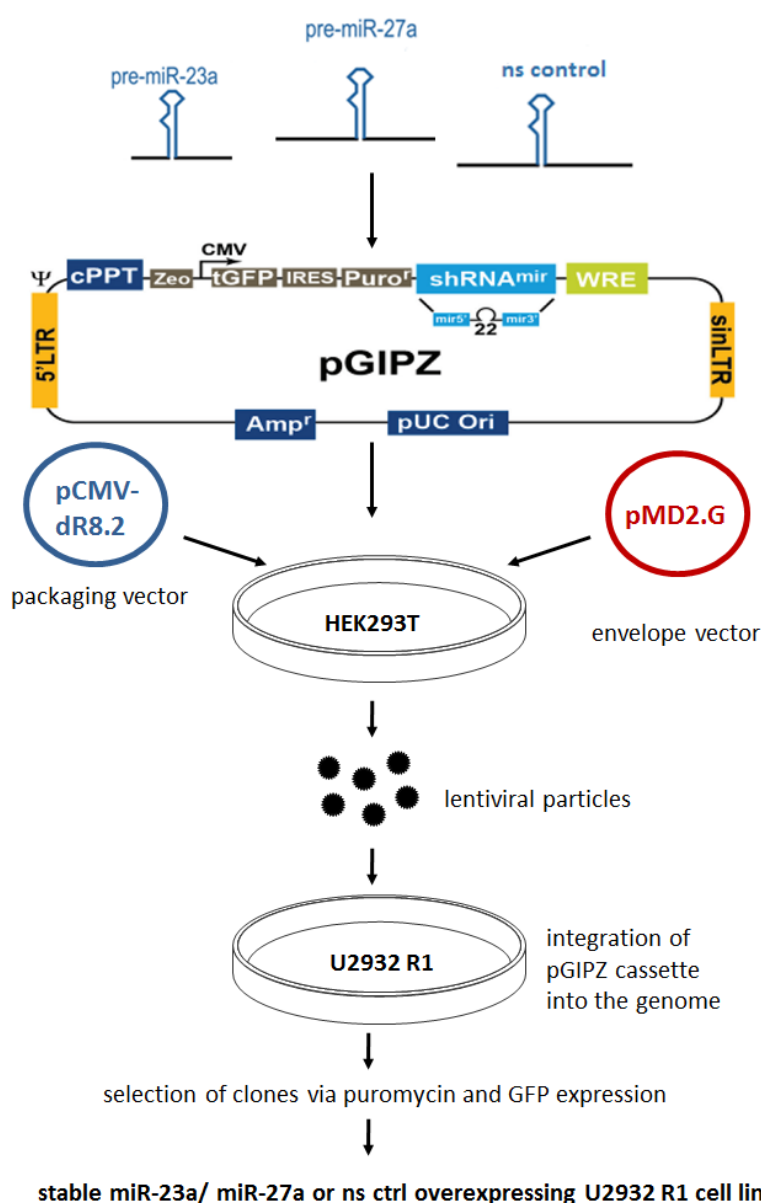
Figure 2.8.: Experimental outline for the generation of stable overexpressing clones
Pre-miR-23a, pre-miR-27a and non silencing control sequences were cloned into the stable transduction vector pGIPZ. Triple tansfection of HEK293T cells with envelope vector pMD2.G, packaging vector pCMV∆R8.2 and miRNA encoding vector pGIPZ in a ratio of 1:2:3 and lead to the secretion of lentiviruses coding for the respective miRNA or non silencing control. The virus containing supernatant of HEK293T cells was subsequently used to infect the DLBCL cell line U2932 R1. Positive clones were selected by puromycin and GFP expression.

2.10.8. Flow cytometry

FACS (fluorescence activated cell sorting) analysis was performed with the BD FACS Calibur
and FACS Aria III flow cytometer and the BD FACS DIVA software. To analyze the cells, 1 x
10^6 cells were harvested, washed once with PBS and resuspended in 500 µL PBS. Cells were
either stained with antibody according to the manufacturer's instructions or directly supple-
mented with propidiumiodide in an end concentration of 0.004 mg/mL before measurement.
Cells were gated to living PI negative population. For AnnexinV/7AAD staining, cells were not
gated.

2.11. Protein biochemistry

2.11.1. Whole cell lysates and cell fractionation

Whole cell lysates

Cells were harvested by centrifugation at 178 x g for 5 min at 4°C, washed once with PBS
and centrifuged for 4 min at 300 x g at 4°C. For whole cell lysates, cell pellets of 1 x 10^6 to
2 x 10^6cells were resuspended in 50 µL RIPA lysis buffer (supplemented with Protease and
Phosphatase Inhibitor) respectively and incubated on ice for 25 min. Subsequently, residual
cell debris was lost by centrifuging cell suspensions at 20,000 x g for 15 min at 4°C. Super-
natants were transferred to new reaction tubes and total protein amount was measured using
Bradford Assay.

Cell fractionation

Cell fractionation has been performed as described by (Schreiber *et al.*, 1989). In short, cell
pellets of 5 x 10^6 cells were resuspended in 400 µl Nuclear Extract Buffer A and incubated
on ice for 13 min. Afterwards 25 µL 10 % NP-40 solution was added to each tube, mixed
thoroughly for 5 seconds and immediately centrifuged at 15.800 x g for 5 min at 4°C. The
supernatant containing the cytosolic fraction was transferred to a new tube. The pellets were
resuspended in 50 µl Nuclear Extract Buffer B and shaken thoroughly for 1-4 h at 4°C. After
centrifugation at 15.800 x g for 5 min at 4°C the supernatant, containing the nuclear fraction,
was transferred to a new tube and protein amount of both fractions was measured using Brad-
ford assay.

2.11.2. Determination of protein concentration by Bradford assay

Determination of protein concentration was carried out by photometrical analysis using a modified Bradford assay (Bradford, 1976). A BSA standard curve was prepared and protein samples were diluted 1:200. 100 µL of Bradford solution was added to 50 µL diluted samples and BSA standards and incubated for 10 min at RT. Measurement was performed at 620 nm with Thermo Multiscan Ex Platereader. Protein concentration was calculated, adjusted with RIPA to 1 µg/µL and boiled for 5 min at 95°C in 6x Laemmli Buffer. Samples were stored at -20°C.

2.11.3. SDS PAGE and Western Blotting

SDS PAGE

Sodium dodecyl sulfate (SDS) polyacrylamide gel electrophoresis (PAGE) was used for separation of proteins according to molecular weight (Laemmli, 1970). Modified buffers listed in table 2.3 were used to prepare a gel composed of a 5% stacking and a 10-15% separation gel. 15 -25 µg total protein per sample was loaded onto the gel and electrophoresis was performed in 1x Running buffer at constant 15 mA per gel for the stacking gel and 30 mA per gel for the separation gel.

Western blotting and immunodetection

Separated proteins were transferred from SDS gel onto a hydrophobic PVDF membrane using wet tank sandwich method (Renart *et al.*, 1979; Towbin *et al.*, 1979). The membrane was activated for 30 sec in 100% MeOH, rehydrated in H_2O for 2 min and equilibrated in transfer buffer prior to use. Membrane and gel were stacked between filter papers into a wet tank chamber filled with ice cold transfer buffer. Protein transfer was performed at 4°C and 100V for 1 h. Effective transfer of proteins was visualized by ponceau S staining and unspecific binding sites were blocked using 5% BSA-TBS-T for 1 h at RT. After blocking, antibody solutions listed in table 2.8 were added over night at 4°C. Next day, blots were washed four times 5 min with 1x TBS-T. The secondary HRP coupled antibody against the species of origin of the first antibody was added in a dilution of 1:10,000 in 5% BSA-TBS-T for 1 h at RT. The membrane was washed four times for 5 min with TBS-T, before detection of bound antibody using Western lightning Plus ECL Solution and Western Lightning Image Reader. For reblotting, the membrane was stripped of bound antibody for 20 min with 1x ReBlot mild buffer, blocked in 5% BSA-TBS-T for 60 min at RT and another primary antibody was added over night as described before.

2.11.4. Ago2-RNA immunoprecipitation

The protocol for Ago2-RNA Immunoprecipitation (Ago2-RIP) used in this thesis was based on the paper "Systematic Analysis of Viral and Cellular MicroRNA Targets in Cells Latently Infected with Human γ-Herpesvirus by RISC Immunoprecipitation Assay" (Dölken *et al.*, 2010).

1.5×10^8 cells per replicate were harvested and washed twice in cold PBS before lysis in 4.2 mL Ago2-RIP lysis buffer in DNAlo bind reaction tubes. DTT, protease inhibitors and RNase-Out were prepared freshly and added immediately before use. Lysates were incubated for 20 min on ice, frozen at -80°C for 10 min and thawed for 8 min at 30°C and 300 rpm. Cell lysates were cleared by centrifugation at 15,000 x g for 30 min at 4°C. An aliquot was taken as input control for Western blotting. Supernatants were supplemented with 4.5 mg magnetic beads that were coupled to 3.6 µg rat anti human Ago2 antibody or isotype control over night at 4°C and washed once with Ago2-RIP wash buffer supplemented with protease and RNase inhibitors. After incubation for 2.5 h rotating at 4°C, an aliquot from the supernatant was taken as depletion control for Western blotting and the beads were washed 5 times with ice cold Ago2-RIP wash buffer supplemented with protease and RNase inhibitors followed by two wash steps with ice cold PBS supplemented with RNase inhibitor. An aliquot of beads was taken for Western blotting output control. RNA was recovered from the remaining beads by adding 1 mL Qiazol. Total RNA was prepared using the miRNeasy kit (QIAGEN) following the manufacturer's instructions including DNase digestion.

CDNA library preparation and Next Generation Sequencing were performed at the GMAK, HZI Brunswick using Illumina kits and technology. For mRNA sequencing, poly A enrichment was applied (ScriptSeq™ v2 RNA-Seq Library Preparation kit, Illumina). For small RNA sequencing no enrichment was performed (TruSeq Small RNA Library Preparation kit). For sequencing library pool of 12 pM was multiplexed on a single lane. Cluster generation was performed with cBot (Illumina) using TruSeq SR Cluster Kit v3–cBot-HS (Illumina). Samples were sequenced (50 bp single-end) on the Illumina High Seq 2500 using TruSeq SBS Kit v3 - HS (Illumina) for 50 cycles.

RNA sequencing reads were pre-processed including trimming of reads (fastq-mcf, ea-utils) and quality control (FastQC) ensuring high quality reads and removal of adapter sequences. Trimmed reads were mapped to the human genome (hg38) by STAR (Dobin *et al.*, 2013) and counted by HTseq (Anders *et al.*, 2015). Further analysis was performed using the software environment R/Bioconductor and the respective software packages. Normalization was performed according to total number of reads within a sample and between samples (Anders *et al.*, 2010). Thresholds for differentially expressed genes were set to at least 2-fold enrichment and a Benjamini-Hochberg adjusted p-value lower than 0.05.

For gene ontology analyses of differentially expressed genes sets, the R-packages goseq and Go.db were used (Young *et al.*, 2010).

2.12. Molecular Biology

2.12.1. Total RNA isolation

Total RNA of cell pellets (1-5 x 10^6 cells, beads from Ago2-RIP assay) was isolated using the miRNeasy kit (QIAGEN) t according to the manufacturer's instructions. Total RNA was eluted in 40 µl RNAse free water and the corresponding concentration has been determined using the NanoDrop2000.

2.12.2. Reverse transcription

The Superscript II first-strand synthesis kit (Invitrogen) and random hexamer primers have been used for the reverse transcription of mRNA to cDNA. For the cDNA synthesis 1 - 2 µg total RNA were mixed with RNAse free water to a final volume of 10 µL. 2 µL random hexamer primers (100 µM) were added, mixed and incubated at 70°C for 10 min in a thermocycler. Subsequently, the tubes were cooled on ice before adding 8 µL master mix. The mixture was incubated for 10 min at RT, before incubation in a thermocycler with the program shown in table 2.12.

Master mix		Thermocycler program	
4 µL	5x First Strand Buffer	60 min	42°C
2 µL	0.1 M DTT	10 min	65°C
1 µL	dNTPs (10 mM each)	constant	4°C
1 µL	SuperScript RT II		

Table 2.12.: Master mix and thermocycler program for reverse transcription of mRNAs

For miRNA detection, the miScript cDNA kit (Qiagen) was used. 1 µg total RNA (isolated with the miRNeasy kit, Qiagen) was adjusted to a volume of 10 µL with RNase free water. 10 µL RT-Mastermix (see table 2.13) was added. High Flex buffer was used for parallel reverse transcription of miRNA, mRNA and pre-miRNA. For reverse transcription of mature miRNAs only, the High Spec buffer was used. The RNA-Mastermix solution was incubated for 1-2 min at ice before starting the reverse transcription using the following protocol:

Master mix		Thermocycler program	
4 μL	5x miScript Buffer	60 min	37°C
2 μL	miScript Nucleics Mix	5 min	95°C
1 μL	miScript II RT Mix	constant	4°C

Table 2.13.: Master mix and thermocycler program for reverse transcription of mRNAs, pre-miRNAs and miRNAs

2.12.3. Quantitative real-time polymerase chain reaction (qRT-PCR)

For relative transcript quantification, the fluorescent DNA binding dye SYBR Green was used. If SYBR Green binds double-stranded DNA, this complex of DNA and the SYBR Green dye will absorb blue light (λmax = 488 nm) and emit green light (λmax = 522 nm). Therefore, the increasing fluorescence is used to quantify the amount of transcripts, which corresponds to the number of PCR cycles with an exponential increase of fluorescence (cycle threshold = C_T-value). For the PCR reaction and the simultaneous fluorescence detection, the Applied Biosytems 7500 Fast Real-Time PCR System was used.

For detection of mRNAs each reaction contained 10 μL SsoFast™ EvaGreen® Supermix (Bio-rad), 10 pmol of each primer and 2-25 ng cDNA mRNA and had a final volume of 20 μl. For detection of miRNAs or pre-miRNAs each reaction contained 10 μL 2 x QuantiTect SYBR Mix, 2 μL 10 x Universal Primer and 2 μL 10 x miScript Primer (for pre miRNA detection no Universal primer was added) and 2 -10 ng miScript cDNA in an final volume of 20 μL.

Each analysis has been performed in technical triplicates. The corresponding qRT-PCR programs are shown in table 2.14. A melt curve was performed after each PCR run to identify unspecific PCR products.

Gene expression was evaluated relative to a house keeper using the SDS 2.4 and RQ Manager 1.2.1 (Applied Biosystems). Target gene transcript abundance was calculated using the $\Delta\Delta C_T$ method. Therefore, the actual C_T-values of genes of interest have been normalized to the C_T-values of the house keeper:

$$\Delta C_T = C_{T\ geneofinterest} - C_{T\ housekeeper}$$

The changes between a treated sample and untreated controls is formed as follows:

$$\Delta\Delta C_T = \Delta C_{T\ treatment} - \Delta C_{Tcontrol}$$

The number of cycles exponentially correlates with the amount of detected DNA in the sample, thus relative n-fold changes can be calculated as:

$$RQ = 2^{-\Delta\Delta C_T}$$

For mRNA detection C_T values in this study were normalized to *GAPDH.* For miRNA or pre-miRNA detection C_T values were normalized to *SNORD48.*

miScript PCR			SSoFast mix PCR		
95°C	15 min		95°C	2 min	
94°C	15 s		95°C	3 s	
55°C	30 s	40x			40x
70°C	34 s		60°C	25 s	

Table 2.14.: qRT-PCR programs

2.12.4. Conventional PCR

Polymerase chain reaction (PCR; (Mullis *et al.*, 1986)) was used for amplification of DNA-fragments and addition of restriction sites for cloning purposes. A typical PCR reaction, was performed according to following protocol:

component	amount
template	1 colony/100 ng DNA
reaction buffer	1x
primer fw	20 pmol
primer rev	20 pmol
dNTP mix	4 mmol
polymerase	1 U
total volume	15 µL

thermocycling conditions:

initial denaturation	5 min	95°C	
denaturation	30 s	95°C	
annealing	30 s	$T_{melting}$	25x
elongation	1 min/kb	72°C	
final elongation	5 min	72°C	

Table 2.15.: conventional PCR

2.12.5. DNA restriction digestion

For sequence specific hydrolysis of plasmid DNA, restriction endonucleases and the corresponding buffers from Thermo Scientific were used. For hydrolysis of plasmid DNA with two different restriction endonucleases the following protocol was used:

	analytical		preparative
1 µg	plasmid DNA	3 µg	plasmid DNA
3 U	restriction endonuclease 1	10 U	restriction endonuclease 1
3 U	restriction endonuclease 2	10 U	restriction endonuclease 2
2 µL	10 x reaction buffer	5 µL	10 x reaction buffer
x	dd H_2O	x	dd H_2O
20 µL	final volume	50 µL	final volume

Table 2.16.: DNA restriction digestion

Analytical samples were incubated for 1 h and preparative samples over night at 37°C. Temperatures and buffers were chosen according to the manufacturer's instructions.

2.12.6. Agarose gel electrophoresis

The negative charged DNA fragments can be separated according to their molecular weight within an electrical field. Therefore, the DNA was mixed with 6 x loading dye (50% (v/v) glycerol, 0.21% (w/v) bromphenole blue, 0.1% (w/v) xylene blue, 0.2 M EDTA pH 8.0) and loaded onto a TAE-agarose gel (1-2 % (w/v) agarose in TAE buffer containing 0.5 μg/mL EtBr). The percentage depended on the expected fragment size. Horizontal agarose gel electrophoresis was performed for 30-60 min at 100-120 V in TAE buffer (40 mM Tris-HCL, pH 7.5, 1 mM Na_2-EDTA, pH 8.0, 0.2% (v/v) CH_3COOH). Due to the intercalation of EtBr into double stranded DNA, the DNA fragments could be visualized by exposure to UV-light.

2.12.7. DNA fragment extraction

DNA fragments were extracted from the agarose gel using QIAquick gel extraction kit (Qiagen, Hilden, Germany) according to the manufacturer's instructions.

2.12.8. Determination of DNA and RNA concentration

DNA and RNA concentration was photometrically determined using NanoDrop2000 (Thermo Scientific, St.Leon-Rot, Germany). DNA was measured at 360 nm and 280 nm. The ratio of extinction at 260 nm to 280 nm should be ~1.8 for high quality DNA. RNA was measured at 260 nm and 230 nm. The ratio of extinction at 260 nm to 230 nm should be ~2.0 for high quality RNA.

Before RNA sequencing, the RNA concentration and quality was assessed using Agilent RNA 6000 Pico Kit and Agilent Small RNA kit according to the manufacturer's instructions. RNA was measured at Bioanalyzer2100 and quantified using Agilent Bioanalyzer expert B.02.08.SI648 software. High quality RNA has a RIN value of 8-10.

2.12.9. Ligation of DNA fragments

To mediate covalent linking of DNA fragments, 50 ng of dephosphorylated vector was mixed with the insert in a molecular ratio of 5:1 (sticky end ligation) and incubated with T_4DNA ligase

(Thermo Scientific, St.Leon-Rot, Germany) over night at 16°C. Following standard protocol was used:

amount	component
50 ng	linearized vector
x ng	insert
2 Weiss U	T_4DNA ligase
1 µL	10 x T_4DNA ligase buffer
x	dd H_2O
10 µL	final volume

Table 2.17.: Ligation of DNA fragments

5 µL of the ligation mix was used for transformation into *E.coli DH5* α.

2.12.10. Transformation

Transformation of *E.coli DH5* α was performed by heat shock procedure: an aliquot with 50 µL of chemical competent bacteria were thawed for several minutes on ice before gently mixing with low amounts of plasmid DNA or 1-5 µL of ligation mix. After an incubation of 30 min on ice, heat shock was performed for 90 s at 42°C. The cells were cooled down on ice immediately and afterwards incubated with 200 µL LB-medium for 45 min at 37°C under constant shaking. Finally, the cells were plated onto LB-Agar plates or pipetted into 200 mL fluid LB-medium containing appropriate antibiotics for selection. Flasks or plates were incubated for 16 h at 37°C.

2.12.11. Cultivation of Bacteria

Escherichia coli (E.coli) bacteria were cultured in Luria-Bertani medium (LB medium) at 37°C. For selection of transformed bacteria, media were supplemented with the corresponding antibiotics (final concentration of ampicillin 100 µg/mL).

2.12.12. Plasmid Isolation

Plasmid DNA was isolated using innuPREP Plasmid Mini Kit (Analytic Jena) for cloning approaches or NucleoBond® Xtra Midi Plus EF kit (Machery-Nagel) for transfections in cell lines. Plasmid DNA was dissolved in water and concentration was determined using NanoDrop2000.

3. Results

3.1. Identification of signaling pathways regulating the MIR23A cluster

One aim of this thesis was to identify the signaling pathways responsible for MIR23A regulation in DLBCL. Since the MIR23A cluster expression is induced during normal GC reaction, factors present in the microenvironment of the GC were used to stimulate the cells and tested whether MIR23A cluster expression can be induced.

3.1.1. CD40L signaling does not change MIR23A cluster expression in B-NHL

Signaling via the CD40 receptor plays an important role during B cell maturation (see section 1.2.2). The CD40 receptor activates a cascade of signaling molecules including PI3K and MAPK signaling (JNK, p38 and ERK), resulting in the activation of many transcription factors (Basso *et al.*, 2004). Many described CD40 effects are NF$\varkappa$B dependent, hence it can be considered as main downstream effector (Berberich *et al.*, 1994). Previous data from our group already confirmed for BL that CD40L stimulation changes global gene expression (Dissertation Alexandra Schrader 2011, published in (Schrader *et al.*, 2012)).

To test whether CD40 signaling regulates the MIR23A cluster in GC derived lymphoma, a BL and a DLBCL cell line were treated with sCD40L and analyzed for MIR23A expression by qRT-PCR.

In order to detect only miR-24 levels that originate from MIR23A cluster and not from MIR23B cluster, the pre-miR-24-2 levels were detected, because the mature miR-24 sequences are identical and cannot be distinguished from each other.

The relative expression levels of mature miR-23a, miR-27a and pre-miR-24-2 do not change upon stimulation with sCD40L, neither in BL-2 nor in U2932 R1 within the tested time period (fig. 3.1). Only in U2932 R1, the pre-miR-23a and pre-miR-27a levels slightly increase after 4 hours of treatment. But this does not affect mature miR-23a and miR-27a levels. Both cell lines respond on CD40L treatment with an increase in *ICAM1* expression levels (Schrader *et al.*, 2012), indicating, that the stimulation was successful.

Lymphoma cells are transformed cells with altered signaling characteristics. Therefore, CD77 germinal center B-cells, which represent the precursor cells of GC derived B cell lymphoma (centroblasts) (Pascual *et al.*, 1994; Klein *et al.*, 2003), were isolated from human pediatric tonsils by MACs technology and treated for 10 h with 200 ng/mL sCD40L. In contrast to the BL and DLBCL cell lines, primary CD77 GCBs respond to sCD40L treatment with a 2-fold

induction of miR-23a and a slight induction of miR-27a (fig. 3.2). Successful CD40L stimulation was verified by the induction of *ICAM1*.

These data indicate that CD40 signaling is not responsible for regulation of the MIR23A in BL and DLBCL.
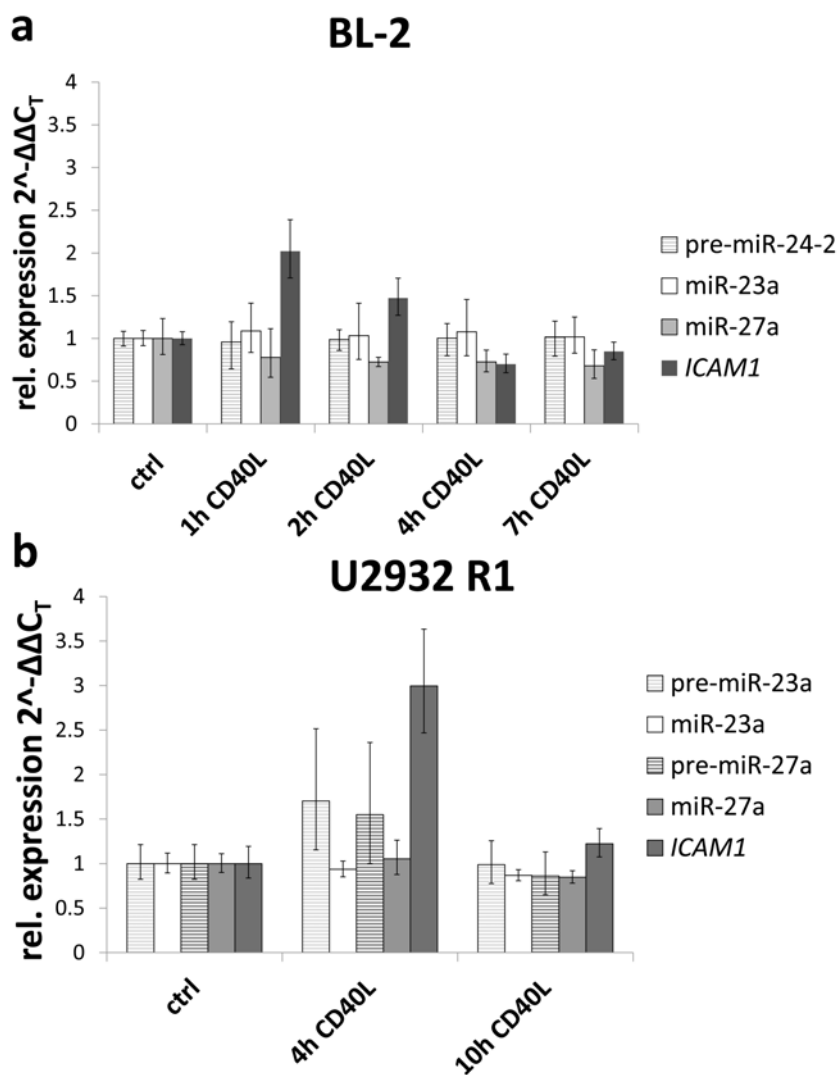
Figure 3.1.: CD40L does not change MIR23A cluster expression in B-NHL cell lines
(a) BL cell line BL-2 and (b) DLBCL cell line U2932 R1 were treated for the indicated time points with 200 ng/µL sCD40L. Relative MIR23A and *ICAM1* levels were detected by qRT-PCR analyses. Mean with 95% CI, endogenous control: *SNORD48* for miRNA, *GAPDH* for mRNA.
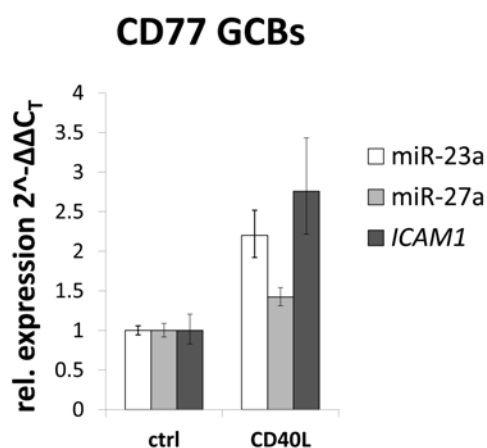
Figure 3.2.: CD40L induces MIR23A cluster expression in primary CD77 GCBs
Primary CD77 positive germinal center B-cells were isolated by MACS technology from human pediatric tonsils and treated for 10h with 200 ng/μL sCD40L. Relative MIR23A levels were detected by qRT-PCR analyses. *ICAM1* served as control for successful CD40L stimulation. One of two experiments is shown. Mean with 95% CI, endogenous control: *SNORD48* for miRNAs, *GAPDH* for *ICAM1*.

3.1.2. LPS does not change MIR23A cluster expression

Bacterial lipopolysaccharide (LPS) is a component of the cell wall of gram negative bacteria. As an T cell independent antigen LPS activates Toll-like receptor 4 (TLR4). TLR4 signaling was shown to activate GC response, resulting in the production of high affinity class switched antibodies of plasma cells (reviewed in (Defranco *et al.*, 2012)).

Activation of TLR4 recruits MyD88 and activates via TRAF6 and TAK1 the MAPK (JNK and p38) and NF$\varkappa$B signaling (reviewed in (Doyle and O'Neill, 2006)). One LPS responsive target gene is *CD58*, which served in this experiment as a control for successful stimulation (Schrader *et al.*, 2012).
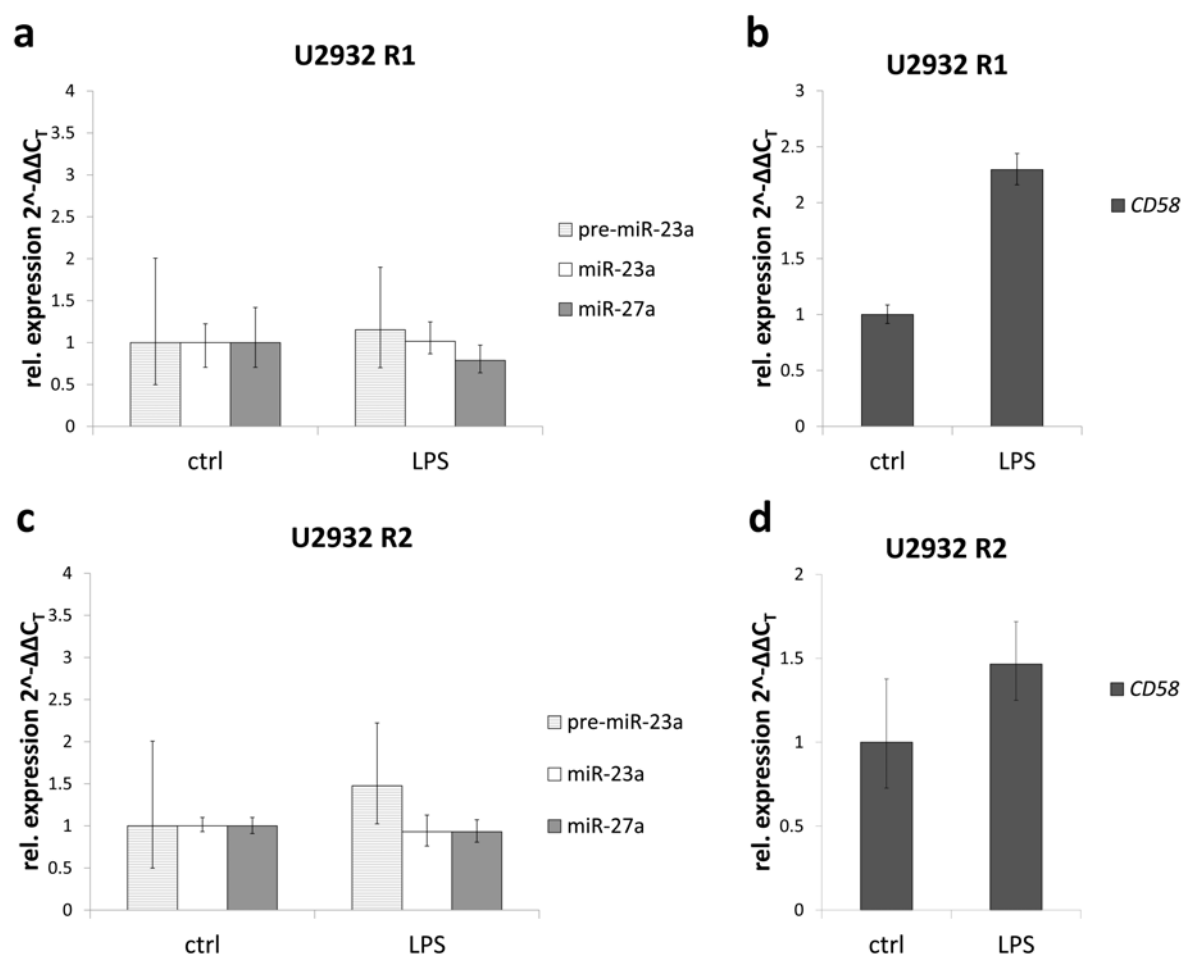
Figure 3.3.: LPS does not change MIR23A expression in DLBCL cell lines U2932 R1 and R2
U2932 R1 (a and b) and U2932 R2 (c and d) were stimulated for 16h with 1 µg/mL LPS. (a and c) relative pre-miR-23a, miR-23a and miR-27a expression levels measured by qRT-PCR. (b) and (d) relative *CD58* levels measured by qRT-PCR. This experiment was performed once. Mean with 95% CI, house keeper: *GAPDH* for *CD58* and *SNORD48* for pre-miR23a and miR-23a/27a.

The U2932 R2 clone responds to LPS stimulation with an increase of 50% of *CD58* expression, but the MIR23A levels are not affected (fig. 3.3 c and d). Although, the U2932 R1 clone responds stronger to LPS treatment with an upregulation of nearly 2.5-fold of *CD58* expression, LPS treatment does not change pre-miR-23a, miR-23a or miR-27a levels.

In summary, together with the previous experiments (section 3.1.1) these data indicate, that downstream NF$\varkappa$B signaling is not central for the regulation of the MIR23A cluster in BL and DLBCL cell lines.

3.1.3. BCR signaling activates the MIR23A cluster in BL and DLBCL

3.1.3.1. BCR signaling activates the MIR23A cluster in BL cell line BL-2

Previous data from our group revealed a large set of transcripts that is altered upon stimulation of the B-cell receptor in the human BL cell line BL-2 (Schrader *et al.*, 2012; Pirkl *et al.*, 2015). The gene expression micro array used in the latter publication to detect transcript expression in this cell line covers the whole human transcriptome including non-coding RNAs and is therefore able to detect precursor transcripts of miRNAs (dissertation Elisabeth Hand 2013, published in (Pirkl *et al.*, 2015)). Hence, this micro array data set was used in this study to analyze MIR23A and paralogous MIR23B cluster expression patterns upon BCR stimulation during a time course in BL-2 (fig. 3.4). An increase of pre-miR-24-2 transcript 60 min upon anti-IgM F(ab)2-fragment stimulation, followed by pre-miR-23a after 210 min, but no induction of pre-miR-27a in the examined time span of stimulation was observed (fig. 3.4 a). Since all pre-miRs of the MIR23A cluster are processed from a single polycistronic transcript one would expect, that all pre-miRs are induced. Moreover, one could speculate that the time order in which the pre-miRs are induced may correlate with the position at which they are encoded on the primary transcript.

The paralogous MIR23B cluster is also induced upon anti-IgM F(ab)2-fragment stimulation as pre-miR-27b expression increases 180 min after stimulation (fig. 3.4 b). Instead, pre-miR-23b and pre-miR-24-1 levels are not affected. These observations raise the question, whether the DNA probes of the micro array correctly detect the small precursor transcripts.
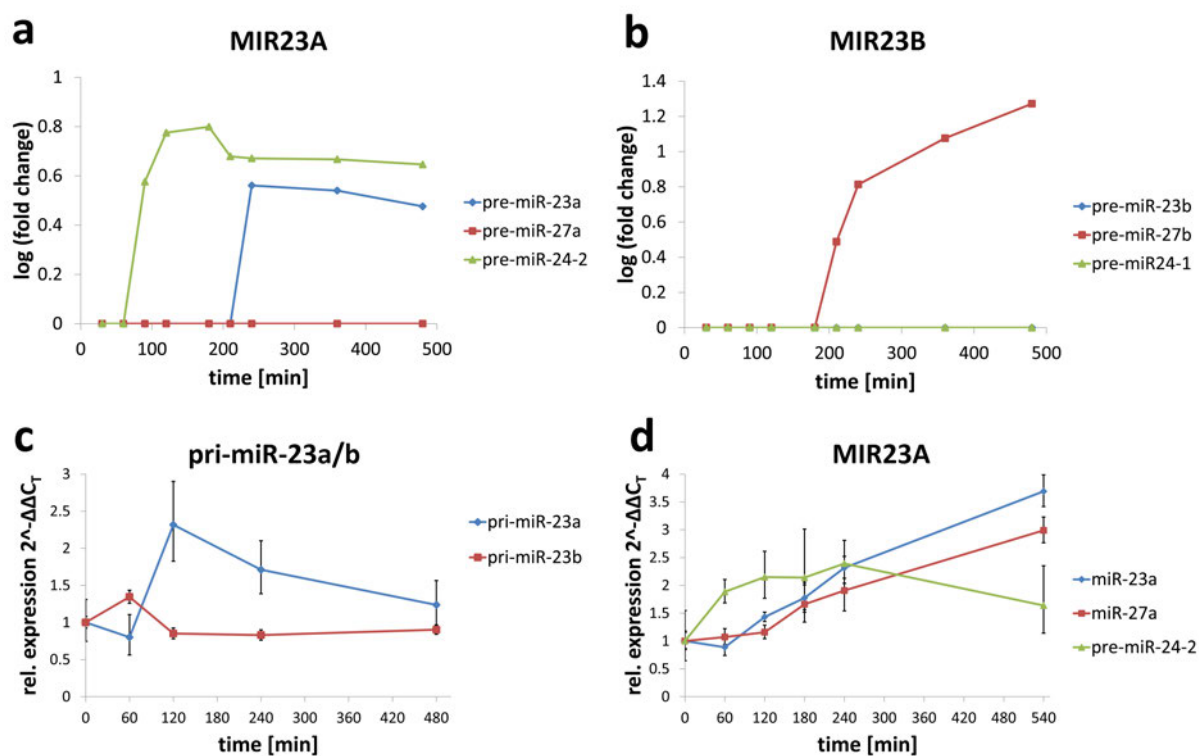
Figure 3.4.: Induction of MIR23A cluster in BL cell line BL-2 upon BCR stimulation
(a) and (b) Micro array gene expression analyses of MIR23A cluster (a) and MIR23B cluster (b) in BL cell line BL-2 upon stimulation with 13 µg/mL anti-IgM F(ab)2-fragment for a 480 min time course. The mean of three experiments is shown. Microarray gene expression dataset taken from the dissertation of Elisabeth Hand in 2013, published in (Pirkl *et al.*, 2015). (c) and (d) qRT-PCR gene expression analyses of relative (c) pri-miR-23a/b and (d) miR-23a, miR-27a and pre-miR-24-2 expression in BL-2 upon 13 µg/mL anti-IgM F(ab)2-fragment stimulation in a time course experiment. Mean with 95% CI, endogenous controls: c) *GAPDH* d) *SNORD48*. One out of two representative experiments is shown.

Therefore, the micro array data were validated by quantitative real time PCR analyses (see fig. 3.4 c an d). According to the micro array data both MIR23 clusters are activated upon BCR stimulation. Interestingly, the qRT-PCR data show, that the primary transcript of the MIR23A cluster is clearly induced, while the primary transcript of the MIR23B cluster shows only minor expression changes (fig. 3.4 c). Next the expression of the mature miRNAs was analyzed by qRT-PCR (fig. 3.4 d). Because the mature miR-24 sequence is identical disregarding from which locus it is transcribed, the precursor transcript pre-miR-24-2, which can be clearly distinguished from the pre-miR-24-1 transcript, was analyzed. As expected the pre-miR24-2 transcript is induced first followed by an induction of mature miR-23a and miR-27a after 120 min. While the expression of the mature miRNAs constantly increases, the pre-miR-24-2 transcript reaches its maximum of 2-fold induction after two hours followed by a decrease.

In summary, these data show for the first time that BCR signaling is responsible for the activation of the MIR23A cluster in BL.

3.1.3.2. BCR signaling activates the MIR23A cluster in DLBCL cell line U2932 R1

Since BCR signaling was demonstrated to activate the MIR23A cluster in BL-2 cell line (see section 3.1.3.1), it was questioned whether a DLBCL cell line, which develops from later stages in GC reaction can also activate the MIR23A cluster expression in response to BCR signaling. Therefore, the DLBCL cell line U2932 R1 was chosen as a model cell line (Quentmeier *et al.*, 2013). This cell line is on the one hand well characterized and shows on the other hand relatively low levels of MIR23A cluster, making it favorable for induction and overexpression experiments. Indeed, the MIR23A levels are induced upon BCR cross-link in DLBCL cell line U2932 R1 (fig. 3.5 a).
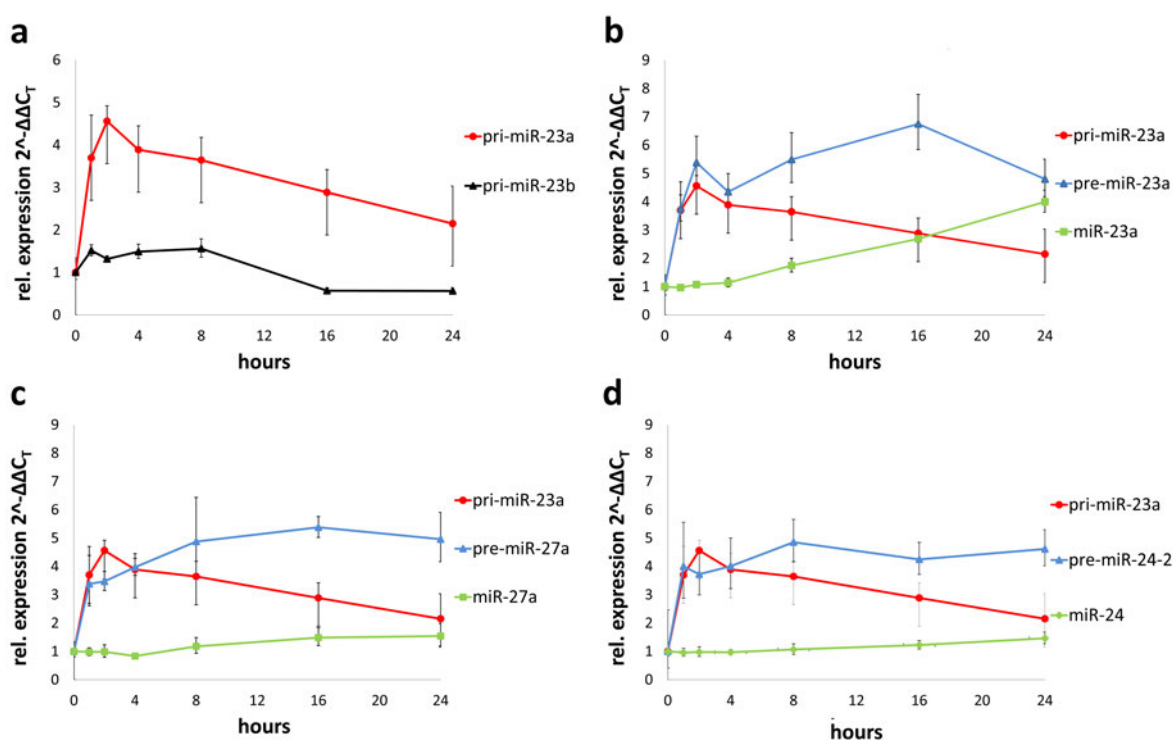
Figure 3.5.: Induction of the MIR23A cluster in DLBCL cell line U2932 R1 upon BCR stimulation
The DLBCL cell line U2932 R1 was treated with 13 µg/mL anti-IgM F(ab)2-fragment . Relative MIR23A expression was measured after 1, 2, 4, 8, 16 and 24 hours of stimulation by qRT-PCR. (a) primary transcript expression of MIR23A and paralogous MIR23B cluster. (b) pri-/pre- and mature miR-23a expression. (c) pri-miR-23a, pre-miR-27a and mature miR-27a expression. (d) pri-miR-23a, pre-miR-24-2 and mature miR-24 expression. Mean with 95% CI, endogenous control: *GAPDH* for pri-miRs and *SNORD48* for mature and pre-miRs, one representative experiment out of two is shown.

The primary miR-23a transcript is induced already after 60 min of BCR stimulation reaching its maximum of 4.5-fold induction after 2 hours followed by a slow decrease. Instead, the primary transcript of the paralogous cluster (pri-miR-23b) is only induced 1.5-fold after 60 min, stays constant before it starts to decrease after 8 hours (fig. 3.5 a). Because the induction of the paralogous cluster is weak compared to the MIR23A cluster all following analyses focus on the MIR23A cluster.

Interestingly, the kinetics of miRNA processing are fast, since the precursor transcripts of all three miRNAs (blue lines in fig. 3.5 b, c and d) are induced already within 60 min, at the same time as the primary transcript does. All precursor transcripts reach their maximum between 8 and 16 hours and decrease afterwards very slowly. With a short time delay after precursor induction the mature miRNAs (green lines fig. 3.5 b, c and d) levels increase. The miR-23a expression is induced after 5-8 hours followed by a slight induction of miR-27a after 8 hours of stimulation, while miR-24 is not induced.

These data together with data from section 3.1.3.1 demonstrate that BCR signaling is responsible for the MIR23A cluster activation in BL and in DLBCL cell lines.

3.1.3.3. BCR dependent MIR23A activation is a general mechanism in DLBCL, but not in healthy germinal center B cells

BCR signaling induced the MIR23A cluster expression in a BL and a DLBCL cell line (section 3.1.3.1 and 3.1.3.2). The focus of this study was to elucidate the regulation of MIR23A cluster in DLBCL. To analyze whether the activation of the MIR23A cluster is a general mechanism in DLBCL, the DLBCL cell lines U2932 R2 (sister clone of U2932 R1, "ABC-like" DLBCL), OCI-LY3 (ABC-DLBCL) and OCI-LY7 (GCB-DLBCL) were stimulated with anti-IgM F(ab)2-fragment or anti-IgG F(ab)2-fragment, respectively. Furthermore, primary non transformed CD77 positive germinal center B cells (CD77 GCBs) (Pascual *et al.*, 1994; Klein *et al.*, 2003) were isolated from human pediatric tonsils and treated in the same manner as the DLBCL cell lines in order to analyze whether the induction of MIR23A cluster by BCR signaling is a physiological or an aberrant process.

All tested DLBCL cell lines respond with an induction of MIR23A cluster expression upon BCR stimulation. In general, the miR-23a induction is stronger than the miR-27a induction, except for OCI-LY3, where both were induced 2-fold. In contrast, primary non-transformed CD77 GCBs do not respond with an increase of miR-23a or miR-27a upon BCR cross-link, although the BCR signaling is clearly activated since one BCR target gene *SLAMF7* (Schrader *et al.*, 2012) is induced (fig. 3.6 b).

These data strongly indicate that BCR mediated MIR23A cluster activation is a general mechanism in BL and DLBCL. Although GCBs show active BCR signaling upon stimulation, they do not upregulate the MIR23A cluster upon activation. This indicates that BCR signaling is aberrantly modified in BL and DLBCL.
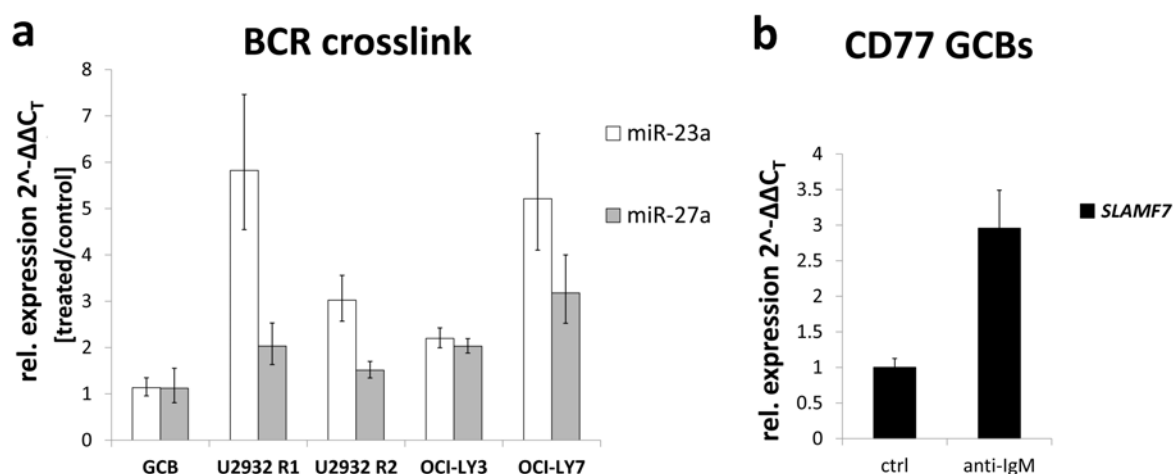
Figure 3.6.: BCR signaling activates MIR23A cluster in different DLBCL cell lines, but not in healthy control cells
The BCR was cross linked in different DLBCL cell lines for 16 hours with 13 µg/mL anti-IgM F(ab)2- or anti-IgG F(ab)2-fragment and in primary CD77 germinal center cells for 10 hours with 13 µg/mL anti-IgM F(ab)2-fragment. (a) miR-23a, miR-27a and (b) SLAMF7 expression were detected by qRT-PCR. Mean with 95% CI, endogenous control: *GAPDH* for *SLAMF7* and *SNORD48* for miRNAs. One representative experiment of three for the cell lines and two for GCBs is shown.

3.1.3.4. Inhibition of protein de-novo synthesis does not affect the MIR23A activation upon BCR stimulation

To test whether the MIR23A cluster is induced by direct downstream signaling, the U2932 R1 cells were treated with cyclohexamide (CHX) simultaneously to BCR stimulation. CHX inhibits protein de-novo synthesis by blocking translation elongation of the ribosome. Under this conditions only transcription factors, that were activated by direct upstream signaling, but not by secondary effects, are translocated into the nucleus and can induce MIR23A cluster expression. In order to control effective CHX treatment, the c-MYC protein levels were analyzed. C-MYC has a high protein turnover rate, being rapidly degraded by the proteasome (Gregory and Hann, 2000). Thus, it functions perfectly as an indicator for effective ribosomal inhibition.

As depicted in fig. 3.7 a) the MIR23A levels (pri-miR-23a, pre-miR-23a and pre-miR-27a) can still be activated upon BCR stimulation with anti-IgM F(ab)2-fragment, when protein de-novo synthesis is effectively blocked by CHX treatment. Notably, c-MYC accumulates upon BCR stimulation in U2932 R1 fig. 3.7 b), hence it was further analyzed as a potential transcription factor responsible for MIR23A regulation in section 3.1.3.6.

In summary, no protein de-novo synthesis is required for BCR dependent activation of the MIR23A cluster, indicating a direct activation of MIR23A promoter.
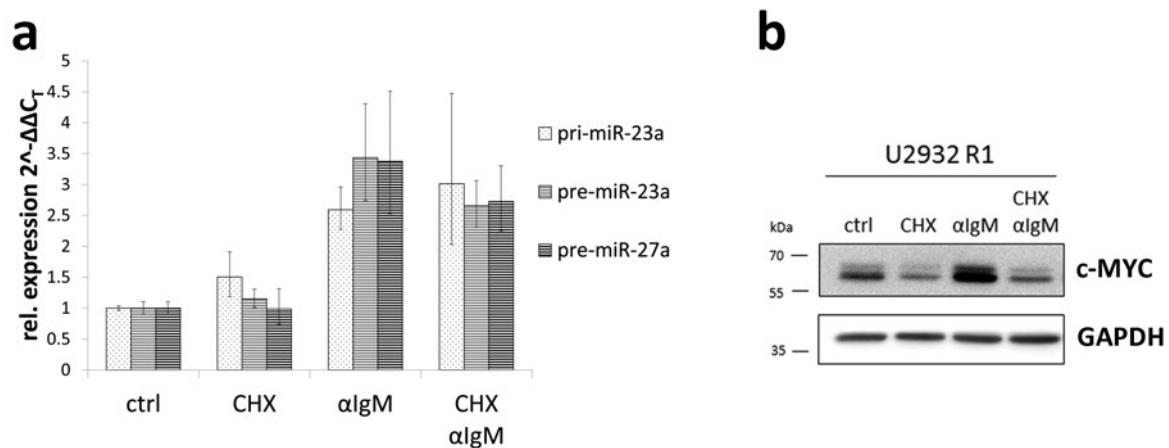
Figure 3.7.: Inhibition of protein de-novo synthesis does not interfere with MIR23A activation upon BCR cross-link

U2932 R1 was pre-treated for 1 h with 100 µg/mL cyclohexamide (CHX) before stimulation with 13 µg/mL anti-IgM F(ab)2-fragment for 2 h. (a) qRT-PCR analyses of pri-miR-23a, pre-miR-23a and pre-miR-27a (b) Western blot analyses of c-MYC. GAPDH served as loading control. Mean with 95% CI, endogenous control: *SNORD48* for pre-miRNAs and *GAPDH* for pri-miR, one representative experiment of three is shown.

3.1.3.5. BTK/MEK/ERK signaling activates the MIR23A cluster

In order to narrow down which signaling cascade downstream of the BCR is responsible for activation of the MIR23A cluster in U2932 R1, the key enzymes BTK, MEK, PI3K and AKT, which mediate the downstream effects of BCR (section 1.2.1), were systematically inhibited by treatment with chemical inhibitors. These pre-treated cells were then stimulated with anti-IgM F(ab)2-fragment followed by MIR23A cluster expression analyses. NF$\varkappa$B signaling was excluded, because previous experiments showed no effect on MIR23A cluster expression when stimulating this pathway in BL (BL-2) or DLBCL (U2932 R1) cell lines (fig. 3.1.1 and 3.1.2).

Ibrutinib irreversibly inhibits the Burton tyrosine kinase (BTK) by covalent binding to Cys-481 in the ATP binding domain (Davids and Brown, 2014). BTK is one of the first proteins that is phosphorylated upon antigen binding. Importantly, BTK plays a key role in BCR signaling, because it spreads the message by phosphorylation of PLCγ2 onto different downstream cascades: the ERK, NF$\varkappa$B and PI3/AKT signaling. As a consequence, BTK inhibition should impair all signaling cascades downstream of the B cell receptor. As a proof of principle it should no longer be possible to activate the MIR23A cluster, when treating the cells with Ibrutinib and anti-IgM F(ab)2-fragment simultaneously. This is exactly what could be observed when performing this experiment with U2932 R1 (fig. 3.8 a): The pre-miR-23a and pre-miR-27a levels are activated upon anti-IgM F(ab)2-fragment stimulation as already previously observed. Treatment with Ibrutinib alone does not alter pre-miR-23a and pre-miR-27a expression levels. Furthermore, the used ibrutinib concentration was not toxic to the cells, as shown in MTT assays (fig. A.3). As expected, the MIR23A cluster is not activated upon double treatment with Ibrutinib and anti-IgM F(ab)2-fragment. As shown in fig. 3.8 b) and 3.9 b) Ibrutinib effectively inhibited phosphorylation of BTK and further downstream of P-ERK.
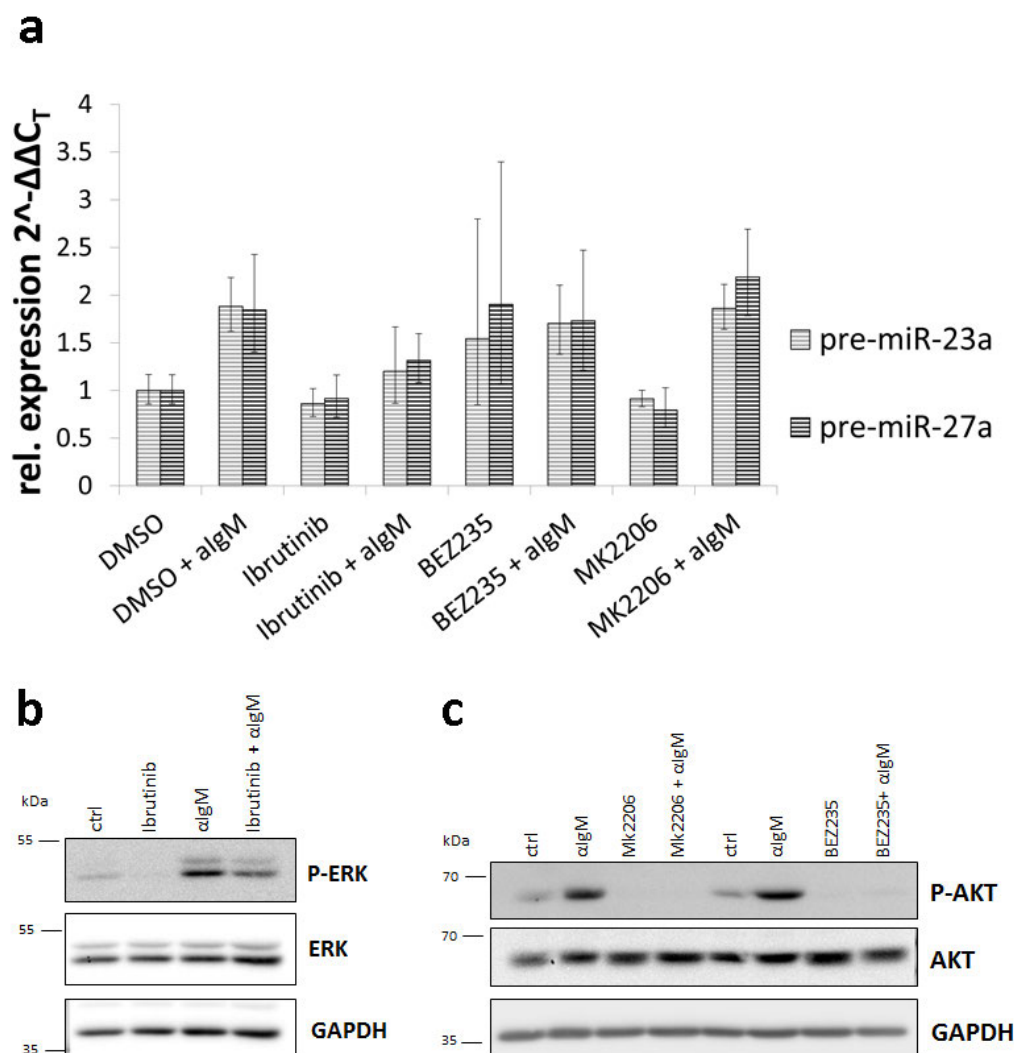
Figure 3.8.: MIR23A cluster expression upon inhibition of key enzymes of BCR signaling
U2932 R1 was pre-treated for 2 hours with the respective inhibitor (1 μM Ibrutinib, 200 nM BEZ235, 3 μM MK2206) before simultaneous stimulation with 13 μg/mL anti-IgM F(ab)2-fragment for 2h. Relative expression levels of (a) pre-miR-23a and pre-miR-27a were detected by qRT-PCR analyses. (Mean with 95% CI, endogenous control: SNORD48) (b-c) Western blot analyses of BCR downstream kinases P-ERK/ERK and P-AKT/AKT. GAPDH served as loading control. One representative experiments of three is shown.

BEZ235 is an ATP-competitive PI3-kinase (p110α/γ/δ/β) and mTOR (p70S6K) inhibitor. PI3K phosphorylates PIP2 to make PIP3, which recruits PDK1 and AKT to the cell membrane, where AKT is activated by phosphorylation of mTORC2 and PDK1. Treatment with BEZ235 inhibits therefore effectively the PI3K/mTOR/AKT signaling (Barrett *et al.*, 2012). Indeed, Western blot analyses show effective inhibition of P-AKT in U2932 R1 (fig. 3.8 c). The pre-miR-23a and pre-miR-27a levels are slightly increased upon treatment of U2932 R1 with BEZ235 alone, but can not be further increased when treated together with anti-IgM F(ab)2-fragment (fig. 3.8 a). However, the error bars are high, making interpretations difficult. In order to interpret these data

correctly, in a next experiment the cells were treated with an additional inhibitor specific for AKT: MK2206. MK2206 allosterically inhibits auto-phosphorylation of T308 and S473 of AKT1, 2 and 3. It thereby prevents the AKT-dependent phosphorylation of numerous downstream targets. Indeed, the control Western blot shows an effective inhibition of AKT phosphorylation (fig. 3.8 c). In contrast to BEZ235, MK2206 itself does not increase the pre-miR-23a or pre-miR-27a levels (fig. 3.8 a). However, double treatment with MK2206 and anti-IgM F(ab)2-fragment lead to an activation of the MIR23A cluster. Therefore, AKT signaling is not responsible for MIR23A cluster activation upon BCR stimulation in U2932 R1.

Next, the MAPK/ERK signaling was studied by inhibition of MEK1/2 with Trametinib in U2932 R1. Trametinib is a high specific inhibitor acting allosterically and reversible (Lugowska *et al.*, 2015). Non-toxic concentrations of trametinib were used for the following experiments (see MTT assays fig. A.3) Interestingly, Trametinib alone slightly downregulated pri-miR-23a, pre-miR-23a and pre-miR-27a levels (fig. 3.9 a). Furthermore, cells that were pre-treated with Trametinib were not able to activate the MIR23A cluster when simultaneously stimulated with anti-IgM F(ab)2-fragment. As a control, Western blot analyses (fig. 3.9 b) show that Trametinib effectively inhibited downstream ERK phosphorylation.

These observations indicate that BTK/MEK/ERK signaling is the BCR downstream cascade that is predominantly responsible for the MIR23A cluster activation in DLBCL model cell line U2932 R1.
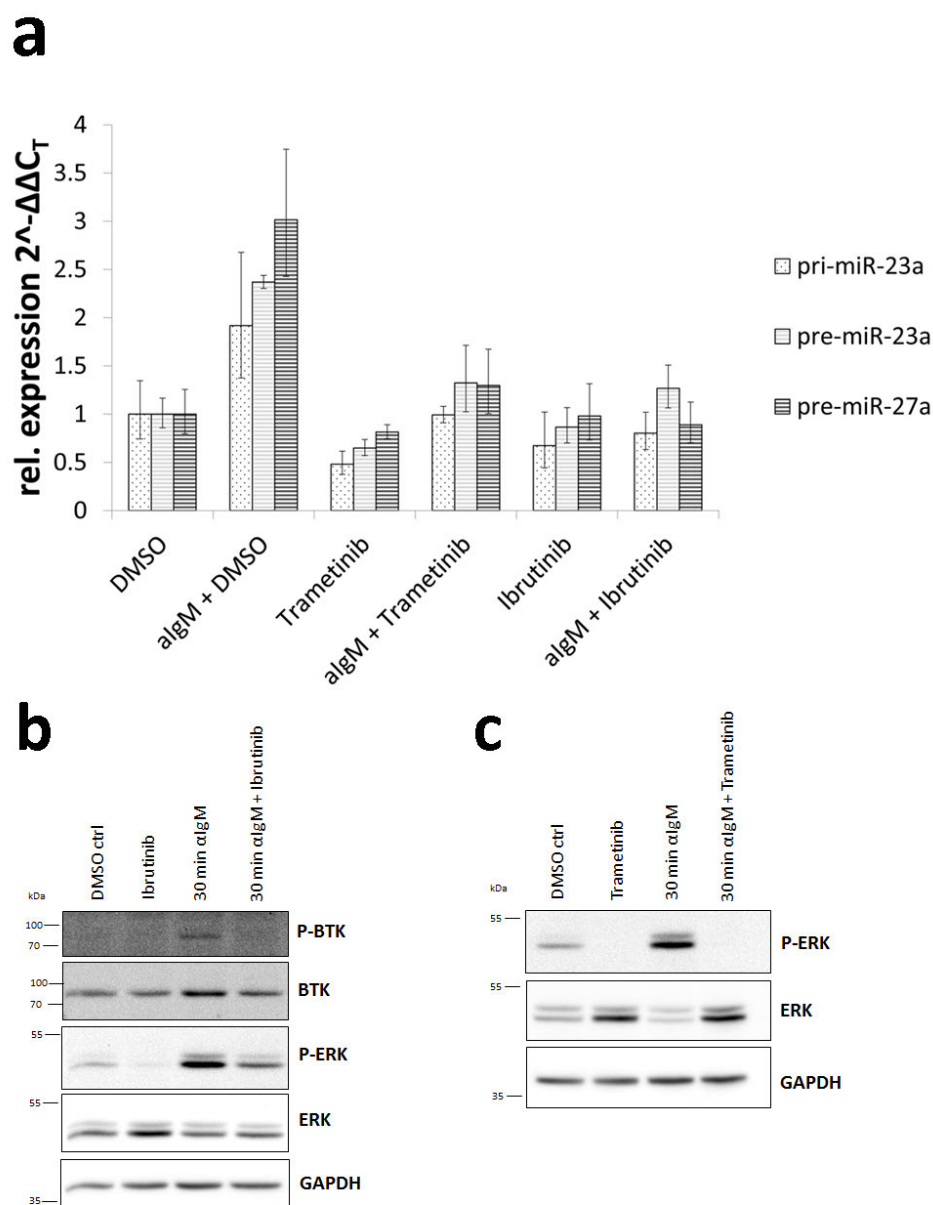
Figure 3.9.: Inhibition of BTK and MEK1/2 prevents MIR23A activation upon BCR stimulation in U2932 R1
DLBCL cell line U2932 R1 was pretreated with Ibrutinib (1 µM) and Trametinib (125 nM) for 2 hours, before BCR stimulation by 13 µg/mL anti-IgM F(ab)2-fragment. Protein samples were taken after 30 min and RNA samples after 2 h of stimulation. (a) qRT-PCR analyses of pri-miR-23a, pre-miR-23a and pre-miR-27a expression upon inhibitor/anti-IgM F(ab)2-fragment double treatment. (Mean with 95% CI, endogenous control: *SNORD48* for miR-NAs, *GAPDH* for pri-miR-23a) (b and c) Western blot analyses verifying effective inhibition of P-BTK by Ibrutinib and P-ERK by Trametinib. GAPDH served as loading control. (Ibrutinib n=3, Trametinib n=2)

3.1.3.6. c-MYC as a potential activator of MIR23A cluster in DLBCL

The proto-oncogene *c-MYC (MYC)* plays an important role in early B-cell development where it induces proliferation and contributes to lymphomagenesis (section 1.1). Previous experiments

(fig. 3.7) indicated that MYC is activated upon BCR signaling in U2932 R1. Indeed, it was already reported that MEK/ERK and PI3K signaling phosphorylate MYC, which leads to an extended half life and accumulation of MYC protein (Sears *et al.*, 2000), exactly as observed for U2932 R1 (fig. 3.7).

Additionally, the sister clones of U2932 (subclones U2932 R1 and U2932 R2) differ in *MYC* expression (Quentmeier *et al.*, 2013). The subclone U2932 R1 expresses low MYC levels, while the subclone U2932 R2 expresses high MYC levels (fig. 3.11). Interestingly, the MYC low subclone U2932 R1 shows also low MIR23A levels, while the MYC high subclone U2932 R2 exhibits higher MIR23A levels. Furthermore, gene expression analyses showed that *MYC* and pri-miR-23a are induced simultaneously upon BCR stimulation, indicating that MYC might be a target gene of BCR signaling and might activate the MIR23A cluster in U2932 R1 (fig. 3.10). Moreover, previous studies showed that MYC can either activate (Li *et al.*, 2013b) or repress the MIR23A cluster (Gao *et al.*, 2009), depending on the cellular context.
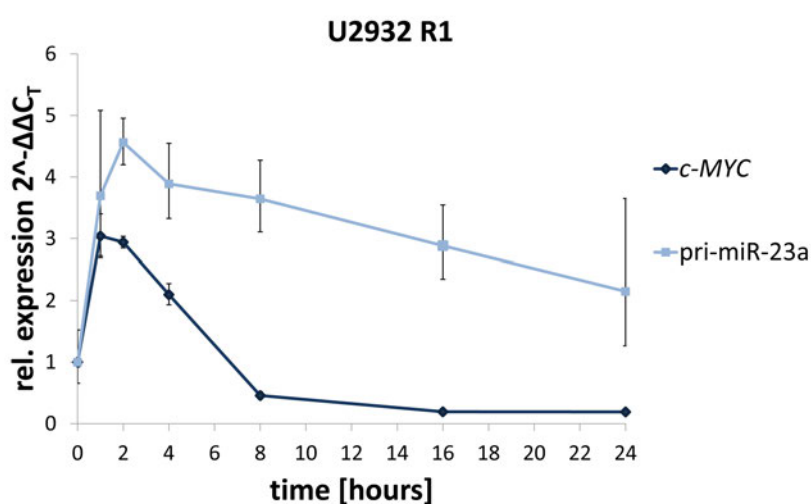
Figure 3.10.: *c-MYC* and pri-miR-23a are simultaneously induced upon BCR cross-link
Relative expression levels of pri-miR23a and *c-MYC* upon 13 μg/mL anti-IgM F(ab)2-fragment treatment in U2932 R1. Endogenous control: *GAPDH*, mean with 95% CI, one representative experiment of two is shown.
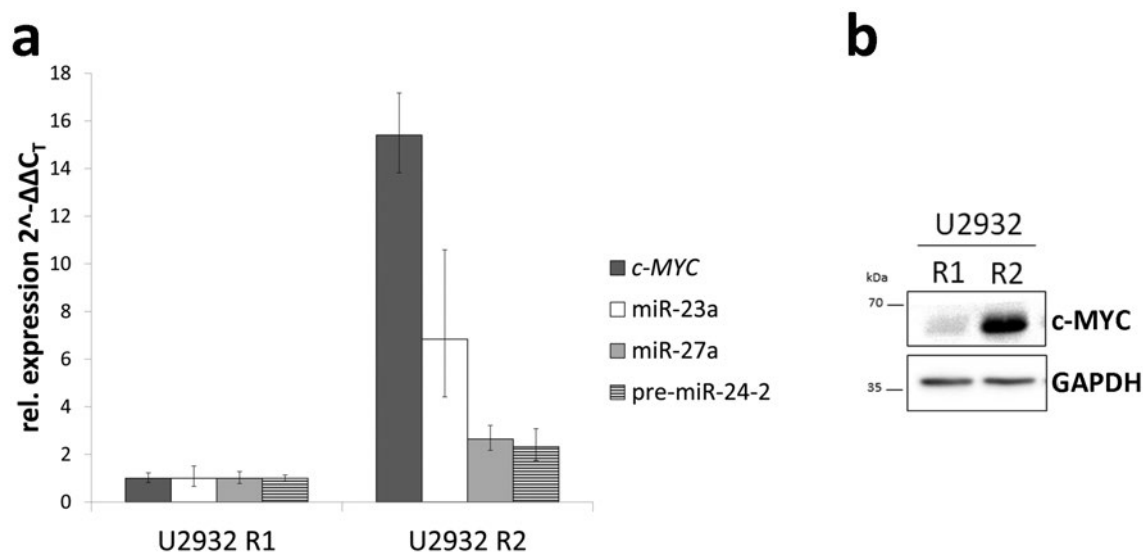
Figure 3.11.: U2932 subclones R1 and R2 differ in *c-MYC* and MIR23A cluster expression
(a) qRT-PCR analysis of relative miR-23a/-27a, pre-miR-24-2 and *c-MYC* levels in U2932 subclones R1 and R2. (Mean with 95% CI, endogenous control: *SNORD48* or *GAPDH*) (b) Western blot analysis of MYC protein levels in U2932 subclones R1 and R2. GAPDH served as loading control. One representative experiment out of three is shown.

Taken together these positive correlations led to the hypothesis that MYC might be a good candidate transcription factor for regulation of the MIR23A cluster. This hypothesis is further supported by Gao and colleagues, who showed that c-MYC binds to the paralogous MIR23B promoter by chromatin immunoprecipitation (ChIP) assay in P493-6 B cells (Gao *et al.*, 2009). Whether MYC can bind to the MIR23A promoter is not known. Controversial to the hypothesis in this thesis, MYC inhibited miR-23a and the miR-23b levels in P493-6 B cells. The P493-6 cell line contains a tetracycline inducible *c-MYC* expression cassette (Tet-off system) by which *MYC* levels can be regulated.
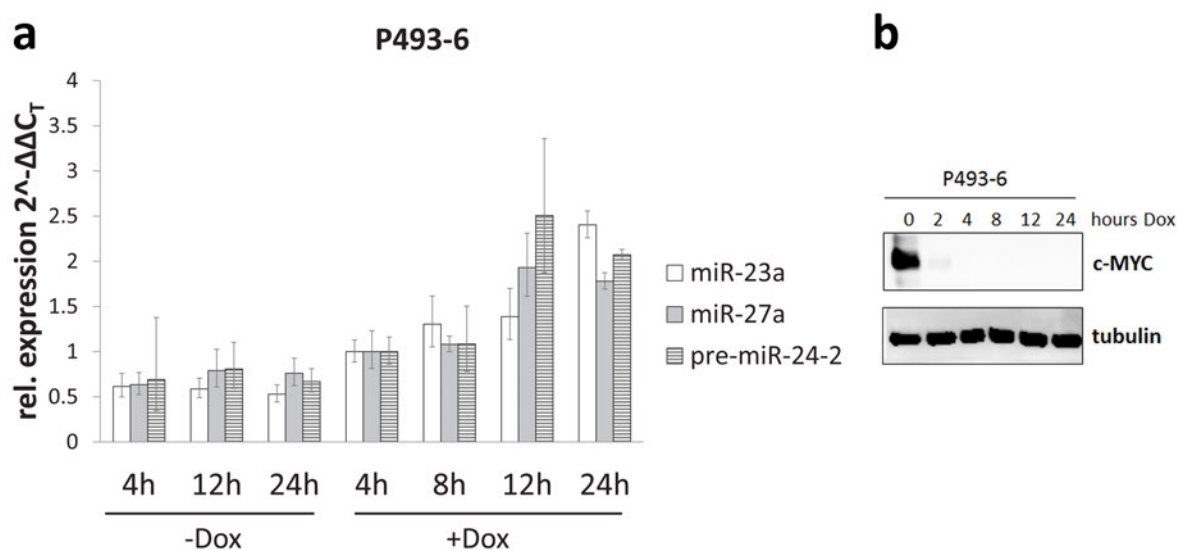
Figure 3.12.: c-MYC inhibits MIR23A in P493-6

P493-6 cells were treated for the indicated time points with 1 ng/mL doxycycline to downregulate c-MYC protein levels. a) qRT-PCR analysis of MIR23A cluster expression with and without doxycycline. (Mean with 95% CI, endogenous control: *SNORD48*) b) control Western Blot showing efficient downregulation of c-MYC protein levels upon doxycycline treatment. Dox = doxycycline. This experiment was performed once, samples were kindly provided by Maren Schmidt.

To confirm the observations from Gao *et al.* 2009, the P493-6 cell line was treated for 4, 8, 12, and 24 hours with doxycycline to efficiently downregulate c-MYC levels (samples were kindly provided by Maren Schmidt). These MYC low samples where then analyzed for MIR23A cluster expression by qRT-PCR. Indeed, miR-23a is activated upon withdrawal of MYC (fig. 3.12), exactly as shown by Gao *et al.* in 2009. Additionally, the miR-27a and pre-miR-24-2 levels increase, indicating that the whole MIR23A cluster and not only miR-23a or miR-23b is inhibited by MYC in P493-6.

However, the P493-6 is a model cell line for BL. In order to answer the question whether MYC is the transcription factor, which activates the MIR23A cluster in DLBCL, classical ectopic overexpression experiments were performed in U2932 R1. 24 hours after nucleofection of the eukaryotic *c-MYC* expression vector, cells were analyzed for primary miR-23a transcript expression via qRT-PCR. MYC overexpression was analyzed by Western blotting. Although, MYC was strongly overexpressed (fig. 3.13 b), the relative expression levels of pri-miR-23a were not altered.
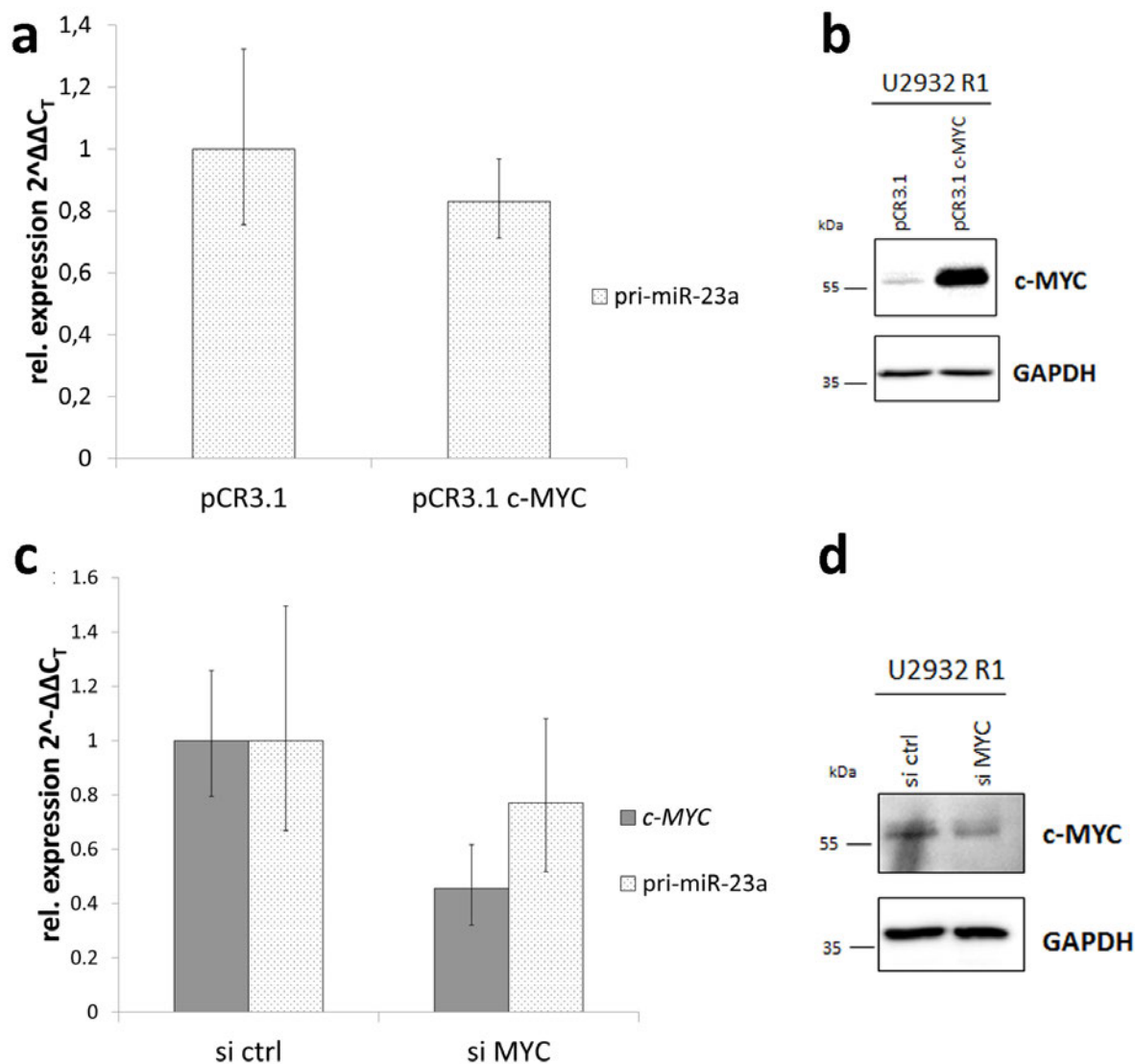
Figure 3.13.: Overexpression and knockdown of *c-MYC* do not alter pri-miR-23a levels in U2932 R1

5 µg plasmid per 5x10^6 cells was transfected by nucleofection in U2932 R1 (a and b). For *MYC* knock down 100 pmol siRNA per 5x10^6 cells was transfected (c and d). 24h after nucleofection pri-miR-23a expression levels were detected by qRT-PCR (a and c). Mean with 95% CI, endogenous control: *GAPDH*. MYC protein levels were detected by Western blotting (b and d). GAPDH served as loading control. One representative experiment of three is shown.

The interpretation of ectopic overexpression experiments can be problematic in some cases, because many proteins act in complexes. When their binding partners are not available in excess, overexpression of the target protein might not exert any effect. Therefore, in a second approach *c-MYC* was knocked down in the same cell line by a specific siRNA against *c-MYC*. 24h after nucleofection the pri-miR-23a levels and the MYC protein levels were analyzed (fig. 3.13 c and d). Although, the MYC protein levels were clearly reduced, the primary miR-23a transcript levels were not significantly altered.

This data are supported by another experiment, where MIR23A levels can be induced upon BCR signaling although c-MYC protein levels were abolished by CHX treatment (section 3.1.3.4, fig. 3.7).

In conclusion, the hypothesis that c-MYC is responsible for activation of the MIR23A cluster in response to BCR signaling, was refused for DLBCL cell line U2932 R1.

3.1.3.7. ELK1 as a potential activator of MIR23A in response to BCR

One transcription factor acting downstream of MEK/ERK signaling, is the E26-like kinase 1 (ELK1). ELK1 is a member of the ternary complex factor (TCF) subfamily of ETS-domain transcription factors and is phosphorylated by ERK2 (MAPK1). Acunzo *et al.* showed by chromatin immunoprecipitation, that ELK1 binds to the MIR23A promoter in lung cancer cells, and that knockdown of *ELK1* leads to a decrease in pri-miR-23a expression (Acunzo *et al.*, 2013). To check whether ELK1 might be a potential candidate to activate the MIR23A cluster in DLBCL, U2932 R1 cells were stimulated with anti-IgM F(ab)2-fragment and/or treated with the MEK1/2 inhibitor Trametinib using non-toxic concentrations (see MTT assays fig. A.3).
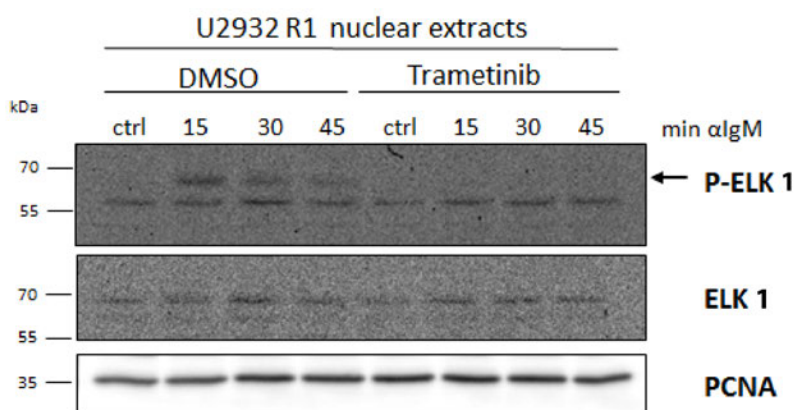
Figure 3.14.: ELK1 phosphorylation is MEK1/2 dependent
Western blot analyses of nuclear extracts of DLBCL cell line U2932 R1 treated with 125 nM Trametinib and/or 13 µg/mL anti-IgM F(ab)2-fragment. PCNA serves as loading control. One of three independent experiments is shown.

Western blot analyses of nuclear extracts show that P-ELK1 is induced within 15 min of BCR stimulation (fig. 3.14). The P-ELK1 signal rapidly vanishes within one hour after stimulation. In contrast, cells stimulated with anti-IgM F(ab)2-fragment and simultaneously treated with Trametinib show no phosphorylation of ELK1. ELK1 protein levels are not affected by the treatments. Consequently, ELK1 is activated by MEK/ERK pathway in U2932 R1. These observation together with the Chip data from Acunzo *et al.* 2013 lead to the hypothesis that ELK1 might be the MEK/ERK downstream transcription factor responsible for the activation of the MIR23A cluster in response to B-cell receptor stimulation in U2932 R1.
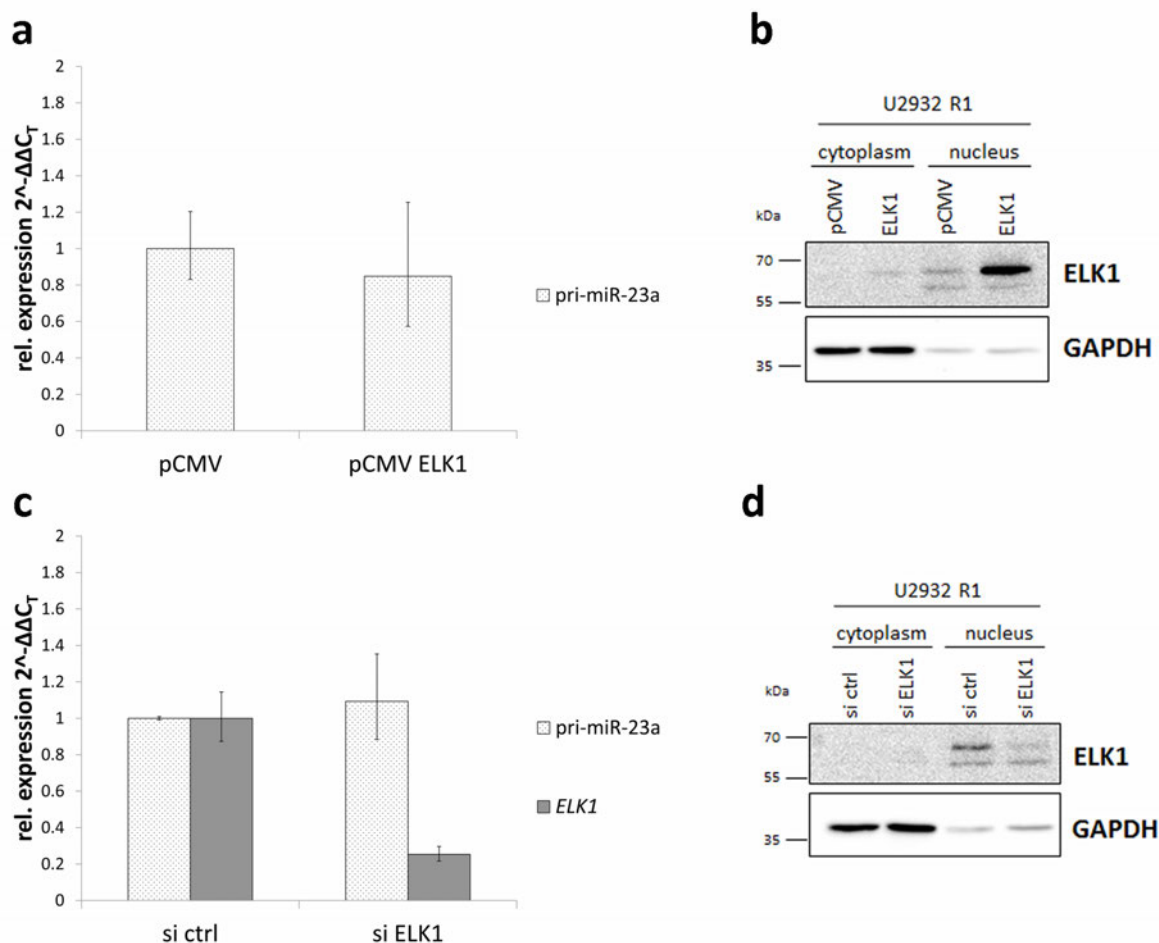
Figure 3.15.: Overexpression and knockdown of *ELK1* does not alter pri-miR-23a levels

5 µg plasmid (pCMV or pCMV_ELK1) per 5×10^6 cells was transfected by nucleofection in U2932 R1 (a and b). For *ELK1* knock down 100 pmol siRNA (si ctrl or si ELK1) per 5×10^6 cells was transfected (c and d). 24h after nucleofection pri-miR-23a expression levels were detected by qRT-PCR (a and c). Mean with 95% CI, endogenous control: *GAPDH.* ELK1 protein levels were detected by Western blotting. GAPDH served as loading control (b and d). One representative experiment of three is shown.

In order to test this hypothesis, ectopic overexpression experiments were performed in U2932 R1 cells. An eukaryotic expression plasmid coding for *ELK1* was transfected by nucleofection in U2932 R1. 24h after transfection, cells were harvested and analyzed for MIR23A expression by qRT-PCR and ELK1 protein overexpression by Western blotting. Although the ELK1 protein is markedly overexpressed, the pri-miR-23a levels are not affected (fig. 3.15 a and b). *Vice versa*, knocking *ELK1* down by siRNA has the same effect: the pri-miR-23a levels stay constant while ELK1 is clearly down regulated (fig. 3.15 c and d).

These classical overexpression and knock down experiments are critical, because on the one hand simple overexpression does not necessarily mean, that more ELK1 is phosphorylated. Only the phosphorylated form acts as a transcription factor. On the other hand, it is very difficult to detect pri-miR-23a, because it is already very low expressed in U2932 R1. Knocking

ELK1 down should lead to further decreased pri-miR-23a levels. Therefore, one additional experiment was performed to prove that ELK1 does not activate the MIR23A cluster: *ELK1* was overexpressed in U2932 R1 and 24 h post transfection the overexpressing cells were stimulated with anti-IgM F(ab)2-fragment. By this approach, the overexpressed ELK1 is activated by phosphorylation and transported into the nucleus where it can bind to its target genes.
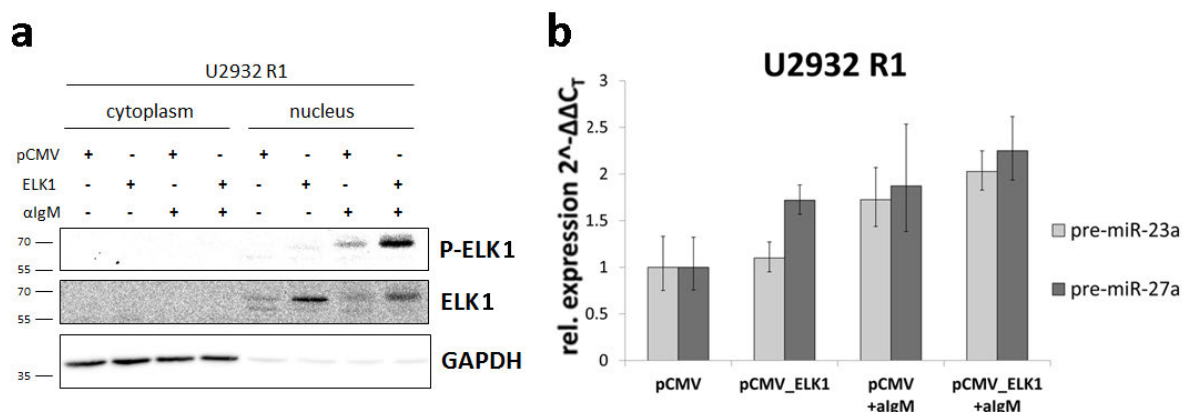
Figure 3.16.: Overexpression and activation of ELK1 in U2932 R1

5 µg plasmid (pCMV or pCMV_ELK1) per $5x10^6$ cells was transfected by nucleofection in U2932 R1. 24 h post transfection cells were stimulated with 13 µg/mL anti-IgM F(ab)2-fragment for 15 min. (a) ELK1 and P-ELK1 levels were detected by Western blotting. GAPDH served as loading control. (b) Relative pre-miR-23a and pre-miR-27a expression levels by qRT-PCR analyses. Endogenous control: *SNORD48*. One of two independent experiments is shown.

Figure 3.16 a shows that cells transfected with *ELK1* express enhanced ELK1 protein levels. Additionally, BCR stimulation leads to an induction of P-ELK1 in the nuclear fractions. As expected, cells that overexpress ELK1 and are subsequently stimulated with anti-IgM F(ab)2-fragment (aIgM) show higher P-ELK levels as control transfected cells. However, higher nuclear P-ELK1 levels did not enhance the pri-miR-23a levels compared to cells that were transfected with control vector and simultaneously stimulated with anti-IgM F(ab)2-fragment (fig. 3.16 a and b). Although high P-ELK1 levels are present in the nucleus, the induction of the MIR23A cluster is not stronger than normal BCR stimulation.

Taken together, these knockdown and overexpression results show that, although MEK/ERK signaling is active upon BCR stimulation leading to phosphorylation of ELK1, P-ELK1 is not the downstream transcription factor responsible for induction of the MIR23A cluster.

3.2. Identification of the MIR23A targetome

3.2.1. Experimental setup for MIR23A targetome identification

In order to analyze the biological function of the MIR23A cluster in DLBCL, the targetomes of miR-23a and miR-27a were identified for the DLBCL model cell line U2932 R1. This approach was achieved by an Ago2-RNA immunoprecipitation (Ago2-RIP), followed by high-throughput RNA-Sequencing (fig. 3.17). Ago2 protein mediates the interaction of miRNA and mRNA within the RISC. Hence, Ago2 immunoprecipitation captures miRNAs and RISC associated mRNAs. These were compared between a miRNA overexpressing cell line to a non-silencing control cell line. Under the assumption that the proportion of overexpressed miRNAs incorporated in the Ago2-RISC complex is enhanced, the comparison of RNA-sequencing data from non silencing control cells (ns ctrl) to miR-23a or miR-27a overexpressing cells should provide an enrichment of a) the miRNA of interest and b) a set of mRNA sequences that are bound to and therefore targeted by the respective miRNA. In detail, mRNA sequencing was performed for Ago2-RIP input and output samples (fig. 3.18). Additionally, small RNAs of the input samples were sequenced, to check whether the global miRNA expression is affected by lentiviral miRNA overexpression. In total, three independent experiments were performed resulting in triplicates for each cell line (U2932 R1 pGIPZ ns ctrl1, miR-23a1 and miR-27a1) and each sample (Ago2-RIP input and output).

In order to identify the mRNAs that are targeted by the respective miRNA, first the enriched transcripts of Ago2-RIP output vs. input were compared. This comparision identifies all transcripts that are incorporated within the RISC complex and bound to Ago2. In a next step, these Ago2-bound transcripts were compared between miRNA overexpressing cell line to ns ctrl cell line. The differentially expressed mRNAs of this comparison are identified as targets of the respective miRNA (enrichment higher than two-fold, p-value less than 0.05; see section 3.2.7).

This approach will give insight into the yet unknown DLBCL specific MIR23A targetome and may predict in which cellular processes the MIR23A cluster is involved in DLBCL.
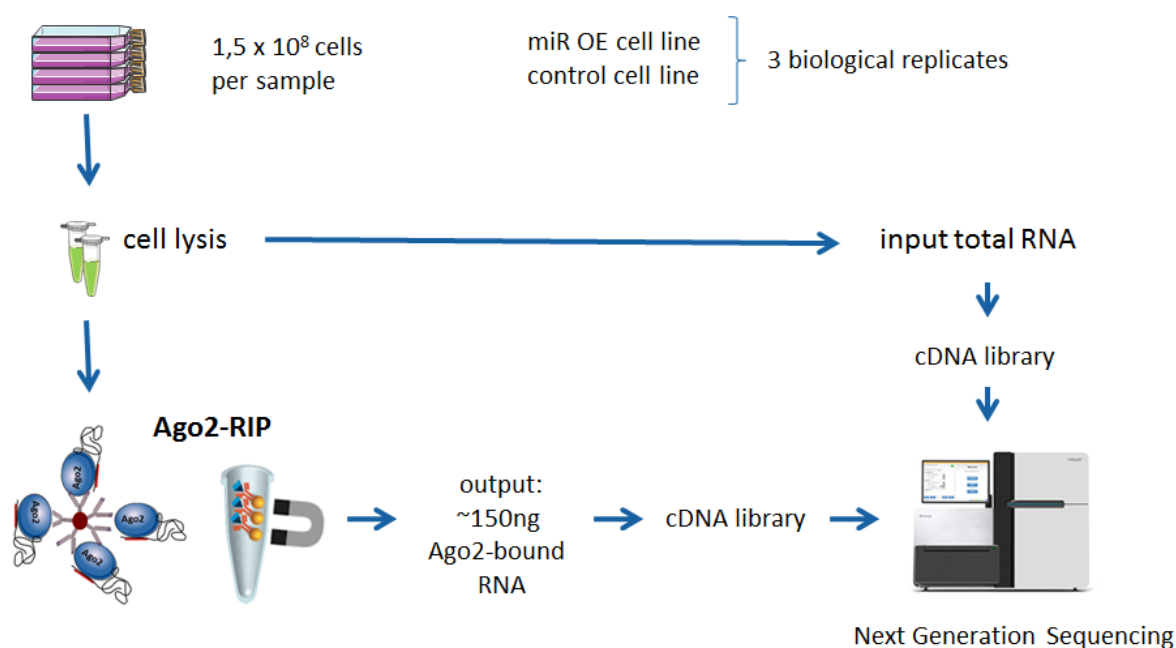
Figure 3.17.: Experimental design of miR-23a/27a targetome identification *via* Ago2-RIP
Scheme of Ago2-RIP approach for identification of the miRNA targetome of a DLBCL cell line. $1,5x10^8$ cells of control or miRNA overexpressing (miR OE) cell line are lysed and cell lysates are used for Ago2-RNA immunoprecipitation (Ago2-RIP) with an Ago2-specific antibody that is coupled to magnetic beads. The RNA from Ago2-RIP input and output samples is isolated and used for cDNA library preparation, which is subsequently analyzed by Next Generation Sequencing.
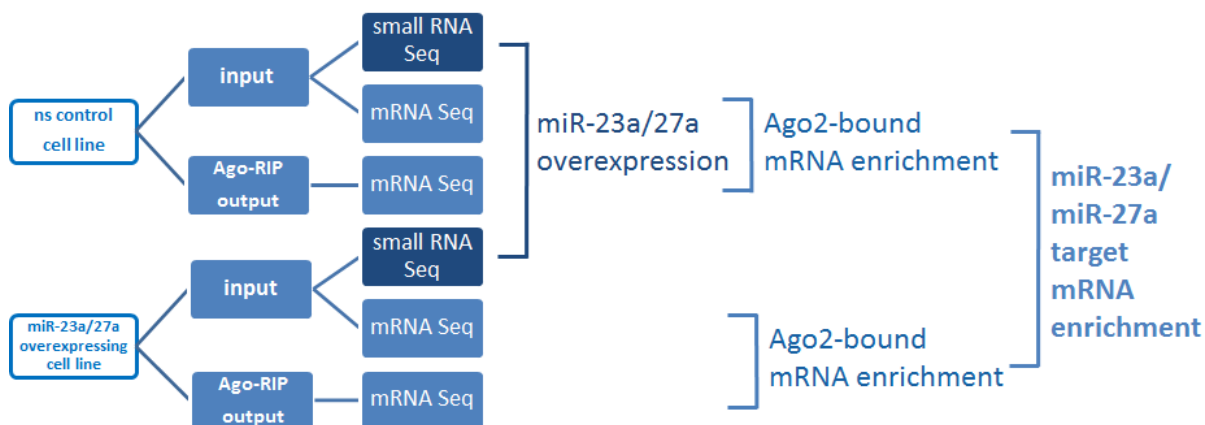
Figure 3.18.: Bioinformatical comparisons for miRNA targetome identification
Scheme of bioinformatical comparisons of Ago2-RIP sequencing data performed for miRNA target identification. Compared are Ago2-RIP samples of miR-23a or miR-27a overexpressing cell lines to non silencing control. First the enrichment of Ago2-bound mRNAs are analyzed by comparison of Ago2-RIP input and output samples for each cell line. Next, these enriched transcripts from miRNA overexpressing cell line are compared to non silencing ctrl. These transcripts are identified as miR-23a or miR-27a bound targets within the Ago2-RISC complex.

Since a large cell number is needed for such an experiment, a DLBCL cell line stably overexpressing the miRNA of interest (miR-23a or miR-27a) or a non silencing control (ns ctrl), was generated. For this purpose, the cell line U2932 R1 was chosen as a DLBCL model cell line,

because it is on the one hand well characterized (Quentmeier *et al.*, 2013) and shows on the other hand relatively low levels of MIR23A, making it favorable for induction and overexpression experiments. Therefore, lentiviral expression vectors for stable miR-23a, miR-27a and ns ctrl overexpression were cloned. MiR-24 was not cloned, because it is not expressed in B cells and it did not respond to B-cell receptor activation (fig. 3.5 d). In parallel, also vectors for transient miRNA overexpression were cloned in order to validate the identified MIR23A targets in transient overexpression experiments.

3.2.2. Cloning of pre-miR-23a and pre-miR-27a into the transient expression vector pSG5 for miRNA overexpression

The pSG5 expression vector coding for miR-23a~miR-27a was kindly provided by Friedrich Grässer. Using PCR the restriction sites for XhoI and MluI were added 74 bp in 5' direction and 62 bp in 3' direction of the pre-miR-23a sequence. The flanking sequences ensure that the miRNA processing machinery is able to bind correctly to the stem loop sequence. The PCR product was subcloned into the TopoTA cloning vector pCR2.1, excised by EcoRI and ligated into the pSG5 expression vector (section 2.9).

The same cloning strategy was applied for miR-27a. In this case the XhoI and MluI restriction sites were added 81 bp 5' direction and 98 bp in 3' direction of miR-27a stem loop sequence.

The restriction sites XhoI and MluI were used for subcloning into a lentiviral expression vector.

3.2.3. Cloning of pre-miR-23a and pre-miR-27a into the lentiviral vector pGIPZ

The lentiviral transduction vector pGIPZ ns ctrl (coding for a non silencing control, GFP and a puromycin resistance) was chosen to generate lentiviral particles that transduce miR-23a and miR-27a into U2932 R1 (section 2.9). The non-silencing sequence is flanked by a XhoI and a MluI restriction site. These were used to excise the ns ctrl sequence and replace it by the pre-miR23a or pre-miR-27a sequences described in section 3.2.2.

3.2.4. Generation of stable miR-23a and miR-27a overexpressing clones

HEK293T cells were used to produce lentiviral particles harboring the ns ctrl, miR-23a or miR-27a sequences. These lentiviral particles were harvested from HEK293T supernatant, the virus titer was determined and the virus solution was used for transduction of the target cell line U2932 R1. Successfully transduced clones were selected by Puromycin resistance and GFP expression (strategy see fig. 2.8). Next, the miRNA expression of each selected clone was verified by qRT-PCR (figure 3.19).

By this approach, many clones overexpressing ns ctrl, miR-23a and miR-27a were generated. Selection criteria for new generated cell lines were: homogeneous and constant GFP expression over several generations, functional mature miRNA expression and unchanged c-MYC, BCL-6 and Ago2 expression. U2932 R1 pGIPZ ns ctrl1, ns ctrl2, miR-23a1, miR-23a2 and miR-27a1 fulfilled this criteria, whereas the miR-27a10 clone was found to be a double clone, showing two distinct GFP populations. Since only two miR-27a clones were obtained, both were used for further experiments (fig. 3.19, supplementals A.1 and A.2).
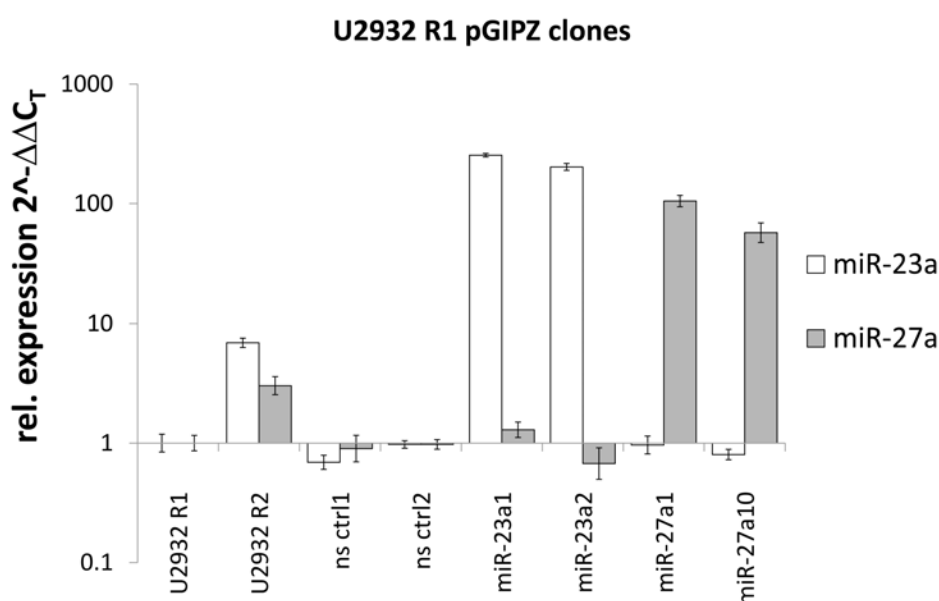
Figure 3.19.: MIR23A expression of stable ns ctrl/miR-23a/miR-27a overexpressing U2932 R1 pGIPZ clones

QRT-PCR results of mature miR-23a and miR-27a expression in lentiviral transduced U2932 R1 clones compared to U2932 R1 qnd R2. (Mean with 95% CI, endogenous control: *SNORD48*.) These cell lines fulfilled all selection criteria (for details refere to main text) and were used for all further experiments. Note that U2932 R1 pGIPZ miR-27a10 is a GFP-double clone.

3.2.5. Characterization of stable miR-23a and miR-27a overexpressing clones

Since miR-23a and miR-27a were previously described to be associated with proliferation and growth (Liu *et al.*, 2013; Jahid *et al.*, 2012; Jiang and Melnick, 2015; Pan *et al.*, 2014), cell numbers of the parental cell line U2932 R1 and the ns ctrl, miR-23a and miR-27a overexpressing U2932 R1 pGIPZ clones were assessed to identify differences in proliferation rates. In detail, equal cell numbers were seeded and cell number as well as cell viability were determined after 24, 48, 72 and 96 hours.
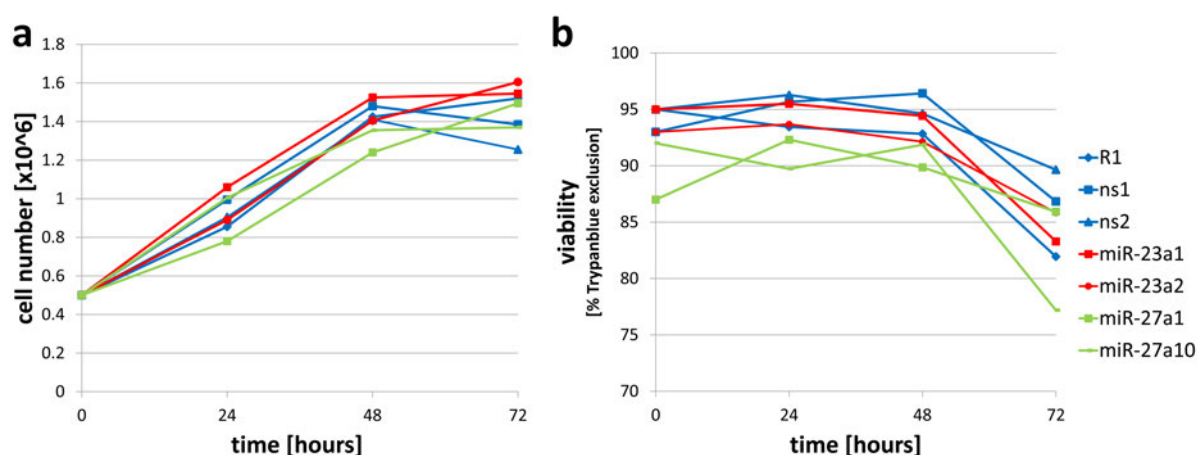
Figure 3.20.: Proliferation of U2932 R1 pGIPZ clones
U2932 R1 pGIPZ clones and U2932 R1 were seeded at a density of $5x10^5$ cells/mL in RPMI1640 +20% FCS. After 24, 48 and 72 hours cell were manually counted using a Neubauer counting chamber. Viability was determined by trypanblue exclusion. One representative experiment of two is shown.

Neither the overexpression of ns ctrl, nor miR-23a or miR-27a altered the proliferation rate of U2932 R1 (fig. 3.20 a). The cell numbers of all clones increase with time, doubling after around 30 hours and stagnate between 48 and 72 hours. Cell viability of all clones stays constant between 90 to 95% for 48 hours before slightly decreasing between 48 and 72 hours (fig. 3.20 b). The miR-23a and ns ctrl overexpressing cell lines did not differ from the parental clone in cell viability, while the miR-27a overexpressing clones showed a slight worse viability by ca. 5%. Stagnation of cell growth and reduction of viability is possibly due to starvation, because the cells were not fed during this time span.

3.2.6. Establishment of an Ago2-RNA immunoprecipitation assay for miRNA targetome identification in DLBCL

In order to identify the miR-23a and miR-27a mRNA targets in DLBCL, an Ago2-RNA immunoprecipitation assay (Ago2-RIP) was established for the DLBCL cell line U2932 R1. The protocol used in this thesis was based on the paper "Systematic Analysis of Viral and Cellular

MicroRNA Targets in Cells Latently Infected with Human g-Herpesvirus by RISC Immunopre-cipitation Assay" (Dölken *et al.*, 2010). It was optimized for the use with the suspension cells U2932 R1. Most important was to obtain enough high quality RNA for mRNA Sequencing, therefore cell number, lysis volume, number of freeze and thaw cycles and antibody to bead ratio were systematically tested and adjusted.
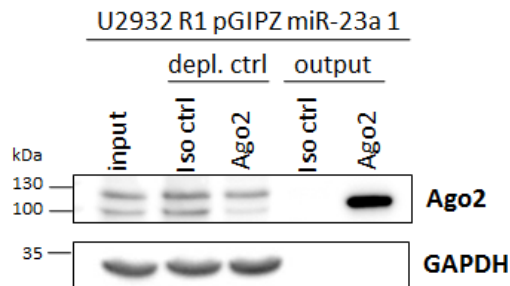
Figure 3.21.: Ago2 protein is enriched by immunoprecipitation
Control Western blot of Ago2-RIP from U2932 R1 pGIPZ miR-23a1. The 100 kDa band represents Ago2. 40 µg total protein per lane. Output 1/40 (v/v) of input. Iso ctrl = isotype control, depl. ctrl = depletion control. Housekeeper: GAPDH. One representative blot from more than three is shown.

As could be seen on the Western blot in fig. 3.21 the Ago2 protein (ca. 100 kDa) could successfully be enriched upon immunoprecipitation in the output fraction, especially because only 1/40 of input volume was loaded on the lanes. The depletion controls (or flow through) show a depletion of Ago2 protein when Ago2-antibody was used, but not when an isotype control was used. Additionally, no Ago2 protein was enriched in the output fraction of isotype control, showing that the immunoprecipitation was specific for Ago2 protein.
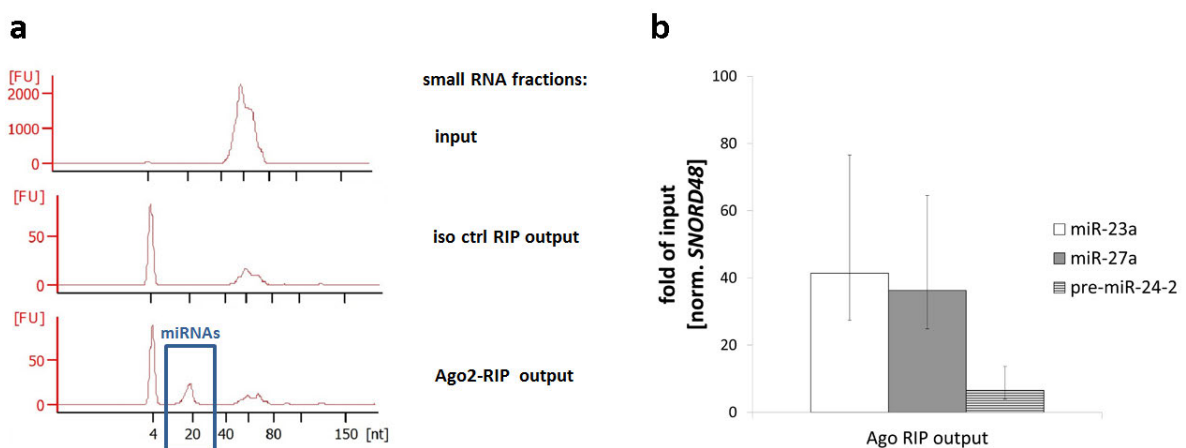
Figure 3.22.: MiRNAs are enriched in Ago2-RIP output
(a) Bioanalyzer small RNA chip data of small RNA fractions of U2932 R1 Ago2 RIP. The 4 nt peak resembles the marker nucleotide. (b) Ago2-RNA immunoprecipitation in U2932 R1. qRT-PCR analyzes show an 40-fold enrichment of mature miRNAs and only 6-fold enrichment of pre-miR-24-2 compared to input fractions. Mean with 95% CI, endogenous control: *SNORD48.*

To check whether the Ago2 immunoprecipitation also includes an enrichment of miRNAs, the output RNA was fractionated into small and large RNAs and analyzed using Bioanalyzer agarose chips (fig. 3.22 a). Input as well as output RNA fractions show a peak between 40 and 80 nt, which represent small RNAs, such as 5S and 5.8S rRNA, tRNAs and other small RNA species. As expected, the Ago2 output shows an additional peak at 20 bp, which is not present in the isotype control output. This peak represents the enrichment of mature miRNAs, that bind within the RISC complex to Ago2 and have a size between 18-22 bp. The relative abundance of miRNAs in the input fraction is low, so this 20 bp peak is not visible without enrichment. Comparing the height of the small RNA peak (40-80 bp), one can clearly see that the peak decreases upon immunoprecipitation, showing that the immunoprecipitation is specific, but still there is a background of other RNA species. Over all, about 150 ng high quality total RNA per sample was obtained upon Ago2-RNA immunoprecipitation from 1.5 x 10^8 cells (RIN values > 8 , supplementary fig. A.4).

In a next step, it was validated by qRT-PCR analyses that these 20 nt long RNA sequences, which were enriched in the Ago2-RIP output fractions, are mature miRNAs (fig. 3.22 b). Indeed, the mature miR-23a and miR-27a transcripts were 40-fold enriched compared to input. As a proof of principle, the precursor miRNA of miR-24 was only 6-fold enriched. Pre-miRNAs were not expected to be bound to Ago2, because they are not incorporated into the RISC. Notably, the ratio of miR-23a to miR-27a did not change upon immunoprecipitation in unmodified parental cell line U2932 R1, showing that the procedure per se did not alter the composition of different miRNAs incorporated into the RISC complex.

Nevertheless, still other RNA species can be found after immunoprecipitation. Especially, ribosomal RNA is still present in the output samples (supplementary fig. A.4). Therefore, and in order to enrich mRNAs, poly A enrichment was applied before cDNA library generation for next generation sequencing of mRNA transcripts. For small RNA sequencing (only of miR-23a1 and ns ctrl1 inputs) the 5'-phosphate and 3'-hydroxyl groups of mature miRNAs, that are generated by Drosha and Dicer processing, were used for adapter ligation before cDNA library preparation.

In summary, the Ago2-RIP could successfully be established for DLBCL cell line U2932 R1. The Ago2 protein together with its bound miRNAs could be specifically and highly enriched upon immunoprecipitation. The RNA amount gained from Ago2-RIP output (~150 ng total RNA per sample) was sufficient for RNA sequencing. Additionally, the RNA quality was still high upon Ago2-RNA immunoprecipitation.

3.2.7. RNA sequencing & analysis

In order to identify the MIR23A targetome in DLBCL an Ago2-RIP assay was established for the DLBCL cell line U2932 R1 (section 3.2.6). Ago2-RIP assays were performed for U2932 R1 pGIPZ clones: miR-23a1, miR-27a1 and ns ctrl 1 (section 3.2.1, fig. 3.17 and 3.18). Total RNA was isolated from Ago2-RIP input and output samples for each cell line in triplicates (three independent experiments). Besides mRNA sequencing of Ago2-RIP input and output samples, small RNA sequencing was performed for U2932 R1 miR-23a1 and ns ctrl1 inputs to check whether global miRNA expression was affected by miR-23a overexpression.

cDNA library preparation and Next Generation Sequencing were performed at the GMAK, HZI Brunswick. For mRNA sequencing, poly A enrichment was applied. For small RNA sequencing no enrichment was performed. All Ago2-RIP samples were sequenced (50 bp single-end) on the Illumina High Seq 2500.

Sequencing yield was 20-50 Mio reads per mRNA sample and 12-16 Mio reads per small RNA sample. Reads were trimmed form adapter sequences and low quality bases, mapped to the human genome (hg38) by STAR and counted by HTseq. Normalization was performed according to total number of reads within a sample and between samples , followed by the comparison of the sequences according to the scheme in fig. 3.18 (Claudia Pommerenke, unpublished). Thresholds for differentially expressed genes were set to at least two-fold enrichment and a Benjamini-Hochberg adjusted p-value lower than 0.05.

The mapping efficiency of ~83% of all reads to the human genome resulted in ~25 Mio uniquely mapped reads per sample, which is suitable to analyze global gene expression profiles (fig. 3.23).

Principal Component Analyses (PCA) of all sequencing data showed that the input and output samples formed as expected two different groups distinct from each other (fig. 3.24). The only exception was input sample ns ctrl1 batch b (fig. 3.24 blue squares b), which differs from all other samples.

In summary, the sequencing data obtained from the input and output samples of Ago2-RIP were consistent and reliable. Hence, they could further be analyzed as depicted in fig. 3.18.

a

b
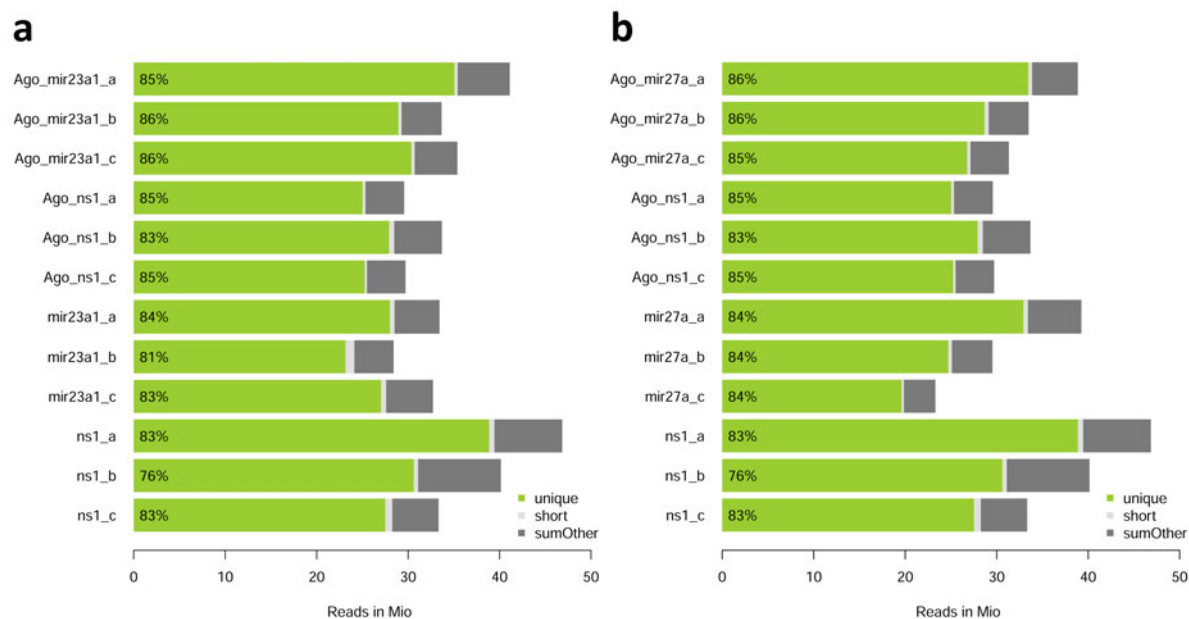
Figure 3.23.: Alignment efficiency for all mRNA sequencing samples

Sequences gained by mRNA sequencing of Ago2-RIP samples were mapped to human genome (hg38). Percent of uniquely mapped reads to annotated gene regions of Ago2-RIP samples are depicted in green. Light grey: sequences, that are too short for uniquely mapping to annotated regions. Dark grey: sequences that could not be uniquely aligned. (a) Ago2-RIP samples of U2932 R1 miR-23a1 and ns ctrl1. (b) Ago2-RIP samples of U2932 R1 miR-23a1 and ns ctrl 1. Note, that ns1 ctrl samples are identical in (a) and (b). a, b, c = different triplicates, Ago_XXX_X = output sample, miR/ns_X = input sample.
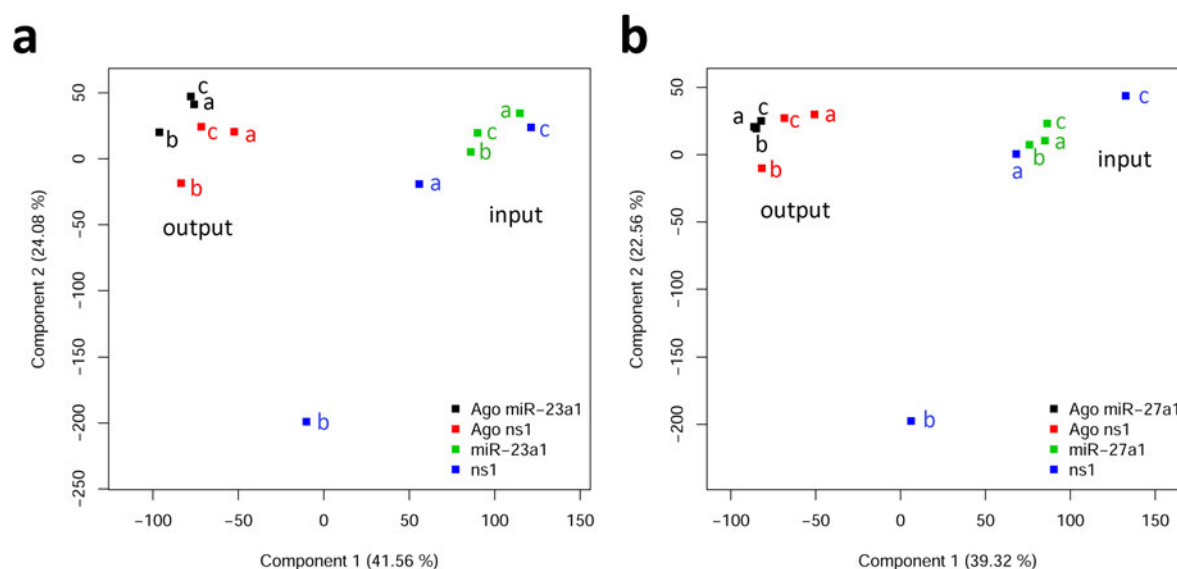
Figure 3.24.: Principal component analysis of Ago2-RIP RNA sequencing samples
PCA analyses of mRNA sequencing data gained from Ago2-RIP input and output samples: (a) miR-23a1 compared to ns ctrl1 Ago2-RIP RNA sequencing samples. (b) miR-27a1 compared to ns ctrl1 Ago2-RIP RNA sequencing samples. a, b, c = different triplicates of Ago2-RIP RNA samples, black squares = Ago2-RIP output RNA sequencing samples of U2932 R1 pGIPZ miR-23a1/miR-27a1, red squares = Ago2-RIP output RNA sequencing samples of U2932 R1 pGIPZ ns ctrl1, green squares = Ago2-RIP input RNA sequencing samples of U2932 R1 pGIPZ miR-23a1/miR-27a1, blue squares = Ago2-RIP input RNA sequencing samples of U2932 R1 pGIPZ ns ctrl 1.

3.2.8. MiR-23a and miR-27a targetome in DLBCL

In order to identify the miR-23a and miR-27a targetome, Ago2-RIPs were performed for the miRNA overexpressing cell lines U2932 R1 pGIPZ miR-23a1, miR-27a1 and ns ctrl1 (detailed description in section 3.2.1, fig. 3.17 and 3.18). Total RNA of input and output samples was sequenced. Additionally, small RNA sequencing was performed for the inputs of U2932 R1 pGIPZ miR-23a1 and ns ctrl1.

As a proof of principle, small RNA sequencing revealed that only miR-23a was highly enriched (190-fold) in the miR-23a overexpressing cell line compared to ns ctrl cell line (fig. 3.25 inner circle). However, also seven other miRNAs (miR-3919, miR-4662B, miR-618, miR-129-1, miR-199B, miR-99a and miR-150) were enriched, but the base mean values of these miRNAs lay between 11-300 reads compared to 29643 reads for miR-23a. It is therefore highly probable, that the identified targets are only targeted by miR-23a and no other miRNA.

In total, the comparison of enriched RNA sequences from Ago2-RIP input to output of miR-23a or miR-27a overexpressing cells to non silencing control cells lead to the identification of 26 miR-23a and 20 miR-27a targets in the DLBCL cell line U2932 R1 (fig. 3.25 and 3.26, table 3.1 and 3.2). The threshold of enrichment was set to a minimum of two-fold and the p-value was set to less than 0.05 (see section 3.2.7). Many of the targets were already predicted by the

algorithm the web tool "Target Scan" uses. Nearly all identified targets (see table 3.3 and 3.4) harbor at least one miR-23a or miR-27a 7mer binding sites. Notably, most binding sites are located in the 3'UTR, except for the identified Zinc finger proteins (ZNFs), which have more miR-23a 7mer binding sites in their coding sequences (CDS).

Interestingly, this approach also detected two long non coding RNAs (lncRNA), one targeted by miR-23a the other by miR-27a. Long non-coding RNAs are transcribed by Pol II and are therefore also polyadenylated. Since the RNA samples were enriched over poly A tails at cDNA synthesis, it is not surprising to find lncRNAs among the sequencing data. Nevertheless, this study focused on the protein coding mRNAs that are targeted by the MIR23A cluster.

For miR-23a 25 novel protein coding target mRNAs were identified for DLBCL cell line U2932 R1. 12 of them were zinc finger proteins, that contain a DNA binding ZNF domain. All these identified ZNFs belong to the same protein family: KRAB-C2H2-ZNFs. Members of this family comprise a high sequence homology, which might be an explanation why so many are targeted by miR-23a. Notably, many ZNFs as well as other miR-23a targets are encoded on chromosome 19, where also the MIR23A cluster itself is encoded. In fact, the identified ZNFs belong to two separate ZNF clusters, that were generated due to gene duplication during evolution: ZNF cluster 269 on chromosome 19 and ZNF cluster 114 on chromosome 7. For the other miR-23a targets no such similarities could be identified. Those targets, that are already described, function in a wide range of cellular processes (table 3.1). The same is true for the 19 newly identified protein coding mRNAs of miR-27a (table 3.2). Strikingly, many of the miR-27a targets are encoded on chromosome 19, as already observed for the miR-23a targets.

Taken together, 37% of all identified miR-23a and miR-27a targets are encoded on chromosome 19, where also the MIR23A is encoded, indicating an unknown mechanism underlying these observations (see section 3.2.8.1).

Comparing the identified miR-23a/27a targets with the differentially expressed genes between miRNA overexpressing cell line compared to control (at least two-fold difference), 12 of 46 targets are differentially expressed (fig. 3.27). These targets are possibly targeted for RNA-degradation by the respective miRNA (Braun *et al.*, 2011). Technically, the miRNA effect on these targets can be analyzed by qRT-PCR.
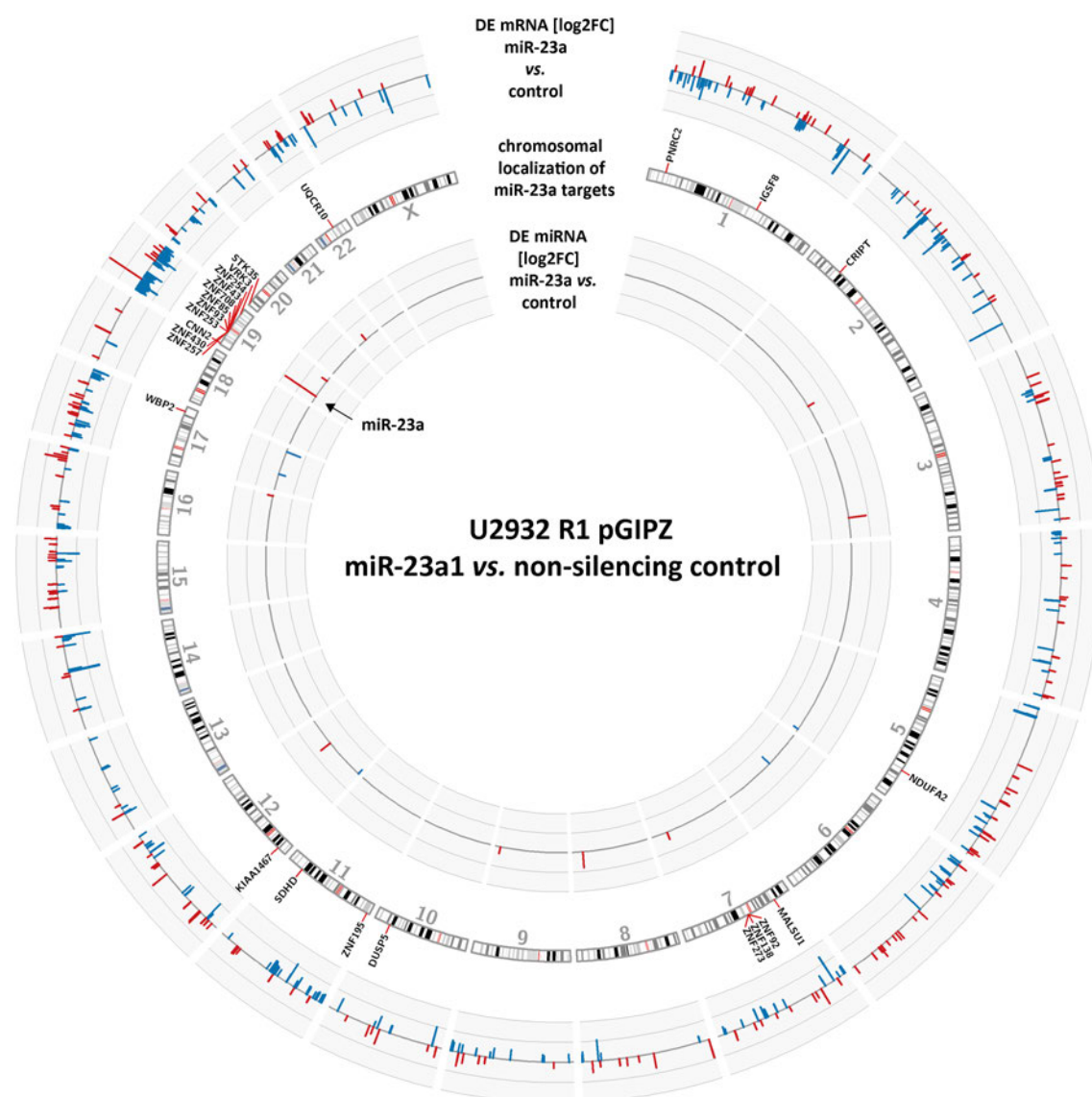
Figure 3.25.: MiR-23a targetome and differentially expressed transcripts in U2932 R1 pGIPZ miR-23a1 *vs.* ns ctrl1
Outer circle: differential expressed transcripts (log2FC) of miR-23a1 clone vs. non silencing control clone. blue: downregulated, red: upregulated; middle circle: chromosomal localization of identified miR-23a targets (enrichment at least two-fold, p-value $\leq$ 0.05); inner circle: differential expressed miRNAs (log2FC) of miR-23a1 clone vs. non silencing control clone. blue: downregulated, red: upregulated; DE: differential expression, FC: fold change.
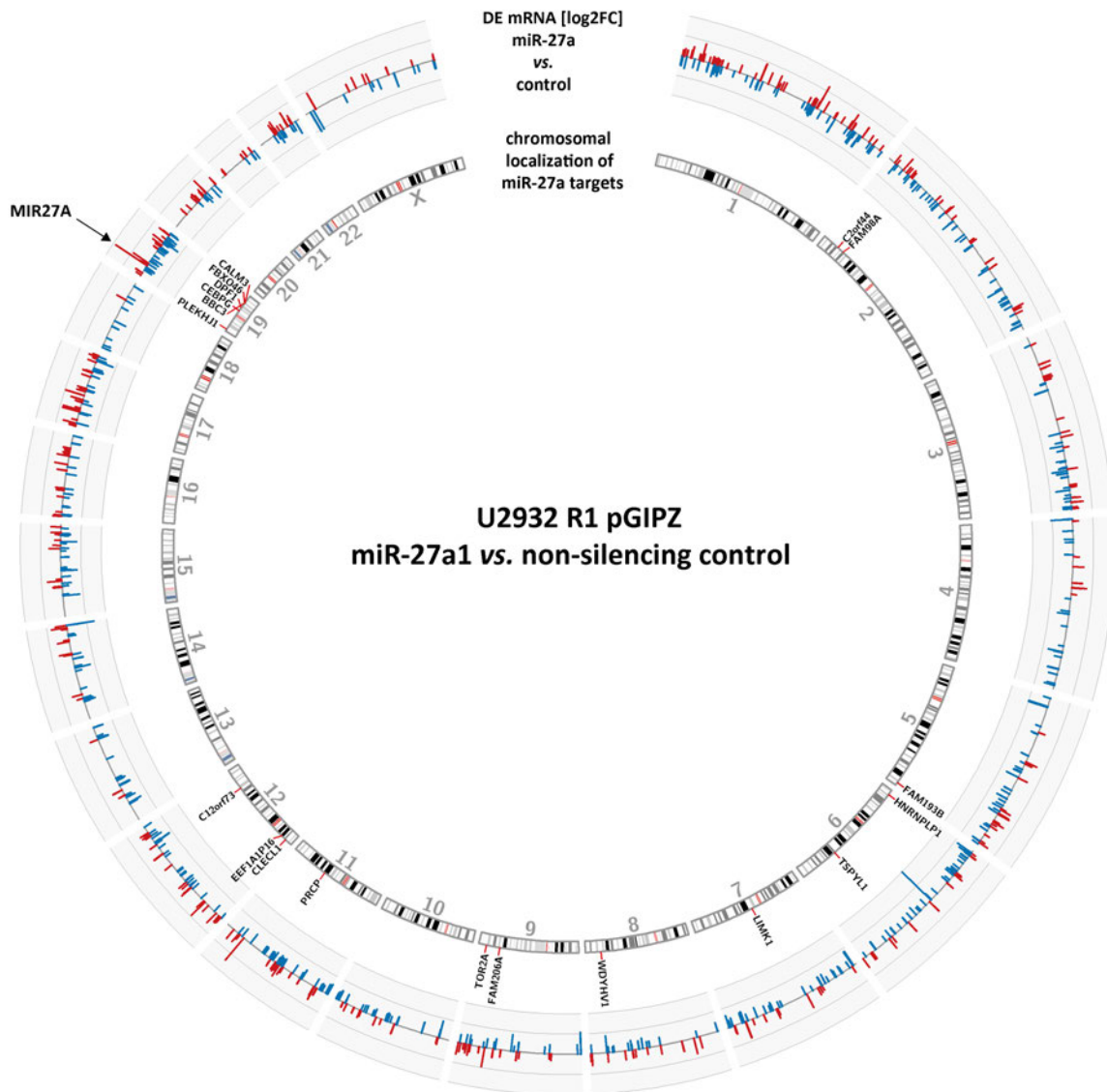
Figure 3.26.: MiR-27a targetome and differentially expressed transcripts in U2932 R1 pGIPZ miR-27a1 *vs.* ns ctrl1

Outer circle: differentially expressed transcripts (log2FC) of miR-27a1 clone *vs.* non silencing control clone. blue: downregulated, red: upregulated; middle circle: chromosomal localization of identified miR-27a targets (enrichment at least two-fold, p-value $\leq$ 0.05); inner circle: differentially expressed miRNAs (log2FC) of miR-27a1 clone vs. non silencing control clone. blue: downregulated, red: upregulated; DE: differential expression, FC: fold change.

Table 3.1.: miR-23a targets in DLBCL cell line U2932 R1

gene	description	chromosome	log2(fc)	padj	predicted
ZNF92	zinc finger protein 92	7	3.21	1.06E-04	yes
ZNF708	zinc finger protein 708	19	3.05	4.41E-04	yes
KIAA1467	KIAA1467	12	2.69	5.31E-13	yes
ZNF257	zinc finger protein 257	19	2.62	3.36E-03	yes
ZNF253	zinc finger protein 253	19	2.56	1.17E-02	yes
UQCR10	ubiquinol-cytochrome c reductase, complex III subunit X	22	2.49	3.20E-02	no
ZNF254	zinc finger protein 254	19	2.44	1.27E-02	yes
ZNF273	zinc finger protein 273	7	2.43	1.12E-02	yes
WBP2	WW domain binding protein 2	17	2.42	1.78E-03	yes
MALSU1	mitochondrial assembly of ribosomal large subunit 1	7	2.32	3.88E-04	no
IGSF8	immunoglobulin superfamily, member 8	1	2.22	3.90E-02	yes
ZNF43	zinc finger protein 43	19	2.19	2.79E-02	yes
NDUFA2	NADH dehydrogenase (ubiquinone) 1 alpha subcomplex, 2	5	2.17	4.11E-02	yes
RP11-1017G21.5	lncRNA RP11-1017G21.5	14	2.08	3.09E-02	no
ZNF430	zinc finger protein 430	19	1.95	3.77E-02	yes
CNN2	calponin 2	19	1.95	3.36E-03	yes
ZNF138	zinc finger protein 138	7	1.91	3.17E-02	yes
VRK3	vaccinia related kinase 3	19	1.75	1.25E-05	yes
SDHD	succinate dehydrogenase complex, subunit D, integral membrane protein	11	1.72	3.17E-02	yes
ZNF85	zinc finger protein 85	19	1.62	6.56E-03	yes
PNRC2	proline-rich nuclear receptor coactivator 2	1	1.61	3.88E-04	yes
CRIPT	cysteine-rich PDZ-binding protein	2	1.60	2.79E-02	no
ZNF93	zinc finger protein 93	19	1.50	8.97E-03	yes
DUSP5	dual specificity phosphatase 5	10	1.38	1.27E-02	yes
ZNF195	zinc finger protein 195	11	1.33	3.17E-02	yes
STK35	serine/threonine kinase 35	20	1.18	3.09E-02	yes

Table 3.2.: miR-27a targets in DLBCL cell line U2932 R1

gene	description	chromosome	log2(fc)	p value	predicted
CTC-246B18.10	lncRNA CTC-246B18.10	19	3.32	1.28E-02	n.d.
HNRNPLP1	heterogeneous nuclear ribonucleoprotein L pseudogene 1	6	3.26	1.45E-03	n.d.
PLEKHJ1	pleckstrin homology domain containing, family J member 1	19	2.90	3.42E-03	no
TOR2A	torsin family 2, member A	9	2.84	1.43E-02	no
C12orf73	chromosome 12 open reading frame 73	12	2.50	8.63E-05	yes
CLECL1	C-type lectin-like 1	12	2.15	1.03E-03	yes
LIMK1	LIM domain kinase 1	7	1.90	1.23E-02	yes
EEF1A1P16	eukaryotic translation elongation factor 1 alpha 1 pseudogene 16	12	1.83	2.63E-03	n.d.
DPF1	D4, zinc and double PHD fingers family 1	19	1.80	1.40E-02	no
BBC3	BCL2 binding component 3	19	1.77	3.92E-03	yes
FBXO46	F-box protein 46	19	1.68	4.99E-02	yes
CALM3	calmodulin 3 (phosphorylase kinase, delta)	19	1.68	1.68E-03	yes
C2orf44	chromosome 2 open reading frame 44	2	1.68	3.55E-08	no
FAM193B	family with sequence similarity 193, member B	5	1.51	3.20E-05	yes
WDYHV1	WDYHV motif containing 1	8	1.50	1.36E-03	no
CEBPG	CCAAT/enhancer binding protein (C/EBP), gamma	19	1.33	1.36E-03	no
TSPYL1	TSPY-like 1	6	1.30	1.27E-03	no
FAM206A	family with sequence similarity 206, member A	9	1.23	1.28E-02	yes
FAM98A	family with sequence similarity 98, member A	2	1.22	1.91E-02	yes
PRCP	prolylcarboxypeptidase (angiotensinase C)	11	1.14	1.27E-03	no

Table 3.3.: Number and location of 7 mer miR-23a binding sites in identified miR-23a targets

target	3'UTR	CDS	5'UTR
CNN2	1	0	0
CRIPT	3	1	0
DUSP5	1	0	0
IGSF8	2	1	0
KIAA1467	3	1	0
MALSU1	0	1	0
NDUFA2	2	0	0
PNRC2	4	0	0
SDHD	3	0	0
STK35	5	3	0
UQCR10	2	0	0
VRK3	2	5	0
WBP2	2	0	0
ZNF138	34	27	1
ZNF195	10	77	2
ZNF253	3	21	0
ZNF254	5	45	0
ZNF257	5	28	1
ZNF273	4	19	0
ZNF43	6	89	4
ZNF430	5	28	0
ZNF708	4	20	0
ZNF85	6	158	0
ZNF92	3	58	2
ZNF93	1	10	0
RP11-1017G21.5	n.d.	1	n.d

Table 3.4.: Number and location of 7 mer miR-27a binding sites in identified miR-27a targets

target	3'UTR	CDS	5'UTR
BBC3	2	0	0
C12orf73	1	0	0
C2orf44	4	2	0
CALM3	1	0	0
CEBPG	1	1	1
CLECL1	5	0	0
DPF1	1	9	0
FAM193B	1	5	6
FAM206A	2	0	0
FAM98A	1	0	1
FBXO46	1	0	0
LIMK1	3	1	0
PLEKHJ1	3	0	0
PRCP	0	2	0
TOR2A	4	0	0
TSPYL1	1	1	0
WDYHV1	1	4	2
HNRNPLP1	n.d.	3	n.d.
EEF1A1P16	n.d.	0	n.d.
CTC-246B18.10	n.d.	1	n.d.

a

654

CNN2
IGSF8
KIAA1467
RP11-1017G21.5
UQCR10
WBP2
ZNF93
ZNF257

18

differentially expressed genes
miR-23a *vs.* ns ctrl

identified
miR-23a targets

b

900

BBC3
FAM206A
CTC-246B18.10
C12orf73

16

differentially expressed genes
miR-27a *vs.* ns ctrl

identified
miR-27a targets
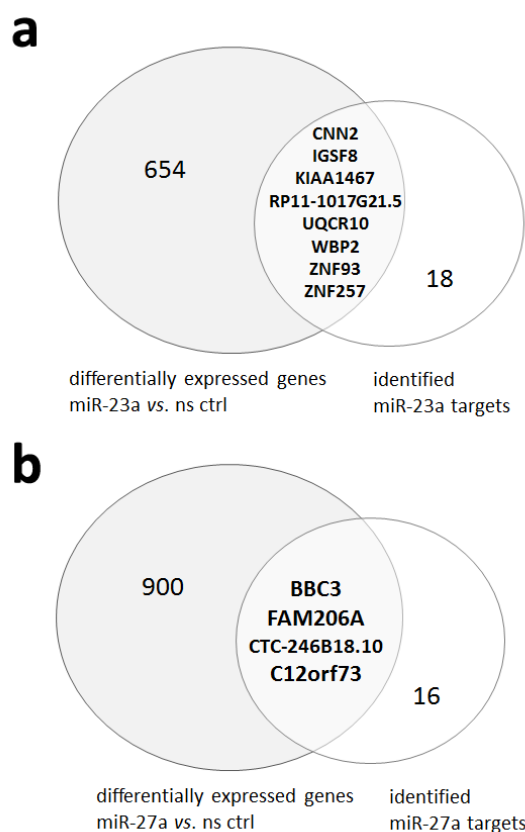
Figure 3.27.: Differentially expressed miR-23a and miR-27a targets

Dark grey: number of differentially expressed genes between (a) miR-23a overexpressing cell line compared to non silencing control (ns ctrl) and (b) miR-27a overexpressing cell line compared to ns ctrl. light grey: newly identified miR-23a/-27a targets. overlap: differentially expressed miR-23a/-27a targets.

3.2.8.1. Clustering of miR-23a and miR-27a target genes on chromosome 19

When examining the lists of newly identified miR-23a and miR-27a targets in detail (table 3.1 and 3.2), one can observe that 17 of 46 identified targets (37%) are encoded on chromosome 19, where also the MIR23A cluster is encoded (fig. 3.28). Plotting the number of identified miR-23a/27a targets against the number of expressed genes per chromosome, one can observe a linear positive correlation (fig. 3.29). The more genes are expressed from a certain chromosome, the more targets are identified from it. However, chromosome 19 shows a clear overrepresentation of miR-23a/27a target genes compared to other chromosomes. Moreover, chromosome 7 also codes for slightly more miR-23a/27a targets than expected for a linear correlation of miRNA targets and expressed genes per chromosome.
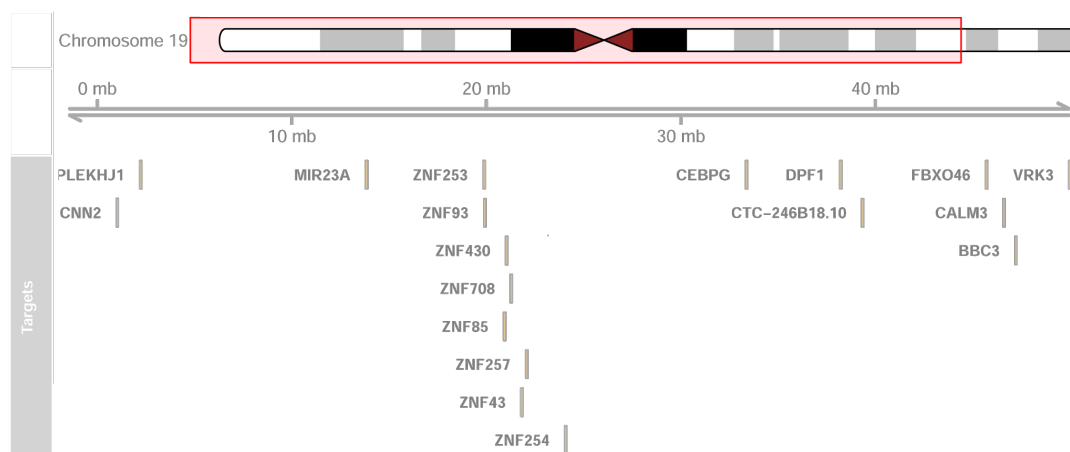
Figure 3.28.: Clustering of targets on chromosome 19
Location of the MIR23A cluster compared to the identified miR-23a and miR-27a targets that are also encoded on chromosome 19.
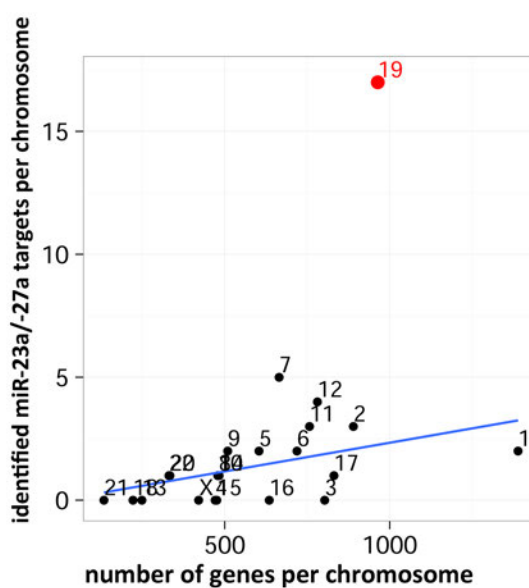
Figure 3.29.: MiR-23a and miR-27a targets are enriched on chromosome 19
Number of genes expressed per chromosome in ns ctrl 1 cell line plotted against the number of identified targets per chromosome.

A possible explanation for this observation could be, that the model cell line expresses more transcripts encoded on chromosome 19 than transcripts from other chromosomes, leading to an increased probability of the miRNAs to target those transcripts. However, this was not the case. As depicted in fig. 3.30 a) the most expressed transcripts are encoded by chromosome 1. The transcript expression of chromosome 19 was similar to that of chromosome 2,3,11,12 and 17, which showed no accumulation of targets.
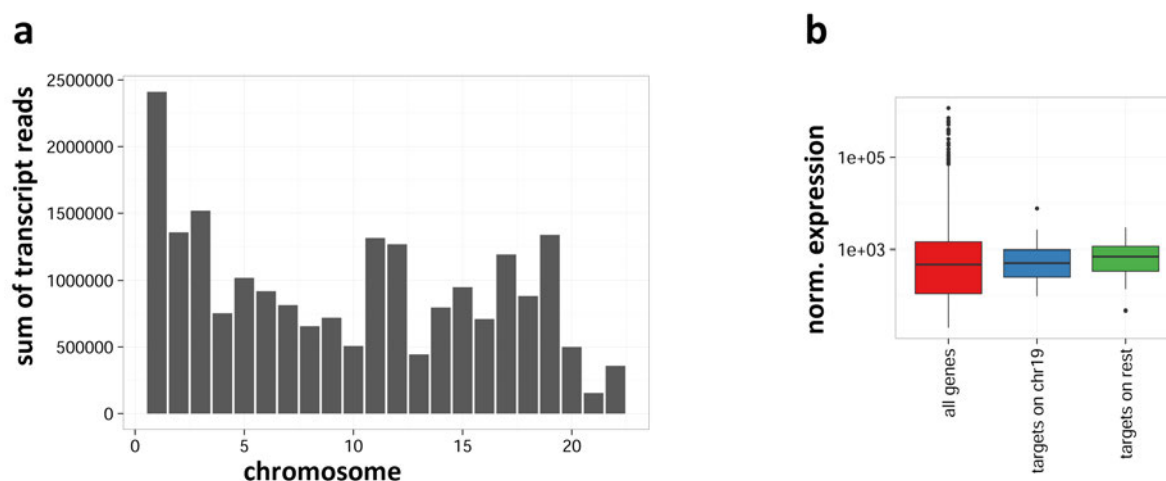
Figure 3.30.: Transcripts of chromosome 19 are not overrepresented
Transcript expression analyses of U2932 R1 pGIPZ non silencing control cell line 1 (a) Sum of reads per chromosome. (b) normalized gene expression for all genes (red), identified miR-23a/-27a targets encoded on chromosome 19 (blue) and identified miR-23a/-27a targets encoded on other chromosomes (green).

Moreover, it was tested whether miR-23a/miR-27a targets are overexpressed compared to other genes (fig. 3.30 b). Neither the expression of miR-23a/miR-27a targets on chromosome 19, nor the expression of miR-23a/miR-27a targets on the other chromosomes differed from the mean expression of all genes. The transcripts of chromosome 19 are not overrepresented in the cell.

One further reason, that could explain the observation of target clustering on chromosome 19, could be that chromosome 19 codes for more miR-23a and miR-27a binding sites in the 3'UTR of its expressed genes. Plotting the number of miR-23a/27a binding sites against the number of 3'UTRs per Mb per chromosome, one can observe the exact opposite: the miR-23a/-27a binding sites are underrepresented in the 3'UTR of chromosome 19 transcripts (fig. 3.31).

Taken together, the observation that the miR-23a/27a targets cluster on chromosome 19 is not due to overrepresentation of transcripts encoded on chromosome 19, nor due to accumulation of miRNA binding sites in transcripts encoded by chromosome 19.
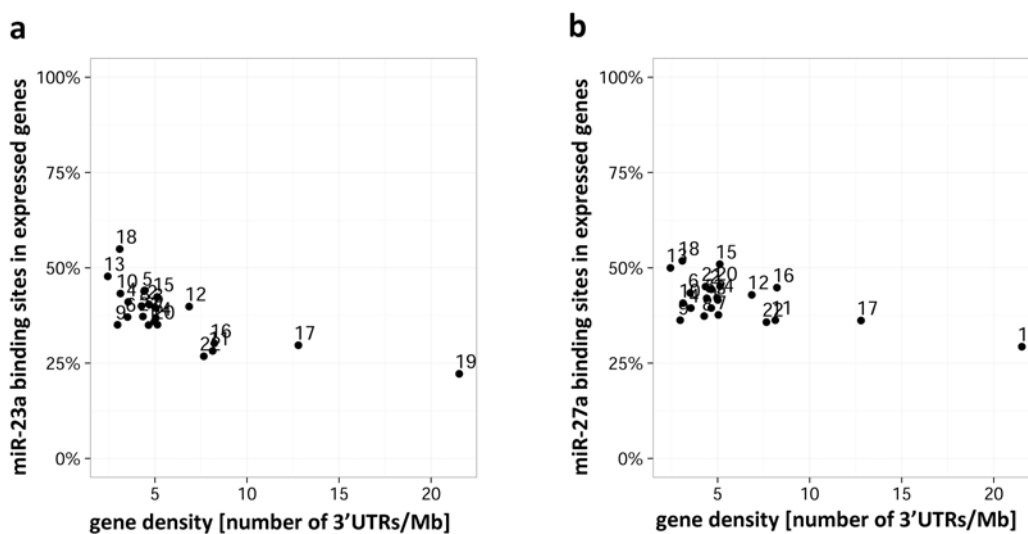
Figure 3.31.: MiR-23a/-27a binding sites are underrepresented on chromosome 19 transcripts Percentage of 7mer binding sites for miR-23a (a) and miR-27a (b) in 3'UTRs of genes expressed in ns ctrl1 cell line in respect to chromosomal gene density.

3.2.9. Validation of Ago2-RIP targets

The Ago2-RIP approach led to a list of 26 miR-23a and 20 miR-27a newly identified mRNA targets in U2932 R1, from which three were chosen for *in vitro* validation. Selection criteria were: transcript expression, high enrichment in Ago2-RIP samples, p-value, possible contribution in tumorigenesis, availability of an specific antibody and previous description as a MIR23A target in literature. Since miRNAs inhibit protein biosynthesis, the protein levels of the target candidates were investigated in miR-23a/miR-27a overexpressing cells compared to control cells.

3.2.9.1. VRK3 protein is not regulated by miR-23a

The newly identified miR-23a target vaccina related kinase 3 (VRK3) was chosen for validation on protein level. VRK3 is a serine/threonine kinase, localized to the endoplasmatic reticulum (ER) and the nucleus. It was 3.3-fold enriched with a very low p-value of 1.25×10^{-5} in miR-23a1 Ago2-RIP samples compared to control (table 3.1). VRK3 was shown to play an important role in negative feedback loop of MAPK/ERK signaling by targeting a phosphatase of ERK (Kang and Kim, 2006). Because MEK/ERK signaling was identified to activate the MIR23A cluster (section 3.1.3), VRK3 might therefore be involved in a negative feedback loop of MIR23A activation upon BCR stimulation.

To test whether VRK3 protein level is indeed downregulated by miR-23a, total cell lysates of stable miR-23a overexpressing clones were analyzed by Western blotting using an antibody specific against VRK3 (fig. 3.32). Comparing the intensity of the VRK3 protein band on West-
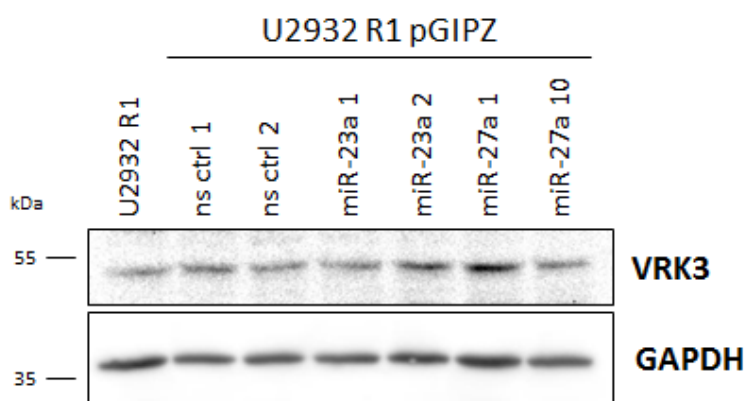
Figure 3.32.: VRK3 protein levels are not changed by miR-23a overexpression
Western blot of VRK3 in total cell lysates of U2932 R1 pGIPZ miR-23a/27a or non silencing control overexpressing clones. Loading control: GAPDH, one representative result of three is shown.

ern blot membrane, no difference between miR-23a overexpressing U2932 R1 pGIPZ clones vs. ns ctrls or miR-27a overexpressing clones could be observed. Consequently, VRK3 protein levels are, at least under default conditions, not downregulated by miR-23a.

3.2.9.2. LIMK1 protein is downregulated by miR-27a

The novel identified miR-27a target, LIM domain kinase 1 (LIMK1) was chosen for validation on protein level. It was enriched 3.7-fold in miR-27a1 Ago2-RIP samples compared to controls with a p-value of 1.23×10^{-2} (table 3.2). The LIMK1 is a serine/threonine kinase, that is implicated in migration by inhibition of Cofilin (Arber *et al.*, 1998) and in mitosis by inhibition of p25/TPPP (Acevedo *et al.*, 2007) (for details see discussion). Additionally, LIMK1 was already shown to be a target of the paralogous miR-27b in non small cell lung cancer (NSCLC), where it regulates invasion and proliferation (Wan *et al.*, 2014).

To validate LIMK1 as a miR-27a target in DLBCL, LIMK1 protein levels from total cell lysates of miR-27a stable overexpressing U2932 R1 pGIPZ clones and ns ctrl clones were compared by Western blotting (fig. 3.33 a). The LIMK1 protein levels are downregulated to 38% in miR-27a1 and to 28% in miR-27a10 stable overexpressing U2932 R1 pGIPZ clones. The sister clone U2932 R2, which expresses higher miR23A levels than the U2932 R1 clone (fig. 3.11) shows also considerable low LIMK1 levels. Surprisingly, the U2932 R1 pGIPZ miR-23a1 clone shows also a slight downregulation of LIMK1 to 76%. However, the miR-23a2 clone showed no such effect. The ns ctrl 3 clone is different from the other two control clones, hence LIMK1 level are downregulated by 17%. This observation may be due to other reasons, but not a direct miR-27a effect.
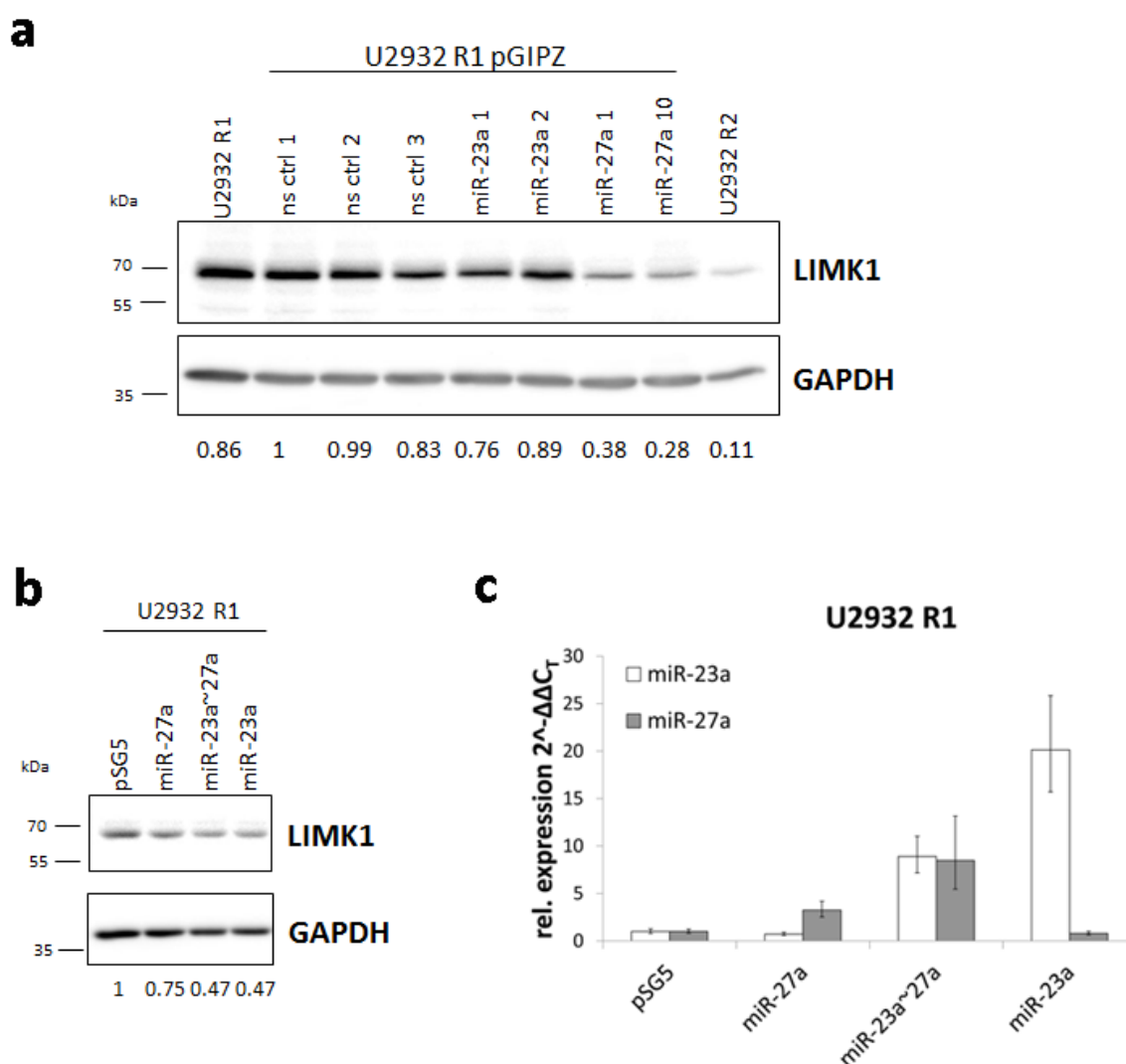
Figure 3.33.: LIMK1 is a miR-27a and miR-23a target
(a) Total cell lysates of U2932 R1 pGIPZ non silencing control, miR-23a or miR-27a stable overexpressing clones. (Loading control: GAPDH, one representative result of three is shown). b) Total cell lysates of parental U2932 R1 48 h post transient transfection with miR-23a, miR-27a or miR-23a~27a expression vector (pSG5). 5 µg plasmid DNA per 5x10^6 cells, one representative result of three is shown. (c) corresponding relative expression of miR-23a and miR-27a upon transfection in U2932 R1. Endogenous control: *GAPDH.*

To validate these results and to clarify whether miR-23a also targets LIMK1, transient over-expression experiments were performed. Therefore, the parental cell line U2932 R1 was transfected with pSG5_miR-23a, pSG5_miR-27a or pSG5_miR-23a~27a expression vector (section 3.2.2). Mature miR-23a and miR-27a expression levels were detected by qRT-PCR (fig. 3.33 c) and LIMK1 protein levels were analyzed by Western blotting 48 hours after transfection (3.33 b). Indeed, the LIMK1 protein levels decreased by 25%, when miR-27a was overexpressed only 5-fold compared to empty vector pSG5. Furthermore, the double transfection with miR-23a and miR-27a, which led to higher levels of miR-27a (ca. 9-fold) than the single-miR-27a transfection, decreased LIMK1 levels to a higher degree (down to 47%). To

test whether this effect was due to higher miR-27a level or due to an additive effect of miR-23a, the same cells were transfected with miR-23a alone. Surprisingly, the same effect (downregulation to 47%) could also be obtained when overexpressing miR-23a 20-fold higher than the empty vector control.

Taken together, LIMK1 protein levels are downregulated by miR-23a and miR-27a in stable and transient miRNA overexpressing experiments for DLBCL cell line U2932 R1, although LIMK1 mRNA was only 3.7-fold enriched in miR-23a Ago2-RIP samples compared to ns control.

3.2.9.3. PUMA protein can not be induced in miR-27a overexpressing cells

BCL-2 binding component 3 (BBC3) or P53 upregulated modulator of apoptosis (PUMA) is a pro-apoptotic protein and was described as a tumor suppressor in different cancer entities. It was chosen as a target candidate for validation on protein level, because it was enriched 3.4-fold, had a good p-value of 3.92×10^{-3} (see table 3.2) and is implicated in apoptosis, which plays an important role during B cell maturation process (section 1.1). Moreover, it was shown in mice, that PUMA is targeted by mmu-miR-23a and mmu-miR-27a in a traumatic brain injury model (Sabirzhanov *et al.*, 2014).

Because of low PUMA levels, it was difficult to detect PUMA by Western blotting. Consequently, PUMA levels were induced by etoposide treatment of miR-27a or ns ctrl overexpressing U2932 R1 pGIPZ clones. Etoposide induces DNA double strand breaks, that activate p53, which subsequently induces PUMA. Although p53 was induced in all samples upon etoposide treatment, only the β-isoform, but not the α-isoform, of PUMA was induced in the parental cell line U2932 R1 and the ns ctrl clones (fig. 3.34). Notably, PUMA-β was not induced in the miR-27a overexpressing clone miR-27a1. It seems as if it is only slightly induced in miR-27a10 clone, but this is due to unequal loading as indicated by the endogenous control GAPDH. When comparing the basal PUMA levels in DMSO treated controls of the stable overexpressing clones to ns ctrl clones, unexpectedly no regulatory pattern could be observed. Obviously, PUMA has to be induced in order to monitor the inhibitory miR-27a effect.

In summary, the expression of PUMA-β isoform is inhibited by miR-27a upon etoposide-induced DNA damage in DLBCL cell line U2932 R1.
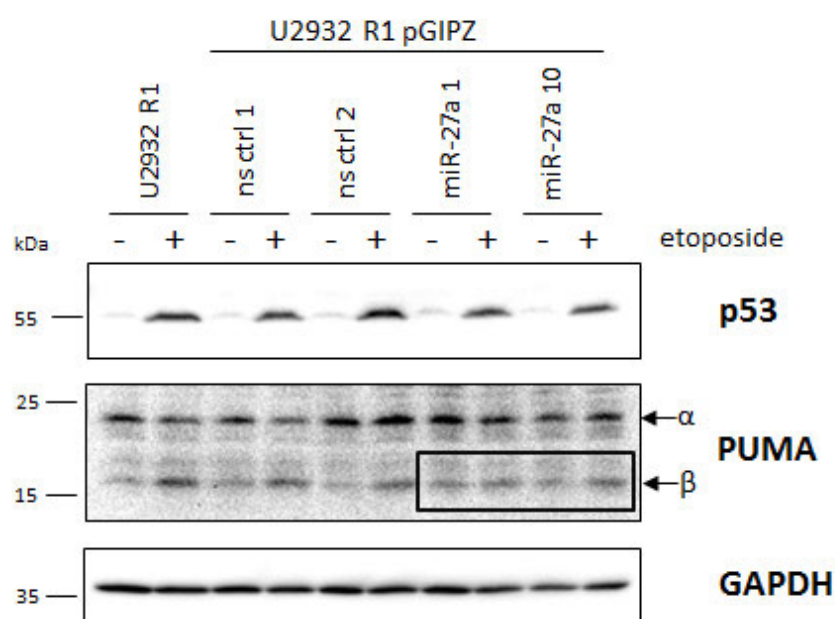
Figure 3.34.: PUMA is a miR-27a target
U2932 R1 pGIPZ miR-27a and non silencing control (ns ctrl) overexpressing cells were treated for 7 hours with 100 µM etoposide (+) or 1:500 DMSO (-). Loading control: GAPDH, one representative experiment of three is shown.

3.3. MIR23A function

3.3.1. Global affected processes by miR-23a or miR-27a overexpression

The identification of the direct miR-23a and miR-27a targets in DLBCL cell line U2932 R1 by Ago2-RIP resulted in two different gene sets with no overlap. Thus, miR-23a and miR-27a have distinct direct targets. However, it is likely that miRNAs of the same cluster act in the same cellular processes. Because miRNA overexpression resulted in differential gene expression profiles, these genes can be considered as indirect miRNA targets. Their expression is not altered by direct binding of the miRNA and subsequently inhibition of proteinbiosynthesis, but by indirect means, such as downregulation of a transcriptional repressor or activator, etc.. To analyze in which biological processes these indirect targets are involved, gene ontology analyses for differentially expressed genes were performed.
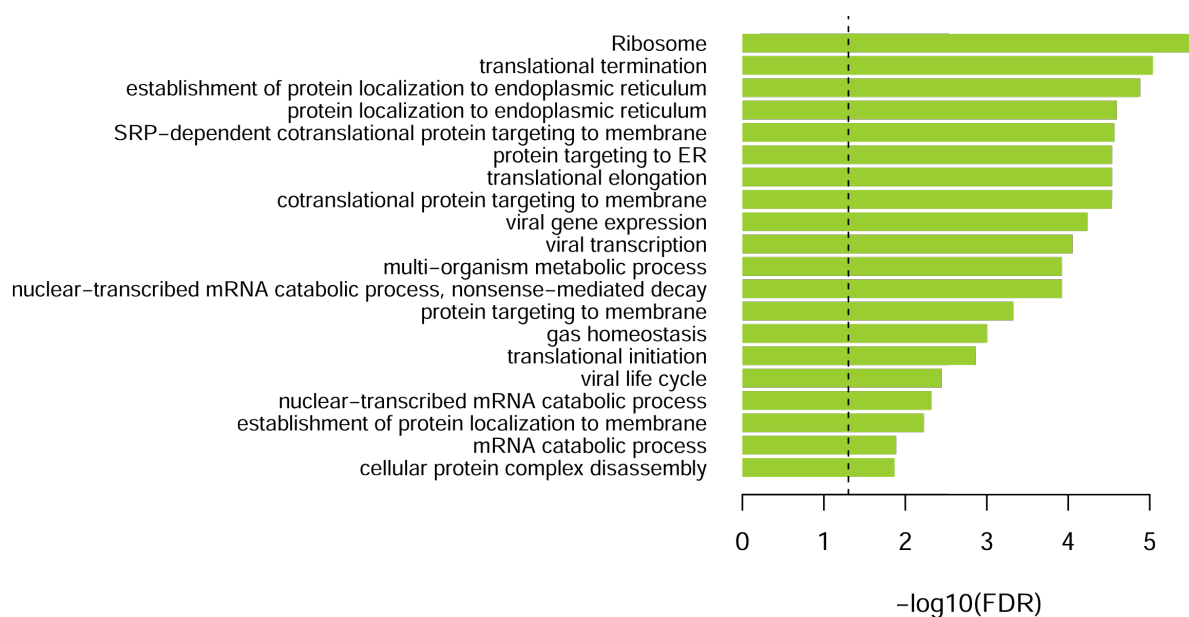
Figure 3.35.: Top 20 GO terms enriched in U2932 R1 pGIPZ miR-23a1 *vs*. ns ctrl1
Hypergeometrical test for overrepresentation of gene ontology terms (GO) of differentially expressed genes between U2932 R1 pGIPZ miR-23a1 and ns ctrl1 cell lines. FDR = false discover rate. Shown are GO terms with p-value ≤0.05. FDR = false discovery rate, FDR q-value is the correction of the p-value for multiple testing using the Benjamini and Hochberg method.

Gene ontology analyses of differentially expressed genes (DEG) upon miR-23a overexpression in U2932 R1 show that genes are affected, which are involved in many different cellular processes (fig. 3.35). Notably, processes involved in ribosomal protein biosynthesis are enriched. Additionally, processes that direct proteins to membranes emerge, indicating that protein trafficking or secretion might be affected by miR-23a overexpression. Gene ontology terms related to a virus might be explained by the lentivirus, that was introduced to gain miRNA overexpression in these cells.
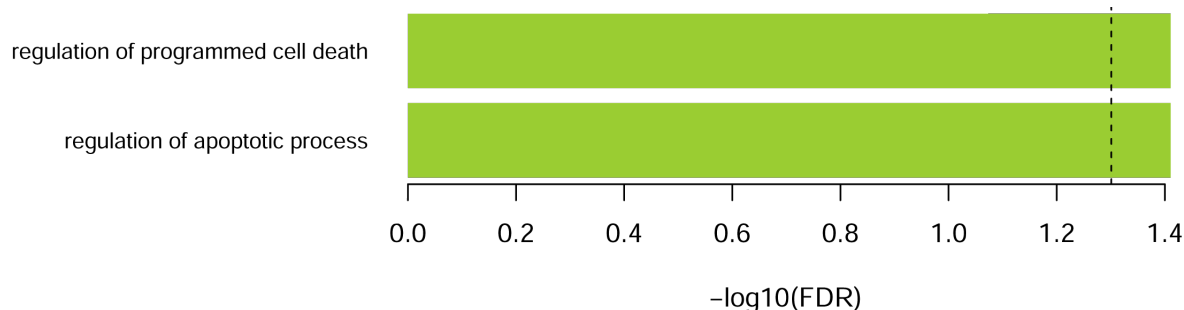
Figure 3.36.: GO terms enriched in U2932 R1 pGIPZ miR-27a1 *vs*. ns ctrl1
Hypergeometrical test for overrepresentation of gene ontology terms (GO) of differentially expressed genes between U2932 R1 pGIPZ miR-27a1 and ns ctrl1 cell lines. FDR = false discover rate. Shown are GO terms with p-value ≤0.05. FDR = false discovery rate, FDR q-value is the correction of the p-value for multiple testing using the Benjamini and Hochberg method.

Gene ontology analyses of differentially expressed genes upon miR-27a overexpression in U2932 R1 revealed interestingly only two significantly enriched GO terms: "regulation of apoptotic process" and "regulation of programmed cell death" (fig. 3.36). This was one reason to test the rate of apoptosis in U2932 R1 miR23a/27a overexpressing cells (fig. 3.38).

To assess a possible cooperative effect of miR-23a and miR-27a the overlap of differentially expressed genes upon miR-23a and miR-27a overexpression in U2932 R1 was analyzed. These overlap generated a list of 104 genes that are affected by overexpression of both, miR-23a and miR-27a (fig. 3.37 and table A.1). Surprisingly, GO term analyses with these genes could not identify significantly enriched cellular processes, indicating that miR-23a and miR-27a act separately to regulate different cellular processes.

miR-23a1 *vs.* ns ctrl1

547

104

800
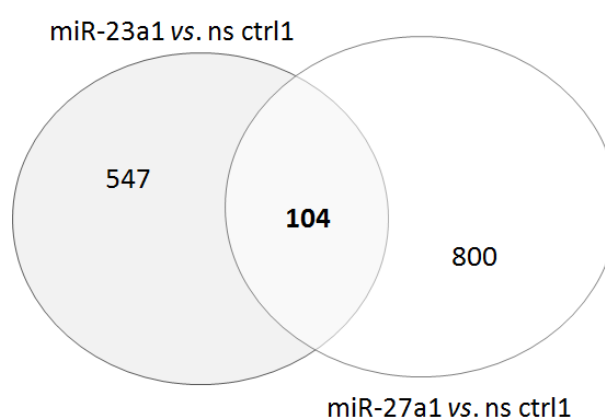
miR-27a1 *vs.* ns ctrl1

Figure 3.37.: Venn diagram of DEG of miR-23a1 *vs.* ns ctrl1 compared to ns ctrl1 *vs.* miR-27a1
Differentially expressed genes (DEG) of U2932 R1 pGIPZ miR-23a1 *vs.* ns ctrl1 compared to ns ctrl1 *vs.* miR-27a1 identifies 104 genes affected by both, miR-23a and miR-27a overexpression.

In conclusion, miR-23a and miR-27a might act separately regulating different cellular processes. Neither the overlap of direct nor indirect miR-23a with miR-27a targets leads to a significant enrichment of GO terms using a hypergeometrical test.

3.3.2. miR-27a attenuates the sensitivity of DLBCL cells to undergo apoptosis

The pro apoptotic protein PUMA could be validated in U2932 R1 as a miR-27a target on protein level (section 3.2.9.3), favouring together with the GO term analyses of indirect miR-27a targets (fig. 3.36) apoptosis as a possible cellular function in which the MIR23A cluster is involved. The introduction of DNA double strand breaks led to the induction of p53, which in turn activated the β-isoform of PUMA in the control cells (parental cell line U2932 R1 and U2932 R1 pGIPZ ns ctrl1 and 2), but not in the miR-27a overexpressing cells (fig. 3.34). Furthermore, also LIMK1, which could also be validated as an miR-27a target on protein level (section 3.2.9.2),

was shown to be implicated in apoptosis (Tomiyoshi *et al.*, 2004). It is therefore probable that overexpression of miR-27a attenuates apoptosis by targeting PUMA-β and LIMK1.

To test this hypothesis, apoptosis was induced for 16h in the parental cell line U2932 R1 and the stable miR-23a, miR-27a and ns ctrl overexpressing U2932 R1 pGIPZ clones using etoposide. The apoptosis rate was determined by AnnexinV/7AAD staining following FACS analyses. Percent of positive cells were normalized to DMSO control (fig. 3.38, for FACS profiles see supplementals).
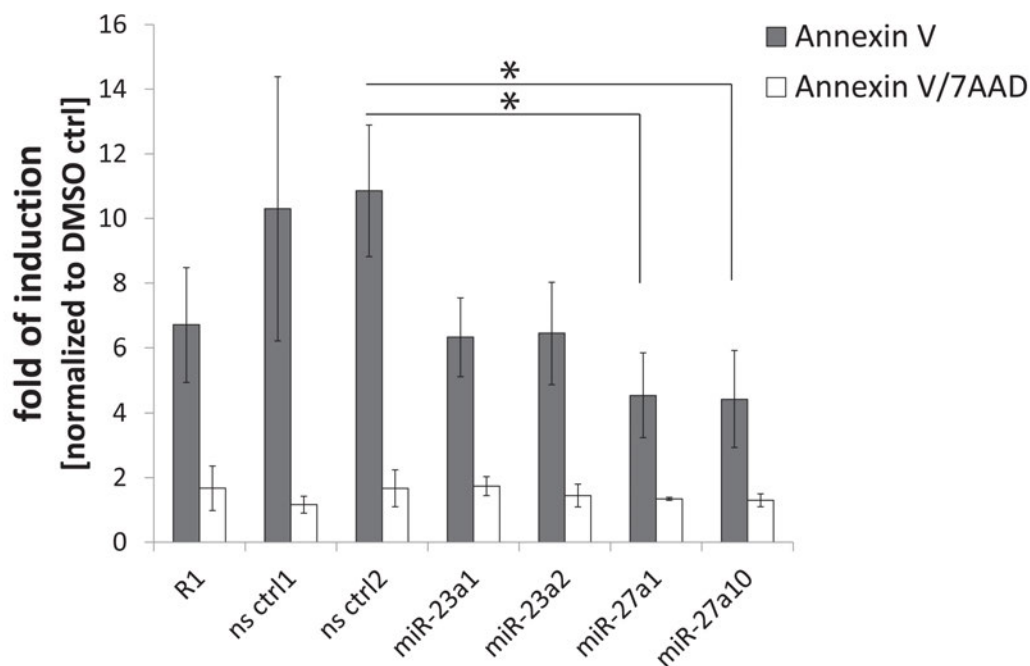
Figure 3.38.: Overexpression of miR-27a reduces sensitivity to etoposide induced apoptosis in DLBCL cell line U2932 R1

Parental cell line U2932 R1, U2932 R1 non silencing control (ns1, ns2), miR-23a (miR-23a1, miR-23a2) and miR-27a (miR-27a1, miR27a10) overexpressing cell lines were treated for 16h with 100 µM etoposide to induce apoptosis. Cells were double stained with Annexin V-PE and 7AAD prior to FACS analysis. Mean +/- SD, n=3, students t-test, *p≤0.05

Comparing the induction of Annexin V positive cells from parental cell line U2932 R1 to U2932 R1 pGIPZ non silencing control cell lines ns ctrl1 and ns ctrl2, one can observe an higher apoptosis rate for the control clones. The parental clone showed an induction rate of 7-fold compared to DMSO treated control, while ns ctrl cell lines showed an induction rate of approximately 11-fold. It may be speculated that the genetical modification of the cells by insertion of the lentivirus, overexpression of eGFP as well as overexpression of an hairpin sequence might induce cellular stress leading to an enhanced disposition to undergo apoptosis. Therefore, the correct controls to compare the miRNA overexpressing clones to, are the non silencing control cell lines. While U2932 R1 pGIPZ ns ctrl cells have an induction rate of early apoptotic cells (Annexin V positive) of 11-fold, the miR-23a overexpressing clones show decreased apoptotic

rates of 7-fold. Notably, the miR-27a overexpressing clones show a significant reduction of apoptosis rate (5-fold) compared to controls. The rate of double positive (Annexin V/7AAD) late apoptotic or dead cells is not affected by miRNA overexpression.

In conclusion, the overexpression of miR-23a and miR-27a reduces the ability of etoposide treated cells to undergo apoptosis.

3.4. The MIR23A cluster in BL and DLBCL patients

The role of the MIR23A cluster is discussed controversially in literature. Although intensively investigated in many different human diseases and cancers, the miRNAs encoded in this cluster can have diverse functions. MiR-23a was reported to act as a tumor suppressor or as an onco-miR, depending on the cellular context (Cao *et al.*, 2012; He *et al.*, 2014). Nevertheless, several studies have shown altered expression of MIR23A cluster in different cancers, among these also some hematopoietic malignancies (APL (Saumet *et al.*, 2009), ALL and AML (Mi *et al.*, 2007)). For B-NHL it was shown by Lenze *et al.* that miR-23a is differentially expressed between BL *vs*. DLBCL (Lenze *et al.*, 2011). Wang *et al.* already indicated that miR-23a is aberrantly expressed in DLBCL compared to healthy controls (Wang *et al.*, 2014). However, the expression status of the whole MIR23A cluster in DLBCL compared to germinal center cells, which are the healthy progenitor cells from which DLBCL develops, was unknown so far.

Therefore, the publicly available data base of the International Cancer Genome Consortium (ICGC) Project "Determining Molecular Mechanisms in Malignant Lymphoma by Sequencing" (ICGC-MMML, release v22, published in (Hezaveh *et al.*, 2016)) was retrieved to compare the MIR23A expression of BL and DLBCL patients to healthy GCBs (fig. 3.39). The differential expression of miR-23a in BL *vs*. DLBCL described by Lenze *et al.* in 2011 could be verified. Additionally, the comparison of the MIR23A cluster expression of BL and DLBCL patients to healthy GCBs reveals a significant overexpression of miR-23a, miR-27a and miR-24 in the patient samples (fig. 3.39).

Taken together, the patient sequencing data show that the whole MIR23A cluster is aberrantly activated in BL and in DLBCL compared to healthy controls (GCBs).
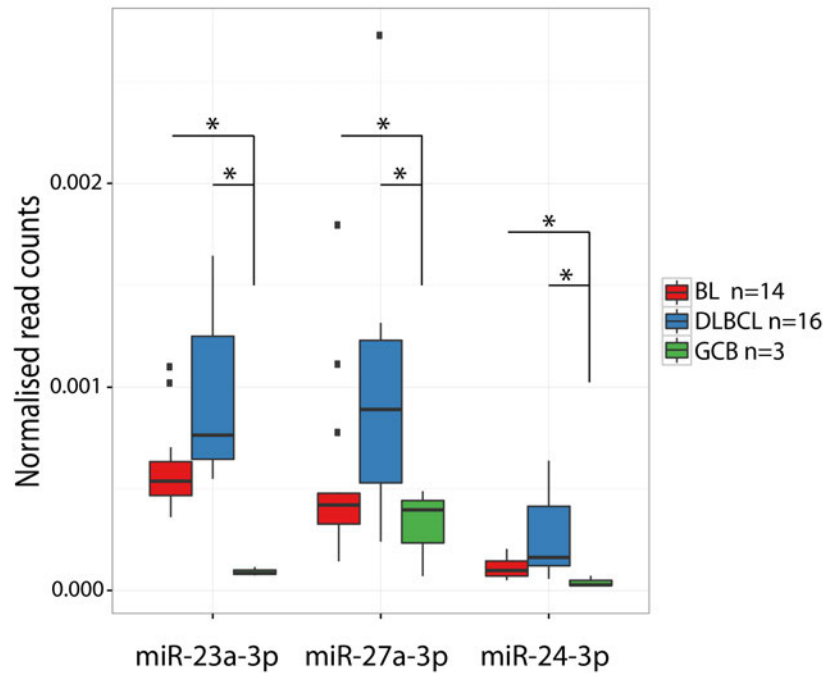
Figure 3.39.: MIR23A cluster expression in B-NHL patients
MicroRNA sequencing data of 14 BL and 16 DLBCL patients compared to GCB isolated from three healthy controls (ICGC v22 published in Hezaveh *et al.* 2016). Mann-Whitney U-test *p≤ 0.05.

3.4.1. Expression of newly identified and validated miR-23a and miR-27a targets in BL and DLBCL patients

The observation that MIR23A levels are aberrantly high in BL and DLBCL compared to controls raises the question which consequences arise from this aberrant high expression of MIR23A cluster for the DLBCL patients. Wang *et al.* showed already in 2014 that high miR-23a levels were correlated with a worse overall survival rate of DLBCL patients. Thus, the MIR23A cluster might have an onco-miR function in DLBCL. Although a miRNA does not necessarily downregulate their targets on RNA level, the expression of the direct miR-23a/27a targets, identified in this study, were analyzed for BL and DLBCL patients on RNA sequencing data provided by the ICGC data base.

Although VRK3 protein could not be validated to be downregulated by miR-23a overexpression under normal conditions in DLBCL cell line U2932 R1 (fig. 3.32), its mRNA levels are decreased in BL and DLBCL patients compared to healthy GCBs (fig. 3.40 a).

In the case of LIMK1, a validated target gene of miR-27a in this study (fig. 3.2.9.2), BL and DLBCL patients show a decrease in *LIMK1* mRNA levels (fig. 3.40 b).
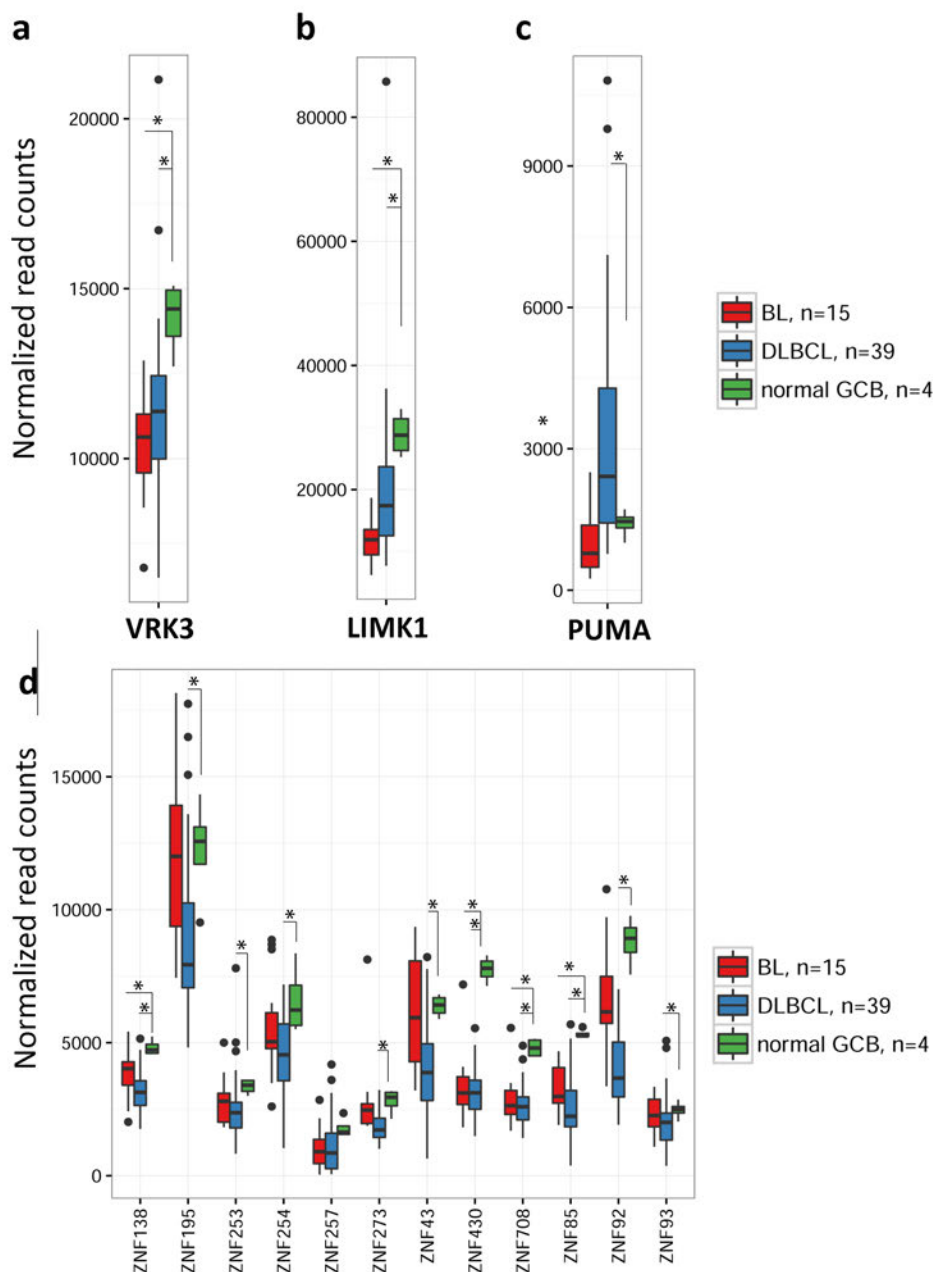
Figure 3.40.: MiR-23a and miR-27a target expression in BL and DLBCL patients
Expression of selected targets in BL and DLBCL patients and normal GCBs (ICGC v22 published in Hezaveh *et al.* 2016). (a) Expression of possible miR-23a target VRK3. (b) Expression of validated miR-27a target LIMK1. (c) Expression of validated miR-27a target PUMA. (d) Expression of ZNFs that are targeted by miR-23a. BL = Burkitt lymphoma, DLBCL = diffuse large B cell lymphoma, GCB = germinal center B cells, VRK3 = Vaccina related kinase 3, LIMK1 = LIM domain kinase 1, PUMA = p53 upregulated modulator of apoptosis, ZNF = zinc finger. Mann-Whitney U-test *p$\leq$ 0.05.

In contrast, the mRNA levels of validated miR-27a target *PUMA* (fig. 3.34) are downregulated in BL, whereas the mean expression of DLBCL patients is higher compared to controls (fig. 3.40 c).

Interestingly, most ZNFs, that were identified as possible miR-23a targets in DLBCL model cell line U2932 R1, are downregulated in BL and DLBCL patients compared to healthy GCBs.

In general, miRNA regulation in mammalia must not result in downregulation of target mRNA levels. However, the mRNA transcripts of *VRK3*, *LIMK1* and most *ZNFs* are decreased in B-NHL compared to healthy GCBs.

4. Discussion

This study had two major aims: the first one was to identify signaling pathways that regulate the expression of MIR23A cluster in DLBCL, in order to enlighten the processes that lead to aberrant high MIR23A cluster expression in DLBCL. The second aim was to identify the targetomes of miR-23a and miR-27a in DLBCL in order to predict the cellular functions in which miR-23a and miR-27a are involved and to test the onco-miR hypothesis for the MIR23A cluster.

DLBCL and BL patients show increased miR-23a levels compared to healthy controls (Wang *et al.*, 2014) (fig. 3.39), indicating that the MIR23A cluster is de-regulated in aggressive B cell lymphoma. Furthermore, DLBCL patients with higher miR-23a levels show a worse overall survival rate than patients with low miR-23a levels, suggesting the MIR23A cluster to have a onco-miR function in DLBCL (Wang *et al.*, 2014).

This thesis shows that the MIR23A cluster is activated by BCR signaling in BL and DLBCL cell lines. In detail, the BCR downstream MEK/ERK signaling cascade was identified to mediate the activation of MIR23A cluster in DLBCL cell lines. Furthermore the onco-miR hypothesis for the MIR23A cluster in DLBCL could be supported by identification and validation of the miR-23a and miR-27a specific targetome in a DLBCL model cell line.

4.1. Regulation of the MIR23A cluster

4.1.1. BCR signaling activates the MIR23A cluster

This study identified MEK/ERK dependent BCR signaling in DLBCL cell lines as a general mechanism responsible for the activation of the MIR23A cluster.

The MIR23A cluster is activated during normal GC reaction: while naive B cells and centroblasts show low MIR23A cluster expression, memory B cells have high MIR23A cluster expression (Malumbres *et al.*, 2009; Tan *et al.*, 2009; Zhang *et al.*, 2009; Iqbal *et al.*, 2015). DLBCL develops from GCB cells, thus DLBCL cells still harbor GC characteristics and a related gene expression profile (Küppers, 2005). However, tumor samples of DLBCL patients express aberrant high MIR23A levels compared to healthy controls ((Wang *et al.*, 2014) and fig. 3.39). Notably, the healthy controls used in both studies were different. Wang *et al.* used paraffin embedded reactive lymph nodes, while primary tonsillar GCBs were sorted in the ICGC-MMML project to get a normal control, which represents the precursor cells from BL and DLBCL. However, the results were similar. This indicates that a deregulated process during GC reaction

might lead to aberrant high MIR23A cluster expression in GC derived lymphoma. The BCR signaling, which plays a key role in GC reaction (section 1.2.1), was identified in this study to be responsible for MIR23A cluster activation. This might be a general mechanism for GC derived lymphoma, since BCR dependent activation of the MIR23A cluster was observed in several DLBCL and one BL cell line (section 3.1.3). The observation, that CD77 positive GCBs isolated from human pediatric tonsils, which represent centroblasts (Pascual *et al.*, 1994; Klein *et al.*, 2003), did not respond to BCR stimulation with an upregulation of MIR23A cluster expression (fig. 3.6), supports the hypothesis of aberrant BCR signaling in BL and DLBCL. However, these experiments were only performed twice. Although widely accepted, the CD77 marker was questioned as an appropriate marker for centroblasts (Högerkorp and Borrebaeck, 2006). Thus, it was shown, that CD77 positive and negative populations are both actively cycling and that gene expression profiles of both populations did not fit to functional characteristics of centroblasts or centrocytes (Högerkorp and Borrebaeck, 2006). Additionally, GCBs used in this study were isolated from pediatric tonsils due to frequent infections and abnormal growth, asking whether these cells are an appropriate normal control. The MIR23A cluster levels might not be further increased by BCR stimulation, because the GCB cells are already fully activated due to antigen response and inflammation.

During GC reaction SHM and CSR lead to affinity maturation of the BCR. These processes include genetic modifications, such as chromosomal translocations and somatic mutations. Errors that occur during these processes can lead to malignant transformation of these cells, as observed in BL, DLBCL and FL. Indeed, many activating mutations within BCR signaling components were reported occurring in aggressive B cell lymphoma (Seda and Mraz, 2015). Importantly, B cell lymphoma are dependent on the survival signals provided by BCR signaling, as shown by their sensitivity to chemical inhibitors that specifically target effectors of the BCR signaling network (Young and Staudt, 2013; Blachly and Baiocchi, 2014; Gaudio *et al.*, 2016). E.g. for ABC DLBCL a chronic BCR signaling due to different mutations was reported: many ABC DLBCL patients carry CARD11 mutations that cause the spontaneous formation of aggregates, which recruit all downstream signaling components of the NF$\varkappa$B pathway (Lenz *et al.*, 2008). Additionally, the ITAMs of CD79 are frequently mutated preventing endocytosis of the BCR and inhibit the activity of LYN to deliver negative feedback signals that attenuate BCR activity (Davis *et al.*, 2010). Another mechanism for chronic active BCR signaling is the reactivity against self antigen (Young *et al.*, 2015). The presence of BCR clusters on the cell surface of ABC DLBCL, resembling the clusters that are formed after antigen encountering, support this observation (Rui *et al.*, 2011). In contrast to chronic active BCR signaling in ABC DLBCL, in GCB DLBCL and BL tonic BCR signaling was reported (Young and Staudt, 2013; Efremov, 2016). It predominantly activates the PI3K pathway in an antigen-independent manner to provide the cell with survival signals. Responsible for tonic BCR signaling are alterations of signaling pathway components, such as SYK amplification (Monti *et al.*, 2005) or

tensin homolog (PTEN) deletion in GCB DLBCL (Pfeifer *et al.*, 2013). Many BL cases harbor *transcription factor 3 (TCF3)* mutations that prevent ID3 to inhibit TCF3 resulting in increased activity of PI3K (Richter *et al.*, 2012; Schmitz *et al.*, 2013). However, inhibition of PI3K/AKT signaling did not inhibit MIR23A cluster activation upon BCR stimulation in U2932 R1 (fig. 3.8), indicating that it is not responsible for MIR23A cluster activation in this cell line. Furthermore, when comparing differential expressed miRNAs from ABC DLBCL with GCB DLBCL cell lines, the MIR23A cluster does not appear in these analyses (Malumbres *et al.*, 2009), indicating, that neither the NFϰB pathway nor PI3K/AKT signaling are predominantly responsible for the activation of the MIR23A cluster in DLBCL.

Indeed, this study could identify MEK/ERK signaling as the major BCR downstream signaling cascade responsible for activation of the MIR23A cluster in DLBCL cell line U2932 R1. Although mutations of Ras/Raf, which act upstream of MEK and ERK, were reported for different cancers (Masliah-Planchon *et al.*, 2015; Downward, 2003), including hairy cell leukemia, where BRAF mutations were shown to result in constitutive active RAF/MEK/ERK signaling (Vaqué *et al.*, 2014), no such mutations are known for DLBCL. However, constitutive active ERK signaling was found in DLBCL (Hollmann *et al.*, 2006). ERK2 itself can bind to DNA and act as a transcriptional repressor (Hu *et al.*, 2009). Furthermore, ERK2 was reported to promote a "poised" state of developmental genes by potentiating PRC2-mediated trimethylation of H3K27 and phosphorylation of RNA Pol II in mice (Tee *et al.*, 2014). Indeed, the MIR23A promoter harbors six canonical ERK2 binding sites, but as the MIR23A cluster is induced upon ERK1/2 activation, ERK2 itself might not be the transcription factor responsible for the activation of the MIR23A cluster. Instead, a downstream factor of ERK1/2 might exert this function. Many downstream factors were already described for the MAP kinase ERK1/2 (Yoon and Seger, 2006). Among these downstream ERK1/2 targets are many transcription factors, including MYC and ELK1 (Gille *et al.*, 1995; Yoon and Seger, 2006).

4.1.2. BCR downstream transcription factors

Proto-oncogene *MYC* was of special interest, because it is downstream of the BCR signaling and many lymphomas harbor *MYC* translocations (Küppers, 2005). Furthermore, *MYC* is considered to promote lymphomagenesis (Dalla-Favera *et al.*, 1982). In regard to transcriptional regulation of the MIR23A cluster, *MYC* was reported to bind to the paralogous MIR23B promoter and suppress miR-23a and miR-23b levels in BL model cell line P493-6 (Gao *et al.*, 2009). This observation was validated in this study and extended to the whole MIR23A cluster in P493-6 (fig. 3.12), indicating that MYC might also bind to the MIR23A promoter. Instead, Li *et al.* showed that c-MYC induced the MIR23A cluster expression in mammary carcinoma (Li *et al.*, 2013a). However, in DLBCL model cell line U2932 R1 ectopic *MYC* overexpression

and siRNA knockdown approaches revealed, that MYC does neither activate nor repress the MIR23A cluster in DLBCL. Furthermore, the MIR23A cluster could still be activated by BCR stimulation, when MYC protein levels were abolished by CHX treatment (fig. 3.7). These data indicate, that MYC is not responsible for the regulation of the MIR23A cluster in DLBCL cell line U2932 R1.

The first transcription factor described to be a substrate of ERK1/2 was ELK1 (Gille *et al.*, 1995). Indeed, this was validated in U2932 R1 (fig. 3.14). Upon BCR stimulation ERK and ELK1 were phosphorylated. Furthermore, the inhibition of ERK phosphorylation by trametinib also inhibited ELK1 phosphorylation. ELK1 forms a ternary complex with serum response factor (SRF) and serum response element (SRE) of *c-Fos* promoter (Gille *et al.*, 1995). Induction of *c-Fos* is important for cell proliferation and differentiation. Furthermore, phosphorylated ELK1 induces the binding of c-Fos to c-Jun, which together form the transcriptionally active AP-1 complex (Whitmarsh and Davis, 1996). AP-1 subsequently induces *cyclin D1*, which is responsible for cell cycle progression (Shaulian and Karin, 2001). ELK1 was regarded as candidate for MIR23A cluster activation, because Acunzo *et al.* showed by ChIP assay that ELK1 binds to the promoter of MIR23A cluster in non-small cell lung cancer (NSCLC) and activates it. However, systematical *ELK1* overexpression and knockdown experiments could not confirm this hypothesis for DLBCL cell line U2932 R1 (fig. 3.15).

Although both transcription factors MYC and ELK1 were described to regulate the miR-23a levels in other cancer entities, neither did this in DLBCL model cell line U2932 R1. One possible explanation might be, that the binding sites of ELK1 and MYC within the MIR23A promoter are not available due to chromatin modifications. Indeed, somatic mutations of epigenetic modifier proteins are a hallmark of DLBCL (Morin *et al.*, 2010, 2011) (Pasqualucci and Dalla-Favera, 2014). One example is *EZH2* in GCB DLBCL. It is upregulated during normal GC reaction in centroblasts and induces bivalent chromatin at genes required for memory and plasma cell differentiation (e.g. *IRF4* and *PRDM1*) (Béguelin *et al.*, 2013). Importantly, *EZH2* mutation of the key tyrosine in catalytic site of SET domain enhances EZH2 activity (Sneeringer *et al.*, 2010) and subsequently leads to permanent silencing of target genes, resulting in a differentiation block and accelerated lymphoid transformation (Béguelin *et al.*, 2013).

Another possibility is that the co-factors, which bind to MYC or ELK1, are de-regulated or mutated. One co-factor of ELK1 is cyclic AMP response element binging (CREB) protein (CBP) (Janknecht and Nordheim, 1996). Indeed, CBP translocations were reported for several hematopoietic diseases, such as acute myeloid leukemia (AML) (Borrow *et al.*, 1996; Giles *et al.*, 1997; Panagopoulos *et al.*, 2001), but not for aggressive B cell lymphoma. Interestingly, CBP loss was shown to induce T cell lymphomagenesis in mice (Kang-Decker *et al.*, 2004). For cofactors of MYC, such as MIZ1, ATAD2, Mad or MAX, no alterations were described in

lymphoma. However, mutations for PIM1, a serine/threonine kinase, which strongly synergizes with MYC, were reported for ABC DLBCL (Peters *et al.*, 2016).

ERK was described to phosphorylate various different proteins, including transcription factors (Yoon and Seger, 2006). It would therefore be necessary to analyze whether binding sites of these ERK downstream transcription factors can be found within the MIR23A promoter region.

Other transcription factors regulating the MIR23A cluster are described in literature, such as PU.1, NFAT and NF$\varkappa$B family members. PU.1 was reported to activate the MIR23A cluster in early stages of B cell development in the bone marrow, where the MIR23A cluster inhibits the development of the lymphoid line (Kong *et al.*, 2010), an observation that was recently validated in a MIR23A knockout mice (Kurkewich *et al.*, 2016). Indeed, PU.1 is also expressed in GCB cells (centroblasts) (Torlakovic *et al.*, 2005; Cattoretti *et al.*, 2006) and might therefore be an interesting candidate for further analyses.

Another interesting candidate is NFAT, because it can be activated upon BCR signaling by PLCγ-Ca^{2+}-Calcineurin signaling (Gachet and Ghysdael, 2009). In detail, NFATc3 was shown to activate the MIR23A cluster in cardiomyocytes (Lin *et al.*, 2009). Indeed, it was reported, that another NFAT family member, NFATc1 was localized in the nucleus of BL and DLBCL samples (Marafiot *et al.*, 2005) and constitutively activated together with NF$\varkappa$B in DLBCL (Fu *et al.*, 2006). Bioinformatical analyses of the MIR23A cluster promoter for transcription factor binding sites revealed ETS1 as a promising candidate, since ETS1 deregulation was reported in BL and DLBCL (Testoni *et al.*, 2015). Furthermore, ETS1 deregulation was shown to contribute to pathogenesis in DLBCL (Bonetti *et al.*, 2013). Moreover, ETS1 is a substrate of ERK (Yoon and Seger, 2006; Plotnik *et al.*, 2014).

Although the NF$\varkappa$B members cRel and p65 were already shown to activate the MIR23A cluster in a T cell leukemic cell line (Rathore *et al.*, 2012), initial stimulation experiments did not support these findings for DLBCL cell line U2932 R1. In detail, the activation of CD40 signaling and LPS stimulation, which predominantly activate NF$\varkappa$B signaling, did not result in an activation of the MIR23A cluster in U2932 R1 and BL-2 (fig. 3.1 and 3.3). However, the CD77 positive GCBs responded to CD40L stimulation with an increase of MIR23A expression, showing that NF$\varkappa$B signaling might activate the MIR23A cluster in healthy GCBs, but not in the DLBCL cell line U2932 R1.

In summary, this study shows for the first time, that BCR dependent MEK/ERK signaling activates the MIR23A cluster in DLBCL cell lines. The activation of MIR23A cluster in DLBCL is aberrant compared to healthy GCB cells, suggesting that aberrant BCR signaling might be responsible for the high MIR23A cluster expression in BL and DLBCL patients.

4.2. MiR-23a & miR-27a targetome identification in DLBCL

In order to identify the cellular processes in which miR-23a and miR-27a are involved, their mRNA targets in DLBCL cell line U2932 R1 were analyzed using Ago2-RIP approach. This led to the identification of 26 novel direct miR-23a and 20 novel direct miR-27a targets for the DLBCL model cell line U2932 R1. Both, direct (miRNA bound mRNAs) and indirect targets (differentially expressed genes) identified in this study indicate, that the MIR23A cluster acts as an onco-miR in DLBCL.

4.2.1. Ago2-RIP assay

Many different methods for the identification of miRNA targets are available, such as *in silico* predictions, expression profiling or ribosome profiling, proteomic approaches (stable isotope labeling with amino acids in cell culture (SILAC)), immunoprecipitation of miRISC proteins with/without cross-linking and pull-down experiments (Thomson *et al.*, 2011; Martinez-Sanchez and Murphy, 2013). Each of these methods has its own advantages and disadvantages. No matter by which means the targets were identified, for each target the downregulation of a protein by a miRNA has to be validated experimentally.

The Ago2-RIP approach, applied in this study, identifies genome wide direct miRNA-mRNA interactions mediated within the RISC complex. Furthermore, targets that are targeted by non-canonical binding of the miRNA can be identified, a great benefit compared to *in silico* predictions. Moreover, miRNAs that do not alter the target mRNA levels can be identified. This is of importance in mammalia, because many miRNAs are thought to mediate mild changes in mRNA levels, since they are supposed to work as fine tuners, which generate thresholds for their target mRNAs (Mukherji *et al.*, 2011; Hadjimichael *et al.*, 2016).

A major disadvantage of an Ago2-RIP, as well as for other experimental approaches, is the ectopic overexpression of the miRNA (miRNA mimics, stable or transient expression vectors). Unphysiological overexpression might overload the miRNA biogenesis machinery and alter the composition of different miRNAs incorporated into the RISC complex. This might disturb other cellular processes not related to the specific miRNA, leading to undesired secondary effects and false interpretations. Furthermore, low affinity targets might be overrepresented. Therefore, inhibition of miRNA by an anti-sense miRNAs or miRNA-sponges can help to avoid these problems. However, it is difficult to determine effective miRNA inhibition, because the miRNA is sequestered by anti-sense miRNAs or miRNA-sponges, leaving miRNA levels constant.

In this study, stable overexpression of pre-miR-23a and pre-miR-27a was used. Small RNA sequencing revealed an overexpression rate of miR-23a of 190-fold compared to control. This high miRNA levels did not significantly alter the global miRNA expression profile, as shown by small RNA sequencing of miR-23a overexpressing U2932 R1 pGIPZ clones compared to control (fig. 3.25 inner ring). However, the composition of miRNAs in Ago2-RIP output samples could not be analyzed because the RNA amount was not enough for mRNA and small RNA sequencing.

To gain most reliable results, Ago2-RIP assay was optimized and performed in three independent experiments. Most challenging was the aim to obtain enough RNA amounts of high quality for RNA sequencing. The immunoprecipitation was shown to specifically pull down Ago2 protein and enrich mature miRNAs (fig. 3.21 and 3.22). Furthermore, the RNA quality was high after immunoprecipitation (fig. A.4) and sequencing reads could successfully be mapped against the human genome (fig. 3.23). Three independent experiments were performed to identify possible outliers. Only targets that were at least 2 times enriched compared to control and had a p-value lower than 0.05 were considered as possible miR-23a or miR-27a targets, thereby lowering the chance to get unspecific results.

4.2.2. Direct miR-23a and miR-27a targets in DLBCL

The majority of identified targets of miR-23a and miR-27a in DLBCL cell line U2932 R1 harbor canonical miRNA binding sites for the respective miRNA, showing that the applied Ago2-RIP approach successfully enriched mRNAs that directly bind to the respective miRNA. All targets, except of one, harbor at least one canonical 7 mer binding site (table 3.3 and 3.4). The pseudogene EEF1A1P16, which has no canonical binding site, might be targeted by non-canonical binding of miR-27a. However, since it is not coding for a protein, it was excluded from further analyses. Interestingly, most identified miR-23a and miR-27a targets were novel in human cells, indicating that indeed the targetome of a miRNA is context and cell type specific.

4.2.2.1. PUMA and apoptosis

Apoptosis was the only GO term, that was significantly enriched in differential gene expression analyses of miR-27a overexpressing U2932 R1 pGIPZ clones to controls. Therefore PUMA (or BBC3) was chosen as a miR-27a candidate for validation on protein level. Furthermore, it was already described as a miR-23a and miR-27a target in mice upon traumatic brain injury (Sabirzhanov *et al.*, 2014).

PUMA is a pro-apoptotic protein belonging to the family of BCL-2 homology (BH) domain 3-only proteins, which mediate canonical mitochondrial apoptosis in response to intrinsic stress,

such as DNA damage (Lomonosova and Chinnadurai, 2008). In response to cellular stress p53 is activated, which in turn induces *PUMA*. In a next step PUMA activates pro-apoptotic BH domain proteins, such as Bax and Bak, which subsequently cause permeabilization of mitochondrial outer membrane and the release of pro-apoptotic molecules from mitochondria (Cytochrome c and apoptosis inducing factor (AIF)) resulting in controlled cell death (Shamas-Din *et al.*, 2011; Ashkenazi, 2008).

The basal level of PUMA is low in U2932 R1 cell line, as expected in a viable and proliferating cell line. It was therefore not expected, that miR-27a overexpression will not further reduce miR-27a levels under normal conditions. Indeed, it was reported, that *PUMA* expression is silenced as a consequence of DNA methylation in human BL and loss of PUMA induces lymphomagenesis in mouse (Garrison *et al.*, 2008; Michalak *et al.*, 2009), supporting the onco-miR hypothesis for the MIR23A cluster. Furthermore, *PUMA* levels are lower in BL compared to healthy controls, while DLBCL patients show similar or higher levels compared to control (fig. 3.40). In order to induce PUMA protein levels, DNA double strand breaks were introduced by etoposide treatment. This led to the induction of p53, which activates PUMA. Only under these stress conditions, the miR-27a effect on PUMA-β could be observed. MiR-27a inhibited the induction of PUMA-β in stable overexpressing clones upon etoposide treatment (fig. 3.34). Interestingly, the alpha isoform of PUMA was neither induced by p53, nor inhibited by miR-27a. Previously, both isoforms were reported to be induced upon p53 in p53-inducible NSCLC cells (Nakano and Vousden, 2001). The 3'UTRs of both isoforms are identical and harbor the same canonical miR-27a 8mer binding site and could therefore both be targeted by miR-27a. PUMA-α is encoded by exon 1a, 2, 3 and 4 while PUMA-β is encoded by exon 1b, 3 and 4. However, no additional canonical 7mer or 8mer miR-27a binding sites can be found in exons coding for PUMA-β, but not for PUMA-α. This indicates, that miR-27a might target PUMA-β by a non-canonical binding site within exon 1b, which could be missing in PUMA-α. Another possibility is, that in principle all PUMA isoforms are targeted by the common binding site in their 3'UTR, but the PUMA-α isoform is specifically stabilized, e.g. by RNA editing in the 3'UTR. Thus, it can no longer be targeted by miR-27a (Liang and Landweber, 2007; Zhang *et al.*, 2016).

NOXA is another BH3-only protein, which is induced by p53 and promotes apoptosis in the same way as PUMA (Ashkenazi, 2008). Previously, Roufayel and colleagues demonstrated that NOXA is a miR-23a target under heat-stress conditions (Roufayel *et al.*, 2014). This indicates, that the whole cluster might regulate apoptosis. Furthermore, this might explain why miR-23a and miR-27a attenuated the ability of U2932 R1 cells to undergo apoptosis upon etoposide treatment (fig. 3.38). This aspect has to be addressed in further experiments. First it has to be shown that this effect can be reversed by miRNA inhibition. Secondly, it has to

be proven whether PUMA-β or NOXA can rescue the attenuated apoptosis of miR-23a and miR-27a overexpressing cells.

4.2.2.2. LIMK1 and migration

Another newly identified miR-27a target in DLBCL cell line U2932 R1 was LIMK1. It is a serine/threonine kinase, activated by p21-activated kinase 6 (PAK6). PAKs are kinases, that are frequently upregulated or hyperactivated in various human cancers (Kumar *et al.*, 2006). Moreover, it was already shown that PAK6 is a miR-23a target in prostate cancer (Cai *et al.*, 2014), leading to the hypothesis, that the whole MIR23A cluster might act in the PAK/LIMK signaling pathway. Indeed LIMK1 levels are lower in BL and DLBCL patients compared to GCBs, showing a negative correlation to MIR23A cluster expression (fig. 3.39 and 3.40). LIMK1 could be validated as a miR-27a target in stable and transient overexpressing cells (fig. 3.33). Notably, also miR-23a was able to decrease LIMK1 protein levels. This can be explained due to three 7mer1A binding sites for miR-23a in the CDS of LIMK1 mRNA. However, this raises the question, why LIMK1 was not found in the miR-23a-Ago2-RIP. Indeed, LIMK1 was shown to be a target for the paralogous miR-27b in non-small cell lung cancer (NSCLC) (Wan *et al.*, 2014). MiR-27b has the identical seed region to miR-27a, thus targeting presumably the same mRNAs.

LIMK1 phosphorylates and thereby inactivates actin depolymerizing factor (ADF)/Cofilin (Arber *et al.*, 1998), which regulates actin dynamics to modulate cell polarity and motility. LIMK1 is therefore involved in cancer cell invasion and metastasis. Unphosphorylated Cofilin binds to actin filaments (f-actin) and induces fragmentation of the filament and depolymerisation of the pointed end of the filament (Bailly and Jones, 2003). This increases the actin filament turnover resulting in the generation of barbed ends that subsequently form lamellipodial protrusions, which are required for directed cell migration (Bailly and Jones, 2003; Nishita *et al.*, 2005). Phosphorylation of Cofilin inhibits the ability of Cofilin to bind to f-actin and to generate barbed ends (Zebda *et al.*, 2000). It was shown that overexpression of LIMK1 or constitutive active LIMK1 led to high levels of P-Cofilin, which inhibited cell polarity and the formation of lamellipodia (Zebda *et al.*, 2000; Dawe *et al.*, 2003). Therefore, the downregulation of LIMK1 by miR-27a might lead to unphosphorylated Cofilin, which increases cell polarity and migratory potential. Enhanced cell migration might result in dissemination of the primary tumor and the formation of distant secondary tumors. Although, very hypothetical, this might support the onco-miR hypothesis for the MIR23A cluster.

However, there are also studies showing that miR-23a inhibits migration and invasion by targeting PAK6 in prostate cancer (Cai *et al.*, 2014). Downregulation of PAK6 led to low P-LIMK1 and consequently low P-Cofilin levels (Cai *et al.*, 2014). In contrast to other studies, were phos-

phorylated Cofilin abolished cell migration (Zebda *et al.*, 2000; Dawe *et al.*, 2003; Nishita *et al.*, 2005), in this study unphosphorylated Cofilin also abolished migration and invasion (Cai *et al.*, 2014). This paradoxon was not addressed by the authors. Moreover, another study reported similar findings: the inhibition of LIMK1 by a cell-permeable peptide led to unphosphorylated Cofilin and to impaired migration of Jurkat cells (Nishita *et al.*, 2002). These observations show, that actin dynamics are very sensitive to perturbations in protein concentration. Possibly the balance of P-Cofilin to Cofilin or the correct distribution of Cofilin within the cell determines whether a cell responds to a stimulus with cell polarity and consequently directed migration or not.

LIMK1 does not only regulate actin dynamics, but also microtubule dynamics during mitosis. In detail, it was shown to mediate microtubule disassembly by phosphorylation of p25 (also known as tubulin polymerization promoting protein (TPPP)) (Acevedo *et al.*, 2007). TPPP/p25 is responsible for correct spindle formation during mitosis (Tirián *et al.*, 2003). Moreover, it was shown that LIMK1 mediated phosphorylation of Cofilin was also implicated in accurate spindle orientation during mitosis (Chakrabarti *et al.*, 2007; Kaji *et al.*, 2008). Incorrect spindle formation might lead to unequal distribution of chromosomes to the daughter cells (Bakhoum and Compton, 2012). However, chromosomal instability is not a common feature of lymphomas.

Since Wan *et al.* showed, that high miR-27b levels downregulated LIMK1 and thereby inhibited cell invasion as well as cell growth (Wan *et al.*, 2014), it would be interesting to check in future studies whether miR-27a has the same effect in DLBCL.

4.2.2.3. VRK3 and MEK/ERK signaling

The miR-23a target candidate VRK3 was of special interest in this study, because it is known to be involved in negative regulation of ERK (Kang and Kim, 2006). Because MEK/ERK signaling was identified in this study to activate the MIR23A cluster, VRK3 might therefore be involved in a feedback loop of MIR23A activation upon BCR stimulation.

VRK3 is a serine/threonine kinase, mainly located in the ER and the nucleus (Nichols and Traktman, 2004), which binds and activates vaccinia H1-related (VHR) (Kang and Kim, 2006), also known as dual-specificity phosphatase 3 (DUSP3). DUSP3 is a nuclear phosphatase that specifically de-phosphorylates and thereby inactivates ERK (Kang and Kim, 2006). Interestingly, another dual-specificity phosphatase DUSP5, which was previously reported to de-phosphorylate ERK1 (Ishibashi *et al.*, 1994) (Ueda *et al.*, 2003), was found to be enriched in the miR-23a Ago2-RIP, indicating that miR-23a might regulate several levels of ERK feedback loop. Targeting ERK dephosphorylating enzymes might lead to enhanced ERK signaling,

which would reinforce the MIR23A cluster expression, creating a positive feedback loop for the MIR23A cluster.

Strikingly, miR-23a did not decrease VRK3 protein levels in stable overexpressing U2932 R1 cell lines under normal conditions. Although VRK3 harbors two miR-23a binding sites in the 3'UTR and five in the CDS, the VRK3 protein levels were not affected in stable overexpressing cells. Indeed, VRK3 protein levels are already very low and may not be further decreased by miRNA action. Maybe miR-23a is responsible to hold VRK3 protein levels on a constant low level. Increased VRK3 levels would lead to decreased survival signals by BCR signaling, being a disadvantage for the tumor cell. Indeed, patient samples show, that *VRK3* levels in BL and DLBCL patients are lower compared to GCB controls. This supports the onco-miR hypothesis for the MIR23A cluster. It is possible, that the inhibitory function of the miRNA can not be observed until VRK3 levels are induced in response to a certain stimulus. The same was observed for the miR-27a target PUMA. A reasonable stimulus might be the activation of the BCR, which activates ERK, that subsequently should be dephosphorylated by VRK3 activated DUSP3 activity.

However, it can not be excluded, that VRK3 might be a false positive miR-23a target candidate, identified by secondary interactions during immunoprecipitation. Direct physical interaction of miR-23a to VRK3 mRNA can be analyzed by Luciferase reporter gene assays and mutation of miRNA binding sites in future studies.

4.2.2.4. Zinc finger proteins

12 of 25 novel identified miR-23a targets were zinc finger proteins (ZNF), that contain a DNA binding ZNF domain and therefore potentially act as transcription factors. All these identified ZNFs belong to the same protein family: KRAB-C2H2-ZNFs. Members of this family comprise a high sequence homology, which might be an explanation why so many are targeted by miR-23a. This sequence homology makes it difficult to analyze ZNF expression by qRT-PCR or Western Blot. The identified ZNFs belong to two separate ZNF clusters, that were generated due to gene duplication during evolution: ZNF cluster 269 on chromosome 19 and ZNF cluster 114 on chromosome 7. Notably, many ZNFs as well as other miR-23a targets are encoded on chromosome 19, where also the MIR23A cluster itself is encoded (see section 4.2.3). Interestingly, all identified ZNFs were downregulated in BL and DLBCL patients compared to healthy controls (fig. 3.40d), indicating that they might have cooperative or redundant functions. Indeed, ZNFs belonging to the KRAB ZNF family were reported to be highly expressed in T-lymphoid cells (Bellefroid *et al.*, 1993). Since the MIR23A cluster was reported to suppress the B cell development (Kong *et al.*, 2010) one might speculate, that this inhibition is mediated through the downregulation of these ZNFs.

4.2.3. Enrichment of targets on chromosome 19

More than one third (37%), namely 17 out of 46 newly identified miR-23a and miR-27a tar-
gets in the DLBCL model cell line U2932 R1, are encoded on chromosome 19, where also
the MIR23A cluster is encoded (fig. 3.28). A closer look at the location of the targets on chro-
mosome 19 reveals that they are encoded on both arms of the chromosome, although this
finding is referred to as "clustering of targets". This study could show, that it is not due to an
overrepresentation of expressed transcripts from chromosome 19 in the used cell line or due
to a higher percentage of potential miR-23a or miR-27a binding sites on transcripts from chro-
mosome 19. This indicates, that it might not just be a coincidence, but that there might be a
biological mechanism underlying this observation.

It is well known that during interphase the chromosomes are arranged in a highly defined
manner within the nucleus (Marshall *et al.*, 1997). Furthermore, fluorescent in situ hybridiza-
tion (FISH) analyses and chromosome conformation capture (C3) assays revealed, that there
is a correlation between chromatin topology and gene activity (Sexton and Cavalli, 2015). It
would therefore be of interest to find out whether the MIR23A cluster is in near proximity of its
targets. Chen *et al.* addressed this question on a global scale by Chromatin Interaction Analy-
sis by Paired-End Tag Sequencing (ChIA-PET) analyses, where they identified the interactions
of miRNA genes with target genes (Chen *et al.*, 2014). They could show that miRNA genes
and protein coding genes were organized in functionally compartmentalized chromatin com-
munities that are expressed together when they are spatially co-located (Chen *et al.*, 2014).
Furthermore, miRNA-target interactions were enriched between communities with functional
homogeneity (Chen *et al.*, 2014). Instead, no miRNA-target interactions were detected when
miRNA and target originated from the same community (Chen *et al.*, 2014). These chromatin
communities were related to topologically associated domain (TAD) structures of the genome
(Chen *et al.*, 2014; Pombo and Dillon, 2015). This might represent a mechanism by which a
miRNA is co-expressed with its targets.

Another mechanism which could explain the co-expression would be a coordinated activation
of the MIR23A cluster together with its targets by the same transcription factor, as suggested in
other studies (Wang *et al.*, 2011; Le *et al.*, 2014). Indeed, the MIR23A cluster and most of the
identified miR-23a and miR-27a target harbor putative myeloid zinc finger 1 (MZF1) binding
sites in their promoter regions. MZF1 was already implicated to play a role in various cancer
entities (Mudduluru *et al.*, 2010).

Furthermore, miRNAs as well as the miRNA processing machinery and Ago2 protein are
present in the nucleus (Hwang *et al.*, 2007; Park *et al.*, 2010). It was shown, that a long
non coding RNA (lncRNA) silences gene expression at certain loci by the recruitment of tran-
scriptional repressors, such as the polycomb repressive complex 2 (PRC2) (Roberts, 2014).

Silencing of the lncRNA by a miRNA disrupts this complex, leading to the activation of the target gene (Roberts, 2014). Since the Ago2-RIP identified several lncRNAs (RP11-1017G21.5, CTC-246B18.10 and KIAA1467), this might be an interesting aspect for further investigations, especially because CTC-246B18.10 is also expressed on chromosome 19.

4.3. Biological function & global effects of MIR23A cluster in DLBCL

Targetome identification via Ago2-RIP assay in DLBCL cell line U2932 R1 revealed many novel and direct targets for miR-23a and miR-27a, from which two (LIMK1 and PUMA) were verified on protein level by miRNA overexpression experiments.

Furthermore, this study showed, that miR-23a and miR-27a are both implicated in the regulation of apoptosis. In detail, miR-23a and miR-27a attenuated the ability of DLBCL cell line U2932 R1 to undergo apoptosis when DNA damage was induced (fig. 3.38). This strongly supports the onco-miR hypothesis for the MIR23A cluster, which was tested in this study. In addition, this observation could contribute to an explanation for the worse overall survival rate of patients with higher miR-23a levels. Cells that have a lower ability to undergo apoptosis, might not respond to chemotherapy. Future experiments have to address, whether PUMA is indeed the key player mediating this observation. Indications that this cluster is involved in multidrug resistance came also from Zhang *et al*., who showed that miR-27a downregulation increased the sensitivity of eosphageal cancer to undergo apoptosis (Zhang *et al.*, 2010).

Interestingly, identified miR-27a target LIMK1, which is mainly known to function in migration, was also shown to be cleaved by caspase-3 like proteases, generating an N-terminally truncated, constitutively active fragment, that induces membrane blebbing, a common feature of apoptotic cells (Tomiyoshi *et al.*, 2004).

Besides these direct targets, miR-23a and miR-27a overexpression also affected global gene expression profiles of U2932 R1. 904 genes were differentially expressed between miR-27a overexpressing and ns ctrl cell line. These genes are referred to as indirect miRNA targets. GO-term enrichment analyses of these indirect target genes revealed a significant enrichment for gene sets associated with apoptosis (fig. 3.36). This indicates that the direct miR-27a target PUMA is definitely not the only player mediating apoptosis in the context of miR-27a overexpressing DLBCL cells, as expected for a miRNA that can have several direct and indirect targets. Furthermore, the onco-miR hypothesis is supported by this results.

GO-term enrichment analyses of the 651 differentially expressed genes of miR-23a overexpressing *vs*. ns ctrl U2932 R1 cells revealed an enrichment of many different cellular processes (fig. 3.35). The majority is associated with the ribosome and proteinbiosynthesis, because

many ribosomal proteins are differentially regulated. Indeed, cancer cells frequently exhibit increased ribosome biogenesis (Takada and Kurisaki, 2015).

Strikingly, GO-term enrichment analyses of the overlap of indirect targets of miR-23a with indirect targets of miR-27a did not show any significant enriched cellular process. This indicates, that both miRNAs might function in different cellular processes and do not have any cooperative effect. However, this is contradictory to the observation, that both, miR-23a and miR-27a, attenuate the ability of U2932 R1 cells to undergo apoptosis. GO-term enrichment analyses using the hypergeometrical test has some limitations. It does not include the direction and fold change of gene expression changes. If a certain process is e.g. targeted by the miRNA directly, one might expect, that the differentially expressed genes involved in this process are downregulated. This is not covered by GO-term analyses. Moreover, this analyses strongly depend on the information listed in the provided gene sets. Thus, it is possible that many identified indirect targets are not functionally described yet and are therefore not found in these GO-terms gene sets.

In summary, functional analyses showed that the MIR23A cluster is involved in the regulation of apoptosis. High levels of miR-23a and miR-27a decreased the ability of the DLBCL model cell line to undergo apoptosis. This supports the onco-miR hypothesis for the MIR23A cluster and might be one possible explanation for the worse outcome of DLBCL patients with higher miR-23a levels.

5. Summary and Conclusion

The MIR23A cluster, encoding miR-23a, miR-27a and miR-24 is aberrantly activated in BL and DLBCL cells compared to their normal counterparts, the germinal center B cells. This study identified the BCR signaling as a general mechanism in BL and DLBCL cell lines responsible for the induction of the MIR23A cluster. Since normal GCBs did not increase MIR23A cluster levels in response to BCR signaling, it is hypothesized that aberrant BCR signaling together with factors of the microenvironment might cause high MIR23A cluster expression in BL and DLBCL patients compared to healthy controls. As the main BCR-downstream signaling cascade mediating MIR23A cluster activation the MEK/ERK signaling pathway was identified. Downstream transcription factors ELK1 and c-MYC were not involved in the activation of the MIR23A cluster in DLBCL cell lines.

Ago2-RIP assay followed by RNA-sequencing identified 46 novel direct miR-23a and miR-27a targets in a DLBCL model cell line. Interestingly, 37% of the newly identified targets were encoded on chromosome 19. Moreover, LIMK1 and PUMA-β were validated as direct miR-27a targets being downregulated on protein level upon miR-27a overexpression. Bioinformatical prediction of MIR23A cluster function based on DEG upon miR-27a overexpression in DLBCL cell line U2932 R1 indicated, that the MIR23A cluster might regulate apoptosis. Indeed, this could be verified in functional analyses. Hence, this study demonstrated that miR-23a and miR-27a attenuate the ability of DLBCL cells to undergo apoptosis in response to DNA damage. This might be one possible explanation why DLBCL patients with high miR-23a expression levels have a worse overall survival rate than patients with low levels, supporting the onco-miR hypothesis for the MIR23A cluster.

Bibliography

Acevedo, K., Li, R., Soo, P., Suryadinata, R., Sarcevic, B., Valova, V. A., Graham, M. E., Robinson, P. J., and Bernard, O. (2007). The phosphorylation of p25/TPPP by LIM kinase 1 inhibits its ability to assemble microtubules. *Experimental Cell Research*, 313(20):4091–4106.

Acunzo, M., Romano, G., Palmieri, D., Laganá, A., Garofalo, M., Balatti, V., Drusco, A., Chiariello, M., Nana-Sinkam, P., and Croce, C. M. (2013). Cross-talk between MET and EGFR in non-small cell lung cancer involves miR-27a and Sprouty2. *Proceedings of the National Academy of Sciences of the United States of America*, 110(21):8573–8.

Alizadeh, A. a., Eisen, M. B., Davis, R. E., Ma, C., Lossos, I. S., Rosenwald, A., Boldrick, J. C., Sabet, H., Tran, T., Yu, X., Powell, J. I., Yang, L., Marti, G. E., Moore, T., Hudson, J., Lu, L., Lewis, D. B., Tibshirani, R., Sherlock, G., Chan, W. C., Greiner, T. C., Weisenburger, D. D., Armitage, J. O., Warnke, R., Levy, R., Wilson, W., Grever, M. R., Byrd, J. C., Botstein, D., Brown, P. O., and Staudt, L. M. (2000). Distinct types of diffuse large B-cell lymphoma identified by gene expression profiling. *Nature*, 403(6769):503–511.

Ameres, S. L. and Zamore, P. D. (2013). Diversifying microRNA sequence and function. *Nature reviews. Molecular cell biology*, 14(8):475–88.

Anders, S., Huber, W., Nagalakshmi, U., Wang, Z., Waern, K., Shou, C., Raha, D., Gerstein, M., Snyder, M., Mortazavi, A., Williams, B., McCue, K., Schaeffer, L., Wold, B., Robertson, G., Hirst, M., Bainbridge, M., Bilenky, M., Zhao, Y., Zeng, T., Euskirchen, G., Bernier, B., Varhol, R., Delaney, A., Thiessen, N., Griffith, O., He, A., Marra, M., Snyder, M., Jones, S., Licatalosi, D., Mele, A., Fak, J., Ule, J., Kayikci, M., Chi, S., Clark, T., Schweitzer, A., Blume, J., Wang, X., Darnell, J., Darnell, R., Smith, A., Heisler, L., Mellor, J., Kaper, F., Thompson, M., Chee, M., Roth, F., Giaever, G., Nislow, C., Marioni, J., Mason, C., Mane, S., Stephens, M., Gilad, Y., Wang, L., Feng, Z., Wang, X., Wang, X., Zhang, X., Robinson, M., Smyth, G., Whitaker, L., Robinson, M., McCarthy, D., Smyth, G., Robinson, M., Smyth, G., Cameron, A., Trivedi, P., Robinson, M., Oshlack, A., Loader, C., McCullagh, P., Nelder, J., Agresti, A., Engström, P., Tommei, D., Stricker, S., Smith, A., Pollard, S., Bertone, P., Morrissy, A., Morin, R., Delaney, A., Zeng, T., McDonald, H., Jones, S., Zhao, Y., Hirst, M., Marra, M., Kasowski, M., Grubert, F., Heffelfinger, C., Hariharan, M., Asabere, A., Waszak, S., Habegger, L., Rozowsky, J., Shi, M., Urban, A., Hong, M., Karczewski, K., Huber, W., Weissman, S., Gerstein, M., Korbel, J., Snyder, M., Benjamini, Y., Hochberg, Y., Bullard, J., Purdom, E., Hansen, K., Dudoit, S., Bloom, J., Khan, Z., Kruglyak, L., Singh, M., Caudy, A., Smyth, G., Smyth, G., Lönnstedt, I., Speed, T., Gentleman, R., Carey, V., Bates, D., Bolstad, B., Dettling, M., Dudoit, S., Ellis, B., Gautier, L., Ge, Y., Gentry, J., Hornik, K., Hothorn, T., Huber, W., Iacus, S., Irizarry, R., Leisch, F., Li, C., Maechler, M., Rossini, A., Sawitzki, G., Smith, C., Smyth, G., Tierney, L., Yang, J., Zhang, J., Bliss, C., Fisher, R., Clark, S., Perry, J., Lawless, J., Saha, K., Paul, S., Langmead, B., Trapnell, C., Pop, M., and Salzberg, S. (2010). Differential expression analysis for sequence count data. *Genome Biology*, 11(10):R106.

Anders, S., Pyl, P. T., and Huber, W. (2015). HTSeq-A Python framework to work with high-throughput sequencing data. *Bioinformatics*, 31(2):166–169.

Arber, S., Barbayannis, F. a., Hanser, H., Schneider, C., Stanyon, C. a., Bernard, O., and Caroni, P. (1998). Regulation of actin dynamics through phosphorylation of cofilin by LIM-kinase. *Nature*, 393(June):805–9.

Armitage, J. O., Mauch, P. M., Harris, N. L., Coiffier, B., and Dalla-Favera, R. (2009). *Non-Hodgkin Lymphomas*.

Ashkenazi, A. (2008). Directing cancer cells to self-destruct with pro-apoptotic receptor agonists. *Nature Reviews Drug Discovery*, 7(12):1001–1012.

Bailly, M. and Jones, G. E. (2003). Polarised migration: Cofilin holds the front. *Current Biology*, 13(4):128–130.

Bakhoum, S. F. and Compton, D. a. (2012). Science in medicine Chromosomal instability and cancer : a complex relationship with therapeutic potential. *The Journal of Clinical Investigation*, 122(4):1138–1143.

Baldwin, A. S. (2001). Control of oncogenesis and cancer therapy resistance by the transcription factor NF-kB. *Journal of Clinical Investigation*, 107(3):241–246.

Bao, Y., Chen, Z., Guo, Y., Feng, Y., Li, Z., Han, W., Wang, J., Zhao, W., Jiao, Y., Li, K., Wang, Q., Wang, J., Zhang, H., Wang, L., and Yang, W. (2014). Tumor Suppressor MicroRNA-27a in Colorectal Carcinogenesis and Progression by Targeting SGPP1 and Smad2. *PloS one*, 9(8):e105991.

Barrett, D., Brown, V. I., Grupp, S. A., and Teachey, D. T. (2012). *Targeting the PI3KAKTmTOR signaling axis in children with hematologic malignancies*, volume 14.

Bartel, D. P. (2004). MicroRNAs: Genomics, Biogenesis, Mechanism, and Function. *Cell*, 116(2):281–297.

Basso, K., Klein, U., Niu, H., Stolovitzky, G. A., Tu, Y., Califano, A., Cattoretti, G., and Dalla-Favera, R. (2004). Tracking CD40 signaling during germinal center development. *Blood*, 104(13):4088–4096.

Basso, K., Sumazin, P., Morozov, P., Schneider, C., Maute, R. L., Kitagawa, Y., Mandelbaum, J., Haddad, J., Chen, C.-Z., Califano, A., and Dalla-Favera, R. (2009). Identification of the human mature B cell miRNome. *Immunity*, 30(5):744–52.

Baumjohann, D., Okada, T., and Ansel, K. M. (2011). Cutting Edge: Distinct Waves of BCL6 Expression during T Follicular Helper Cell Development. *Journal of immunology (Baltimore, Md. : 1950)*, 187(5):2089–2092.

Béguelin, W., Popovic, R., Teater, M., Jiang, Y., Bunting, K. L., Rosen, M., Shen, H., Yang, S. N., Wang, L., Ezponda, T., Martinez-Garcia, E., Zhang, H., Zheng, Y., Verma, S. K., McCabe, M. T., Ott, H. M., VanAller, G. S., Kruger, R. G., Liu, Y., McHugh, C. F., Scott, D. W., Chung, Y. R., Kelleher, N., Shaknovich, R., Creasy, C. L., Gascoyne, R. D., Wong, K. K., Cerchietti, L., Levine, R. L., Abdel-Wahab, O., Licht, J. D., Elemento, O., and Melnick, A. M. (2013). EZH2 Is Required for Germinal Center Formation and Somatic EZH2 Mutations Promote Lymphoid Transformation. *Cancer Cell*, 23(5):677–692.

Bellefroid, E. J., Marine, J. C., Ried, T., Lecocq, P. J., Rivière, M., Amemiya, C., Poncelet, D. a., Coulie, P. G., de Jong, P., and Szpirer, C. (1993). Clustered organization of homologous KRAB zinc-finger genes with enhanced expression in human T lymphoid cells. *The EMBO journal*, 12(4):1363–1374.

Berberich, I., Shu, G. L., and Clark, E. A. (1994). Cross-linking CD40 on B cells rapidly activates nuclear factor-kappa B. *Journal of immunology (Baltimore, Md. : 1950)*, 153(10):4357–66.

Bertrand, S., Berger, R., Philip, T., Bernheim, A., Bryon, P. A., Bertoglio, J., Doré, J. F., Brunat-Mentigny, M., and Lenoir, G. M. (1981). Variant translocation in a non endemic case of Burkitt's lymphoma: t

(8;22) in an Epstein-Barr virus negative tumour and in a derived cell line. *European Journal of Cancer (1965)*, 17(5):577–581.

Bhattacharyya, S. N., Habermacher, R., Martine, U., Closs, E. I., and Filipowicz, W. (2006). Relief of microRNA-Mediated Translational Repression in Human Cells Subjected to Stress. *Cell*, 125(6):1111–1124.

Blachly, J. S. and Baiocchi, R. A. (2014). Targeting PI3-kinase (PI3K), AKT and mTOR axis in lymphoma. *British Journal of Haematology*, 167(1):19–32.

Bohnsack, M. T., Czaplinski, K., and Gorlich, D. (2004). Exportin 5 is a RanGTP-dependent dsRNA-binding protein that mediates nuclear export of pre-miRNAs. *RNA (New York, N.Y.)*, 10(2):185–91.

Bojarczuk, K., Bobrowicz, M., Dwojak, M., Miazek, N., Zapala, P., Bunes, A., Siernicka, M., Rozanska, M., and Winiarska, M. (2015). B-cell receptor signaling in the pathogenesis of lymphoid malignancies. *Blood Cells, Molecules, and Diseases*, 55(3):255–265.

Bonetti, P., Testoni, M., Scandurra, M., Ponzoni, M., Piva, R., Mensah, A. a., Rinaldi, A., Kwee, I., Tibiletti, M. G., Iqbal, J., Greiner, T. C., Chan, W. C., Gaidano, G., Piris, M. a., Cavalli, F., Zucca, E., Inghirami, G., and Bertoni, F. (2013). Deregulation of ETS1 and FLI1 contributes to the pathogenesis of diffuse large B-cell lymphoma. *Blood*, 122(13):2233–2241.

Borrow, J., Stanton, V. P., Anderson, J. M., Becher, R., Behm, F. G., Chaganti, R. S. K., Civin, C. I., Disteche, C., Dube, I., Frischauf, A. M., Horsman, D., Mitelman, F., Volinia, S., Waltore, A. E., and Housman, D. E. (1996). The translocation t(8;16)(p11;p13) of acute myeloid leukaemia fuses a putative acetyltransferase to the CREB-binding protein. *Nat Genet.*, 14(3):353–6.

Bradford, M. (1976). Rapid and Sensitive Method for Quantification of Microgram Quantities of Protein utilizing principle of Protein-Dye-Binding. *Analytical Biochemistry*, 72(1-2):248–254.

Braun, J. E., Huntzinger, E., Fauser, M., and Izaurralde, E. (2011). GW182 proteins directly recruit cytoplasmic deadenylase complexes to miRNA targets. *Molecular Cell*, 44(1):120–133.

Brennecke, J., Stark, A., Russell, R. B., and Cohen, S. M. (2005). Principles of microRNA-target recognition. *PLoS biology*, 3(3):e85.

Buck, a. M. Y. H., Perot, J., Chisholm, M. a., Kumar, D. S., Cognat, R. I. E., Marcinowski, L., Do, L., and Tuddenham, L. E. E. (2010). Post-transcriptional regulation of miR-27 in murine cytomegalovirus infection. *Rna*, 16:307–315.

Burkitt, D. (1958). A sarcoma involving the jaws in african children. *British Journal of Surgery*, 46(197):218–223.

Burroughs, A. M., Ando, Y., de Hoon, M. L., Tomaru, Y., Suzuki, H., Hayashizaki, Y., and Daub, C. O. (2011). Deep-sequencing of human Argonaute-associated small RNAs provides insight into miRNA sorting and reveals Argonaute association with RNA fragments of diverse origin. *RNA Biology*, 8(1):158–177.

Cai, S., Chen, R., Li, X., Cai, Y., Ye, Z., and Li, S. (2014). Downregulation of microRNA-23a suppresses prostate cancer metastasis by targeting the PAK6-LIMK1 signaling pathway. *Oncotarget*, 6(6):3904–3917.

Cai, X., Hagedorn, C. H., and Cullen, B. R. (2004). Human microRNAs are processed from capped, polyadenylated transcripts that can also function as mRNAs. *RNA (New York, N.Y.)*, 10(12):1957–66.

Caimi, P. F., Hill, B. T., Hsi, E. D., and Smith, M. R. (2016). Clinical Approach to Diffuse Large B Cell Lymphoma. *Blood Reviews*.

CancerresearchUK (2016). www.cancerresearch.org 24.09.2016.

Cao, M., Seike, M., Soeno, C., Mizutani, H., Kitamura, K., Minegishi, Y., Noro, R., Yoshimura, A., Cai, L., and Gemma, A. (2012). MiR-23a regulates TGF-β-induced epithelial-mesenchymal transition by targeting E-cadherin in lung cancer cells. *International journal of oncology*, 41(3):869–75.

Cattoretti, G., Pasqualucci, L., Ballon, G., Tam, W., Nandula, S. V., Shen, Q., Mo, T., Murty, V. V., and Dalla-Favera, R. (2005). Deregulated BCL6 expression recapitulates the pathogenesis of human diffuse large B cell lymphomas in mice. *Cancer Cell*, 7(5):445–455.

Cattoretti, G., Shaknovich, R., Smith, P. M., Jäck, H.-M., Murty, V. V., and Alobeid, B. (2006). Stages of Germinal Center Transit Are Defined by B Cell Transcription Factor Coexpression and Relative Abundance. *Journal of Immunology*, 177:6930–6939.

Chakrabarti, R., Jones, J. L., Oelschlager, D. K., Tapia, T., Tousson, A., and Grizzle, W. E. (2007). Phosphorylated LIM kinases colocalize with gamma-tubulin in centrosomes during early stages of mitosis. *Cell Cycle*, 6(23):2944–2952.

Chen, D., Fu, L. Y., Zhang, Z., Li, G., Zhang, H., Jiang, L., Harrison, A. P., Shanahan, H. P., Klukas, C., Zhang, H. Y., Ruan, Y., Chen, L. L., and Chen, M. (2014). Dissecting the chromatin interactome of microRNA genes. *Nucleic Acids Research*, 42(5):3028–3043.

Chendrimada, T. P., Gregory, R. I., Kumaraswamy, E., Cooch, N., Nishikura, K., and Shiekhattar, R. (2005). TRBP recruits the Dicer complex to Ago2 for microRNA processing and gene silencing. 436(7051):740–744.

Chhabra, R., Dubey, R., and Saini, N. (2010). Cooperative and individualistic functions of the microR-NAs in the miR-23a˜27a˜24-2 cluster and its implication in human diseases. *Molecular cancer*, 9:232.

Ci, W., Polo, J. M., and Melnick, A. (2008). B-cell lymphoma 6 and the molecular pathogenesis of diffuse large B-cell lymphoma. *Current opinion in hematology*, 15(4):381–390.

Coiffier, B., Lepage, E., Brière, J., Herbrecht, R., Tilly, H., Bouabdallah, R., Morel, P., Van Den Neste, E., Salles, G., Gaulard, P., and Reyes, F. (2002). CHOP Chemotherapy plus Rituximab Compared with CHOP Alone in Elderly Patients with Diffuse Large-B-Cell Lymphoma. *N Engl J Med*, 346(4):235–242.

Compagno, M., Lim, W. K., Grunn, A., Nandula, S. V., Shen, Q., Bertoni, F., Ponzoni, M., Scandurra, M., Califano, A., Bhagat, G., Chadburn, A., Dalla-favera, R., and Pasqualucci, L. (2010). Mutations of multiple genes cause deregulation of NF-kB in diffuse large B-cell lymphoma. 459(7247):717–721.

Cubedo, E., Gentles, A. J., Huang, C., Natkunam, Y., Bhatt, S., Lu, X., Jiang, X., Romero-Camarero, I., Freud, A., Zhao, S., Bacchi, C. E., Martínez-Climent, J. A., Sanchez-García, I., Melnick, A., and Lossos, I. S. (2012). Identification of LMO2 transcriptome and interactome in diffuse large B-cell,lymphoma. *Blood*, 119(23):5478–5491.

Cultrera, J. L. and Dalia, S. M. (2012). Diffuse large B-cell lymphoma: Current strategies and future directions. *Cancer Control*, 19(3):204–213.

Dalla-Favera, R., Bregni, M., Eriksont, J., Pattersonf, D., Gallo, R. C., and Crocet, C. M. (1982). Human c-myc onc Gene is Located on the Region of Chromosome 8 that is Translocated in Burkitt Lymphoma Cells. *Proceedings of the National Academy of Sciences*, 79(December):7824–7827.

Dave, S., Fu, K., Wright, G., Lam, L., Kluin, P., Boerma, E., Greiner, T., Weisenburger, D., Rosenwald, A., Ott, G., and Others (2006). Molecular diagnosis of Burkitt's lymphoma. *The New England Journal of Medicine*, 354(23):2431–2442.

Davids, M. S. and Brown, J. R. (2014). Ibrutinib: a first in class covalent inhibitor of Bruton's tyrosine kinase. *Future Oncology*, 10(6):957–967.

Davis, B. N., Hilyard, A. C., Lagna, G., and Hata, A. (2008). SMAD proteins control DROSHA-mediated microRNA maturation. *Nature*, 454(7200):56–61.

Davis, R. E., Brown, K. D., Siebenlist, U., and Staudt, L. M. (2001). Constitutive nuclear factor kappaB activity is required for survival of activated B cell-like diffuse large B cell lymphoma cells. *The Journal of experimental medicine*, 194(12):1861–74.

Davis, R. E., Ngo, V. N., Lenz, G., Tolar, P., Young, R. M., Romesser, P. B., Kohlhammer, H., Lamy, L., Zhao, H., Yang, Y., Xu, W., Shaffer, A. L., Wright, G., Xiao, W., Powell, J., Jiang, J.-K., Thomas, C. J., Rosenwald, A., Ott, G., Muller-Hermelink, H. K., Gascoyne, R. D., Connors, J. M., Johnson, N. a., Rimsza, L. M., Campo, E., Jaffe, E. S., Wilson, W. H., Delabie, J., Smeland, E. B., Fisher, R. I., Braziel, R. M., Tubbs, R. R., Cook, J. R., Weisenburger, D. D., Chan, W. C., Pierce, S. K., and Staudt, L. M. (2010). Chronic active B-cell-receptor signalling in diffuse large B-cell lymphoma. *Nature*, 463(7277):88–92.

Dawe, H. R., Minamide, L. S., Bamburg, J. R., and Cramer, L. P. (2003). ADF/cofilin controls cell polarity during fibroblast migration. *Current Biology*, 13(3):252–257.

De Jong, D. and Balagué Ponz, O. (2011). The molecular background of aggressive B cell lymphomas as a basis for targeted therapy. *Journal of Pathology*, 223(2):274–282.

De Silva, N. S. and Klein, U. (2015). Dynamics of B cells in germinal centres. *Nature Reviews Immunology*, 15(3):137–148.

de Yébenes, V. G., Bartolomé-Izquierdo, N., and Ramiro, A. R. (2013). Regulation of B-cell development and function by microRNAs. *Immunological reviews*, 253(1):25–39.

Defranco, A. L., Rookhuizen, D. C., and Hou, B. (2012). Contribution of Toll-like receptor signaling to germinal center antibody responses. *Immunological Reviews*, 247(1):64–72.

Dobin, A., Davis, C. A., Schlesinger, F., Drenkow, J., Zaleski, C., Jha, S., Batut, P., Chaisson, M., and Gingeras, T. R. (2013). STAR: Ultrafast universal RNA-seq aligner. *Bioinformatics*, 29(1):15–21.

Dölken, L., Malterer, G., Erhard, F., Kothe, S., Friedel, C. C., Suffert, G., Marcinowski, L., Motsch, N., Barth, S., Beitzinger, M., Lieber, D., Bailer, S. M., Hoffmann, R., Ruzsics, Z., Kremmer, E., Pfeffer, S., Zimmer, R., Koszinowski, U. H., Grässer, F., Meister, G., and Haas, J. (2010). Systematic analysis of viral and cellular microRNA targets in cells latently infected with human gamma-herpesviruses by RISC immunoprecipitation assay. *Cell host & microbe*, 7(4):324–34.

Dominguez-Sola, D., Victora, G. D., Ying, C. Y., Phan, R. T., Saito, M., Nussenzweig, M. C., and Dalla-Favera, R. (2012). The proto-oncogene MYC is required for selection in the germinal center and cyclic reentry. *Nature immunology*, 13(11):1083–91.

Downward, J. (2003). Targeting RAS signalling pathways in cancer therapy. *Nat Rev Cancer*, 3(1):11–22.

Doyle, S. L. and O'Neill, L. A. J. (2006). Toll-like receptors: From the discovery of NF??B to new insights into transcriptional regulations in innate immunity. *Biochemical Pharmacology*, 72(9 SPEC. ISS.):1102–1113.

Efremov, D. G. (2016). FOXO discriminates tonic from chronic in DLBCL. *Blood*, 127(6):667–669.

Elgueta, R. (2009). Molecular mechanism and function of CD40/CD40L engagement in the immune system. 229(1):189.

Esquela-Kerscher, A. and Slack, F. J. (2006). Oncomirs - microRNAs with a role in cancer. *Nature Reviews Cancer*, 6(4):259–269.

Evan, G. I., Wyllie, A. H., Gilbert, C. S., Littlewood, T. D., Land, H., Brooks, M., Waters, C. M., Penn, L. Z., and Hancock, D. C. (1992). Induction of apoptosis in fibroblasts by c-myc protein. *Cell*, 69(1):119–128.

Fabian, M. R., Mathonnet, G., Sundermeier, T., Mathys, H., Zipprich, J. T., Svitkin, Y. V., Rivas, F., Jinek, M., Wohlschlegel, J., Doudna, J. A., Chen, C. Y. A., Shyu, A. B., Yates, J. R., Hannon, G. J., Filipowicz, W., Duchaine, T. F., and Sonenberg, N. (2009). Mammalian miRNA RISC Recruits CAF1 and PABP to Affect PABP-Dependent Deadenylation. *Molecular Cell*, 35(6):868–880.

Fanale, M. A. and Younes, A. (2008). Nodular lymphocyte predominant Hodgkin's lymphoma. In *Rare Hematological Malignancies*, pages 367–381.

Farazi, T. A., Hoell, J. I., Morozov, P., and Tuschl, T. (2013). MicroRNA Cancer Regulation. 774.

Ferlay, J., Steliarova-Foucher, E., Lortet-Tieulent, J., Rosso, S., Coebergh, J. W. W., Comber, H., Forman, D., and Bray, F. (2013). Cancer incidence and mortality patterns in Europe: Estimates for 40 countries in 2012. *European Journal of Cancer*, 49(6):1374–1403.

Ferry, J. A. (2006). L ymphoma S eries : V ariants of L arge- C ell L ymphoma. pages 375–383.

Feugier, P. (2005). Long-Term Results of the R-CHOP Study in the Treatment of Elderly Patients With Diffuse Large B-Cell Lymphoma: A Study by the Groupe d'Etude des Lymphomes de l'Adulte. *Journal of Clinical Oncology*, 23(18):4117–4126.

Fey, D., Matallanas, D., Rauch, J., Rukhlenko, O. S., and Kholodenko, B. N. (2016). The complexities and versatility of the RAS-to-ERK signalling system in normal and cancer cells. *Seminars in Cell and Developmental Biology*, 58:96–107.

Filipowicz, W., Bhattacharyya, S. N., and Sonenberg, N. (2008). Mechanisms of post-transcriptional regulation by microRNAs: are the answers in sight? *Nature reviews. Genetics*, 9(2):102–14.

Franceschi, S., Dal Maso, L. D., and La Vecchia, C. L. (1999). Advances in the epidemiology of HIV-associated non-Hodgkin's lymphoma and other lymphoid neoplasms. *International Journal of Cancer*, 83(4):481–485.

Friedman, R. C., Farh, K. K. H., Burge, C. B., and Bartel, D. P. (2009). Most mammalian mRNAs are conserved targets of microRNAs. *Genome Research*, 19(1):92–105.

Fu, L., Lin-Lee, Y. C., Pham, L. V., Tamayo, A., Yoshimura, L., and Ford, R. J. (2006). Constitutive NFkB and NFAT activation leads to stimulation of the BLyS survival pathway in aggressive B-cell lymphomas. *Blood*, 107(11):4540–4548.

Funakoshi, S., Longo, D. L., Beckwith, M., Conley, D. K., Tsarfaty, G., Tsarfaty, I., Armitage, R. J., Fanslow, W. C., Spriggs, M. K., and Murphy, W. J. (1994). Inhibition of human B-cell lymphoma growth by CD40 stimulation. *Blood*, 83(10):2787–94.

Gachet, S. and Ghysdael, J. (2009). Calcineurin/NFAT signaling in lymphoid malignancies. *General Physiology and Biophysics*, 28.

Gao, P., Tchernyshyov, I., Chang, T.-C., Lee, Y.-S., Kita, K., Ochi, T., Zeller, K. I., De Marzo, A. M., Van Eyk, J. E., Mendell, J. T., and Dang, C. V. (2009). c-Myc suppression of miR-23a/b enhances mitochondrial glutaminase expression and glutamine metabolism. *Nature*, 458(7239):762–5.

Garrison, S. P., Jeffers, J. R., Yang, C., Nilsson, J. a., Hall, M. a., Rehg, J. E., Yue, W., Yu, J., Zhang, L., Onciu, M., Sample, J. T., Cleveland, J. L., and Zambetti, G. P. (2008). Selection against PUMA Gene Expression in Myc-Driven B-Cell Lymphomagenesis. *Molecular and Cellular Biology*, 28(17):5391–5402.

Gaudio, E., Tarantelli, C., Kwee, I., Barassi, C., Bernasconi, E., Rinaldi, A., Ponzoni, M., Cascione, L., Targa, A., Stathis, A., Goodstal, S., Zucca, E., and Bertoni, F. (2016). Combination of the MEK inhibitor pimasertib with BTK or PI3K-delta inhibitors is active in preclinical models of aggressive lymphomas. *Annals of Oncology*, 27(6):1123–1128.

Gayko, U., Fung, M., Clow, F., Sun, S., Faust, E., Price, S., James, D., Doyle, M., Bari, S., and Zhuang, S. H. (2015). Development of the Bruton's tyrosine kinase inhibitor ibrutinib for B cell malignancies. *Annals of the New York Academy of Sciences*, pages n/a–n/a.

Giffin, L. and Damania, B. (2014). *KSHV: Pathways to tumorigenesis and persistent infection*, volume 88. Elsevier Inc., 1 edition.

Giles, R. H., Dauwerse, J. G., Higgins, C., Petrij, F., Wessels, J. W., Beverstock, G. C., Dohner, H., Jotterand-Bellomo, M., Falkenburg, J. H., Slater, R. M., van Ommen, G. J., Hagemeijer, A., van der Reijden, B. A., and Breuning, M. H. (1997). Detection of CBP rearrangements in acute myelogenous leukemia with t(8;16). *Leukemia*, 11(12):2087–2096.

Gille, H., Kortenjann, M., Thomae, O., Moomaw1, C., Slaughterl, C., Cobb2, M. H., and Shaw3, P. E. (1995). ERK phosphorylation potentiates Elk-1-mediated ternary complex formation and transactivation. *The EMBO Journal*, 14(5):951–962.

Gong, J. Z., Stenzel, T. T., Bennett, E. R., Lagoo, A. S., Dunphy, C. H., Moore, J. O., Rizzieri, D. a., Tepperberg, J. H., Papenhausen, P., and Buckley, P. J. (2003). Burkitt lymphoma arising in organ transplant recipients: a clinicopathologic study of five cases. *The American Journal of Surgical Pathology*, 27(6):818–27.

Goswami, R. S., Atenafu, E. G., Xuan, Y., Waldron, L., Reis, P. P., Sun, T., Datti, A., Xu, W., Kuruvilla, J., Good, D. J., Lai, R., Church, A. J., Lam, W. S., Baetz, T., Lebrun, D. P., Sehn, L. H., Farinha, P., Jurisica, I., Bailey, D. J., Gascoyne, R. D., Crump, M., and Kamel-Reid, S. (2013). MicroRNA signature obtained from the comparison of aggressive with indolent non-Hodgkin lymphomas: potential prognostic value in mantle-cell lymphoma. *Journal of clinical oncology : official journal of the American Society of Clinical Oncology*, 31(23):2903–2911.

Gregory, M. A. and Hann, S. R. (2000). c-Myc proteolysis by the ubiquitin-proteasome pathway: stabilization of c-Myc in Burkitt's lymphoma cells. *Molecular and cellular biology*, 20(7):2423–2435.

Grimson, A., Farh, K. K. H., Johnston, W. K., Garrett-Engele, P., Lim, L. P., and Bartel, D. P. (2007). MicroRNA Targeting Specificity in Mammals: Determinants beyond Seed Pairing. *Molecular Cell*, 27(1):91–105.

Guttilla, I. K. and White, B. A. (2009). Coordinate regulation of FOXO1 by miR-27a, miR-96, and miR-182 in breast cancer cells. *Journal of Biological Chemistry*, 284(35):23204–23216.

Hadjimichael, C., Nikolaou, C., Papamatheakis, J., and Kretsovali, A. (2016). MicroRNAs for Fine-Tuning of Mouse Embryonic Stem Cell Fate Decision through Regulation of TGF-β Signaling. *Stem Cell Reports*, 6(3):292–301.

Hafner, M., Landthaler, M., Burger, L., Khorshid, M., Berninger, P., Rothballer, A., Jr, M. A., Munschauer, M., Ulrich, A., Wardle, G. S., Dewell, S., Zavolan, M., and Tuschl, T. (2010). Transcriptome-wide identification of RNA-binding protein and microRNA target sites by PAR-CLIP. *Cell*, 141(1):129–141.

Han, J., Lee, Y., Yeom, K. H., Nam, J. W., Heo, I., Rhee, J. K., Sohn, S. Y., Cho, Y., Zhang, B. T., and Kim, V. N. (2006). Molecular Basis for the Recognition of Primary microRNAs by the Drosha-DGCR8 Complex. *Cell*, 125(5):887–901.

Hanahan, D. and Weinberg, R. A. (2011). Hallmarks of cancer: the next generation. *Cell*, 144(5):646–674.

Hashimoto, A., Okada, H., Jiang, A., Kurosaki, M., Greenberg, S., Clark, E. A., and Kurosaki, T. (1998). Involvement of Guanosine Triphosphatases and Phospholipase C-gamma 2 in Extracellular Signal regulated Kinase, c-Jun NH2-terminal Kinase, and p38 Mitogen-activated Protein Kinase Activation by the B Cell Antigen Receptor. *J. Exp. Med*, 188(7).

Hauer, J., Püschner, S., Ramakrishnan, P., Simon, U., Bongers, M., Federle, C., and Engelmann, H. (2005). TNF receptor (TNFR)-associated factor (TRAF) 3 serves as an inhibitor of TRAF2/5-mediated activation of the noncanonical NF-kappaB pathway by TRAF-binding TNFRs. *Proceedings of the National Academy of Sciences of the United States of America*, 102(8):2874–9.

He, Y., Meng, C., Shao, Z., Wang, H., and Yang, S. (2014). MiR-23a Functions as a Tumor Suppressor in Osteosarcoma. *Cellular physiology and biochemistry : international journal of experimental cellular physiology, biochemistry, and pharmacology*, 34(5):1485–1496.

Hezaveh, K., Kloetgen, A., Bernhart, S. H., Mahapatra, K. D., Lenze, D., Richter, J., Haake, A., Bergmann, A. K., Brors, B., Burkhardt, B., Claviez, A., Drexler, H. G., Eils, R., Haas, S., Hoffmann, S., Karsch, D., Klapper, W., Kleinheinz, K., Korbel, J., Kretzmer, H., Kreuz, M., Küppers, R., Lawerenz, C., Leich, E., Loeffler, M., Mantovani-Loeffler, L., López, C., McHardy, A. C., Möller, P., Rohde, M., Rosenstiel, P., Rosenwald, A., Schilhabel, M., Schlesner, M., Scholz, I., Stadler, P. F., Stilgenbauer, S., Sungalee, S., Szczepanowski, M., Trümper, L., Weniger, M. A., Siebert, R., Borkhardt, A., Hummel, M., and Hoell, J. I. (2016). Alterations of miRNAs and miRNA-regulated mRNA expression in GC B cell lymphomas determined by integrative sequencing analysis. *Haematologica*, (July):haematol.2016.143891.

Hisanaga, K., Sagar, S. M., Hicks, K. J., Swanson, R. A., and Sharp, F. R. (1990). Differentiation or Proliferation But Not Depolarization. 8:69–75.

Högerkorp, C.-M. and Borrebaeck, C. a. K. (2006). The human CD77- B cell population represents a heterogeneous subset of cells comprising centroblasts, centrocytes, and plasmablasts, prompting phenotypical revision. *Journal of immunology (Baltimore, Md. : 1950)*, 177(7):4341–4349.

Hollmann, C. A., Owens, T., Nalbantoglu, J., Hudson, T. J., and Sladek, R. (2006). Constitutive activation of extracellular signal-regulated kinase predisposes diffuse large B-cell lymphoma cell lines to CD40-mediated cell death. *Cancer Research*, 66(7):3550–3557.

Hu, S., Xie, Z., Onishi, A., Yu, X., Jiang, L., Lin, J., sool Rho, H., Woodard, C., Wang, H., Jeong, J. S., Long, S., He, X., Wade, H., Blackshaw, S., Qian, J., and Zhu, H. (2009). Profiling the Human Protein-DNA Interactome Reveals ERK2 as a Transcriptional Repressor of Interferon Signaling. *Cell*, 139(3):610–622.

Hummel, M., Barth, T. F. E., Bernd, H.-w., Cogliatti, S. B., Dierlamm, J., Ph, D., Feller, A. C., Hansmann, M.-l., Haralambieva, E., Harder, L., Hasenclever, D., Kühn, M., Lenze, D., Lichter, P., Martin-subero, J. I., Möller, P., Ott, G., Parwaresch, R. M., Pott, C., Rosenwald, A., Rosolowski, M., Schwaenen, C., Stürzenhofecker, B., Szczepanowski, M., Trautmann, H., Wacker, H.-h., Spang, R., Loeffler, M., Trümper, L., Stein, H., and Siebert, R. (2006). A Biologic Definition of Burkitt's Lymphoma from Transcriptional and Genomic Profiling. *The New England Journal of Medicine*, 354(23):2419–2430.

Hutvágner, G., McLachlan, J., Pasquinelli, A. E., Bálint, E., Tuschl, T., and Zamore, P. D. (2001). A cellular function for the RNA-interference enzyme Dicer in the maturation of the let-7 small temporal RNA. *Science (New York, N.Y.)*, 293(5531):834–838.

Hutvagner, G. and Simard, M. J. (2008). Argonaute proteins: key players in RNA silencing. *Nature reviews. Molecular cell biology*, 9(1):22–32.

Hwang, H.-W., Wentzel, E. A., and Mendell, J. T. (2007). A Hexanucleotide Element Directs MicroRNA Nuclear Import. 315:97–100.

Iizasa, H., Wulff, B. E., Alla, N. R., Maragkakis, M., Megraw, M., Hatzigeorgiou, A., Iwakiri, D., Takada, K., Wiedmer, A., Showe, L., Lieberman, P., and Nishikura, K. (2010). Editing of Epstein-Barr virus-encoded BART6 microRNAs controls their dicer targeting and consequently affects viral latency. *Journal of Biological Chemistry*, 285(43):33358–33370.

Iqbal, J., Gupta, S., Chen, Q. H., Brody, J. P., and Koduru, P. (2007). Diffuse large B-cell lymphoma with a novel translocation involving BCL6. *Cancer Genetics and Cytogenetics*, 178(1):73–76.

Iqbal, J., Shen, Y., Huang, X., Liu, Y., Wake, L., Liu, C., Deffenbacher, K., Lachel, C. M., Wang, C., Rohr, J., Guo, S., Smith, L. M., Wright, G., Bhagavathi, S., Dybkaer, K., Fu, K., Greiner, T. C., Vose, J. M., Jaffe, E., Rimsza, L., Rosenwald, A., Ott, G., Delabie, J., Campo, E., Braziel, R. M., Cook, J. R., Tubbs, R. R., Armitage, J. O., Weisenburger, D. D., Staudt, L. M., Gascoyne, R. D., Mckeithan, T. W., and Chan, W. C. (2015). Global microRNA expression profiling uncovers molecular markers for classification and prognosis in aggressive B-cell lymphoma. *Blood*, 125(7):1137–1146.

Ishibashi, T., Bottaro, D. P., Michieli, P., Kelley, C. A., and Aaronson, S. A. (1994). A novel dual specificity phosphatase induced by serum stimulation and heat shock. *Journal of Biological Chemistry*, 269(47):29897–29902.

Jahid, S., Sun, J., Edwards, R. a., Dizon, D., Panarelli, N. C., Milsom, J. W., Sikandar, S. S., Gümüs, Z. H., and Lipkin, S. M. (2012). miR-23a promotes the transition from indolent to invasive colorectal cancer. *Cancer discovery*, 2(6):540–53.

Janas, M. M., Wang, B., Harris, A. S., Aguiar, M., Shaffer, J. M., Subrahmanyam, Y. V. B. K., Behlke, M. a., Wucherpfennig, K. W., Gygi, S. P., Gagnon, E., and Novina, C. D. (2012). Alternative RISC

assembly: binding and repression of microRNA-mRNA duplexes by human Ago proteins. *RNA (New York, N.Y.)*, 18(11):2041–55.

Janeway, C. A., Murphy, K. M., Travers, P., and Walport, M. (2001). *Janeway Immunologie*, volume 5. Auflage.

Janknecht, R. and Nordheim, A. (1996). MAP Kinase-Dependent Transcriptional Coactivation by Elk-1 and Its Cofactor CBP of signals such as growth factors or cytokines . Many of these signals enter the c-fos promoter in vivo , SRF and a ternary complex factor , one of which is the Elk-1 protein . 837:831–837.

Jiang, Y. and Melnick, A. (2015). The Epigenetic basis of diffuse large B-cell lymphoma. *Semin Hematol.*, 52(2):86–96.

Kahl, B. (2008). Chemotherapy Combinations With Monoclonal Antibodies in Non-Hodgkin's Lymphoma. *Seminars in Hematology*, 45(2):90–94.

Kaji, N., Muramoto, A., and Mizuno, K. (2008). LIM kinase-mediated cofilin phosphorylation during mitosis is required for precise spindle positioning. *Journal of Biological Chemistry*, 283(8):4983–4992.

Kang, T.-H. and Kim, K.-T. (2006). Negative regulation of ERK activity by VRK3-mediated activation of VHR phosphatase. *Nature cell biology*, 8(8):863–869.

Kang-Decker, N., Tong, C., Boussouar, F., Baker, D. J., Xu, W., Leontovich, A. A., Taylor, W. R., Brindle, P. K., and Van Deursen, J. M. A. (2004). Loss of CBP causes T cell lymphomagenesis in synergy with p27 Kip1 insufficiency. *Cancer Cell*, 5(2):177–189.

Khan, W. N. (2009). B cell receptor and BAFF receptor signaling regulation of B cell homeostasis. *Journal of immunology (Baltimore, Md. : 1950)*, 183:3561–3567.

Khvorova, A., Reynolds, A., and Jayasena, S. D. (2003). Functional siRNAs and miRNAs exhibit strand bias. *Cell*, 115(2):209–216.

Kidger, A. M. and Keyse, S. M. (2016). The regulation of oncogenic Ras/ERK signalling by dual-specificity mitogen activated protein kinase phosphatases (MKPs). *Seminars in Cell and Developmental Biology*, 50:125–132.

Kim, Y. K., Heo, I., and Kim, V. N. (2010). Modifications of Small RNAs and their associated proteins. *Cell*, 143(5):703–709.

Klein, U. and Dalla-Favera, R. (2008). Germinal centres: role in B-cell physiology and malignancy. *Nature reviews. Immunology*, 8(1):22–33.

Klein, U., Tu, Y., Stolovitzky, G. a., Keller, J. L., Haddad, J., Miljkovic, V., Cattoretti, G., Califano, A., and Dalla-Favera, R. (2003). Transcriptional analysis of the B cell germinal center reaction. *Proceedings of the National Academy of Sciences of the United States of America*, 100(5):2639–44.

Kluiver, J., Haralambieva, E., De Jong, D., Blokzijl, T., Jacobs, S., Kroesen, B. J., Poppema, S., and Van Den Berg, A. (2006). Lack of BIC and microRNA miR-155 expression in primary cases of Burkitt lymphoma. *Genes Chromosomes and Cancer*, 45(2):147–153.

Kluiver, J., Poppema, S., de Jong, D., Blokzijl, T., Harms, G., Jacobs, S., Kroesen, B.-J., and van den Berg, A. (2005). BIC and miR-155 are highly expressed in Hodgkin, primary mediastinal and diffuse large B cell lymphomas. *The Journal of pathology*, 207(July):243–249.

Konforte, D., Simard, N., and Paige, C. J. (2009). IL-21: an executor of B cell fate. *J Immunol*, 182(4):1781–1787.

Kong, K. Y., Owens, K. S., Rogers, J. H., Mullenix, J., Velu, C. S., Grimes, H. L., and Dahl, R. (2010). MIR-23A microRNA cluster inhibits B-cell development. *Experimental hematology*, 38(8):629–640.e1.

Kozomara, A. and Griffiths-Jones, S. (2011). MiRBase: Integrating microRNA annotation and deep-sequencing data. *Nucleic Acids Research*, 39.

Kuersten, S. and Goodwin, E. B. (2003). The power of the 3' UTR: translational control and development. *Nature reviews. Genetics*, 4(8):626–637.

Kulkarni, M., Ozgur, S., and Stoecklin, G. (2010). On track with P-bodies. *Biochemical Society transactions*, 38(Pt 1):242–51.

Kumar, R., Gururaj, A. E., and Barnes, C. J. (2006). P21-Activated Kinases in Cancer. *Nature Reviews Cancer*, 6(6):459–471.

Küppers, R. (2005). Mechanisms of B-cell lymphoma pathogenesis. *Nature reviews. Cancer*, 5(4):251–62.

Kurkewich, J. L., Bikorimana, E., Nguyen, T., Klopfenstein, N., Zhang, H., Hallas, W. M., Stayback, G., McDowell, M. a., and Dahl, R. (2016). The mirn23a microRNA cluster antagonizes B cell development. *J Leukoc Biol*, 100(November):1–13.

Laemmli, U. K. (1970). Cleavage of structural proteins during the assembly of the head of bacteriophage T4. *Nature*, 227(5259):680–685.

Lawrence, T. (2009). The nuclear factor NF-kappaB pathway in inflammation. *Cold Spring Harbor perspectives in biology*, 1(6):1–10.

Lawrie, C. H. (2013). MicroRNAs and lymphomagenesis: a functional review. *British Journal of Haematology*, 160(5):571–81.

Le, T. D., Liu, L., Zhang, J., Liu, B., and Li, J. (2014). From miRNA regulation to miRNA-TF co-regulation: computational approaches and challenges. *Briefings in Bioinformatics*, 16(3):475–496.

Lee, R. C., Feinbaum, R. L., and Ambros, V. (1993). The C. elegans heterochronic gene lin-4 encodes small RNAs with antisense complementarity to lin-14. *Cell*, 75(5):843–854.

Lee, Y., Kim, M., Han, J., Yeom, K.-H., Lee, S., Baek, S. H., and Kim, V. N. (2004). MicroRNA genes are transcribed by RNA polymerase II. *The EMBO journal*, 23(20):4051–60.

Lenz, G., Davis, R. E., Ngo, V. N., Lam, L., George, T. C., Wright, G. W., Dave, S. S., Zhao, H., Xu, W., Rosenwald, A., Ott, G., Muller-Hermelink, H. K., Gascoyne, R. D., Connors, J. M., Rimsza, L. M., Campo, E., Jaffe, E. S., Delabie, J., Smeland, E. B., Fisher, R. I., Chan, W. C., and Staudt, L. M. (2008). Oncogenic CARD11 mutations in human diffuse large B cell lymphoma. *Science (New York, N.Y.)*, 319(5870):1676–9.

Lenz, G., Nagel, I., Siebert, R., Roschke, A. V., Sanger, W., Wright, G. W., Dave, S. S., Tan, B., Zhao, H., Rosenwald, A., Muller-Hermelink, H. K., Gascoyne, R. D., Campo, E., Jaffe, E. S., Smeland, E. B., Fisher, R. I., Kuehl, W. M., Chan, W. C., and Staudt, L. M. (2007). Aberrant immunoglobulin class

switch recombination and switch translocations in activated B cell-like diffuse large B cell lymphoma. *The Journal of experimental medicine*, 204(3):633–43.

Lenze, D., Leoncini, L., Hummel, M., Volinia, S., Liu, C. G., Amato, T., De Falco, G., Githanga, J., Horn, H., Nyagol, J., Ott, G., Palatini, J., Pfreundschuh, M., Rogena, E., Rosenwald, A., Siebert, R., Croce, C. M., and Stein, H. (2011). The different epidemiologic subtypes of Burkitt lymphoma share a homogenous micro RNA profile distinct from diffuse large B-cell lymphoma. *Leukemia official journal of the Leukemia Society of America Leukemia Research Fund UK*, 25(12):1869–76.

Lewis, B. P., Shih, I.-h., Jones-Rhoades, M. W., Bartel, D. P., and Burge, C. B. (2003). Prediction of Mammalian MicroRNA Targets. *Cell*, 115(7):787–798.

Li, S., Lin, P., Fayad, L. E., Lennon, P. A., Miranda, R. N., Yin, C. C., Lin, E., and Medeiros, L. J. (2012). B-cell lymphomas with MYC/8q24 rearrangements and IGH@BCL2/t(14;18)(q32;q21): an aggressive disease with heterogeneous histology, germinal center B-cell immunophenotype and poor outcome. *Mod Pathol*, 25(1):145–156.

Li, X., Liu, X., Xu, W., Zhou, P., Gao, P., Jiang, S., and Lobie, P. E. (2013a). c-MYC-regulated miR-23a/24-2/27a Cluster Promotes Mammary Carcinoma Cell Invasion and Hepatic Metastasis by Targeting Sprouty2. *J. Biol. Chem*, 288:18121–18133.

Li, X., Liu, X., Xu, W., Zhou, P., Gao, P., Jiang, S., Lobie, P. E., and Zhu, T. (2013b). C-MYC-regulated miR-23a/24-2/27a cluster promotes mammary carcinoma cell invasion and hepatic metastasis by targeting sprouty2. *Journal of Biological Chemistry*, 288(25):18121–18133.

Liang, H. and Landweber, L. F. (2007). Hypothesis: RNA editing of microRNA target sites in humans? *RNA (New York, N.Y.)*, 13(4):463–7.

Lin, Z., Murtaza, I., Wang, K., Jiao, J., Gao, J., and Li, P.-F. (2009). miR-23a functions downstream of NFATc3 to regulate cardiac hypertrophy. *Proceedings of the National Academy of Sciences of the United States of America*, 106(29):12103–12108.

Liu, D., Xu, H., Shih, C., Wan, Z., Ma, X., Ma, W., Luo, D., and Qi, H. (2015). T-B-cell entanglement and ICOSL-driven feed-forward regulation of germinal centre reaction. *Nature*, 517(7533):214–8.

Liu, J. (2004). Argonaute2 Is the Catalytic Engine of Mammalian RNAi. *Engineer*, 290(7543):22.

Liu, X., Ru, J., Zhang, J., hua Zhu, L., Liu, M., Li, X., and Tang, H. (2013). miR-23a Targets Interferon Regulatory Factor 1 and Modulates Cellular Proliferation and Paclitaxel-Induced Apoptosis in Gastric Adenocarcinoma Cells. *PLoS ONE*, 8(6):1–13.

Lomonosova, E. and Chinnadurai, G. (2008). BH3-only proteins in apoptosis and beyond: an overview. *Oncogene*, 27 Suppl 1(S1):S2–19.

Lu, T.-X., Fan, L., Wang, L., Wu, J.-Z., Miao, K.-R., Liang, J.-H., Gong, Q.-X., Wang, Z., Young, K. H., Xu, W., Zhang, Z.-H., Li, J.-Y., Lu, T.-X., Fan, L., Wang, L., Wu, J.-Z., Miao, K.-R., Liang, J.-H., Gong, Q.-X., Wang, Z., Young, K. H., Xu, W., Zhang, Z.-H., and Li, J.-Y. (2015). MYC or BCL2 copy number aberration is a strong predictor of outcome in patients with diffuse large B-cell lymphoma. *Oncotarget*, 6(21):18374–18388.

Lugowska, I., Koseła-Paterczyk, H., Kozak, K., and Rutkowski, P. (2015). Trametinib: a MEK inhibitor for management of metastatic melanoma. *OncoTargets and therapy*, 8:2251–9.

Lytle, J. R., Yario, T. a., and Steitz, J. a. (2007). Target mRNAs are repressed as efficiently by microRNA-binding sites in the 5' UTR as in the 3' UTR. *Proceedings of the National Academy of Sciences of the United States of America*, 104(23):9667–9672.

Ma, Y., Yu, S., Zhao, W., Lu, Z., and Chen, J. (2010). miR-27a regulates the growth, colony formation and migration of pancreatic cancer cells by targeting Sprouty2. *Cancer letters*, 298(2):150–8.

Malumbres, R., Sarosiek, K. a., Cubedo, E., Ruiz, J. W., Jiang, X., Gascoyne, R. D., Tibshirani, R., and Lossos, I. S. (2009). Differentiation stage-specific expression of microRNAs in B lymphocytes and diffuse large B-cell lymphomas. *Blood*, 113(16):3754–64.

Manzano, M., Shamulailatpam, P., Raja, A. N., and Gottwein, E. (2013). Kaposi's sarcoma-associated herpesvirus encodes a mimic of cellular miR-23. *Journal of virology*, 87(21):11821–30.

Marafiot, T., Pozzobon, M., Hansmann, M. L., Ventura, R., Pileri, S. A., Roberton, H., Gesk, S., Gaulard, P., Barth, T. F. E., Du, M. Q., Leoncini, L., Möller, P., Natkunam, Y., Siebert, R., and Mason, D. Y. (2005). The NFATc1 transcription factor is widely expressed in white cells and translocates from the cytoplasm to the nucleus in a subset of human lymphomas. *British Journal of Haematology*, 128(3):333–342.

Marshall, W. F., Fung, J. C., and Sedat, J. W. (1997). Deconstructing the nucleus: global archetecture from local interactions. *Curr. Opin. Genet. Develop.*, 7:259–263.

Martinez-Climent, J. A., Alizadeh, A. A., Segraves, R., Blesa, D., Rubio-Moscardo, F., Albertson, D. G., Garcia-Conde, J., Dyer, M. J. S., Levy, R., Pinkel, D., and Lossos, I. S. (2003). Transformation of follicular lymphoma to diffuse large cell lymphoma is associated with a heterogeneous set of DNA copy number and gene expression alterations. *Blood*, 101(8):3109–3117.

Martinez-Sanchez, A. and Murphy, C. L. (2013). MicroRNA Target Identification-Experimental Approaches. *Biology*, 2(1):189–205.

Masliah-Planchon, J., Garinet, S., and Pasmant, E. (2015). RAS-MAPK pathway epigenetic activation in cancer: miRNAs in action. *Oncotarget*, 7(25).

Matranga, C., Tomari, Y., Shin, C., Bartel, D. P., and Zamore, P. D. (2005). Passenger-strand cleavage facilitates assembly of siRNA into Ago2-containing RNAi enzyme complexes. *Cell*, 123(4):607–620.

Maxwell, S. A. and Mousavi-Fard, S. (2013). Non-Hodgkin's B-cell lymphoma: advances in molecular strategies targeting drug resistance. *Experimental biology and medicine (Maywood, N.J.)*, 238(9):971–90.

McNally, R. J. Q. and Parker, L. (2006). Environmental factors and childhood acute leukemias and lymphomas. *Leukemia & Lymphoma*, 47(4):583–598.

Melchers, F. (2015). Checkpoints that control B cell development. 125(6):2203–2210.

Mi, S., Lu, J., Sun, M., Li, Z., Zhang, H., Neilly, M. B., Wang, Y., Qian, Z., Jin, J., Zhang, Y., Bohlander, S. K., Le Beau, M. M., Larson, R. a., Golub, T. R., Rowley, J. D., and Chen, J. (2007). MicroRNA expression signatures accurately discriminate acute lymphoblastic leukemia from acute myeloid leukemia. *Proceedings of the National Academy of Sciences of the United States of America*, 104(50):19971–19976.

Michalak, E. M., Jansen, E. S., Happo, L., Cragg, M. S., Tai, L., Smyth, G. K., Strasser, A., Adams, J. M., and Scott, C. L. (2009). Puma and to a lesser extent Noxa are suppressors of Myc-induced lymphomagenesis. *Cell death and differentiation*, 16(5):684–96.

Michlewski, G. and Cáceres, J. F. (2010). Antagonistic role of hnRNP A1 and KSRP in the regulation of let-7a biogenesis. *Nature structural & molecular biology*, 17(8):1011–8.

Monti, S., Monti, S., Savage, K. J., Savage, K. J., Kutok, J. L., Kutok, J. L., Feuerhake, F., Feuerhake, F., Kurtin, P., Kurtin, P., Mihm, M., Mihm, M., Wu, B., Wu, B., Pasqualucci, L., Pasqualucci, L., Neuberg, D., Neuberg, D., Aguiar, R. C. T., Aguiar, R. C. T., Cin, P. D., Cin, P. D., Ladd, C., Ladd, C., Pinkus, G. S., Pinkus, G. S., Salles, G., Salles, G., Harris, N. L., Harris, N. L., Dalla-favera, R., Dalla-favera, R., Habermann, T. M., Habermann, T. M., Aster, J. C., Aster, J. C., Golub, T. R., Golub, T. R., Shipp, M. a., and Shipp, M. a. (2005). Molecular profiling of diffuse large B-cell lymphoma identifies robust subtypes including one characterized by host infl ammatory response. *Response*, 105(5):1851–1861.

Morin, R. D., Johnson, N. A., Severson, T. M., Mungall, A. J., Goya, R., Paul, J. E., Boyle, M., Woolcock, B. W., Yap, D., Humphries, R. K., Griffith, O. L., Shah, S., Kimbara, M., Shashkin, P., Charlot, J. F., Tcherpakov, M., Corbett, R., Tam, A., Varhol, R., Smailus, D., Moksa, M., Zhao, Y., Delaney, A., Qian, H., Birol, I., Schein, J., Holt, R., Horsman, D. E., Connors, J. M., Jones, S., Hirst, M., Gascoyne, R. D., and Marra, M. A. (2010). Somatic mutation of EZH2 (Y641) in Follicular and Diffuse Large B-cell Lymphomas of Germinal Center Origin. *Nature genetics*, 42(2):181–185.

Morin, R. D., Mendez-Lago, M., Mungall, A. J., Goya, R., Mungall, K. L., Corbett, R. D., Johnson, N. A., Severson, T. M., Chiu, R., Field, M., Jackman, S., Krzywinski, M., Scott, D. W., Trinh, D. L., Tamura-Wells, J., Li, S., Firme, M. R., Rogic, S., Griffith, M., Chan, S., Yakovenko, O., Meyer, I. M., Zhao, E. Y., Smailus, D., Moksa, M., Chittaranjan, S., Rimsza, L., Brooks-Wilson, A., Spinelli, J. J., Ben-Neriah, S., Meissner, B., Woolcock, B., Boyle, M., McDonald, H., Tam, A., Zhao, Y., Delaney, A., Zeng, T., Tse, K., Butterfield, Y., Birol, I., Holt, R., Schein, J., Horsman, D. E., Moore, R., Jones, S. J. M., Connors, J. M., Hirst, M., Gascoyne, R. D., and Marra, M. A. (2011). Frequent mutation of histone-modifying genes in non-Hodgkin lymphoma. *Nature*, 476(7360):298–303.

Morlando, M., Ballarino, M., Gromak, N., Pagano, F., Bozzoni, I., and Proudfoot, N. J. (2008). Primary microRNA transcripts are processed co-transcriptionally. *Nature structural & molecular biology*, 15(9):902–9.

Mudduluru, G., Vajkoczy, P., and Allgayer, H. (2010). Myeloid zinc finger 1 induces migration, invasion, and in vivo metastasis through Axl gene expression in solid cancer. *Molecular cancer research : MCR*, 8(2):159–169.

Mukherji, S., Ebert, M. S., Zheng, G. X. Y., Tsang, J. S., Sharp, P. A., and van Oudenaarden, A. (2011). MicroRNAs can generate thresholds in target gene expression. *Nature genetics*, 43(9):854–9.

Mullis, K., Faloona, F., Scharf, S., Saiki, R., Horn, G., and Erlich, H. (1986). Specific enzymatic amplification of DNA in vitro: The polymerase chain reaction.

Na, Y.-J. and Kim, J. H. (2013). Understanding cooperativity of microRNAs via microRNA association networks. *BMC genomics*, 14 Suppl 5(Suppl 5):S17.

Nakano, H., Sakon, S., Koseki, H., Takemori, T., Tada, K., Matsumoto, M., Munechika, E., Sakai, T., Shirasawa, T., Akiba, H., Kobata, T., Santee, S. M., Ware, C. F., Rennert, P. D., Taniguchi, M., Yagita,

H., and Okumura, K. (1999). Targeted disruption of Traf5 gene causes defects in CD40- and CD27-mediated lymphocyte activation. *Proceedings of the National Academy of Sciences of the United States of America*, 96(17):9803–8.

Nakano, K. and Vousden, K. H. (2001). PUMA, a novel proapoptotic gene, is induced by p53. *Molecular Cell*, 7:683–694.

Nichols, R. J. and Traktman, P. (2004). Characterization of Three Paralogous Members of the Mammalian Vaccinia Related Kinase Family. *Journal of Biological Chemistry*, 279(9):7934–7946.

Nishita, M., Aizawa, H., and Mizuno, K. (2002). Stromal cell-derived factor 1alpha activates LIM kinase 1 and induces cofilin phosphorylation for T-cell chemotaxis. *Molecular and cellular biology*, 22(3):774–83.

Nishita, M., Tomizawa, C., Yamamoto, M., Horita, Y., Ohashi, K., and Mizuno, K. (2005). Spatial and temporal regulation of cofilin activity by LIM kinase and Slingshot is critical for directional cell migration. *Journal of Cell Biology*, 171(2):349–359.

Oom, A. L., Humphries, B. A., and Yang, C. (2014). MicroRNAs: Novel players in cancer diagnosis and therapies. *BioMed Research International*, 2014.

Paepe, P. D. and Wolf-Peeters, C. D. (2007). Diffuse large B-cell lymphoma: a heterogeneous group of non-Hodgkin lymphomas comprising several distinct clinicopathological entities. *Leukemia*, 21(1):37–43.

Pan, W., Wang, H., Jianwei, R., and Ye, Z. (2014). MicroRNA-27a promotes proliferation, migration and invasion by targeting MAP2K4 in human osteosarcoma cells. *Cellular physiology and biochemistry : international journal of experimental cellular physiology, biochemistry, and pharmacology*, 33(2):402–12.

Panagopoulos, I., Fioretos, T., Isaksson, M., Samuelsson, U., Billström, R., Strömbeck, B., Mitelman, F., and Johansson, B. (2001). Fusion of the MORF and CBP genes in acute myeloid leukemia with the t(10;16)(q22;p13). *Human molecular genetics*, 10(4):395–404.

Park, C. W., Zeng, Y., Zhang, X., Subramanian, S., and Steer, C. J. (2010). Mature microRNAs identified in highly purified nuclei from HCT116 colon cancer cells. *RNA biology*, 7(5):606–14.

Pascual, B. V., Liu, Y.-j., Magalski, A., Bouteiller, O. D., Banchereau, J., and Capra, J. D. (1994). Analysis of Somatic Mutation in Five B Cell Subsets of Human Tonsil. *Methods*, 180(July).

Pasqualucci, L., Bhagat, G., Jankovic, M., Compagno, M., Smith, P., Muramatsu, M., Honjo, T., Morse, H. C., Nussenzweig, M. C., and Dalla-Favera, R. (2008). AID is required for germinal center-derived lymphomagenesis. *Nature genetics*, 40(1):108–112.

Pasqualucci, L. and Dalla-Favera, R. (2014). SnapShot: Diffuse large B cell lymphoma. *Cancer Cell*, 25(1):132–132.e1.

Pasquinelli, a. E., Reinhart, B. J., Slack, F., Martindale, M. Q., Kuroda, M. I., Maller, B., Hayward, D. C., Ball, E. E., Degnan, B., Müller, P., Spring, J., Srinivasan, a., Fishman, M., Finnerty, J., Corbo, J., Levine, M., Leahy, P., Davidson, E., and Ruvkun, G. (2000). Conservation of the sequence and temporal expression of let-7 heterochronic regulatory RNA. *Nature*, 408(6808):86–89.

Pedersen, I. M., Otero, D., Kao, E., Miletic, A. V., Hother, C., Ralfkiaer, E., Rickert, R. C., Gronbaek, K., and David, M. (2009). Onco-miR-155 targets SHIP1 to promote TNFalpha-dependent growth of B cell lymphomas. *EMBO Molecular Medicine*, 1(5):288–295.

Peters, T. L., Li, L., Tula-Sanchez, A. A., Pongtornpipat, P., Schatz, J. H., Peters, T. L., Li, L., Tula-Sanchez, A. A., Pongtornpipat, P., and Schatz, J. H. (2016). Control of translational activation by PIM kinase in activated B-cell diffuse large B-cell lymphoma confers sensitivity to inhibition by PIM447. *Oncotarget*, 5(0).

Petersen, C. P., Bordeleau, M. E., Pelletier, J., and Sharp, P. A. (2006). Short RNAs repress translation after initiation in mammalian cells. *Molecular Cell*, 21(4):533–542.

Pfeifer, M., Grau, M., Lenze, D., Wenzel, S.-S., Wolf, A., Wollert-Wulf, B., Dietze, K., Nogai, H., Storek, B., Madle, H., Dörken, B., Janz, M., Dirnhofer, S., Lenz, P., Hummel, M., Tzankov, A., and Lenz, G. (2013). PTEN loss defines a PI3K/AKT pathway-dependent germinal center subtype of diffuse large B-cell lymphoma. *Proceedings of the National Academy of Sciences of the United States of America*, 110(30):12420–5.

Pham, L. V., Tamayo, A. T., Yoshimura, L. C., Lo, P., Terry, N., Reid, P. S., and Ford, R. J. (2002). A CD40 Signalosome anchored in lipid rafts leads to constitutive activation of NF-kB and autonomous cell growth in B cell lymphomas. *Immunity*, 16(1):37–50.

Pirkl, M., Hand, E., Kube, D., and Spang, R. (2015). Analyzing synergistic and non-synergistic interactions in signalling pathways using Boolean Nested Effect Models. *Bioinformatics (Oxford, England)*, 32(November 2015):893–900.

Plotnik, J. P., Budka, J. A., Ferris, M. W., and Hollenhorst, P. C. (2014). ETS1 is a genome-wide effector of RAS/ERK signaling in epithelial cells. *Nucleic Acids Research*, 42(19):11928–11940.

Plotnikov, A., Zehorai, E., Procaccia, S., and Seger, R. (2011). The MAPK cascades: Signaling components, nuclear roles and mechanisms of nuclear translocation. *Biochimica et Biophysica Acta - Molecular Cell Research*, 1813(9):1619–1633.

Polack, A., Hortnagel, K., Pajic, A., Christoph, B., Baier, B., Falk, M., Mautnert, J., Geltinger, C., and G.W. BORNKAMM, B. K. (1996). c-myc activation renders proliferation of Epstein-Barr virus (EBV)-transformed cells independent of EBV nuclear antigen 2 and latent membrane protein 1. *Proc. Natl. Acad. Sci. USA*, 93(September):10411–10416.

Pombo, A. and Dillon, N. (2015). Three-dimensional genome architecture: players and mechanisms. *Nature reviews. Molecular cell biology*, 16(4):245–257.

Quentmeier, H., Amini, R. M., Berglund, M., Dirks, W. G., Ehrentraut, S., Geffers, R., Macleod, R. a. F., Nagel, S., Romani, J., Scherr, M., Zaborski, M., and Drexler, H. G. (2013). U-2932: two clones in one cell line, a tool for the study of clonal evolution. *Leukemia*, 27(5):1155–64.

Rai, D., Kim, S.-W., McKeller, M. R., Dahia, P. L. M., and Aguiar, R. C. T. (2010). Targeting of SMAD5 links microRNA-155 to the TGF-beta pathway and lymphomagenesis. *Proceedings of the National Academy of Sciences of the United States of America*, 107(7):3111–6.

Raman, M., Chen, W., and Cobb, M. H. (2007). Differential regulation and properties of MAPKs. *Oncogene*, 26(22):3100–3112.

Rathore, M. G., Saumet, A., Rossi, J.-F., de Bettignies, C., Tempé, D., Lecellier, C.-H., and Villalba, M. (2012). The NF-κB member p65 controls glutamine metabolism through miR-23a. *The international journal of biochemistry & cell biology*, 44(9):1448–56.

Raut, L. S. and Chakrabarti, P. P. (2014). Management of relapsed-refractory diffuse large B cell lymphoma. *South Asian journal of cancer*, 3(1):66–70.

Reed, D. (1902). On the Pathological Changes in Hodgkin's Disease, with Special Reference to its Relation to Tuberculosis. *The John Hopkins Press*.

Reinhart, B. J., Slack, F. J., Basson, M., Pasquinelli, a. E., Bettinger, J. C., Rougvie, a. E., Horvitz, H. R., and Ruvkun, G. (2000). The 21-nucleotide let-7 RNA regulates developmental timing in Caenorhabditis elegans. *Nature*, 403(6772):901–906.

Renart, J., Reiser, J., and Stark, G. R. (1979). Transfer of proteins from gels to diazobenzyloxymethyl-paper and detection with antisera: a method for studying antibody specificity and antigen structure. *Proceedings of the National Academy of Sciences of the United States of America*, 76(7):3116–20.

Richter, J., Schlesner, M., Hoffmann, S., Kreuz, M., Leich, E., Burkhardt, B., Rosolowski, M., Ammerpohl, O., Wagener, R., Bernhart, S. H., Lenze, D., Szczepanowski, M., Paulsen, M., Lipinski, S., Russell, R. B., Adam-Klages, S., Apic, G., Claviez, A., Hasenclever, D., Hovestadt, V., Hornig, N., Korbel, J. O., Kube, D., Langenberger, D., Lawerenz, C., Lisfeld, J., Meyer, K., Picelli, S., Pischimarov, J., Radlwimmer, B., Rausch, T., Rohde, M., Schilhabel, M., Scholtysik, R., Spang, R., Trautmann, H., Zenz, T., Borkhardt, A., Drexler, H. G., Möller, P., MacLeod, R. a. F., Pott, C., Schreiber, S., Trümper, L., Loeffler, M., Stadler, P. F., Lichter, P., Eils, R., Küppers, R., Hummel, M., Klapper, W., Rosenstiel, P., Rosenwald, A., Brors, B., Siebert, R., and Project, F. T. I. M.-S. (2012). Recurrent mutation of the ID3 gene in Burkitt lymphoma identified by integrated genome, exome and transcriptome sequencing. *Nature Genetics*, 44(12):1316–1320.

Rio, D. C., Clark, S. G., Tjian, R., Science, S., Series, N., and Jan, N. (2015). A Mammalian Host-Vector System that Regulates Expression and Amplification of Transfected Genes by Temperature Induction. *Science (New York, N.Y.)*, 227(4682):23–28.

Roberts, T. C. (2014). The MicroRNA Biology of the Mammalian Nucleus. *Molecular therapy. Nucleic acids*, 3(August):e188.

Roehle, A., Hoefig, K. P., Repsilber, D., Thorns, C., Ziepert, M., Wesche, K. O., Thiere, M., Loeffler, M., Klapper, W., Pfreundschuh, M., Matolcsy, A., Bernd, H.-W., Reiniger, L., Merz, H., and Feller, A. C. (2008). MicroRNA signatures characterize diffuse large B-cell lymphomas and follicular lymphomas. *British journal of haematology*, 142(5):732–44.

Rosenwald, A., Wright, G., et al Chan, W., WC, C., and Al., E. (2002). The use of molecular profiling to predict survival after chemotherapy for diffuse large B-cell lymphoma. *New England Journal of Medicine*, 346(25):1937–1947.

Rossi, D. and Gaidano, G. (2009). Richter syndrome: molecular insights and clinical perspectives. *Hematological oncology*, 27:1–10.

Rottiers, V. and Näär, A. M. (2012). MicroRNAs in metabolism and metabolic disorders. *Nature reviews. Molecular cell biology*, 13(4):239–50.

Roufayel, R., Johnston, D. S., and Mosser, D. D. (2014). The elimination of miR-23a in heat-stressed cells promotes NOXA-induced cell death and is prevented by HSP70. *Cell Death and Disease*, 5(11):e1546.

Rui, L., Schmitz, R., Ceribelli, M., and Staudt, L. M. (2011). Malignant pirates of the immune system. *Nature Immunology*, 12(10):933–940.

Sabirzhanov, B., Zhao, Z., Stoica, B. a., Loane, D. J., Wu, J., Borroto, C., Dorsey, S. G., and Faden, a. I. (2014). Downregulation of miR-23a and miR-27a following Experimental Traumatic Brain Injury Induces Neuronal Cell Death through Activation of Proapoptotic Bcl-2 Proteins. *Journal of Neuroscience*, 34(30):10055–10071.

Sacedon, R., Diez, B., Nunez, V., Hernandez-Lopez, C., Gutierrez-Frias, C., Cejalvo, T., Outram, S. V., Crompton, T., Zapata, A. G., Vicente, A., and Varas, A. (2005). Sonic Hedgehog Is Produced by Follicular Dendritic Cells and Protects Germinal Center B Cells from Apoptosis. *The Journal of Immunology*, 174(3):1456–1461.

Saito, M., Gao, J., Basso, K., Kitagawa, Y., Smith, P. M., Bhagat, G., Pernis, A., Pasqualucci, L., and Dalla-Favera, R. (2007). A Signaling Pathway Mediating Downregulation of BCL6 in Germinal Center B Cells Is Blocked by BCL6 Gene Alterations in B Cell Lymphoma. *Cancer Cell*, 12(3):280–292.

Saumet, A., Vetter, G., Bouttier, M., Portales-Casamar, E., Wasserman, W. W., Maurin, T., Mari, B., Barbry, P., Vallar, L., Friederich, E., Arar, K., Cassinat, B., Chomienne, C., and Lecellier, C.-H. (2009). Transcriptional repression of microRNA genes by PML-RARA increases expression of key cancer proteins in acute promyelocytic leukemia. *Blood*, 113(2):412–21.

Scadden, A. D. J. (2005). The RISC subunit Tudor-SN binds to hyper-edited double-stranded RNA and promotes its cleavage. *Nature Structural & Molecular Biology*, 12(6):489–496.

Schmitz, R., Young, R. M., Ceribelli, M., Jhavar, S., Liu, X., Powell, J., Yang, Y., Xu, W., Zhao, H., Kohlhammer, H., Rosenwald, A., Kluin, P., Müller-hermelink, H. K., Ott, G., Gascoyne, D., Connors, J. M., Rimsza, L. M., Campo, E., Jaffe, E. S., Smeland, E. B., Ogwang, M. D., Reynolds, S. J., and Richard, I. (2013). Burkitt Lymphoma Pathogenesis and Therapeutic Targets from Structural and Functional Genomics. *Nature*, 490(7418):116–120.

Schrader, A., Meyer, K., von Bonin, F., Vockerodt, M., Walther, N., Hand, E., Ulrich, A., Matulewicz, K., Lenze, D., Hummel, M., Kieser, A., Engelke, M., Trümper, L., and Kube, D. (2012). Global gene expression changes of in vitro stimulated human transformed germinal centre B cells as surrogate for oncogenic pathway activation in individual aggressive B cell lymphomas. *Cell communication and signaling : CCS*, 10(1):43.

Schreiber, E., Matthias, P., Miiller, M. M., and Schaffner, W. (1989). Rapid detection of octamer binding proteins with mmini-extracts", prepared from a small number of cells. 17(15):6419.

Sears, R., Nuckolls, F., Haura, E., Taya, Y., Tamai, K., and Nevins, J. R. (2000). Multiple Ras-dependent phosphorylation pathways regulate Myc protein stability. *Genes and Development*, 14(19):2501–2514.

Seda, V. and Mraz, M. (2015). B-cell receptor signalling and its crosstalk with other pathways in normal and malignant cells. *European Journal of Haematology*, 94(3):193–205.

Sehn, L. H. and Gascoyne, R. D. (2015). Diffuse large B-cell lymphoma: optimizing outcome in the context of clinical and biologic heterogeneity. *Blood*, 125(1):22–32.

Seifert, M., Scholtysik, R., and Küppers, R. (2013). Origin and Pathogenesis of B Cell Lymphomas. 971(D).

Sexton, T. and Cavalli, G. (2015). The role of chromosome domains in shaping the functional genome. *Cell*, 160(6):1049–1059.

Shaffer III, A. L., Young, R. M., and Staudt, L. M. (2011). Pathogenesis of Human B Cell Lymphomas. *Annual Review of Immunology*, 30(December 2011):565–610.

Shamas-Din, A., Brahmbhatt, H., Leber, B., and Andrews, D. W. (2011). BH3-only proteins: Orchestrators of apoptosis. *Biochimica et Biophysica Acta - Molecular Cell Research*, 1813(4):508–520.

Shan, D., Ledbetter, J. a., and Press, O. W. (2000). Signaling events involved in anti-CD20-induced apoptosis of malignant human B cells. *Cancer immunology, immunotherapy*, 48(12):673–83.

Shaulian, E. and Karin, M. (2001). AP-1 in cell proliferation and survival. *Oncogene*, 20(19):2390–2400.

Shulman, Z., Gitlin, A. D., Weinstein, J. S., Lainez, B., Esplugues, E., Flavell, R. A., Craft, J. E., and Nussenzweig, M. C. (2014). Dynamic signaling by T follicular helper cells during germinal center B cell selection. *Science (New York, N.Y.)*, 345(6200):1058–1062.

Siomi, H. and Siomi, M. C. (2008). Characterization of endogenous human Argonautes and their miRNA partners in RNA silencing. *Proceedings of the National Academy of Sciences of the United States of America*, 105(23):7964–9.

Siomi, H. and Siomi, M. C. (2010). Posttranscriptional Regulation of MicroRNA Biogenesis in Animals. *Molecular Cell*, 38(3):323–332.

Sneeringer, C. J., Scott, M. P., Kuntz, K. W., Knutson, S. K., Pollock, R. M., Richon, V. M., and Copeland, R. A. (2010). Coordinated activities of wild-type plus mutant EZH2 drive tumor-associated hypertrimethylation of lysine 27 on histone H3 (H3K27) in human B-cell lymphomas. *Proceedings of the National Academy of Sciences of the United States of America*, 107(49):20980–5.

Stein, H. and Hummel, M. (2007). Burkitt's and Burkitt-like lymphoma. Molecular definition and value of the World Health Organisation's diagnostic criteria. *Der Pathologe*, 28(1):41–5.

Sternberg, C. (1897). Über eine eigenartige, unter dem Bilde der Pseudoleukämie verlaufende Tuberkulose des lymphat. Apparates. *Zeitschrift für Heilkunde*.

Swerdlow, S. H., Campo, E., Pileri, S. A., Harris, N. L., Stein, H., Siebert, R., Advani, R., Ghielmini, M., Salles, G. A., Zelenetz, A. D., and Jaffe, E. S. (2016). The 2016 revision of the World Health Organization (WHO) classification of lymphoid neoplasms. *Blood*, 127(20):blood–2016–01–643569.

Takada, H. and Kurisaki, A. (2015). Emerging roles of nucleolar and ribosomal proteins in cancer, development, and aging. *Cellular and Molecular Life Sciences*, 72(21):4015–4025.

Tamaru, J., Hummel, M., Marafioti, T., Kalvelage, B., Leoncini, L., Minacci, C., Tosi, P., Wright, D., and Stein, H. (1995). Burkitt's lymphomas express VH genes with a moderate number of antigen-selected somatic mutations. *The American journal of pathology*, 147(5):1398–1407.

Tan, L. P., Wang, M., Robertus, J.-L., Schakel, R. N., Gibcus, J. H., Diepstra, A., Harms, G., Peh, S.-C., Reijmers, R. M., Pals, S. T., Kroesen, B.-J., Kluin, P. M., Poppema, S., and van den Berg, A. (2009). miRNA profiling of B-cell subsets: specific miRNA profile for germinal center B cells with variation

between centroblasts and centrocytes. *Laboratory investigation; a journal of technical methods and pathology*, 89(6):708–16.

Tee, W. W., Shen, S. S., Oksuz, O., Narendra, V., and Reinberg, D. (2014). Erk1/2 activity promotes chromatin features and RNAPII phosphorylation at developmental promoters in mouse ESCs. *Cell*, 156(4):678–690.

Teng, G., Hakimpour, P., Landgraf, P., Rice, A., Tuschl, T., Casellas, R., and Papavasiliou, F. N. (2008). MicroRNA-155 Is a Negative Regulator of Activation-Induced Cytidine Deaminase. *Immunity*, 28(5):621–629.

Testoni, M., Chung, E. Y. L., Priebe, V., and Bertoni, F. (2015). The transcription factor ETS1 in lymphomas: friend or foe? *Leukemia & Lymphoma*, (October 2014):1–6.

Thapa, D. R., Li, X., Jamieson, B. D., and Martínez-Maza, O. (2011). Overexpression of microRNAs from the miR-17-92 paralog clusters in AIDS-related non-Hodgkin's lymphomas. *PloS one*, 6(6):e20781.

Thomson, D. W., Bracken, C. P., and Goodall, G. J. (2011). Experimental strategies for microRNA target identification. *Nucleic acids research*, 39(16):6845–53.

Tirián, L., Hlavanda, E., Oláh, J., Horváth, I., Orosz, F., Szabó, B., Kovács, J., Szabad, J., and Ovádi, J. (2003). TPPP/p25 promotes tubulin assemblies and blocks mitotic spindle formation. *Proceedings of the National Academy of Sciences of the United States of America*, 100(24):13976–81.

Tomiyoshi, G., Horita, Y., Nishita, M., Ohashi, K., and Mizuno, K. (2004). Caspase-mediated cleavage and activation of LIM-kinase 1 and its role in apoptotic membrane blebbing. *Genes to Cells*, 9:591–600.

Torlakovic, E., Malecka, A., Myklebust, J. H., Tierens, A., Aasheim, H. C., Nesland, J. M., Smeland, E., Kvaløy, S., and Delabie, J. (2005). PU.1 protein expression has a positive linear association with protein expression of germinal centre B cell genes including BCL-6, CD10, CD20 and CD22: Identification of PU.1 putative binding sites in the BCL-6 promotor. *Journal of Pathology*, 206(3):312–319.

Torre, L. A., Bray, F., Siegel, R. L., Ferlay, J., Lortet-tieulent, J., and Jemal, A. (2015). Global Cancer Statistics, 2012. *CA: a cancer journal of clinicians.*, 65(2):87–108.

Towbin, H., Staehelin, T., and Gordon, J. (1979). Electrophoretic transfer of proteins from polyacrylamide gels to nitrocellulose sheets: procedure and some applications. *Proceedings of the National Academy of Sciences of the United States of America*, 76(9):4350–4.

Tweeddale, M., Lim, B., Robinson, J., Jamal, N., Minden, D. M., Zalcberg, J., Lockwood, G., and Messner, H. A. (1987). The Presence of Clonogenic. *Blood*, pages 1307–1315.

Ueda, K., Arakawa, H., and Nakamura, Y. (2003). Dual-specificity phosphatase 5 (DUSP5) as a direct transcriptional target of tumor suppressor p53. *Oncogene*, 22(36):5586–91.

Ueda, Y., Hirai, S. I., Osada, S. I., Suzuki, A., Mizuno, K., and Ohno, S. (1996). Protein kinase C gamma activates the MEK-ERK pathway in a manner independent of Ras and dependent on Raf. *Journal of Biological Chemistry*, 271(38):23512–23519.

Vallabhapurapu, S. and Karin, M. (2009). Regulation and function of NF-kappaB transcription factors in the immune system. *Annual review of immunology*, 27:693–733.

van Rooij, E. (2011). The art of microRNA research. *Circulation research*, 108(2):219–34.

Vaqué, J. P., Martínez, N., Batlle-López, A., Pérez, C., Montes-Moreno, S., Sánchez-Beato, M., and Piris, M. A. (2014). B-cell lymphoma mutations: Improving diagnostics and enabling targeted therapies. *Haematologica*, 99(2):222–231.

Vigorito, E., Perks, K. L., Abreu-Goodger, C., Bunting, S., Xiang, Z., Kohlhaas, S., Das, P. P., Miska, E. A., Rodriguez, A., Bradley, A., Smith, K. G. C., Rada, C., Enright, A. J., Toellner, K. M., MacLennan, I. C. M., and Turner, M. (2007). microRNA-155 Regulates the Generation of Immunoglobulin Class-Switched Plasma Cells. *Immunity*, 27(6):847–859.

Wan, L., Zhang, L., Fan, K., and Wang, J. (2014). MiR-27b targets LIMK1 to inhibit growth and invasion of NSCLC cells. *Molecular and Cellular Biochemistry*, 390(1-2):85–91.

Wang, W.-l., Yang, C., Han, X.-l., Wang, R., Huang, Y., Zi, Y.-m., and Li, J.-d. (2014). MicroRNA-23a expression in paraffin-embedded specimen correlates with overall survival of diffuse large B-cell lymphoma. *Medical oncology (Northwood, London, England)*, 31(4):919.

Wang, Y., Li, X., and Hu, H. (2011). Transcriptional regulation of co-expressed microRNA target genes. *Genomics*, 98(6):445–452.

Whitmarsh, A. J. and Davis, R. J. (1996). Transcription factor AP-1 regulation by mitogen-activated protein kinase signal transduction pathways.

Xie, P., Hostager, B. S., Munroe, M. E., Moore, C. R., and Bishop, G. a. (2006). Cooperation between TNF Receptor-Associated Factors 1 and 2 in CD40 Signaling. *The Journal of Immunology*, 176(9):5388–5400.

Yoon, S. and Seger, R. (2006). The extracellular signal-regulated kinase: Multiple substrates regulate diverse cellular functions. *Growth Factors*, 24(1):21–44.

Young, M. D., Wakefield, M. J., Smyth, G. K., and Oshlack, A. (2010). Gene ontology analysis for RNA-seq: accounting for selection bias. *Genome biology*, 11(2):R14.

Young, R. M. and Staudt, L. M. (2013). Targeting pathological B cell receptor signalling in lymphoid malignancies. *Nat Rev Drug Discov*, 12(3):229–243.

Young, R. M., Wu, T., Schmitz, R., Dawood, M., Xiao, W., Phelan, J. D., Xu, W., Menard, L., Meffre, E., Chan, W.-C. C., Jaffe, E. S., Gascoyne, R. D., Campo, E., Rosenwald, A., Ott, G., Delabie, J., Rimsza, L. M., and Staudt, L. M. (2015). Survival of human lymphoma cells requires B-cell receptor engagement by self-antigens. *Proceedings of the National Academy of Sciences*, 112(44):201514944.

Yu, J., Wang, F., Yang, G.-H., Wang, F.-L., Ma, Y.-N., Du, Z.-W., and Zhang, J.-W. (2006). Human microRNA clusters: genomic organization and expression profile in leukemia cell lines. *Biochemical and biophysical research communications*, 349(1):59–68.

Zebda, N., Bernard, O., Bailly, M., Welti, S., Lawrence, D. S., and Condeelis, J. S. (2000). at the Leading Edge and Subsequent Lamellipod Extension. *Cell*, 151(5).

Zhang, H., Li, M., Han, Y., Hong, L., Gong, T., Sun, L., and Zheng, X. (2010). Down-regulation of miR-27a might reverse multidrug resistance of esophageal squamous cell carcinoma. *Digestive Diseases and Sciences*, 55(9):2545–2551.

Zhang, J., Jima, D. D., Jacobs, C., Fischer, R., Gottwein, E., Huang, G., Lugar, P. L., Lagoo, A. S., Rizzieri, D. a., Friedman, D. R., Weinberg, J. B., Lipsky, P. E., and Dave, S. S. (2009). Patterns of microRNA expression characterize stages of human B-cell differentiation. *Blood*, 113(19):4586–94.

Zhang, L., Yang, C.-S., Varelas, X., and Monti, S. (2016). Altered RNA editing in 3' UTR perturbs microRNA-mediated regulation of oncogenes and tumor-suppressors. *Scientific reports*, 6(November 2015):23226.

A.Supplementals
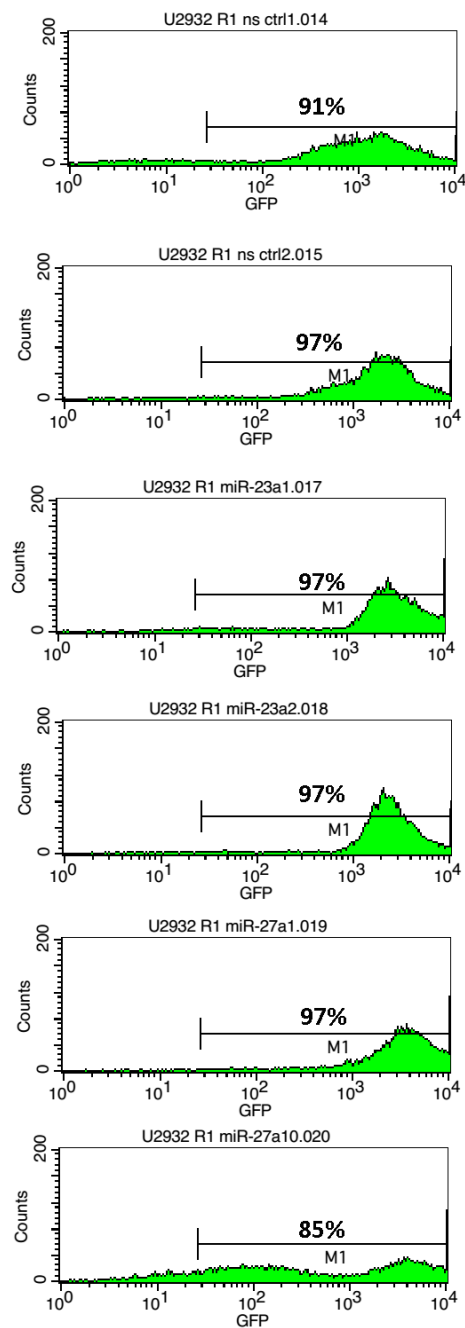
Figure A.1.: GFP expression profile of U2932 R1 pGIPZ clones
FACS analyses of GFP expression profile of stable transduced U2932 R1 pGIPZ clones. 10000 counts were measured. Cells were gated to the living, PI negative population. Percentage of living green M1 population cells are depicted.
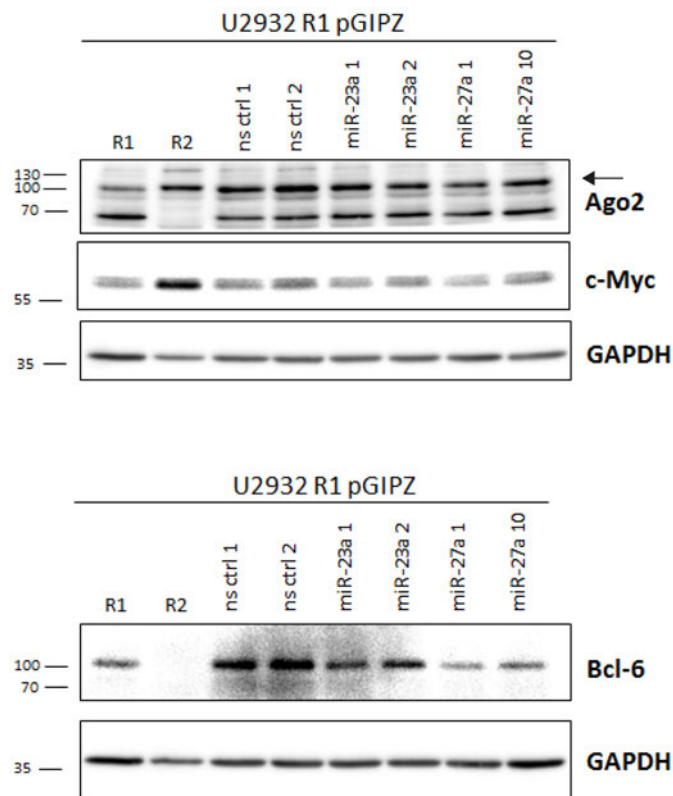
Figure A.2.: Western blot characterization of U2932 R1 pGIPZ clones
Expression of Ago2, c-MYC and Bcl-6 in U2932 R1 pGIPZ miR-23a/-27a and ns ctrl overexpressing clones compared to the parental clone U2932 R1 and sister clone U2932 R2. (20 µg total protein per well, one representative blot of three is shown)
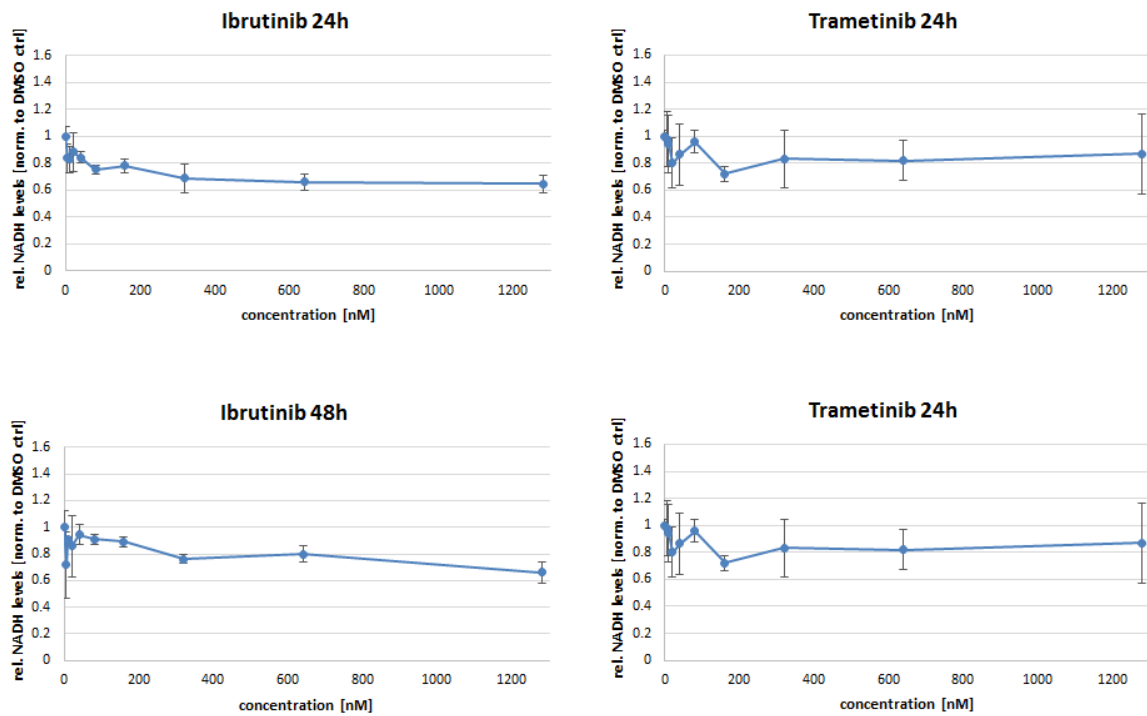
Figure A.3.: MTT Assay for U2932 R1 upon Ibrutinib and Trametinib treatment
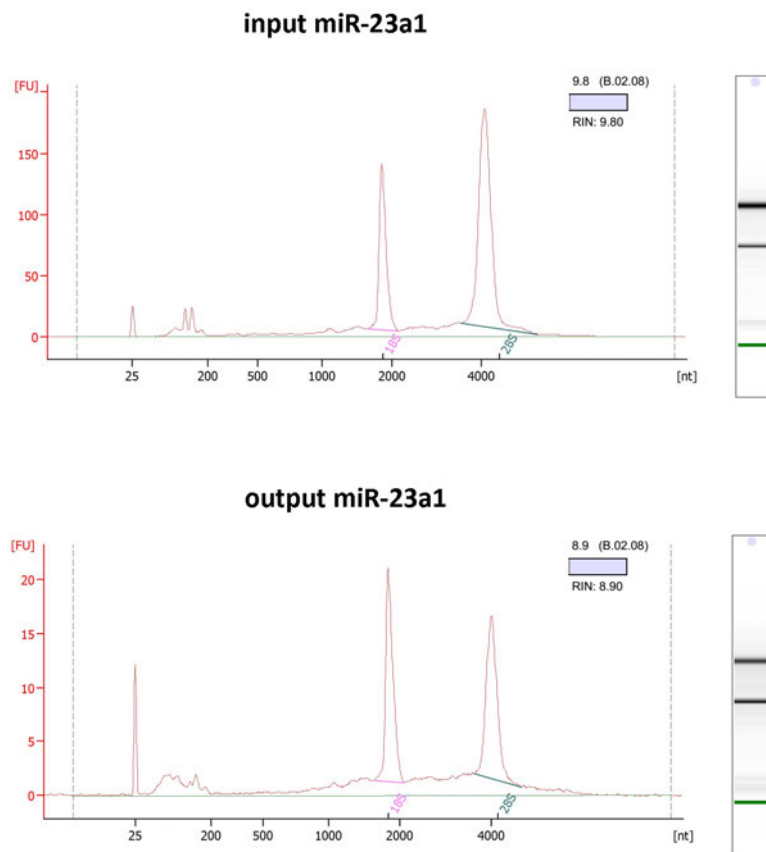
U2932 R1 was treated with inhibitor dilution series for 24h and 48h and cell viability was assesed using MTT assay. Trametinib: 12800 - 50 nM; Ibrutinib 1280 - 5 nM; 0 nM = DMSO ctrl


Figure A.4.: High quality of total RNA after Ago-RIP

Bioanalyzer total RNA Chip analyzes for quality control of Ago2-RIP input and output samples of U2932 R1 miR-23a1. The 25 nt peak represents the marker. In both samples the 18S and 28S RNA peaks are clear and distinct. No RNA degradation could be observed. The RNA Integrity Numbers (RIN) indicate high RNA quality.

Table A.1.: Differentially expressed genes of miR-23a1/ns crtl1 vs. miR-27a1/ns ctrl1

Gene ID	Gene name	Description
ENSG00000207980	**MIR23A**	microRNA 23a
ENSG00000111052	**LIN7A**	lin-7 homolog A (C. elegans)
ENSG00000163618	**CADPS**	Ca++-dependent secretion activator
ENSG00000166503	**HDGFRP3**	Hepatoma-derived growth factor-related protein 3
ENSG00000146938	**NLGN4X**	neuroligin 4, X-linked
ENSG00000196482	**ESRRG**	estrogen-related receptor gamma
ENSG00000113140	**SPARC**	secreted protein, acidic, cysteine-rich (osteonectin)
ENSG00000253941	**IGHVII-51-2**	immunoglobulin heavy variable (II)-51-2 (pseudogene)
ENSG00000128641	**MYO1B**	myosin IB
ENSG00000179455	**MKRN3**	makorin ring finger protein 3
ENSG00000169862	**CTNND2**	catenin (cadherin-associated protein), delta 2
ENSG00000254167	**IGHVIII-51-1**	immunoglobulin heavy variable (III)-51-1 (pseudogene)
ENSG00000151623	**NR3C2**	nuclear receptor subfamily 3, group C, member 2
ENSG00000164362	**TERT**	telomerase reverse transcriptase
ENSG00000100385	**IL2RB**	interleukin 2 receptor, beta
ENSG00000168672	**FAM84B**	family with sequence similarity 84, member B
ENSG00000057657	**PRDM1**	PR domain containing 1, with ZNF domain
ENSG00000184635	**ZNF93**	zinc finger protein 93
ENSG00000111249	**CUX2**	cut-like homeobox 2
ENSG00000203706	**SERTAD4-AS1**	SERTAD4 antisense RNA 1
ENSG00000185668	**POU3F1**	POU class 3 homeobox 1
ENSG00000124491	**F13A1**	coagulation factor XIII, A1 polypeptide
ENSG00000048740	**CELF2**	CUGBP, Elav-like family member 2
ENSG00000213967	**ZNF726**	zinc finger protein 726
ENSG00000126353	**CCR7**	chemokine (C-C motif) receptor 7
ENSG00000076356	**PLXNA2**	plexin A2
ENSG00000188868	**ZNF563**	zinc finger protein 563
ENSG00000207827	**MIR30A**	microRNA 30a
ENSG00000182253	**SYNM**	synemin, intermediate filament protein
ENSG00000213626	**LBH**	limb bud and heart development
ENSG00000105974	**CAV1**	caveolin 1, caveolae protein, 22kDa
ENSG00000171291	**ZNF439**	zinc finger protein 439
ENSG00000163590	**PPM1L**	protein phosphatase, Mg2+/Mn2+ dependent, 1L
ENSG00000198369	**SPRED2**	sprouty-related, EVH1 domain containing 2
ENSG00000156535	**CD109**	CD109 molecule
ENSG00000137285	**TUBB2B**	tubulin, beta 2B class IIb
ENSG00000114790	**ARHGEF26**	Rho guanine nucleotide exchange factor (GEF) 26
ENSG00000173083	**HPSE**	heparanase
ENSG00000064692	**SNCAIP**	synuclein, alpha interacting protein
ENSG00000148600	**CDHR1**	cadherin-related family member 1
ENSG00000124785	**NRN1**	neuritin 1
ENSG00000183813	**CCR4**	chemokine (C-C motif) receptor 4
ENSG00000173198	**CYSLTR1**	cysteinyl leukotriene receptor 1
ENSG00000118985	**ELL2**	elongation factor, RNA polymerase II, 2
ENSG00000119138	**KLF9**	Kruppel-like factor 9
ENSG00000163518	**FCRL4**	Fc receptor-like 4
ENSG00000105997	**HOXA3**	homeobox A3
ENSG00000249679	**RP11-279O9.4**	
ENSG00000106004	**HOXA5**	homeobox A5
ENSG00000081818	**PCDHB4**	protocadherin beta 4
ENSG00000150593	**PDCD4**	programmed cell death 4 (neoplastic transformation inhibitor)
ENSG00000005513	**SOX8**	SRY (sex determining region Y)-box 8
ENSG00000248905	**FMN1**	formin 1
ENSG00000160050	**CCDC28B**	coiled-coil domain containing 28B
ENSG00000235159	**RP6-109B7.4**	

Continued on next page

Gene ID	Gene name	Description
ENSG00000159618	**GPR114**	G protein-coupled receptor 114
ENSG00000186026	**ZNF284**	zinc finger protein 284
ENSG00000196664	**TLR7**	toll-like receptor 7
ENSG00000142178	**SIK1**	salt-inducible kinase 1
ENSG00000072694	**FCGR2B**	Fc fragment of IgG, low affinity IIb, receptor (CD32)
ENSG00000121742	**GJB6**	gap junction protein, beta 6, 30kDa
ENSG00000164484	**TMEM200A**	transmembrane protein 200A
ENSG00000072110	**ACTN1**	actinin, alpha 1
ENSG00000188596	**CFAP54**	cilia and flagella associated 54
ENSG00000158715	**SLC45A3**	solute carrier family 45, member 3
ENSG00000124942	**AHNAK**	AHNAK nucleoprotein
ENSG00000078900	**TP73**	tumor protein p73
ENSG00000164695	**CHMP4C**	charged multivesicular body protein 4C
ENSG00000179431	**FJX1**	four jointed box 1 (Drosophila)
ENSG00000187676	**B3GALTL**	beta 1,3-galactosyltransferase-like
ENSG00000224565	**RP1-148H17.1**	
ENSG00000184702	**SEPT5**	septin 5
ENSG00000177628	**GBA**	glucosidase, beta, acid
ENSG00000115297	**TLX2**	T-cell leukemia homeobox 2
ENSG00000135631	**RAB11FIP5**	RAB11 family interacting protein 5 (class I)
ENSG00000082497	**SERTAD4**	SERTA domain containing 4
ENSG00000138760	**SCARB2**	scavenger receptor class B, member 2
ENSG00000260022	**LA16c-306A4.1**	
ENSG00000124813	**RUNX2**	runt-related transcription factor 2
ENSG00000238287	**RP11-656D10.3**	
ENSG00000134986	**NREP**	neuronal regeneration related protein
ENSG00000249004	**PRMT5P1**	protein arginine methyltransferase 5 pseudogene 1
ENSG00000118515	**SGK1**	serum/glucocorticoid regulated kinase 1
ENSG00000121753	**BAI2**	brain-specific angiogenesis inhibitor 2
ENSG00000204954	**C12orf73**	chromosome 12 open reading frame 73
ENSG00000158792	**SPATA2L**	spermatogenesis associated 2-like
ENSG00000189171	**S100A13**	S100 calcium binding protein A13
ENSG00000075420	**FNDC3B**	fibronectin type III domain containing 3B
ENSG00000151150	**ANK3**	ankyrin 3, node of Ranvier (ankyrin G)
ENSG00000176771	**NCKAP5**	NCK-associated protein 5
ENSG00000003147	**ICA1**	islet cell autoantigen 1, 69kDa
ENSG00000225724	**LL22NC03-80A10.11**	
ENSG00000273619	**RP5-908M14.9**	
ENSG00000069702	**TGFBR3**	transforming growth factor, beta receptor III
ENSG00000071051	**NCK2**	NCK adaptor protein 2
ENSG00000136929	**HEMGN**	hemogen
ENSG00000246095	**LINC01096**	long intergenic non-protein coding RNA 1096
ENSG00000140931	**CMTM3**	CKLF-like MARVEL transmembrane domain containing 3
ENSG00000182175	**RGMA**	repulsive guidance molecule family member a
ENSG00000185792	**NLRP9**	NLR family, pyrin domain containing 9
ENSG00000137266	**SLC22A23**	solute carrier family 22, member 23
ENSG00000064393	**HIPK2**	homeodomain interacting protein kinase 2
ENSG00000175741	**RWDD4P2**	RWD domain containing 4 pseudogene 2
ENSG00000177494	**ZBED2**	zinc finger, BED-type containing 2
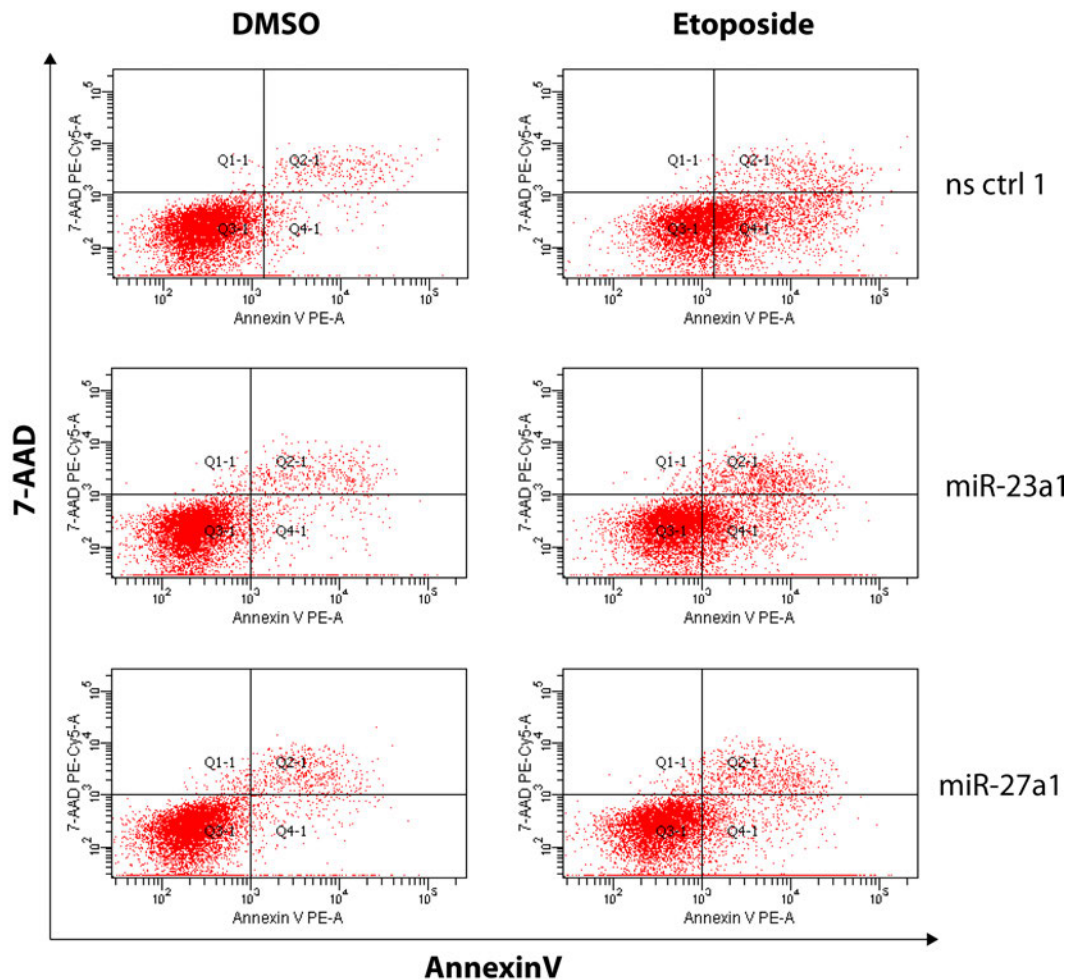
Figure A.5.: FACS analysis of AnnexinV/7AAD staining of U2932 R1 clones upon etoposide treatment

U2932 R1 pGIPZ cell lines overexprssing a non silencing control, miR-23a or miR-27a were treated for 16h with 100 µM etoposide to induce apoptosis. Cells were double stained with AnnexinV-PE and 7AAD prior to FACS analysis. (one representative experiment of three is shown)

Curriculum Vitae

Natalie Veronika Freytag née Klytta

born on February 28th 1986 in Zabrze, Poland

Leibniz-Institut DSMZ

Deutsche Sammlung für Mikroorganismen und Zellkulturen

Molecular Cancer Research

Inhoffenstraße 7B

38124 Braunschweig

2014 -2017	**Doctoral Thesis (continued)**
	"Characterization of the MIR23A Cluster in Diffuse Large B Cell Lymphoma - Regulation and Targetome Identification"
	Leibniz-Institut Deutsche Sammlung für Mikroorganismen und Zellkulturen DSMZ, Braunschweig
	Molecular Cancer Research
	Supervisor: Prof. Dieter Kube (University Medical Center Göttingen)
	Co-Supervisor: Dr. Sonja Eberth (Leibniz-Institut DSMZ Braunschweig)
2013-2014	**Doctoral thesis**
	"Characterization of the MIR23A Cluster in Diffuse Large B Cell Lymphoma - Regulation and Targetome Identification"
	University Medical Center of the Georg-August University Göttingen
	Haematology and Oncology, Supervisor: Prof. Dieter Kube
	Co-Supervisor: Dr. Sonja Eberth
2013 - 2017	**PhD program Molecular Medicine** of the Georg-August University Göttingen
2010 - 2012	**Master of Science**, Developmental, Neural and Behavioral Biology
	Georg-August-Universität Göttingen
	Major: Cell and Developmental Biology
	Master Thesis: "Establishment of an Auxin Inducible Protein Degradation System to Analyze the Function of Chk2 Kinase during Mitosis"
	Supervisor: Prof. Holger Bastians
2007 - 2010	**Bachelor of Science,** Biology
	Georg-August-Universität, Göttingen, Germany
	Bachelor Thesis: "Untersuchung der Funktion der Spermatogonien-spezifischen Gene *Nanos2*, *Dazl*, *Pou5f1* und *Zfp145* in der Maus."
	Supervisor: Prof. Sigrid Hoyer-Fender
2005 - 2007	**Staatlich-anerkannte biologisch technische Assistentin**
	Hans-Böckler-Berufskolleg Marl
2005	**Abitur (A-level)**
	Städtisches Gymnasium Herten